8-2017

Managing exoelectrogenic microbial community development through bioprocess control for conversion of biomass-derived streams

Alex James Lewis
University of Tennessee, Knoxville, alewis53@vols.utk.edu

To the Graduate Council:

I am submitting herewith a dissertation written by Alex James Lewis entitled "Managing exoelectrogenic microbial community development through bioprocess control for conversion of biomass-derived streams." I have examined the final electronic copy of this dissertation for form and content and recommend that it be accepted in partial fulfillment of the requirements for the degree of Doctor of Philosophy, with a major in Energy Science and Engineering.

Abhijeet Borole, Major Professor

We have read this dissertation and recommend its acceptance:

Brian Davison, Terry Hazen, Cong Trinh

Accepted for the Council:
Dixie L. Thompson

Vice Provost and Dean of the Graduate School

(Original signatures are on file with official student records.)

Managing exoelectrogenic microbial community development through bioprocess control for conversion of biomass-derived streams:

A Dissertation Presented for the

Doctor of Philosophy

Degree

The University of Tennessee, Knoxville

Alex James Lewis

August 2017

ACKNOWLEDGEMENTS

First, I want to sincerely thank my advisor Abhijeet Borole for his mentorship during my dissertation. His guidance and open-door policy were invaluable to my development as a scientist and research success. I would also like to thank my committee members for their participation in this process, and for providing guidance and critiques to improve the way I approached science. I want to thank the Bredesen Center, specifically Lee Riedinger, Wanda Davis, and Tracey Bucher for all their help over these 4 years, you guys are the best!

Lastly, I want to thank my friends and family who supported me through this process, and all the long hours and weekend work days! Thanks for always being there.

ABSTRACT

Bioelectrochemical systems are an emerging technology capable of utilizing aqueous waste streams generated during biomass conversion of lignocellulosic feedstocks to produce valuable co-products and thus, have potential to be integrated into biorefineries. In a microbial electrolysis cell, organic compounds are converted to electrons, protons, and CO_2 by fermentative and exoelectrogenic bacteria in the anode compartment. By having the ability to extract electrons from waste streams, these systems can treat water while also producing hydrogen, and thus can improve the efficiency of biomass to fuel production by minimizing external hydrogen requirement and enabling water recycle. The overall goal of this research is to understand how changes in the way the reactors are operated affect the performance of the system, and the structure of microbial community within when converting a biomass-derived stream (BOAP). This can enable the design of optimal community structure for waste stream conversion, which can lead to improved and stable performance of the system.

An integrated approach was taken to test parameters such as flow-rate, recycle, organic loading rate, feeding regime, and electrode potential using a suite of electrochemical, metabolic and genomic techniques to unravel the biocomplexity of these systems and the impact on the reactor microbial communities. Faster flow-rates and recycle operation led to better conversion of BOAP, but efficiencies decreased as organic loading rates increased. Exposure to high concentrations during fed-batch feeding resulted in a substantial loss of electrons that was alleviated through continuous operation. Additionally, high loading/concentration conditions selected for different microbial species. Furthermore, exposing the microbial communities to different anode voltages provided evidence that the benefits of using more negative anode

potentials to increase electrical efficiency can be capture through long-term enrichment without sacrificing substantial output. Lastly, the microbial community was characterized using deep sequencing techniques, revealing novel players directing a wide range of compounds to electrons. The resulting data was used to develop correlations that will serve as the foundation for operating these systems for commercial applications.

TABLE OF CONTENTS

LIST OF TABLES

LIST OF FIGURES

INTRODUCTION

Rapid progress in development of biorefinery technologies is needed to accelerate commercial development. Opportunities to enhance the viability of advanced biofuel technologies lie with the ability to fully utilize the entire feedstock and co-produce high-value commodities in addition to fuel[1]. Many proposed technologies such as pyrolysis, hydrothermal liquefaction of algae, and lingnocellulosic fermentations produce waste streams that must be valorized. Focusing on the production of biofuel from lignocellulosic feedstocks via pyrolysis, a significant amount of hydrogen is needed for upgrading of the produced bio-oil for generating drop-in fuel hydrocarbons. The ability to produce hydrogen from biomass or biomass-derived streams can significantly reduce the greenhouse gas emissions released by use of natural gas as a hydrogen source in this process. Separation of the bio-oil for fuel production produces large amounts of aqueous phase retaining a significant portion of the carbon and energy from the biomass feedstock[2]. If the carbon from the aqueous phase is not recovered, a significant fraction of biomass and energy is lost to the water phase, decreasing the biofuel yield from the process. Besides the pyrolysis process, many other biofuel platform technologies utilize aqueous processing, e.g., fermentation, algal biomass growth, which also have the potential to lose carbon and energy retained in this aqueous phase. Thus, technologies are needed to address these issues related to carbon loss via aqueous phase, regardless of the conversion platform.

Microbial electrolysis is a robust technology capable of producing renewable hydrogen through energy recovery from organic waste streams[3]. As described in abstract, organic compounds are converted to electrons, protons, and CO2 by electroactive bacteria at the anode and the electrons can then travel via an external circuit while protons diffuse through a

membrane to an anaerobic cathode, where they can react with help of a small applied potential to drive H_2 production from incoming electrons and protons at the cathode[4,5]. **Figure 1** diagrams this process.

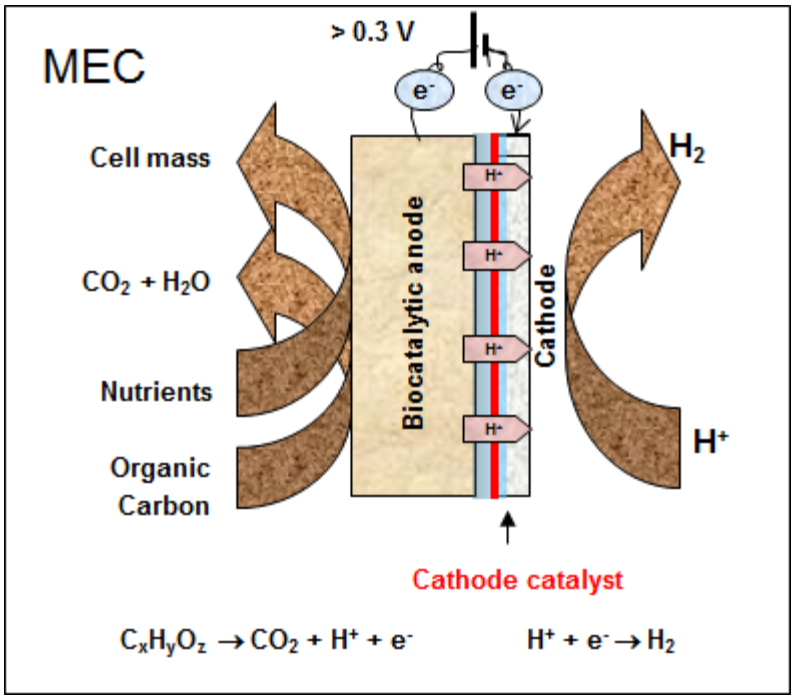

Figure 1: Diagram of microbial electrolysis[6].

The unique aspect of these systems is a solid electron acceptor for microbial processes, imparting a path to oxidize or reduce compounds without the need for adding specific compounds to serve as electron donors or acceptors. This adds an extra element of redox control via setting the applied potential (voltage difference between anode and cathode), which effects the thermodynamics of reactions taking place in anode and cathode. Optimization of electroactive biofilms to handle more complex wastewater streams requires a multipronged approach to operation, system design and biology parameters[7,8]. Complex feedstocks, such as those derived from lignocellulosic biomass can contain hundreds of compounds, which may require multi-step conversion and interactions among different bacteria to effectively convert.

Additionally, proper reactor architecture and operational conditions are required to achieve meaningful levels of performance. Many studies in the literature appear to undervalue enrichment of the microbial community, which drives this process. Unenriched microbial communities are often used, and exposed to the substrate of interest for a very short period before experiments are undertaken, despite evidence of the impact of carbon source on community development, among other selective pressures[7,9]. Several MEC configurations and process conditions have been studied for improving performance and conversion of waste streams into hydrogen. Typical parameters studied for quantifying and understanding performance of continuously fed MECs include hydraulic retention time (HRT) and organic loading rate (OLR), which depend on flow rate and substrate concentration. Increasing the HRT has been reported to affect the hydrogen production rate as well as the efficiency of hydrogen production with mixed results[10,11]. The effect of OLR on anode efficiency and productivity has also been studied[12,13], but primarily in microbial fuel cells (MFCs)[14–16]. The current output usually increases with increasing OLR, however, the anode efficiency, hydrogen recovery, and cathode efficiency can vary depending on other operational parameters. The effect of these operational parameters on MEC performance, in addition to the mode of feeding, needs to be better understood and requires insights into the mechanistic details of the process for MECs treating complex substrates. Additionally as described previously, the applied voltage can change the thermodynamics of the system, but it is the anode electrode potential, which the biofilm uses to transfer electrons, that determines the energy gain available to microbe for a given substrate and impacts the metabolic pathways used to convert it[17]. Studies in the literature have found higher activity per unit biomass at more negative potentials using direct means of electron transfer, while more positive potentials form thicker, less efficient biofilms[18,19]. Additionally,

specific pathways and active redox enzymes have shown preferences depending on anode potential[20–23]. However, the ability of the microbial communities to respond to short-term vs long-term changes and achieve high performance at negative anode potentials is unclear. While the energy gain for the exoelectrogenic microbes are an important factor, interactions with other community members such as fermentative populations are essential for conversion of complex streams. It is well established that even for simple substrates, syntrophic interactions among fermenters and exoelectrogens as well as hydrogen scavengers are required to produce current in the anode[24–27]. For more complex substrates these needs are compounded and but little progress has been made investigating these interactions for conversion of more complex streams.

Improvements in the application of MECs for conversion of biomass streams must start with the biocatalyst. Due to the recalcitrant and inhibitory nature of BOAP containing furanic and phenolic aromatic compounds as well as organic acids, a directed enrichment process is a necessary but overlooked approach needed to develop an effective microbial community. Thus, the 2nd chapter of this study investigates the hypothesis that a targeted enrichment is necessary to reach higher levels of productivities and efficiencies for conversion of complex streams, which is assessed through COD removal, conversion of individual compounds within BOAP, and current/hydrogen output. The inter-related parameters of OLR, flow-rate, HRT, and concentration were then investigated to examine the effect of these variables on MEC performance. The HRT, OLR and substrate concentration are inter-related and cannot truly be studied independently, as is typically done. For example, to reach a desired OLR either the HRT/flow rate of the system or the concentration of the feed must be altered. Thus, when studying the effect of different OLR's, one of the other two variables will also be changing, so, only two of the three variables can be studied independently, while the third remains a dependent

variable. To address this, experiments were carried out holding concentration constant, then again holding OLR constant. While holding concentration constant, our hypothesis is that mass transfer and kinetic limitations exist at low flow-rates and if flow rate in the anode is increased, then mass transfer limitations may be alleviated increasing current and hydrogen production rate. To follow up this experiment that held concentration constant, concentration was allowed to change as function of OLR and flow rate to further study the effect concentration on the microbial community and resulting performance. The hypothesis under investigation was two-fold. First, at the same OLR a higher concentration at lower flow-rate would not improve performance due to losses in mass transfer. Secondly, MECs operated at higher OLRs may increase diversion of electrons to methanogenesis due to higher concentrations of substrate. In the 5th chapter, the abilities of the anode microbial community were explored more in depth to probe the interactions between functional members of the community. Due to the complex nature of BOAP, containing multiple classes of fermentable compounds, our hypothesis was that fermentation to produce acetate for exoelectrogens is limiting. To assess if the observed results from previous chapters were the result of the feeding regime, the impact of continuous vs fed-batch feeding was tested with the hypothesis that continuous operation would result in better performance and community structure.

Switching the focus to exoelectrogens, opposite anode potential levels were used to determine the capacity and mechanism by which microbial communities adapt to different redox environments. Two experimental paths were used for studying the impact of electrode potential: shifting an already mature biofilm to a new potential, and enrichment for a specific anode potential from start-up. Performance outputs and efficiencies were compared for short-term and long-term responses while tracking changes in metabolite profile and microbial community

structure. Building on our enrichment strategy in chapter 2, we hypothesized that if a directed enrichment was carried out, high performance could be achieved at more negative potentials despite less energy gain available to the microbes. Additionally, if diverse communities contain microbes that are able to alter gene expression as the sole means of adaptation in response to different redox conditions, then shifting of the poised potential should only temporarily result in reduced current when looking at short-term vs long-term responses.

To probe deeper into community structure and activity of fermentative, syntrophic, and exoelectrogen populations, the 8th chapter takes a genomics-focused approach using 16S rRNA method, shotgun metagenomics and RNA-seq in addition to metabolite profiles. This enabled community activity to be characterized at a much deeper level. Finally, the resulting data from the previous chapters across experimental conditions was used for a developing correlations and qualitative relationships between process parameters, community structure, and reactor performance via principal component analysis (PCA) and Canonical correspondence analysis (CCA).

References

1. da Silva TL, Gouveia L, Reis A. Integrated microbial processes for biofuels and high value-added products: the way to improve the cost effectiveness of biofuel production. *Appl Microbiol Biotechnol*. 2014;98(3):1043-1053. doi:10.1007/s00253-013-5389-5.
2. Imam T, Capareda S. Characterization of bio-oil, syn-gas and bio-char from switchgrass pyrolysis at various temperatures. *J Anal Appl Pyrolysis*. 2012;93:170-177. doi:10.1016/j.jaap.2011.11.010.
3. Logan BE, Call D, Cheng S, et al. Microbial electrolysis cells for high yield hydrogen gas production from organic matter. *Environ Sci Technol*. 2008;42:8630-8640. doi:10.1021/es801553z.
4. Hong Liu †, Stephen Grot ‡ and, Bruce E. Logan* †. Electrochemically Assisted Microbial Production of Hydrogen from Acetate. 2005. doi:10.1021/ES050244P.
5. Hallenbeck PC, Ghosh D, Skonieczny MT, Yargeau V. Microbiological and engineering aspects of biohydrogen production. *Indian J Microbiol*. 2009;49(1):48-59. doi:10.1007/s12088-009-0010-4.
6. P. Borole A. Improving energy efficiency and enabling water recycling in biorefineries using bioelectrochemical systems. *Biofuels, Bioprod Biorefining*. 2011;5:246-28-36. doi:10.1002/bbb.
7. Borole AP, Reguera G, Ringeisen B, Wang Z-W, Feng Y, Kim BH. Electroactive biofilms: Current status and future research needs. *Energy Environ Sci*. 2011;4(12):4813. doi:10.1039/c1ee02511b.
8. Sleutels THJ a, Ter Heijne A, Buisman CJN, Hamelers HVM. Bioelectrochemical systems: An outlook for practical applications. *ChemSusChem*. 2012;5:1012-1019. doi:10.1002/cssc.201100732.
9. Pant D, Van Bogaert G, Diels L, Vanbroekhoven K. A review of the substrates used in microbial fuel cells (MFCs) for sustainable energy production. *Bioresour Technol*. 2010;101(6):1533-1543. doi:10.1016/j.biortech.2009.10.017.
10. Gil-Carrera L, Escapa a., Carracedo B, Morán a., Gómez X. Performance of a semi-pilot tubular microbial electrolysis cell (MEC) under several hydraulic retention times and applied voltages. *Bioresour Technol*. 2013;146:63-69. doi:10.1016/j.biortech.2013.07.020.
11. Escapa A, Lobato A, García DM, Morán A. Hydrogen production and COD elimination rate in a continuous microbial electrolysis cell: The influence of hydraulic retention time and applied voltage. *Environ Prog Sustain Energy*. 2013;32(2):263-268. doi:10.1002/ep.11619.
12. Gil-Carrera L, Escapa A, Moreno R, Morán A. Reduced energy consumption during low strength domestic wastewater treatment in a semi-pilot tubular microbial electrolysis cell. *J Environ Manage*. 2013;122:1-7. doi:10.1016/j.jenvman.2013.03.001.
13. Escapa A, Gil-Carrera L, García V, Morán A. Performance of a continuous flow microbial electrolysis cell (MEC) fed with domestic wastewater. *Bioresour Technol*. 2012;117:55-62. doi:10.1016/j.biortech.2012.04.060.
14. He Z, Wagner N, Shelley D. Minteer A, Angenent LT. An Upflow Microbial Fuel Cell with an Interior Cathode: Assessment of the Internal Resistance by Impedance Spectroscopy. 2006. doi:10.1021/ES060394F.

15. Aelterman P, Versichele M, Marzorati M, Boon N, Verstraete W. Loading rate and external resistance control the electricity generation of microbial fuel cells with different three-dimensional anodes. *Bioresour Technol*. 2008;99:8895-8902. doi:10.1016/j.biortech.2008.04.061.
16. Borole AP, Hamilton CY, Vishnivetskaya T a. Enhancement in current density and energy conversion efficiency of 3-dimensional MFC anodes using pre-enriched consortium and continuous supply of electron donors. *Bioresour Technol*. 2011;102(8):5098-5104. doi:10.1016/j.biortech.2011.01.045.
17. Peter Aelterman, Korneel Rabaey, Hai The Pham, Nico Boon and, Verstraete* W. Continuous Electricity Generation at High Voltages and Currents Using Stacked Microbial Fuel Cells. 2006. doi:10.1021/ES0525511.
18. Aelterman P, Freguia S, Keller J, Verstraete W, Rabaey K. The anode potential regulates bacterial activity in microbial fuel cells. *Appl Microbiol Biotechnol*. 2008;78(3):409-418. doi:10.1007/s00253-007-1327-8.
19. Torres CI, Krajmalnik-Brown R, Parameswaran P, et al. Selecting anode-respiring bacteria based on anode potential: Phylogenetic, electrochemical, and microscopic characterization. *Environ Sci Technol*. 2009;43(24):9519-9524. doi:10.1021/es902165y.
20. Busalmen JP, Esteve-Nuñez A, Feliu JM. Whole Cell Electrochemistry of Electricity-Producing Microorganisms Evidence an Adaptation for Optimal Exocellular Electron Transport. *Environ Sci Technol*. 2008;42(7):2445-2450. doi:10.1021/es702569y.
21. Zhu X, Yates MD, Hatzell MC, Ananda Rao H, Saikaly PE, Logan BE. Microbial community composition is unaffected by anode potential. *Environ Sci Technol*. 2014;48:1352-1358. doi:10.1021/es404690q.
22. Levar CE, Chan CH, Mehta-Kolte MG, Bond DR. An inner membrane cytochrome required only for reduction of high redox potential extracellular electron acceptors. *MBio*. 2014;5(6):e02034. doi:10.1128/mBio.02034-14.
23. Zacharoff L, Chan CH, Bond DR. Reduction of low potential electron acceptors requires the CbcL inner membrane cytochrome of Geobacter sulfurreducens. *Bioelectrochemistry*. 2016;107:7-13. doi:10.1016/j.bioelechem.2015.08.003.
24. Parameswaran P, Torres CI, Lee HS, Krajmalnik-Brown R, Rittmann BE. Syntrophic interactions among anode respiring bacteria (ARB) and non-ARB in a biofilm anode: Electron balances. *Biotechnol Bioeng*. 2009;103(3):513-523. doi:10.1002/bit.22267.
25. Gao Y, Ryu H, Santo Domingo JW, Lee H-S. Syntrophic interactions between H2-scavenging and anode-respiring bacteria can improve current density in microbial electrochemical cells. *Bioresour Technol*. 2014;153:245-253. doi:10.1016/j.biortech.2013.11.077.
26. Hari AR, Katuri KP, Gorron E, Logan BE, Saikaly PE. Multiple paths of electron flow to current in microbial electrolysis cells fed with low and high concentrations of propionate. *Appl Microbiol Biotechnol*. 2016;100(13):5999-6011. doi:10.1007/s00253-016-7402-2.
27. Miceli JF, Garcia-Peña I, Parameswaran P, Torres CI, Krajmalnik-Brown R. Combining microbial cultures for efficient production of electricity from butyrate in a microbial electrochemical cell. *Bioresour Technol*. 2014;169:169-174. doi:10.1016/j.biortech.2014.06.090.

CHAPTER I

HYDROGEN PRODUCTION FROM SWITCHGRASS VIA AN INTEGRATED PYROLYSIS–MICROBIAL ELECTROLYSIS PROCESS

This chapter was originally published by:

Lewis AJ, Ren S, Ye X, Kim P, Labbe N, Borole AP. Hydrogen production from switchgrass via an integrated pyrolysis-microbial electrolysis process. *Bioresour Technol.* 2015;195:231-241. doi:10.1016/j.biortech.2015.06.085.

No alterations were made to the published article for inclusion in the dissertation. The pyrolysis of switchgrass and generation of bio-oil aqueous phase (BOAP) and its characterization were carried out by Ren S, Ye X, Kim P, and Labbe N. All experiments and analysis utilizing BOAP in the microbial electrolysis cell (MEC), were carried out by AJL as well the writing of this manuscript. APB provided guidance and feedback on experimental design, analysis, and manuscript preparation.

Abstract

A new approach to hydrogen production using an integrated pyrolysis-microbial electrolysis process is described. The aqueous stream generated during pyrolysis of switchgrass was used as a substrate for hydrogen production in a microbial electrolysis cell, achieving a maximum hydrogen production rate of 4.3 L H_2/L (anode)-day at a loading of 10 g COD/L-anode-day. Hydrogen yields ranged from 50 ± 3.2% to 76 ± 0.5% while anode Coulombic efficiency ranged from 54 ± 6.5% to 96 ± 0.21%, respectively. Significant conversion of furfural, organic acids and phenolic molecules was observed under both batch and continuous conditions. The electrical and overall energy efficiency ranged from 149-175% and 48-63%, respectively. The results demonstrate the potential of the pyrolysis-microbial electrolysis process as a sustainable and efficient route for production of renewable hydrogen with significant

implications for hydrocarbon production from biomass.

Introduction

Sustainable hydrogen supply and water management are the two most significant sustainability issues facing biorefinery development. Production of transportation fuels from biomass via pyrolysis enables production of hydrocarbon fuels, making it a high priority alternative for biorefineries. However, due to the high oxygen content of biomass, significant amount of hydrogen is needed for deoxygenation and generation of fuel hydrocarbons. The ability to produce hydrogen from biomass or biomass-derived streams can significantly reduce the greenhouse gas emissions released by use of natural gas as a hydrogen source. Production of hydrogen from natural gas contributes 18% to capital costs via the thermochemical route converting biomass to fuels [1]. Biomass used for pyrolysis typically contains 20% moisture or more resulting in a water-rich bio-oil from the pyrolysis process. Fast pyrolysis and intermediate pyrolysis generate a bio-oil product which is essentially a mixture of aqueous and organic phases. Separation of the bio-oil for fuel production produces large amounts of aqueous phase containing organic carbon from biomass. A bio-oil derived from switchgrass was reported to contain over 70% aqueous phase [2]. If the carbon from the aqueous phase is not recovered, a significant fraction of biomass and energy is lost to the water phase, decreasing the overall efficiency of the process.

Production of renewable hydrogen from biomass is a long-sought technology for moving away from fossil fuels and towards a low-carbon economy. Microbial electrolysis is a versatile technology capable of addressing the issue of hydrogen production as well as water management [3]. By extracting energy from the aqueous stream in the form of hydrogen and treating water, the

efficiency of biomass to fuel production can be increased by minimizing external hydrogen requirement and enabling water recycling [4]. Previous work on bioanode development has resulted in a highly enriched anode consortium using the waste stream from ethanol fermentation, capable of converting furan aldehydes, phenolics, and other normally inhibitory compounds [5,6]. Optimization of electroactive biofilms to handle complex wastewater streams requires a multipronged approach that includes process, system design and biology parameters [7-9]. Recent advancements in understanding of the electrochemical performance of anode biofilms and the dependence of the enrichment process on organic loading, continuous vs. batch substrate delivery and other parameters have led to current densities reaching above 20 A/m^2 [9,10].

In this study, we report conversion of the complex mixture of organics present in the bio-oil aqueous phase (boap) derived from biomass pyrolysis containing phenolic compounds, furan aldehydes, organic acids and sugar derivatives in an MEC to produce hydrogen. This mixture is overall more recalcitrant than the fermentation stream previously utilized in bioanode [5]. The development of an electroactive microbial community capable of handling the toxic compounds and generating hydrogen using a switchgrass pyrolysis-derived aqueous phase is reported. The composition of the microbial community developed for treatment of boap is described. The efficiency of conversion in the anode as well as cathode, and overall hydrogen production efficiency and productivity and their reproducibility in replicate experiments in two different MECs is reported.

Methods

Biomass pyrolysis

The feedstock used in the study was air-dried switchgrass with particle sizes less than 2 mm and a moisture content of 7‑8 wt%, which was obtained from Genera Energy Inc. (Vonore, TN). A semi pilot auger pyrolysis system was used in this study to carry out intermediate pyrolysis. The system was equipped with a feeding system, an auger pyrolysis reactor, a biochar collector, a particle-precipitating chamber, and a condensation section (Supplemental Figure 8). A detailed description of the pyrolysis system used in this study, (located at the Center for Renewable Carbon, University of Tennessee), is provided elsewhere [11]. In brief, the bio-oil used in this study was produced under the following operation conditions. The feedstock was transferred from the feeding hopper to the pyrolysis reactor by a single auger with feeding rate of approximately 8.5 kg/h. The pyrolysis reactor (10 W×10 H×250 L cm) contains internal dual augers. The auger speed controlled the residence time of feedstock at 72 seconds. The heated zone comprised of a 200 cm long electrical resistance furnace operating at 500 °C. The sweeping gas (nitrogen gas, 20 L/min) was introduced into the front of the auger reactor and moved with the evolved vapors to the condensation section. Before the vapors enter the condensers from the auger reactor, the particle chamber (20 cm in diameter and 100 cm long) precipitated fine particles from the vapors. The biochar produced from the feedstock was collected into the biochar drum. The condensation section comprised of three condensers in series (10 cm in diameter and 200 cm long, each). Before the pyrolysis operation, all condensers were cooled to 10 - 15 °C using a circulation water cooling system. The bio-oils collected from three condensers were immediately combined and mixed for homogeneity and stored in the walk-in freezer until

used for characterization. The pyrolysis operation was performed in duplicate.

Bio-oil separation and characterization

The crude bio-oil obtained from the pyrolysis reactor was mixed with distilled water in a ratio of 1:4 (wt.%) to separate bio-oil aqueous phase (boap: water soluble fraction) and an organic phase (water insoluble fraction). The mixture was shaken vigorously and placed at 4°C overnight. Then the mixture was centrifuged in an IEC Clinical centrifuge (model 120) at 5000 rpm for 30 minutes to ensure the phase separation. The boap was collected and weighed to determine the amount of bio-oil dissolved in the water. The separated aqueous phase (boap) was used for hydrogen production in the MEC system.

The chemical compounds in boap were identified by gas chromatography-mass spectrometry (GC-MS) and quantified by GC-flame ionization detector and high performance liquid chromatography (HPLC). A Shimadzu GC–MS (QP2010S) with a Restek Rtx-5MS capillary column was used. The column was programmed at 45°C for 3 min, then at 5°C/min to 150°C without holding, then 10°C/min to 260°C and a hold time of 7 min. The inlet was set at 240°C, and sample injection was made in split mode (1:20). The compounds were identified by comparing their mass spectra with those from the National Institute of Standards and Technology (NIST) mass spectral data library. Due to the very high water content in the boap, organic compounds were first extracted by ethyl lactate and chloroform and then analyzed by GC-MS. The crude bio-oil was diluted a factor 20 times before being injected into the GC-MS.

GC-FID with a HP-5 column was used for quantifying volatile compounds in boap. The same program with the GC-MS was used in GC-FID. A HPLC system (Jasco 2000Plus, Jasco analytical instruments) equipped with PU-2089S Plus pump, a MD-2018 Plus Photodiode Array

detector (PDA), a RI-2031 Plus intelligent RI detector, and an AS-2055 Plus auto sampler was used to analyze boap for non-volatile compounds. The liquid chromatography was conducted at 50.0°C using Bio-rad HPX-87H (300 x 8 mm) column. The volume of injected sample was 20µl. The mobile phase was 5mM H_2SO_4 with or without 15 % acetonitrile (v/v) with a flow rate of 0.6 mL/min. The method using 15% acetonitrile was used primarily to ascertain elution of all peaks from the column and to determine appropriate run time. The use of acetonitrile posed a problem with quantification of organic acids; therefore a method without acetonitrile was used with a longer run time of 120 min.

MFC and MEC construction

The bioelectrochemical system used in this study consisted of a two-chamber cell that was convertible between MFC and MEC. The anode consisted of a carbon felt (projected surface area = 12.56 cm^2, specific surface area = 454 cm^2cm^{-3}, anode volume = 15.96 cm^3) that was plasma treated to increase hydrophilicity [12]. The anode and cathode chambers are separated by a membrane electrode assembly (MEA) consisting of Nafion and platinum-deposited carbon (0.5 mg/cm^2; 10% Pt; E-TEC, FuelCellsEtc., Bryan, TX) on the cathode side. The cathode chamber was 16 ml and included a 12 cm^2 piece of stainless steel mesh as a current collector in contact with the Pt-deposited carbon cathode. The cathode inlet/outlet was open to air during operation of the system as MFC but was sealed and made oxygen-free by sparging with N_2 for MEC operation. The two chambers were connected via an external resistor attached to a carbon rod current collector inserted into the anode and stainless steel wire at the cathode. All enrichment and experiments were carried out at room temperature (22°C).

Inoculation and operation

The MFC was inoculated using previously enriched consortia from two different anodes. The first was from an anode pre-enriched on boap, which used an inoculum from a bioanode grown on a corn stover-derived fermentation process stream [5]. The second came from an anode fed with furan aldehydes and phenolic model compounds as the substrate [6]. Multiple consortia were used to enable broad specificity in the new community to handle the different class of compounds present in boap. The inoculum consisted of a total of two cores (5 mm diameter x 12.5 mm length) cut out of the anode carbon felt along with anodic biofilm grown on the felt from the previously mentioned anodes. The inoculum was immediately transplanted into a similar-sized hole in new MFC anode felt. Two duplicate MFCs were developed in parallel and followed an enrichment procedure similar to that reported previously [13,14]. The operation of the MFC prior to testing included continuous supply of boap added directly in the flow line via syringe pump as shown in Figure 2. The starting load on the MFC was 220 Ω, at which the MFCs reached their peak voltage of 0.36 V after 14 days. The resistance was then dropped to 100 ohms on day 15 and to 51 ohms on day 17. Glucose was supplemented in batches of 0.2 g/l approximately once a month over the first 6 months of operation to facilitate growth of boap converting microbes. A minimal nutrient medium consisting of mineral salts and vitamin solution was used as reported previously [14]. The medium was placed in an external reservoir and circulated through the anode chamber at a flow rate of 5 mL min^{-1}. Media and planktonic cells were replaced intermittently to maintain an optical density (600 nm) of the medium below 0.05 units.

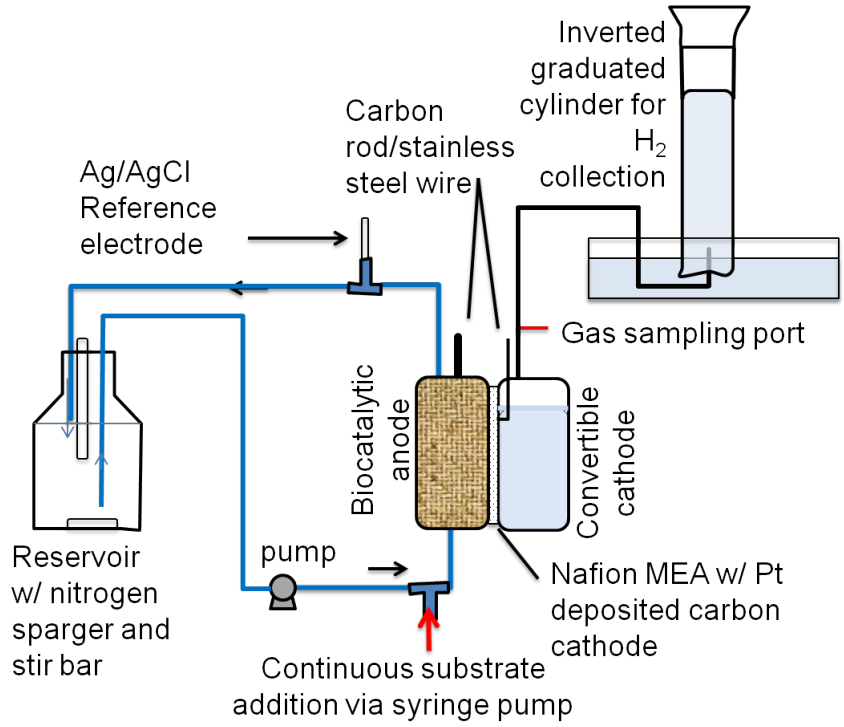

Figure 2: Experimental setup for investigating hydrogen production from BOAP using MEC.

Chronoamperometry - Hydrogen production

The air-cathode was converted to an oxygen-free cathode by sparging with N_2 to enable operation of the system as MEC. Additionally, the cathode chamber was filled with 12 ml of 100 mM phosphate buffer followed by additional sparging with N_2. A viton tube was attached to the cathode outlet and was inserted into an inverted 100 or 250 ml graduated cylinder containing DI water for gas collection. The cathode inlet was then sealed and the nitrogen sparging stopped to allow collection of hydrogen gas. Chronoamperometric measurements were conducted by poising the anode electrode at a potential of -0.2 V relative to a Ag/AgCl reference electrode [15]. The cell potential was also recorded to determine the total energy applied to the cell. The method to operate MEC by poising the anode electrode was used instead of poising the cathode or applying a fixed potential across the cell since it offers the advantage of maintaining the anode

potential at an optimal value and preventing damage to the anode community from excessively positive potentials . The cathode gas outlet line included a T-junction to allow gas sampling via a sealed septa sampling port. Boap was tested in batch at concentrations of 0.3, 0.2 and 0.1 g/L as well as in continuous addition mode at an organic loading of 2, 4, 10 g/L-day. The concentration and loading refer to COD of the boap supplied to the anode. The boap was diluted to 50 g/L and filtered using a 0.45 μm nylon filter before use. During batch tests with boap, time zero samples were taken before poising of the anode or circulation of the aqueous medium. Between experiments, the anode medium was replaced and the inlet and outlet lines flushed with fresh medium. The cathode buffer was also replaced between experiments. The hydrogen production measurements were initiated immediately after starting chronoamperometry. A Reference 3000 potentiostat/galvanostat/zero resistance ammeter (Gamry Instruments, Warminster PA) was used for all MEC experiments. Depending on the substrate level used, each experiment was allowed to run between 8-24 hours. At the end of each run, the volume displaced by hydrogen production was measured, gas samples for GC analysis were taken from the cathode outlet to confirm hydrogen production, and samples for HPLC analysis were taken from the external anode reservoir to measure the extent of conversion of the substrates in boap. HPLC samples from MEC were centrifuged for 10 min at 4500 rpm, and then filtered with 0.2 μm nylon filter and stored at 4 °C for analysis. HPLC samples were analyzed as described in section 2.0.

COD analysis

Samples prepared for HPLC as outlined above in section 2.5 were also analyzed via the Hach COD method. A 2 ml sample was added to a Hach COD digestion vial and inverted several times for mixing. The samples were then placed in a Hach DRB 200 reactor at 150 °C for 2

hours. Upon completion, samples were allowed to cool to room temperature before spectroscopic analysis. A calibration curve was generated prior to running samples, utilizing 10 concentrations from 25 mg to 1000 mg of COD standard solution (Potassium Acid Phthalate). Absorbance readings were taken at 620 nm on Spectronic 20 Genesys and converted to concentration based on the calibration curve.

DNA extraction and 16s rRNA analysis

MFC's were disconnected and moved into an anaerobic glove bag for sampling of the microbial community from the anode felt. The MFC's anode chamber was opened up and a coring tool was used to remove a 5 mm diameter x 12.5 mm long core of felt from above the inlet area in the anode, which was replaced by a fresh piece of matching felt. Cores were stored in either sterile MilliQ water or 25% glycerol in freezer vials for storage at -80°C. Genomic DNA was isolated using the standard freeze–thaw procedure, followed by phenol–chloroform extraction [14,16] . Extracted and purified DNA samples were submitted to Hudson Alpha Genomic Services Lab (Huntsville, AL) for library prep and 16s rRNA analysis. Their methods included PCR reactions were run using 10ng of input template, V3-V4 amplicon primers, and Kapa Master mix (20 cycles). Products were purified using 0.75X beads, and were then put into a second, indexing PCR reaction (Kapa master mix, 12 cycles of PCR, GSL3.7 indexes for I7). Final libraries were purified and quantified by Qubit. Products were pooled using the Biomek liquid handler and profiled using the Agilent Bioanalyzer. Kapa qPCR was also done for another quality control. Sequencing was then carried out with MiSeq 250 bp PE run and sequence data was analyzed on BaseSpace using 16S Metagenomics v1.0.1 (ILLUMINA, INC).

Calculation of Coulombic efficiency and other conversion efficiencies

Performance was characterized by anodic Coulombic efficiency (CE), cathodic conversion efficiency, percent hydrogen yield, electrical efficiency and overall energy efficiency. CE was calculated from the produced current I_{obs}, the moles of substrate n_s used and the number of electrons available per mol of substrate (based on complete conversion to CO_2) n_e, using the following equation:

$$CE_{anode} = \frac{I_{obs}t}{n_s n_e F}$$

F is Faraday constant and t is the duration of the experiment. The boap concentration was measured as COD as well as using HPLC analysis. However, all compounds were not identified by HPLC and therefore the total concentration of organics in boap was not available. Therefore, COD measurements before and after MEC treatment were used to determine the substrate concentration and loading. The total COD of the boap before dilution for MEC treatment was 130 g/L. The compounds identified by HPLC are being reported separately (Ren et al., 2015, manuscript in preparation) and were used to understand the conversion of the individual compounds in the anode. Percent hydrogen yield was calculated as grams of hydrogen produced per gram of hydrogen expected from conversion of substrate utilized in the anode. Since absolute boap concentration was not available, COD was used as a measure of substrate concentration to calculate the percent yield:

$$Y_{H2} = \frac{PV_{H2}/RT}{2\Delta nCOD}$$

where P is the atmospheric pressure, V_{H2} is the volume of hydrogen produced, R is the gas

constant, T is the temperature in Kelvin and ΔnCOD is the moles of COD consumed during the experiment. Hydrogen productivity or rate of hydrogen production was calculated directly from the volume of hydrogen produced per unit anode volume per unit time:

$$Q_{H2} = \frac{V_{H2}/V_{anode}}{t}$$

Cathodic conversion efficiency was calculated as the ratio of the amount of hydrogen produced and the maximum amount of hydrogen that could be produced based on the average current generated over the experiment, I_{obs}. This was calculated by the following equation:

$$CE_{cat} = \left(\frac{V_{H2}}{\frac{I_{obs} tRT}{2FP}} \right)$$

Energy efficiency calculations were done using the method described by Logan et al., 2008 defined by the overall (η_{E+S}), which is calculated from the combustion energy of hydrogen (W_{H2}), substrate input (W_s), and electrical energy input (W_E):

$$\eta_{E+S} = \frac{-W_{H2}}{W_E - W_s}$$

The energy content used for boap was based on COD and estimated to be 14.955 kJ/gCOD [17]. Similarly, electrical efficiency (η_E) is the ratio of total energy recovered as hydrogen (W_{H2}) to the electrical energy input (W_E)

$$\eta_E = \frac{-W_{H2}}{W_E}$$

Results and Discussion

Bio-oil production and pyrolysis yields

Pyrolysis of switchgrass using a pilot-scale auger reactor yielded 50-54% bio-oil, 29% biochar, and 17-21% non-condensable gas. Two separate pyrolysis runs were carried out, but only the bio-oil from the first run was used in the experiments described in this report. The compounds identified in the two bio-oils were similar as described in Section 3.2.

Bio-oil and aqueous phase characterization

After separation of the aqueous phase from the bio-oil via addition of deionized water, about 35.1 wt% organic compounds in the crude bio-oil were extracted to the aqueous phase (boap) to form a solution of about 8.3 wt% of organics in the aqueous phase. This corresponds to a COD of 130 g/L. The aqueous fraction contained about 19.1 wt% of the original biomass as dissolved organics. Figure 9 in Appendix shows a distribution of the pyrolysis products and the organic and aqueous fractions resulting from fractionation of bio-oil after water addition. Compounds identified by GC-MS in the crude bio-oil and aqueous phase are provided in Table 3 in Appendix. The identified compounds were mainly categorized to nine groups: acids, alcohols, aldehydes, esters, furans, ketones, phenolics, sugars, and PAHs (poly aromatic hydrocarbons). The compounds extracted into the aqueous phase based on GC-MS analysis indicated that the boap contained alcohols, furans, ketones, and phenolics. Organic acids and levoglucosan were detected in crude bio-oil at high concentration and were extracted into the aqueous phase. According to the GC-MS analysis for crude bio-oil and boap, a total of 17 compounds including 3 acids, 3 furans, 2 alcohols, 6 phenolics, 2 ketones and 1 anhydrosugar were quantified by GC-

FID and HPLC-PDA. Among these compounds eight major compounds were quantified by HPLC-PDA and another 9 compounds were quantified by GC-FID using external standards. The results for quantification of the compounds in boap are shown in Table 1. Levoglucosan and acetic acid were detected in boap at concentration of 15.33 and 11.96 g/L. Other compounds were present at relatively lower concentrations, generally below 3 g/L. The total amount of compounds quantified by HPLC in boap was about 37g/L.GC-FID analysis quantified 9 volatile compounds in boap. GC-FID analysis showed 1,3-propanediol, 2(5H)-furanone, and 1-hydroxybutanone at relatively higher concentrations (> 1 g/L) with additional 6 other compounds which were below 0.6g/L in boap. Total amount of compounds quantified in boap by GC-FID was about 6.02 g/L. The total concentration of compounds quantified together by HPLC-PDA and GC-FID was 43.01g/L.

Microbial anode development

The duplicate MFCs developed using the methods described in section 2.4 were operated for 8 months prior to this study with boap as the substrate and reached a stable output of 1 mA at a loading of 2 g/L-day. The development of an anode microbial consortium capable of utilizing the complex compounds in boap that are also inhibitory to microbial growth was possible due to addition of glucose as a co-substrate. Previous trials without inclusion of glucose did not yield sufficient current production (data not shown). Acclimation and enrichment of a variety of microbes with different roles is critical to enhance the overall ability of the community to collectively breakdown a wide spectrum of compounds and harvest the electrons [5,7,18].

Table 1: Concentrations of major chemical compounds in bio-oil aqueous phase quantified by HPLC-PDA and GC-FID.

Quantification method	Major chemicals	Concentration based on aqueous phase (g/L)
HPLC-PDA	Furfural	1.01
	1,2-benzendiol	1.77
	Phenol	1.8
	Levoglucosan	15.33
	Acetic acid	11.96
	Proponic acid	1.89
	Vanillic acid	2.69
	HMF	0.54
	Total	36.99
GC-FID	Phenol, 2-methoxy-	0.25
	2-methyl-4-methyphenol	0.07
	Cyclohexanone	0.07
	3-methyl-1,2-cyclophetandiol	0.46
	2,6-Dimethoxyphenol	0.26
	1,3-propanediol	1.84
	3-ethylphenol	0.56
	2(5H)-Furanone	1.17
	1-hydroxybutanone	1.35
	Total	6.02
	Sum	43.01

16s rRNA analysis

Figure 3 shows characterization of the anode community based on 16S rRNA genes, identified to the family level. As expected, Proteobacterium dominated the community likely due to its diverse metabolic capabilities and utilization of the molecules in the complex boap. The duplicate bioanode showed significant similarity in community structure among the major families identified, sharing 5 of the top 8 families, including Geobacteraceae, and Rhodocyclaceae. The relative proportions of members did vary slightly, with the largest difference between duplicates being the presence of Enterococcaceae (16%) and Comamonadaceae (10%) separately at high proportions.

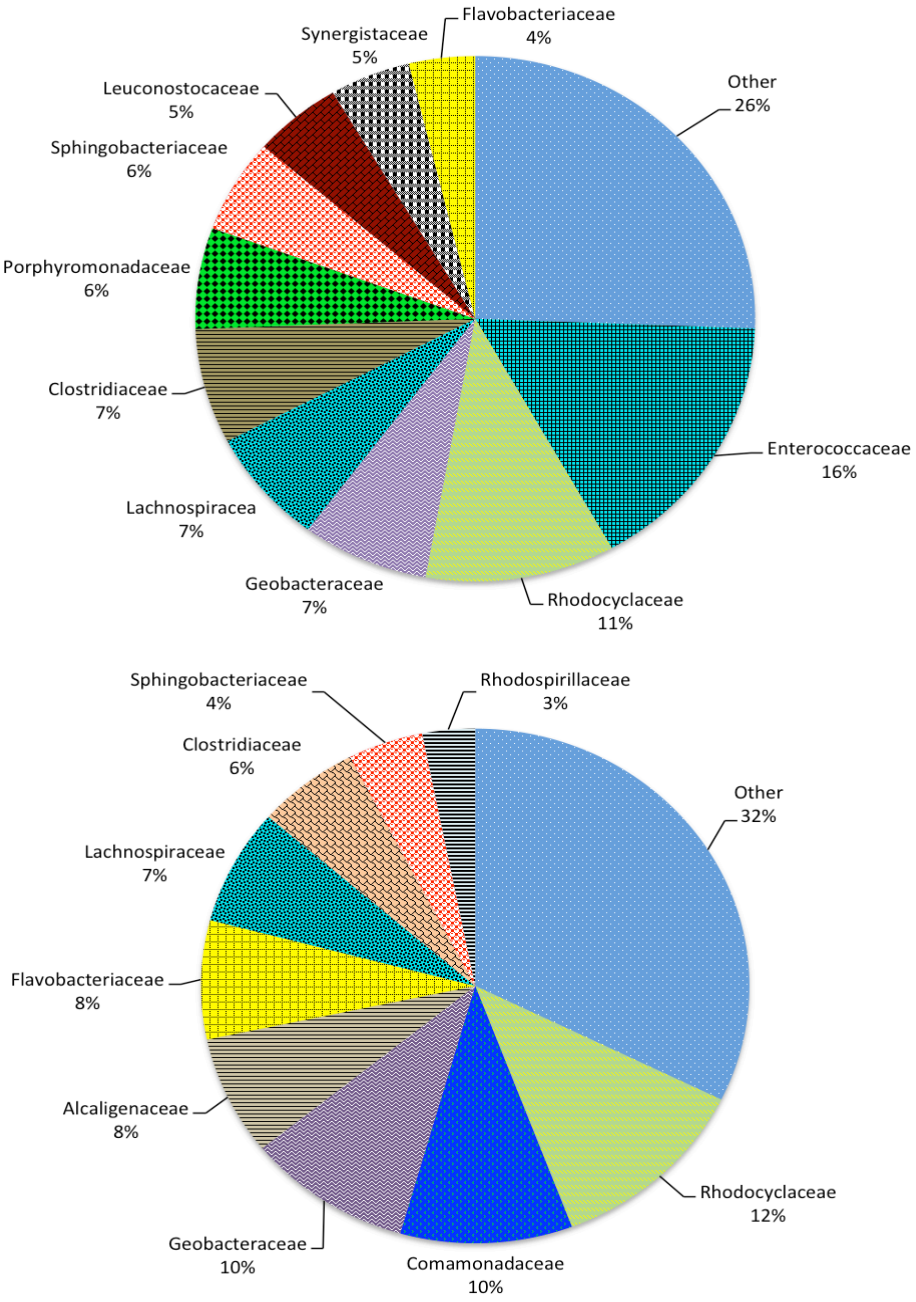

Figure 3: Characterization of anode microbial consortia via 16S rRNA analysis.

While these duplicate MFC's were treated identically, natural variation in the starting inoculum, which was a biofilm growing on carbon felt electrode core removed from other bioanodes, could be a reason for the differences. In addition to the common Geobacteraceae family known for electrogenic activity, Rhodocyclaceae has also been previously found in acetate-fed bioanodes and have also been linked to versatile metabolic capabilities including fatty acid and aromatic conversion [16,19]. The family Comamonadaceae has been found in cellulose-fed bioanodes and can also convert short-chain fatty acids and has been shown to be capable of electricity generation [20-22] . The family Enterococcaceae also contains known electrogens such as *Citrobacter freundii* and *Klebsiella oxytoca* [23]. The presence of a variety of microbes with differing capabilities and unclassified bacteria is likely the result of the complex substrate used in this study, since multiple studies have indicated the effect of carbon source on community development and the establishment of syntrophic interactions [7,24].

Batch operation

Investigations into hydrogen production with batch addition of boap resulted in an average hydrogen production rate of 1.28 ± 0.17 L H_2/L-anode-day (referred to as L/L-day henceforth) at a boap concentration of 0.1 g/L. Increasing the BOAP concentration increased the hydrogen productivity to 1.91 ± 0.47 L/L-day. This rate was an average obtained over a period of 8 -20 hours, depending on the BOAP concentration used. The current production during the MEC operation is shown in Figure 4. An average of four replicates is shown in Supplemental Figure 12 to demonstrate reproducibility. The initial current produced in the MEC during the first hour was in the range of 5-10 mA, depending on the boap concentration, which dropped to less than 1 mA over the duration of the experiment.

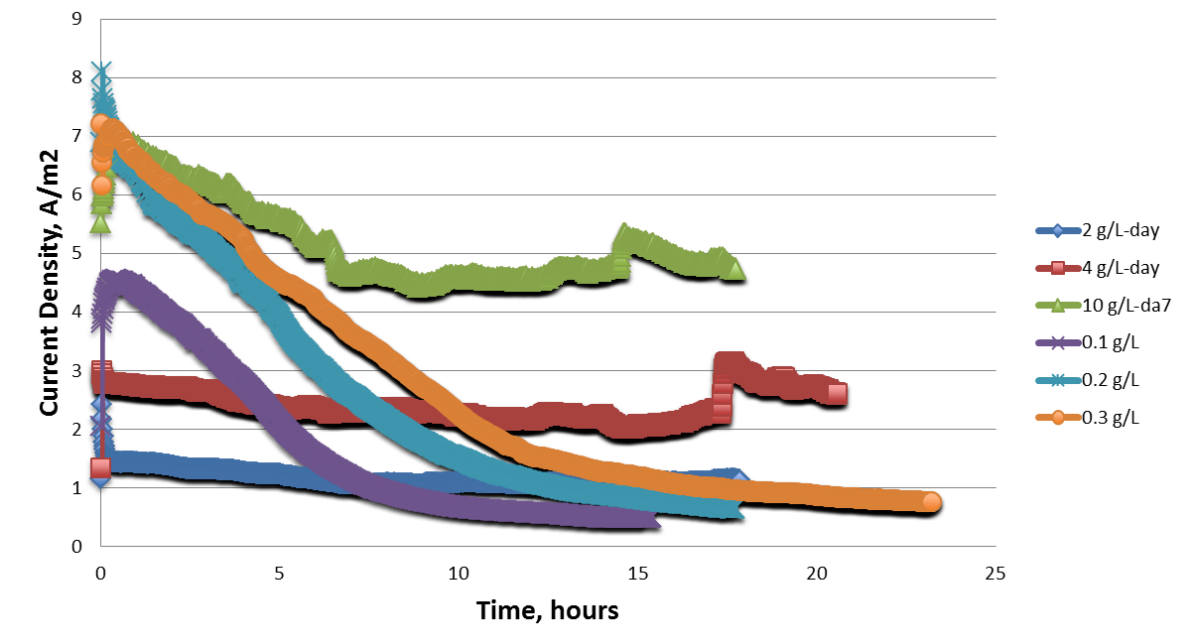

Figure 4: Current production profile during batch and continuous operation of MEC generating hydrogen from bio-oil aqueous phase (BOAP). The concentration of BOAP was varied from a COD of 0.1 to 0.3 g/L. In continuous experiment, the organic loading rate was inreased from 2 to 10 g/L-day resulting in a proportional increase in current production.

This shows that the initial rate of hydrogen production was much higher than the average. At a concentration of 0.3 g/L, the rate of hydrogen production in the first two hours was 9.3 L/L-day, but the average over the duration of the experiment was less than a fifth of the initial rate. Hydrogen collection was halted after the current dropped below 1 mA in all experiments. A replicate MEC (MEC B), operated under the same conditions resulted in a similar hydrogen production profile. The results are shown in Appendix Figure 10. The differences in the two replicates can be attributed to small differences in inoculum and unequal biocatalyst density during growth in the anode. The anode Coulombic efficiency (CE) for the MEC A ranged from 93 ± 1.7% at boap concentration of 0.1 g/L to 76 ± 3.1% at a concentration of 0.3 g/L. The results for the replicate (MEC B) as well as MEC A are shown in Figure 5a. The anode CE was calculated using COD of the samples before and after MEC treatment.

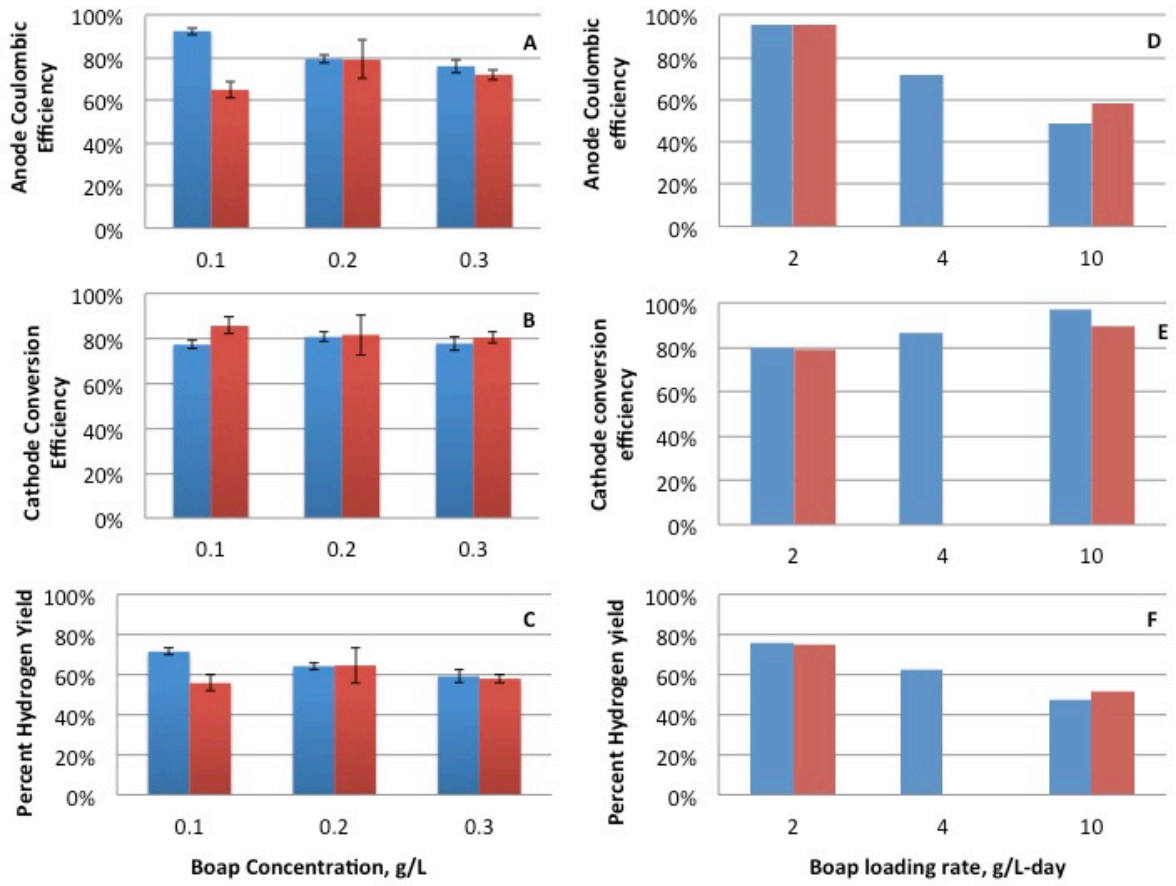

Figure 5: Batch substrate addition: (A) Anode Coulombic efficiency (B) cathode conversion efficiency (C) percent hydrogen yield. Continuous substrate addition: (D) Anode Coulombic efficiency (E) cathode conversion efficiency (F) percent hydrogen yield.

The cathode conversion efficiency ranged from 77 ± 3.4% to 81 ± 2.4% for MEC A and 81 ± 2.99% to 86 ± 7.6% for the duplicate, MEC B (Figure 5b). Thus, the BOAP concentration appears to have a negligible effect on the anode CE and cathode conversion efficiency. The percent hydrogen yield obtained at the three batch concentrations ranged between 56 ± 8.2% and 72 ± 1.8% (Figure 5c). Thus, the percent hydrogen yield also appears to be negligibly affected by BOAP concentration under batch conditions.

Continuous substrate addition

Effect of boap loading on MEC performance was assessed by changing the loading from 2 g/L-day to 10 g/L-day. The hydrogen production rate increased proportionally with the boap loading rate from 0.9 ± 0.06 to 4.3 ± 0.05 L/L-day as shown in Figure 11 in Appendix. The corresponding current density was 1.2 ± 0.1 A/m^2 to 4.5 ± 0.22 A/m^2, respectively. Compared to the batch run, the current production as well as hydrogen generation was relatively constant during the continuous addition experiment. The anode CE, cathode conversion efficiency and percent hydrogen yield are shown in Figure 5d-f. The anode CE decreased from 96 ± 0.2% at 2 g/L-day to 54 ± 6.5% at 10 g/L-day. The cathode conversion efficiency, on the other hand increased from 79 ± 0.7% at 2 g/L-day to 94 ± 5.5% at 10 g/L-day. The hydrogen yield, on the other hand, decreased from 76 ± 0.5% to 50 ± 3.2%, respectively.

Conversion of individual components of boap

In addition to determination of the total COD of boap, the samples were also analyzed by HPLC. It is observed that under batch conditions, more than 98% removal of acetic acid and furfural was achieved Figure 6.

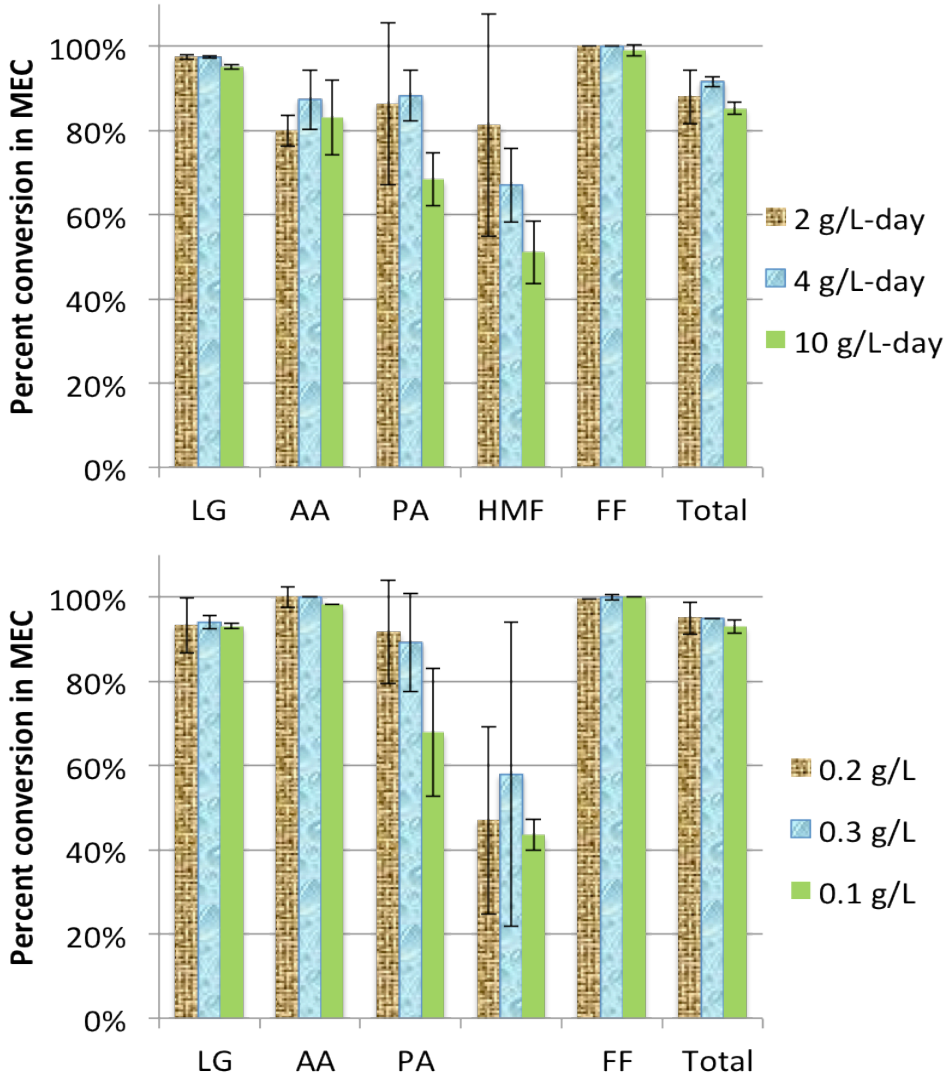

Figure 6: Extent of removal of key compounds from bio-oil aqueous phase via MEC. The column represented by 'Total' includes all peaks quantified by HPLC, which contribute 33% to the COD of BOAP. (LG – Levuglucosan, AA – Acetic acid, PA – Propionic acid, HMF – Hydroxymethylfurfural, FF – Furfural).

Conversion of propionic acid was between 67-100% and that of HMF was between 21-57%. The majority of the phenolic compounds were also removed. Based on all the peaks quantified by HPLC, a total reduction of 92-95% was observed, demonstrating significant conversion of the furan aldehyde and phenolic compounds present in boap as well. Under continuous boap addition experiments, similar results were obtained. This shows that the anode microbial community was very efficient in conversion of the organic acids, levoglucosan and furfural present in boap. A high level of conversion of the quantified phenolic compounds was also observed.This was evidenced by the reduction in the 'Total' percent reduction in Figure 5, which includes phenol, 1,2-benzenediol, vanillic acid, guaiacol and 2,6-dimethoxyphenol.

Energy efficiency

The electrical energy efficiency (EE) and overall energy efficiency for the conversion of boap into hydrogen are shown in Figure 7. Under batch conditions, the overall EE decreased from 58 ± 5.6% at a BOAP concentration of 0.1 g/L to 51 ± 3.3% at 0.3 g/L. The efficiency results provided are the average of the two replicate MECs. The electrical EE also decreased from 175 ± 11% to 149 ± 6%, respectively. Under continuous addition conditions, the efficiencies decreased with increasing loading rate as shown in Figure 7b.

Improvement in treatment of complex feed streams in MEC

In this study, the primary goal was to demonstrate the capability of microbial electrolysis systems to produce hydrogen from carbon/energy rich waste streams such as those resulting from biomass conversion platforms. A bioanode capable of efficiently converting a real-world, complex mixture of organic compounds was developed and its ability to remove major

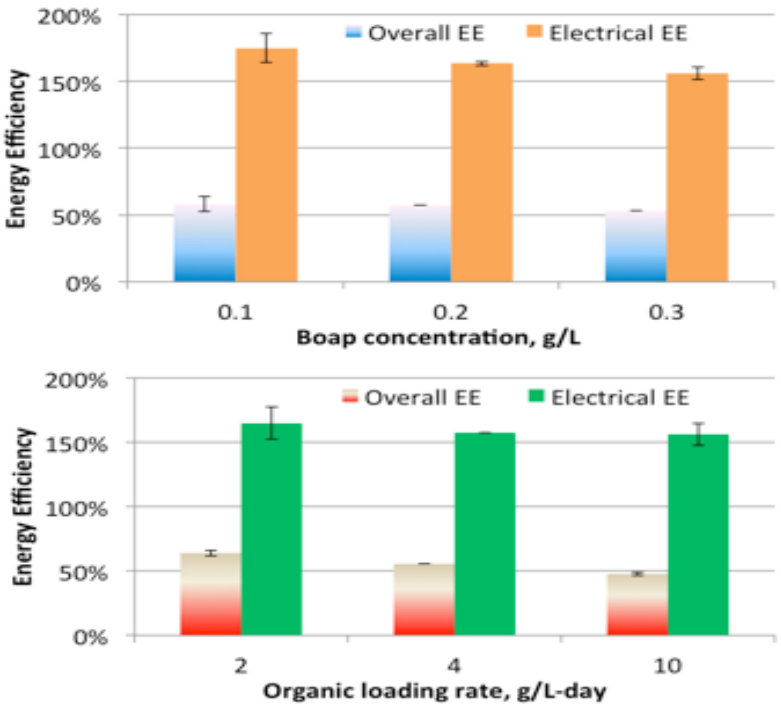

Figure 7: Electrical and overall energy efficiency (EE) obtained during batch (A) and continuous (B) substrate addition experiments.

compounds of interest within the mixture including corrosive and acidic compounds such as acetic acid and phenolic acids was demonstrated. The productivity of 4.3 L H_2/L-day achieved using the boap feedstock is the highest reported productivity for a complex substrate that we know of. Table 2 contains H_2 productivities and system information for MEC studies reported in the literature. Lu et al were able to achieve a productivity of 1.41 L/L-day using a post-fermentation effluent at an applied potential of 0.6 V in a single-chamber membraneless MEC [25]. Escapa et al. were able to achieve a similar productivity of 1.42 L/L-day at mucher larger anode volume > 200 ml using a synthetic fermentation effluent by altering the HRT and increasing the applied voltage to 1 V (Escapa et al., 2013). A common occurrence among other studies with lower output could be the lack of sufficient enrichment of the anode biocatalyst. It is our observation that in many other studies use of an anode with un-enriched inoculum or use of a

Table 2: Hydrogen production from complex substrates in MECs and key efficiency parameters. £ Continuous substrate addition conditions, * batch conditions.

Substrate	MEC Volume (ml)	System	Anode electrode	Cathode electrode	H2 productivity (LH2/L-day)	Applied voltage Eap (V)	Current Density		Coulombic Efficiency	Overall energy Efficiency	References
							A/m3	A/m2			
lignocellulose effluent	28	single	Graphite fiber brush	Carbon cloth/Pt (10% Pt/C)	1.00 ± 0.19	0.5	1.15		110%	61%	(Lalaurette et al., 2009)
Fermentation effluent	72	single	carbon fiber brush	Carbon cloth/Pt 0.5 mg/cm2	0.48	0.435			58%	23%	(Wang et al., 2011
Domestic wastewater	584	two	Carbon paper	Carbon paper/Pt 0.5 mg/cm2	0.154 LH2/g-COD	0.5		< 0.6	23%	9.90%	(Ditzig et al., 2007)
Swine wastewater	28	single	Graphite fiber brush	Carbon cloth/Pt 0.5 mg/cm2	0.9-1.0	0.5	106		29 ± 17% to 43 ± 2%	190 ± 39% (electrical)	(Wagner et al., 2009)
Fermentation effluent	26	single	Graphite brush	Carbon cloth/Pt 0.5 mg/cm2	1.41	0.6	135		87%	70%	(Lu et al., 2009)
A de-oiled refinery wastewater	5	single	Graphite plates	Stainless steel mesh (Type 304)	N/A	0.7		2.1			(Ren et al., 2013)
Industrial and Food processing wastewater	28	single	graphite fiber brush	Carbon cloth/Pt (10 wt% on Vulcan XC-72)	0.58 0.35	0.7		2.1 2.4	12% 35%	3.8 ± 0.2 −1.2 ± 0.2 kWh/kg-COD	(Tenca et al., 2013)
Potato wastewater	28	single	graphite fiber brush	Carbon cloth/Pt 0.5 mg/cm2	0.74	0.9	N/A		80%		(Kiely et al., 2011)
Winery wastewater	1000	single	graphite fiber brush	SS mesh	0.19 ± 0.04	0.9	7.4				(Cusick et al., 2011)
Milk, glycerol, starch	28	single	graphite fiber brush	graphite fiber cloth/Pt,5.0 mg Pt/cm2	0.94	0.8	150		50-70%		(Montpart et al., 2015)
Synthetic fermentation effluent	200	single	graphite felt	Ni-based gas diffusion	1.42	1.0	206			97%	(Escapa et al., 2013)
bio-oil aqueous phase	29.3	two	carbon felt	Carbon cloth/Pt 0.5 mg/cm2	4.3£ 2.5*	0.96 0.8	202 99		54% 79%	48% 60%	This Study

model substrate for enrichment and testing with the substrate of interest is practiced. Our experience has shown this is insufficient for developing a robust community needed for treating complex waste streams, and use of enrichment procedures as that developed in our laboratory for mixtures of various substrates can alter community structure to enhance the functional capabilities of degradation and electron transfer (Borole et al., JPS 2008; ChemElectroChem 2014). Our focus on bioanode enrichment using a patented enrichment process with a previously enriched inoculum over several months resulted in development of a community capable of converting a variety of compounds into electrons. The dominant phyla of Proteobacteria and Firmicutes in the bioanodes have well-established syntrophic interactions for conversion of a variety of carbon compounds, as well as the presence of known electrogenic families such as Geobacteraceae allow for the conversion of a variety of compounds with high CE [26,27]. Furthermore, our two-chamber system has been previously optimized relative to many other studies employing different designs such as H-type reactors, minimizing anode dead space and reducing electrode spacing, etc. (Borole et al., 2009b).

Additionally, where other studies commonly utilize an applied potential difference between anode and cathode, the use of a method setting anode potential at -0.2 V vs. Ag/AgCl reference electrode used in our study may have contributed to maintaining a steady, high bioanode performance. This method also allows the cell voltage to reach the 1 V range, but prevents the anode from reaching damaging positive potentials that can occur when setting a strict potential difference. The bioanode developed for this study also achieved high productivities of 12.4 L/L-day under continuous addition of acetic acid as a substrate (data not shown), even though this community has been enriched for a multi-substrate complex mixture and not pure acetic acid. Further growth of anode biofilm and utilization of alternate cathodes

can potentially improve the performance even higher.

Advancements in conversion efficiency and hydrogen yield

While there was some variation in values for anode Coulombic efficiency among batch experiments due to experimental run time, maximum CE and percent hydrogen yield reached values of 93% ± 1.7% and 81% ± 2.35% respectively. The volume of hydrogen produced over the length of the experiments varied from 9-54 mL depending on the type and rate of loading, reaching the highest value during 10 g/L-day of continuous boap addition. A reduction in both H_2 yield and CE was observed at the higher concentrations, but this reduction was much more pronounced for continuous addition experiments, where the average CE and H_2 yield reduced to 54% ± 6.5% and 54% ± 3.4% at 10 g/L-day, respectively. CE and H_2 yield tend to trend together as H_2 production is a direct function of the electrons and protons harvested from the anode, but H_2 yield values can be slightly lower due to system losses and proton diffusion. Conversely, COD removal increased in opposite fashion, reaching the highest percentage of 52% at 10 g/L-day boap. The increased COD removal and decreased CE and H_2 yield could be explained by higher activity of fermentative organisms in the anode due to increased substrate saturation at higher loading rates, contributing to COD removal without harvesting electrons and protons decreasing CE and H_2 yield. Maximum COD removal for batch studies was 48% ± 1.5% at 0.2 g/L boap. COD removal values were somewhat lower than those reported in the literature for other complex/wastewater streams. This is likely due to the complexity of compounds present in boap, many of which are recalcitrant and commonly inhibitory to many microbes. Additionally, the experiments were stopped when the current production reached below 1 mA, and not continued until the current production ceased, indicating potential for higher COD removal with

longer run times. Nonetheless, overall energy efficiency and electrical efficiency values were in the range of those reported for MEC studies, reaching values of 62% ± 0.67% and 167% ± 2.26% in batch studies.

One of the problems with bioanodes operated at high substrate concentration or loading rate is production of methane [28,29]. Absence of methane in the product gas and absence of archaea in the bioanode demonstrate the effective suppression of methanogenic population from bioanode developed in this study. Experiments conducted in continuous and batch mode of substrate addition further illustrate that even when high substrate loading was used, methane production did not occur. The efficiency of conversion of boap to hydrogen was similar in both modes of operation, further illustrating the advantages of the enrichment and MEC operational procedure employed [14,18].

Implications for biorefinery application

With continuing improvement in the ability to utilize significant portions of compounds present in many biorefinery waste streams at high efficiencies, microbial electrolysis systems have real potential for commercial integration into multiple biomass conversion platforms [5,6]. While commercial-scale pyrolysis technology is still being developed, making it difficult to predict the volume and composition of an aqueous-phase stream, a recent update at the Pacific Northwest National Laboratory (PNNL) estimates that a 2000 ton/day pyrolysis plant would require 1000 m^3 water/day, and produce approximately 1000 m^3 wastewater/day [30] . This high water demand coupled with high GHG emitting natural gas reforming for H_2 production makes microbial electrolysis an attractive alternative for continued development. The PNNL study also alludes to this, stating that alternative, sustainable forms of hydrogen will be necessary for

advancing the technology if they can be developed and made economically viable. Besides the pyrolysis platform, biomass to ethanol bioconversion and algal hydrothermal liquefaction are additional platforms that could be integrated with microbial electrolysis systems. A 2000 ton/day lignocellulosic biorefinery has the theoretical potential to generate 7200 m^3/hr of hydrogen, based on the assumption of 50% conversion efficiency and a biodegradability factor of 0.5 [31] . In order to continue the rapid improvement of bioelectrochemical systems to meet future commercial demands, expanded efforts in under-investigated areas of metagenomics and transcriptomics of anode communities along with development of sustainable cathode materials or biocathodes, will be required in addition to continued efforts in improving reactor design and performance.

Conclusion

An integrated pyrolysis-microbial electrolysis process for hydrogen production was demonstrated. The MEC demonstrated a productivity of 4.3 L H_2/L-day and a percent hydrogen yield of 50.4 ± 3.2% at a loading of 10 g COD/L-anode-day. A maximum anode Coulombic efficiency of 96 ± 0.21% and a maximum cathode conversion efficiency of 94 ± 5.5% were also achieved, albeit at different loading rates. Nearly complete conversion of acetic acid, propionic acid, levoglucosan and furfural was observed with an overall energy efficiency of 48-63%. The hydrogen produced from the integrated process can be used to hydrodeoxygenate bio-oil to make fuel, while reducing lifecycle greenhouse gas emissions.

References

1. Jones S, Valkenburg C, Walton C, et al. *Production of gasoline and diesel from biomass via fast pyrolysis, hydrotreating and hydrocracking: A design case.*: Pacific Northwest National Laboratory;2009. ONNL-18284 Rev.1.
2. Imam T, Capareda S. Characterization of bio-oil, syn-gas and bio-char from switchgrass pyrolysis at various temperatures. *Journal of Analytical and Applied Pyrolysis.* 2012;93:170-177.
3. Logan BE, Call D, Cheng S, et al. Microbial electrolysis cells for high yield hydrogen gas production from organic matter. *Environ. Sci. Technol.* Dec 2008;42(23):8630-8640.
4. Borole AP. Improving energy efficiency and enabling water recycle in biorefineries using bioelectrochemical cells. *Biofuels, Bioproducts & Biorefining.* 2011-09-29 2011;5(1):28-36.
5. Borole AP, Hamilton C, Schell D. Conversion of residual organics in corn stover-derived biorefinery stream to bioenergy via microbial fuel cells. *Environ Sci Technol.* 2013;47(1):642-648.
6. Borole AP, Mielenz J, Vishnivetskaya TA, Hamilton CY. Controlling accumulation of fermentation inhibitors in biorefinery water recycle using microbial fuel cells. *Biotechnol. Biofuels.* 2009;2(1):7.
7. Borole AP, Reguera G, Ringeisen B, Wang Z-W, Feng Y, Kim BH. Electroactive biofilms: Current status and future research needs. *Energy Environ. Sci.* 2011;4:4813-4834.
8. Sleutels T, Darus L, Hamelers HVM, Buisman CJN. Effect of operational parameters on Coulombic efficiency in bioelectrochemical systems. *Bioresource Technology.* Dec 2011;102(24):11172-11176.
9. Sleutels T, Ter Heijne A, Buisman CJN, Hamelers HVM. Bioelectrochemical Systems: An Outlook for Practical Applications. *Chemsuschem.* Jun 2012;5(6):1012-1019.
10. Ichihashi O, Vishnivetskaya T, Borole AP. High-Performance Bioanode Development for Fermentable Substrates via Controlled Electroactive Biofilm Growth. *ChemElectroChem.* 2014;1(11):1940-1947.
11. Kim P, Johnson A, Edmunds CW, et al. Surface functionality and carbon structures in lignocellulosic-derived biochars produced by fast pyrolysis. *Energy & Fuels.* 2011;25(10):4693-4703.
12. Borole AP, LaBarge S, Spott B. Three-dimensional, gas-phase fuel cells with a laccase biocathode. *J. Power Sources.* March 15, 2009 2009;188(2):421-426.
13. Borole AP, Inventor; UT-Battelle, assignee. Microbial fuel cell with improved anode, US Patent 7,695,8342010.
14. Borole AP, Hamilton CY, Vishnivetskaya TA, et al. Integrating engineering design improvements with exoelectrogen enrichment process to increase power output from microbial fuel cells *J. Power. Sources.* June 15, 2009 2009;191(2):520-527.
15. Nam J-Y, Tokash JC, Logan BE. Comparison of microbial electrolysis cells operated with added voltage or by setting the anode potential. *International Journal of Hydrogen Energy.* 2011;36(17):10550-10556.
16. Borole AP, Hamilton CY, Vishnivetskaya TA, Leak D, Andras C. Improving power

production from acetate-fed microbial fuel cells via enrichment of exoelectrogenic organisms in continuous flow systems. *Biochem. Eng. J.* 2009;48:71-80.
17. Lide DR. CRC Handbook of Chemistry and Physics, 76th ed. Boca Raton: CRC Press, Inc; 1995.
18. Borole AP, Hamilton CY, Vishnivetskaya TA. Enhancement in energy conversion efficiency and current density of 3-dimensional MFC anodes using pre-enriched consortium and continuous supply of electron donors. . *Bioresour. Technol.* 2011;102(8):5098-5104.
19. Hesselsoe M, Füreder S, Schloter M, et al. Isotope array analysis of Rhodocyclales uncovers functional redundancy and versatility in an activated sludge. *The ISME journal.* 2009;3(12):1349-1364.
20. Rismani-Yazdi H, Christy AD, Dehority BA, Morrison M, Yu Z, Tuovinen OH. Electricity generation from cellulose by rumen microorganisms in microbial fuel cells. *Biotechnol Bioeng.* Aug 2007;97(6):1398-1407.
21. Xing DF, Cheng SA, Logan BE, Regan JM. Isolation of the exoelectrogenic denitrifying bacterium Comamonas denitrificans based on dilution to extinction. *Applied Microbiology and Biotechnology.* Feb 2010;85(5):1575-1587.
22. Xing DF, Zuo Y, Cheng SA, Regan JM, Logan BE. Electricity generation by Rhodopseudomonas palustris DX-1. *Environ. Sci. Technol.* Jun 2008;42(11):4146-4151.
23. Sun Y, Zuo J, Cui L, Deng Q, Dang Y. Diversity of microbes and potential exoelectrogenic bacteria on anode surface in microbial fuel cells. *The Journal of general and applied microbiology.* 2010;56(1):19-29.
24. Pant D, Van Bogaert G, Diels L, Vanbroekhoven K. A review of the substrates used in microbial fuel cells (MFCs) for sustainable energy production. *Bioresource Technology.* Mar 2010;101(6):1533-1543.
25. Lu L, Ren NQ, Xing DF, Logan BE. Hydrogen production with effluent from an ethanol-H-2-coproducing fermentation reactor using a single-chamber microbial electrolysis cell. *Biosensors & Bioelectronics.* Jun 2009;24(10):3055-3060.
26. Freguia S, Teh EH, Boon N, Leung KM, Keller J, Rabaey K. Microbial fuel cells operating on mixed fatty acids. *Bioresource Technology.* 2010;101(4):1233-1238.
27. Kiely PD, Cusick R, Call DF, Selembo PA, Regan JM, Logan BE. Anode microbial communities produced by changing from microbial fuel cell to microbial electrolysis cell operation using two different wastewaters. *Bioresource Technology.* 2011;102(1):388-394.
28. Escapa A, Lobato A, Garcia DM, Moran A. Hydrogen production and COD elimination rate in a continuous microbial electrolysis cell: The influence of hydraulic retention time and applied voltage. *Environmental Progress & Sustainable Energy.* Jul 2013;32(2):263-268.
29. Ishii S, Hotta Y, Watanabe K. Methanogenesis versus electrogenesis: Morphological and phylogenetic comparisons of microbial communities. *Biosci Biotechnol Biochem.* Feb 2008;72(2):286-294.
30. Jones S, Meyer P, Snowden-Swan L, et al. *Process design and economics for conversion of lignocellulosic biomass to hydrocarbon fuels*: PNNL;2013. PNNL-23053, NREL/TP-5100-61178.
31. Borole AP, Mielenz J. Estimating hydrogen production potential in biorefineries using

microbial electrolysis cell technology *Intl J. Hydrogen Energy.* 2011;36(22):14787-14795.

Appendix

Table 3: Identified compounds in crude bio-oil and aqueous phase by GC/MS

Categories	Compounds	Crude oil	Extracted by ethyl lactate	Extracted by chloroform	Categories	Compounds	Crude oil	Extracted by ethyl lactate	Extracted by chloroform
Acids	Acetic acid	X			Ketones	1-Hydroxy-2-butanone	X	X	X
	propionic acid	X				2-Cyclopenten-1-one, 3-methyl-	X	X	X
	Succinic acid, methyl-	X				Cyclohexanone	X	X	X
	vanilic acid	X	X			2-Butanone, 3,3-dimethyl-	X	X	X
	Benzoic acid, 3-hydroxy-4-methyl-	X				2-Cyclopenten-1-one, 3-ethyl-2-hydroxy-	X	X	X
Alcohols	1,3-Propanediol	X	X			Cyclohexanone, 4-hydroxy-	X	X	
	1,3-Propanediol, 2-(hydroxymethyl)-2-methyl-	X				2,5-Cyclohexadiene-1,4-dione, 2-methyl-5-(1-methylethyl)-	X		X
	3-Hexanol, 2,4-dimethyl-	X			PAHs	Anthracene	X		
	Cyclodecanol	X	X	X		Pyrene	X		
	3-Cyclobutene-1,2-dione, 3,4-dihydroxy-	X	X	X	Phenolics	Phenol	X	X	X
	1,2-Cyclopentanedione, 3-methyl-	X	X	X		Phenol, 3-methyl-	X	X	
	5-Isopropenyl-2-methylcyclohexanol	X				Phenol, 2-methyl-	X	X	

Table 3 Continued

	Categories	Compounds	Crude oil	Extracted by ethyl lactate	Extracted by chloroform	Categories	Compounds	Crude oil	Extracted by ethyl lactate
	Cyclohexanol, 2,3-dimethyl-	X	X	X		Phenol, 2-methoxy-	X	X	X
	4-Cyclopentene-1,3-diol, trans-	X				Phenol, 3-ethyl-	X	X	X
	3-Nonyn-1-ol	X				Phenol, 3-(1-methylethyl)-	X		
	2-Hexen-1-ol, 2-ethyl-	X	X	X		1,2-Benzenediol	X	X	X
	Cyclododecanol	X	X			Phenol, 2-methoxy-4-methyl-	X	X	
	Bicyclo [3.1.1] hept-3-en-2-ol, 4,6,6-trimethyl-	X	X			Phenol, 2,3,5,6-tetramethyl-	X		
	Cyclohexanol, 2-methyl-5-(1-methylethenyl)-	X	X	X		Phenol, 4-ethyl-2-methoxy-	X	X	X
	1-Cyclohexene-1-methanol, 4-(1-methylethenyl)-	X				2(1H)-Naphthalenone, octahydro-, trans-	X		
Aldehyde	2-Furaldehyde, 5-methyl-	X	X	X		Phenol, 2-methoxy-5-(1-propenyl)-, (E)-	X	X	X
	5-Methyl-2-hexanone	X	X			Phenol, 2,6-dimethoxy-	X	X	X
	1-Cyclohexene-1-acetaldehyde, 2,6,6-trimethyl-	X	X	X		Benzaldehyde, 3-hydroxy-4-methoxy-	X	X	X

Table 3 Continued

Categories	Compounds	Crude oil	Extracted by ethyl lactate	Extracted by chloroform	Categories	Compounds	Crude oil	Extracted by ethyl lactate	Extracted by chloroform
Esters	Butyric acid, 3-methyl-, allyl ester	X				1,2,3-Trimethoxybenzene	X	X	X
	Benzoic acid, 4-hydroxy-3-methoxy-, methyl ester	X	X	X		1,4-Benzenediol, 2-(1,1-dimethylethyl)-	X	X	X
	2-Octynoic acid, methyl ester	X	X	X		Benzene, 1,2,3-trimethoxy-5-methyl-	X	X	
	p-Menth-8-en-2-ol, acetate	X				Phenol, 2,6-dimethoxy-4-(2-propenyl)-	X	X	X
	Pentanoic acid, 4-methyl-, ethyl ester	X				Benzaldehyde, 2,4,5-trimethoxy-	X	X	X
Furans	Furfural	X	X	X	Sugars	d-Mannitol, 1,4-anhydro-	X	X	
	2(5H)-Furanone	X	X	X		1,6-Anhydro-.beta.-D-glucopyranose (levoglucosan)	X		
	2(5H)-Furanone, 5-methyl-	X	X						
	Benzofuran, 2,3-dihydro-	X	X	X					

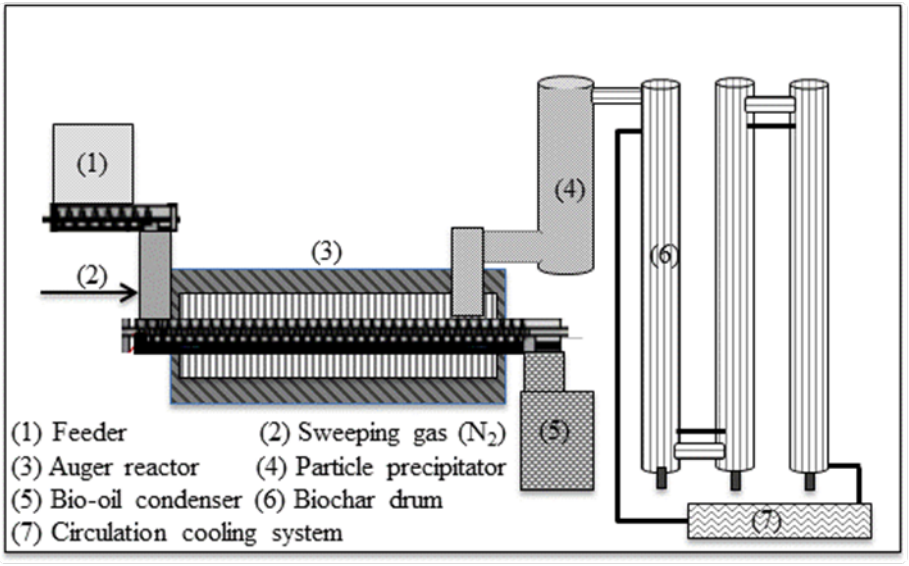

Figure 8: Semi pilot-scaled auger pyrolysis system

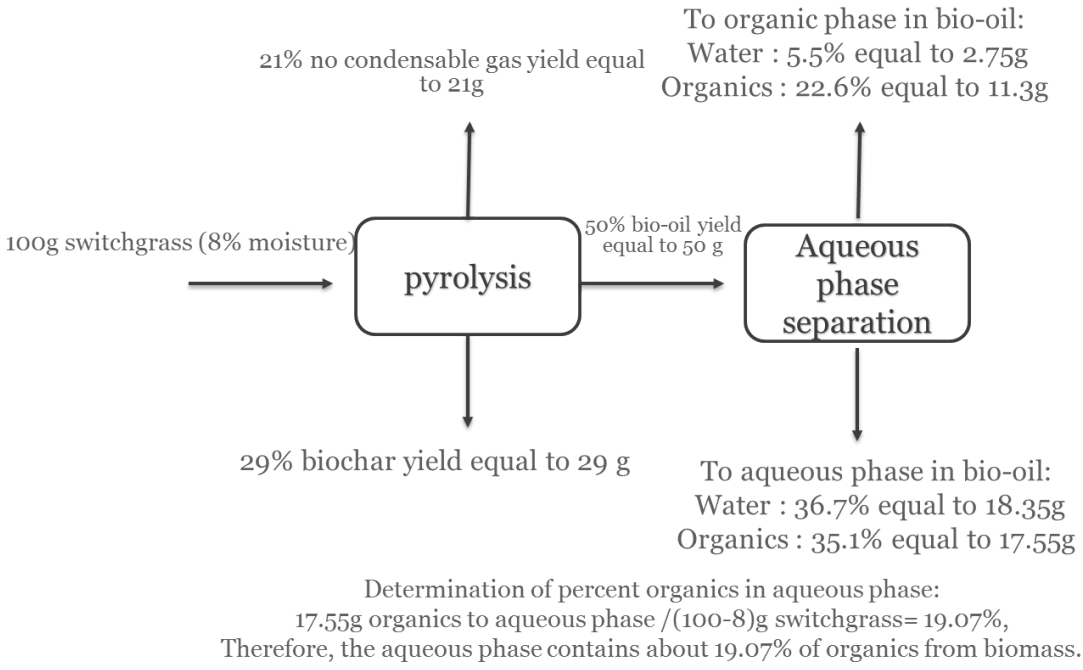

Figure 9: Distribution of products resulting from pyrolysis and after fractionation of bio-oil via addition of water.

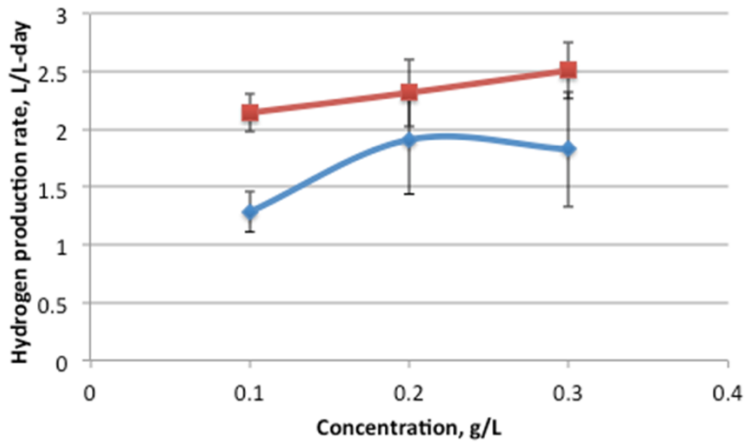

Figure 10: The effect of BOAP concentration on rate of hydrogen production during batch operation.

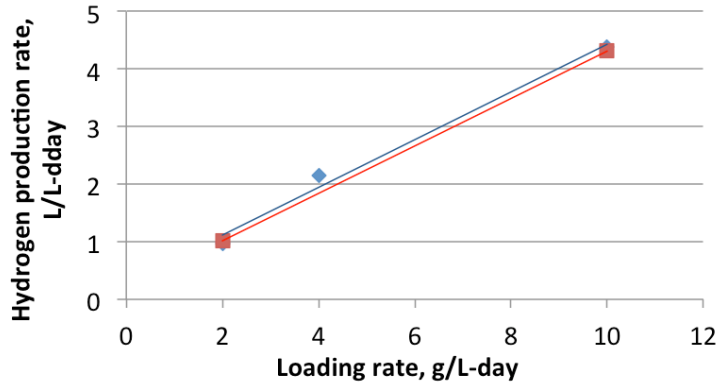

Figure 11: Effect of BOAP loading rate on hydrogen production during continuous addition experiment.

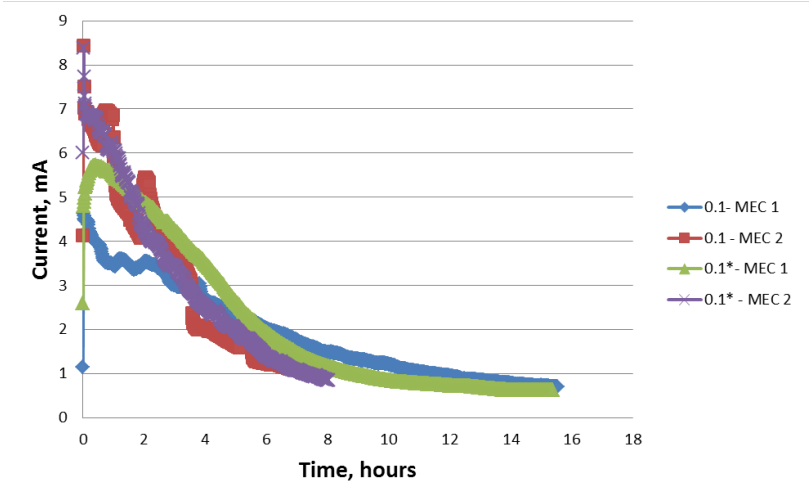

Figure 12: Current production profile during batch operation of MEC generating hydrogen from bio-oil aqueous phase (BOAP) at a COD concentration of 0.1 g/L.

CHAPTER II

UNDERSTANDING THE IMPACT OF FLOW RATE AND RECYCLE ON THE CONVERSION OF A COMPLEX BIOREFINERY STREAM USING A FLOW-THROUGH MICROBIAL ELECTROLYSIS CELL

This chapter was originally published by:

Lewis AJ, Borole AP. Understanding the impact of flow rate and recycle on the conversion of a complex biorefinery stream using a flow-through microbial electrolysis cell. *Biochem Eng J*. 2016;116:95-104. doi:10.1016/j.bej.2016.06.008.

No alterations were made to the published article for inclusion in the dissertation. All experiments and analysis utilizing BOAP in the microbial electrolysis cell (MEC), were carried out by AJL as well the writing of this manuscript. APB provided guidance and feedback on experimental design, analysis, and manuscript preparation.

Abstract

The effect of flow rate and recycle on the conversion of a biomass-derived pyrolysis aqueous phase in a microbial electrolysis cell (MEC) were investigated to demonstrate production of renewable hydrogen in biorefinery. A continuous MEC operation was investigated under one-pass and recycle conditions using the complex, biomass-derived, fermentable, mixed substrate feed at a constant concentration of 0.026 g/L, while testing flow rates ranging from 0.19 to 3.6 mL/min. This corresponds to an organic loading rate (OLR) of 0.54 to 10 g/L-day. Mass transfer issues observed at low flow rates were alleviated using high flow rates. Increasing the flow rate to 3.6 mL/min (3.7 min HRT) during one-pass operation increased the hydrogen productivity 3-fold, but anode conversion efficiency (ACE) decreased from 57.9% to 9.9%. Recycle of the anode liquid helped to alleviate kinetic limitations and the ACE increased by 1.8-fold and the hydrogen productivity by 1.2-fold compared to the one-pass condition at the flow rate of 3.6 mL/min (10 g/L-d OLR). High COD removal was also achieved under recycle

conditions, reaching 74.2 ±1.1%, with hydrogen production rate of 2.92 ± 0.51 L/L-day. This study demonstrates the advantages of combining faster flow rates with a recycle process to improve rate of hydrogen production from a switchgrass-derived stream in the biorefinery.

Introduction

Production of drop-in fuels from biomass requires deoxygenation of the biomass, since it contains over 35% oxygen by weight [1]. Hydrogen generated via steam reforming of natural gas is a typical reductant for this process. Renewable hydrogen generated from biomass has potential to reduce greenhouse gas emissions to mitigate climate change. Microbial electrolysis is one such method to generate hydrogen for biorefinery application [2,3]. Conversion of switchgrass to hydrogen was recently demonstrated using microbial electrolysis cells (MECs) [4]. The process involved pyrolysis of switchgrass to generate bio-oil and an associated aqueous stream rich in carbon, which was used as a feed for microbial electrolysis. The process generates an organic phase which serves as a feedstock for biofuel production using hydrogen generated via microbial electrolysis. Application of the combined pyrolysis-microbial electrolysis process in biorefineries requires further understanding of the influence of process and operating conditions on hydrogen production.

Several MEC configurations and process conditions have been studied for improving performance and conversion of waste streams into hydrogen. Integration of MECs into biorefineries may require development of continuous systems rather than batch systems to supply a steady stream of hydrogen for the hydrodeoxygenation reaction. Continuous MEC operation has been investigated previously for municipal wastewater treatment [5-7], winery wastewater [8], as well as MECs using model substrates [9-11]. Typical parameters studied for quantifying and

understanding performance of continuous MECs include hydraulic retention time (HRT) and organic loading rate (OLR), which depend on flow rate and substrate concentration. However, the number of reports investigating these effects for complex substrates in continuous systems are limited. Typical HRTs for MEC range from a few hours to a day or more. Increasing the HRT has been reported to affect the hydrogen production rate as well as the efficiency of hydrogen production with mixed results [5,12]. The effect of OLR on bioanode efficiency and productivity has also been studied [6,13], but primarily in microbial fuel cells (MFCs) [14-17]. The current output usually increases with increasing OLR, however, the coulombic efficiency, hydrogen recovery, and cathode efficiency can vary depending on other operational parameters. The type of substrate also makes a significant difference in the performance of the MEC. Use of fermentable substrates vs those which can be used directly by exoelectrogens, such as acetate, can lead to variations in performance depending on MEC design and operating conditions [6]. The effect of OLR and HRT on MEC performance is not well understood. The HRT, OLR and substrate concentration are inter-related and cannot truly be studied independently, as is typically done. For example, to reach a desired OLR either the HRT/flow rate of the system or the concentration of the feed has to be altered. Thus, when studying the effect of different OLR's, one of the other two variables will also be changing, so, only two of the three variables can be studied independently, while the third remains a dependent variable. Furthermore, the use of complex substrates or wastewater containing fermentable substrates as feed can significantly complicate these effects [5,6]. Understanding the influence of these operational parameters in MECs treating complex substrates requires insights into the mechanistic details of the process. The contribution of exoelectrogenic vs. fermentative and other accompanying biochemical reactions occurring in the MEC, as well as the kinetics and mass transfer issues underlying the

processes have to be evaluated to provide a better understanding of the effects on MEC performance.

In this study, we investigate the effect of flow rate, which defines HRT and OLR at a given substrate concentration. We examine the effect of these variables on MEC performance treating a complex, biomass-derived pyrolysis aqueous phase [4], but is applicable to any complex wastewater stream. This is important for generation of hydrogen in the biorefinery, since it can allow upgrading of bio-oil to biofuels without the need for external hydrogen. Identifying the operating conditions to maximize hydrogen production is critical, so we investigated the effect of anode fluid recycle on MEC performance operated under continuous flow conditions using two continuously-fed, replicate MECs.. Our goal was to understand the performance of MECs fed with complex substrates such as bio-oil aqueous phase (BOAP) and development of continuous systems for application in the biorefinery.

Methods

MEC construction and experimental set up

Two microbial electrolysis cells were constructed using carbon felt as anode material and Pt-deposited carbon as the cathode material (Figure 13). A carbon rod and stainless steel wire were used as current collectors, respectively, along with Nafion 115 as the separating membrane between the two electrode chambers. The anode and cathode volume were 16 mL each, while the projected area was 12.56 cm^2. The cathode buffer was 100 mM potassium phosphate. Additional details of the MEC construction are given elsewhere [4]. The MECs were operated in a continuous flow mode to study the effect of flow rate and substrate concentration on hydrogen production.

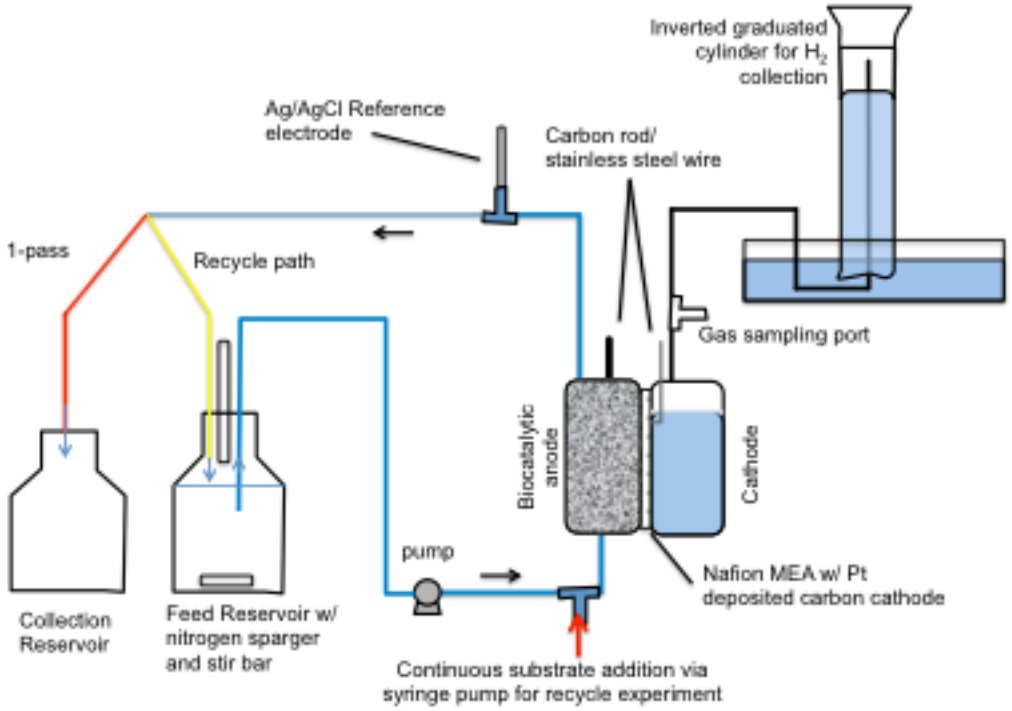

Figure 13: Schematic of MEC system investigating hydrogen production under one-pass and recycle conditions. Substrate was added directly into the feed reservoir for the one-pass condition, while it was added via the syringe pump into the flow line achieving the same OLR for the recycle condition.

Feedstock preparation for bioanode development

The substrate fed into the MEC anode was an aqueous portion of pyrolysate or bio-oil aqueous phase (BOAP) derived from switchgrass. The biomass was pyrolyzed in semi pilot augur reactor system, utilizing a residence time of 72 seconds at 500 °C to produce a bio-oil, which was then separated into an organic and aqueous phase by addition of deionized water (Oil:water ratio = 1:4) [4,18]. The chemical oxygen demand of the BOAP generated through the process was 130 g/L. The main compounds within BOAP consist of organic acid, furans, and phenolic compounds, with more detail information provided in the Appendix Table 5. The primary compounds include levoglucosan, acetic acid, hydroxymethylfurfural (HMF), 2-furfural,

vanillic acid, 2-methoxyphenol, 3-ethylphenol, etc [4,18]. The concentrated BOAP was diluted prior to use in order to minimize any additional effects of overloading and was fed into the MEC at different loading rates ranging from 0.54 to 10 g/L-day.

The MEC's used in this study were established and operated for ~ one year prior to the experiments reported here. The anodes were inoculated from a set of reactors previously acclimated to BOAP to create a new set of duplicate reactors, MEC-A and MEC-B. Furthermore, replicate experiments were conducted in each reactor, producing 4 sets of data for each condition. Results are reported either as average of two replicates with data shown for each of the two MECs or as average of all 4 runs. The error bars describe the method of averaging. A minimal nutrient salt medium containing Wolf's mineral and vitamin solutions was used as reported previously [4]. Glucose was provided as a supplemental carbon source for growth of the biofilm in addition to BOAP during start-up. It was mixed with BOAP and fed continuously into the anode. The glucose concentration was gradually reduced from 50% at the initial loading of 1 g/L-d to 0% (100% BOAP) at the highest loading of 10 g/L-d. Cyclic voltammetry was carried out every 1-2 weeks with a batch addition of 0.1 g/l glucose and 0.1 g/l BOAP separately to assess growth, current output, and BOAP utilization over the first two months of operation. During the period of 2-10 months post inoculation, the reactors were operated in both MFC and MEC modes. Prior to the beginning of this study, the reactors had been operated under only MEC conditions for the past 2 months using BOAP as the only substrate, with the anode poised at -0.2 V vs Ag/AgCl reference electrode. While additional experiments prior to this study did see the reactors reach loading of 10 g/L-d, long-term operation was limited to 2 g/L-d to avoid excess growth of non-exoelectrogens. However, the MECs were operated intermittently under batch conditions of concentration between 0.1 and 0.5 g/L BOAP, prior to this study, which may

have resulted in growth of non-exoelectrogenic organisms and methanogens.

One-pass and recycle operation

The MECs were investigated via chronoamperometry by poising the anodes at -0.2 V vs Ag/AgCl reference electrode. Hydrogen production was studied under two process conditions with continuous substrate addition: a one-pass operation and a recycle operation. The one-pass operation consisted of continuous flow of anode fluid from a feed reservoir containing BOAP through the MEC, with the effluent collection in separate container. During the recycle operation, the anode liquid was continuously recycled to and from the feed reservoir and the BOAP substrate was added via a syringe using a concentrate into the flow line entering the anode as shown in Figure 1. A constant BOAP concentration of 0.026 g /L was maintained in the flow line entering the anode for the majority of one-pass and recycle experiments to test the effect of flow rate on current and hydrogen production. For one-pass operation, the MEC's were operated at different flow rates ranging from 0.19 mL/min to 3.6 mL/min, corresponding to an HRT of 70.6 to 3.7 min. The corresponding OLR ranged from 0.54 g/L-d to 10 g/L-d. For recycle operation, the range was slightly narrowed to 0.3 mL/min to 3.6 mL/min. Figure 14A shows the operating variables and the corresponding operational times for the various conditionsFigure 14B shows the resulting OLR and HRT corresponding to the operational conditions. The order of execution of the experiments was dictated by the time frame of the experiments, which were scheduled to maximize the number of experiments that could be run while facilitating sampling and operational changes. The conditions for the recycle experiments are shown in Figure 14C-D. An additional experiment was carried out at higher concentration of 0.3 g/L at a flow rate of 0.3 mL/min, which served to compare high and low flow rates across the the same loading rate of 10

g/L-d with one-pass and recycle. Prior to the start of each experiment, circulation of media and substrate were stopped to allow current output to decrease to the baseline level, while media was replaced and flushed from the lines, as well as through the anode. The cathode buffer was also replaced between experiments, except for those with short time frames where current output and hydrogen production would not likely result in pH changes (based on previous experimental observations). Anodes remained poised at -0.2 V vs Ag/AgCl at all times, even between experiments, so hydrogen measurements and current outputs were tracked upon re-starting flow of substrate for a specific condition. A Reference 3000 potentiostat/galvanostat/zero resistance ammeter (Gamry Instruments, Warminster PA) was used for all the experiments. Depending on the flow rate used for one-pass operation, most experiments were allowed to run between 4-24 h. A volume of 100 mL was used in the reservoir for recycle experiments.

Analysis and calculations

At the end of each run, the volume displaced by hydrogen production was measured and gas samples for GC analysis were taken from the cathode outlet to confirm hydrogen production. Liquid samples were taken for high performance liquid chromatography (HPLC) analysis from the external anode reservoir for the recycle experiments and from the effluent collector for the one-pass experiments. A Jasco 2000Plus (Jasco analytical instruments) equipped with PU-2089S Plus pump, a MD-2018 Plus Photodiode Array detector (PDA), a RI-2031 Plus intelligent RI detector, and an AS-2055 Plus auto sampler was used to analyze HPLC samples for individual compound conversion. The liquid chromatography was conducted at 50.0°C using Bio-rad HPX-87H (300 x 8 mm) column with an injection volume of 20µl. The mobile phase was 5mM H_2SO_4 with a flow rate of 0.6 mL/min.

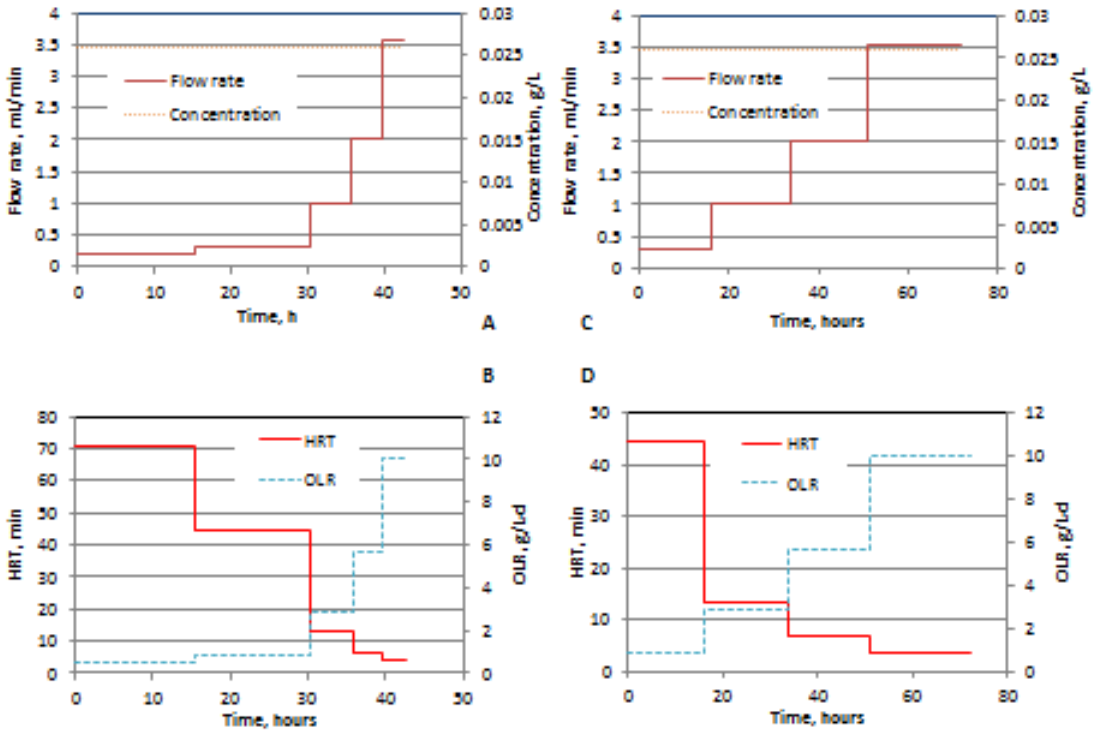

Figure 14: Experimental conditions and operating parameters tested during MEC operation. (A) Range of BOAP concentration and flow rate employed during one-pass operation, (B) OLR and HRT corresponding to one-pass operation, (C) Range of BOAP concentration and flow rate employed during recycle operation, (D) OLR and HRT corresponding to recycle operation.

COD analysis was also conducted to measure the extent of overall BOAP conversion. 2 mL samples were added to Hach HR COD (20-1500 mg/L COD) vials and digested in a Hach DRB 200 reactor at 150 °C for 2 hours. Digested samples were allowed to cool to room temperature and analyzed on Spectronic 20 Genesys with absorbance readings taken at 620 nm.

Performance and conversion efficiency were characterized by anodic conversion efficiency (ACE), cathodic conversion efficiency (CCE), hydrogen efficiency (HE), hydrogen recovery (HRE), Coulombic efficiency (CE). ACE and HE are additional parameters based on the total substrate provided, and not on the COD that was removed. The formulas for ACE and CE are very similar, with CE using (n_s) for moles of substrate removed and ACE uses the total COD added to the anode represented by (n_T).

$$CE/ACE \quad = \frac{I_{obs}t}{(n_s \; or \; n_T)n_eF}$$

where I_{obs} is the current produced, n_e is the number of electrons available per mol of substrate based on complete conversion to CO_2 , F: Faraday constant, and t is the duration of the experiment. HRE and HE equations are altered similarly, with HRE using (ΔnCOD) for moles of COD removed and HEusing total COD added to the system (tCOD).

$$HRE/HE = \frac{PV_{H2}/RT}{2\;(\Delta nCOD \; or \; tCOD)}$$

The other variables consist of (P) for the atmospheric pressure, (V_{H2}) is the volume of hydrogen produced, (R) is the gas constant, (T) is the temperature in Kelvin. Cathode conversion was calculated as previously described, and is based on the ratio of hydrogen produced vs the theoretical amount that could be produced based on the average current generated over the length of the experiment [4,10].

Results and Discussion

Hydrogen production from switchgrass bio-oil aqueous phase

BOAP contains a wide spectrum of compounds such as phenolics, furans, and organic acids, resulting from the thermochemical pyrolytic conversion of lignocellulosic biomass . Our previous study demonstrated the ability to produce hydrogen from these compounds using switchgrass-derived BOAP via microbial electrolysis [4,18]. This current work set out to study a continuous MEC process and to identify the effect of flow rate on MEC performance. The results reported previously [4] only included operation under recycle conditions at a set flow rate of 3.6 mL/min, demonstrating an increase in current with increasing OLR up to the highest level tested of 10 g/L-d. This work expands the investigations to one-pass, continuous operation, at different flow rates, but at a constant feed concentration of 0.026 g/L. The hydrogen productivity for one-pass operation increased with increasing flow rate, but plateaued at a flow rate of 2 mL/min as shown in Figure 15, reaching 1.41 ± 0.14 L-H_2/L-anode volume-day (referred to as L/L-day, henceforth). Hydrogen production under recycle conditions, also studied at different flow rates, resulted in a continued increase up to the highest flow rate studied, reaching a maximum of 2.92 ± 0.51 L/L-d at 3.6 mL/min. This is an improvement in the rate of hydrogen production by 107% compared to the one-pass condition. The effects of the operating conditions on anode and cathode processes leading to this improvement in hydrogen productivity are discussed below. The reproducibility of the MEC performance in the two replicate MECs (A and B) was remarkable with an average coefficient of variation of 6.57% for hydrogen productivity across the recycle experiments.

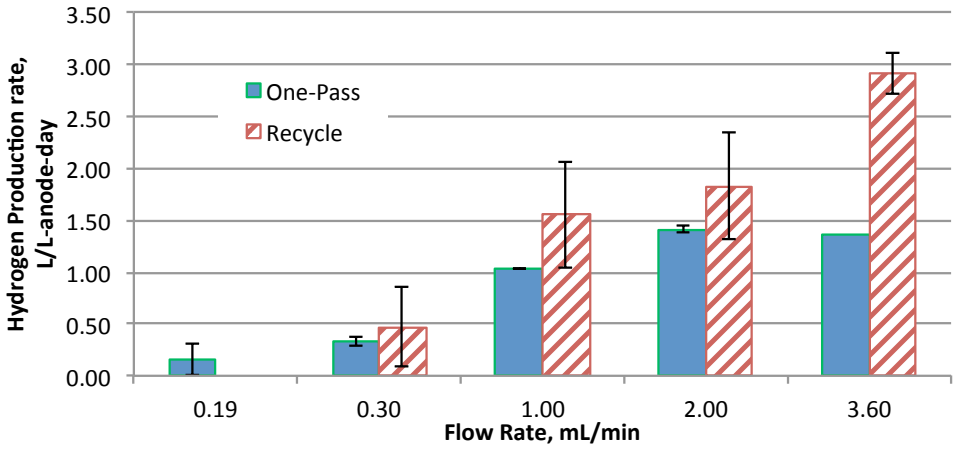

Figure 15: Rate of hydrogen production as a function of flow rate. The error bars represent standard deviation for two duplicate reactors.

Effect of Flow rate on current density and efficiency during one-pass operation

The effect of flow rate on MEC performance was evaluated over ~19-fold range. With BOAP concentration held constant at 0.026 g/L, this corresponds to an OLR range of 0.54 to 10 g/L-d. Two replicate reactors were used, MEC-A and MEC-B, which performed with similar results. Referring to MEC-A, as the flow rate was increased from 0.19 to 3.6 mL/min, the average current density increased from 0.44 A/m^2 ± 0.04 to 1.46 A/m^2 ± 0.11. While the current density increased with flow rate, the anode conversion efficiency (ACE, current yield as a function of substrate provided) followed a reverse trend for the most part as shown in Figure 16. The average ACE was 55.6 ± 4.6% at a flow rate of 0.19 mL/min, however, it decreased steadily to 9.9% ± 0.7% as the flow rate was increased to 3.6 mL/min. Anode Coulombic efficiency (CE) was also determined based on COD analysis of the MEC influent and effluent as reported previously [4]. ACE and HE were used rather than CE and HRE because the change in COD for most one-pass experiments was below the error of analysis due to the low COD concentration used in these experiments.

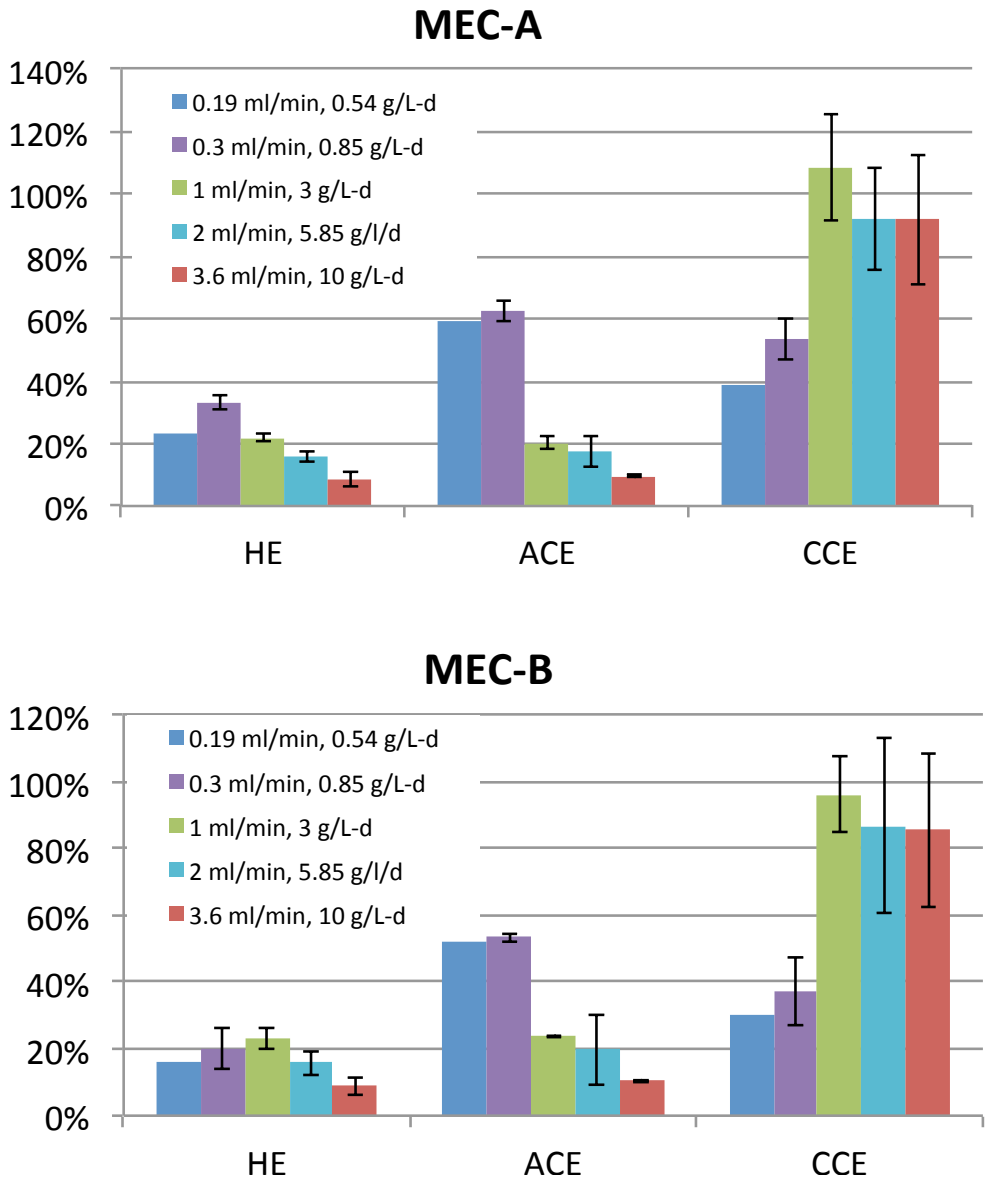

Figure 16: Hydrogen recovery (HE, mol%), Anode conversion efficiency (ACE), and cathode efficiency for MEC operation under one-pass condition for MEC-A and MEC-B. The legend includes flow rate and OLR. The error bars represent standard deviation of two replicate runs conducted in each MEC.

The results for ACE and HE were also reproducible in the two replicate reactors, MEC-A and B, which were operated under the same conditions. All the experiments conducted in this study used the same low BOAP concentration (0.026 g/L), which means that OLR and HRT both changed as function of the flow rate, simultaneously. Compared to ACE, the cathode efficiency showed a reverse trend and increased from 34.55 ± 6.29% to 88.6% ± 4.5% as the flow rate was increased from 0.19 to 3.6 mL/min. There was greater variation in cathode efficiencies at the higher flow rates, which is likely due to the shorter run times, but the overall trend remains and shows a considerable drop off in CCE when flow is reduced below 1 mL/min. Since the anode potential was controlled in these experiments, the cathode potential varied as a function of the current produced. As the rate of substrate delivery to the anode (OLR) is increased, the number of electrons generated and transferred to the cathode increases, thus reducing the cathode potential to more negative values. At low flow rates, the potential difference (ΔV) between the anode and the cathode was smaller. At a flow rate of 0.19 mL/min, the ΔV was only 0.66 V. The low cathode efficiency observed at low flow rates was potentially due to the smaller potential difference between the two electrodes, and more positive value for the cathode. This hypothesis was tested by conducting an additional experiment by setting the ΔV between the anode and cathode to 1.0 V (vs. 0.66 V which was reached when the anode was poised at -0.2V vs. Ag/AgCl electrode). This was done at the flow rate of 0.3 mL/min corresponding to an OLR of 0.85 g/L-d, The higher ΔV increased the CCE to 54.5%, improving the cathode efficiency by 21%. This indicates that the potential difference was at least partially responsible for the lower cathode efficiency. Studies carried out by Escapa et al. (2012) indicated that the benefits of increased voltage are not as pronounced at low OLR's, corroborating our modest increase [13]. The trend for HE is more complicated between the two reactors. On average, the HE increased

initially from 19.4% ± 5.4% at the lowest flow rate to 26.7 ± 2.5% at 0.3 mL/min. From here, HE decreased with increasing flow rate to 8.8 ± 0.2% at 3.6 mL/min. It is clear that HE decreases with increasing flow rate during one pass due to low ACE. However, when flow rate is reduced enough, HE begins to decrease due to the significant drop-off in CCE below 1 mL/min., Thus, a maximum HE would likely be obtained somewhere between a flow rate of 0.3 and 1 mL/min when comparing the two replicate reactors. The drop in ACE and HE with increasing flow rate was suspected to be due to insufficient retention time for conversion during one-pass operation. This hypothesis was investigated further by recycling the anode effluent.

Effect of anode recycle on MEC performance

Since the ACE decreased with increasing flow rate, the effect of recycle was examined as a potential way to boost conversion in the anode. The hypothesis is that when the anode fluid is recycled, the HRT would effectively increase to infinity, enabling higher conversion of the COD increasing current production and ACE. Figure 17 shows the current density as a function of time at a flow rate of 1 and 2 mL/min under recycle conditions. The current production during the one-pass experiment is also shown for comparison. The results show that the current production increased significantly as a result of recycle at and beyond 1 mL/min. Figure 18 shows the comparison of the average current density achieved at different flow rates for the recycle and one-pass conditions. The current density increased by more than 120% at 3.6 mL/min when the anode fluid was recycled. As shown in Figure 17, the current increased during the course of the run under recycle conditions, while it decreased under one-pass conditions. The trends were similar for all experiments at and above the flow rate of 1 mL/min, although the difference was more pronounced at the higher flow rates.

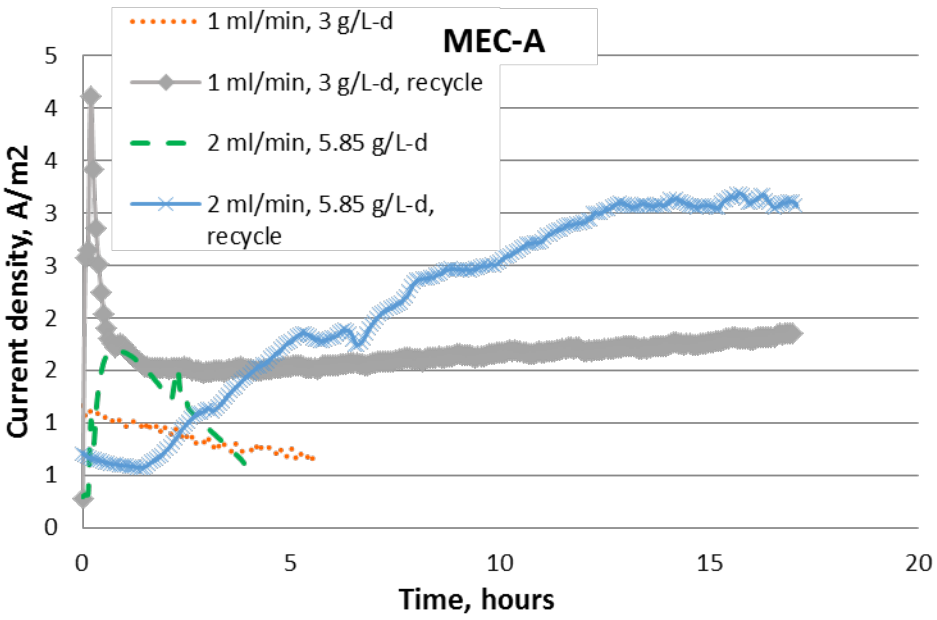

Figure 17: Comparison of one-pass and recycle operation at a flow rate of 1 and 2 mL/min.

To illustrate this effect graphically, the end-point current densities based on the final current obtained during each run were compared with the average current densities (Figure 18). For recycle, the average current densities were less than the end-point current densities, and the opposite was true for one-pass under most conditions as shown in Figure 18. The current produced during the start of the run was typically low and increased gradually with time as substrates and intermediates accumulated during recycle, resulting in higher endpoint currents. In the one-pass condition, faster flow rates alleviated mass transfer issues only up to a certain point due to the complex nature of the substrate, resulting in a reduction in current output at the highest flow rate due to the limited time the substrate spends in the anode. When the anode fluid is recycled, the effective retention time increases, allowing for enhanced production of acetic acid from the complex substrates present in BOAP and any potential degradation products that may be generated via fermentation, hydrolysis and other processes.

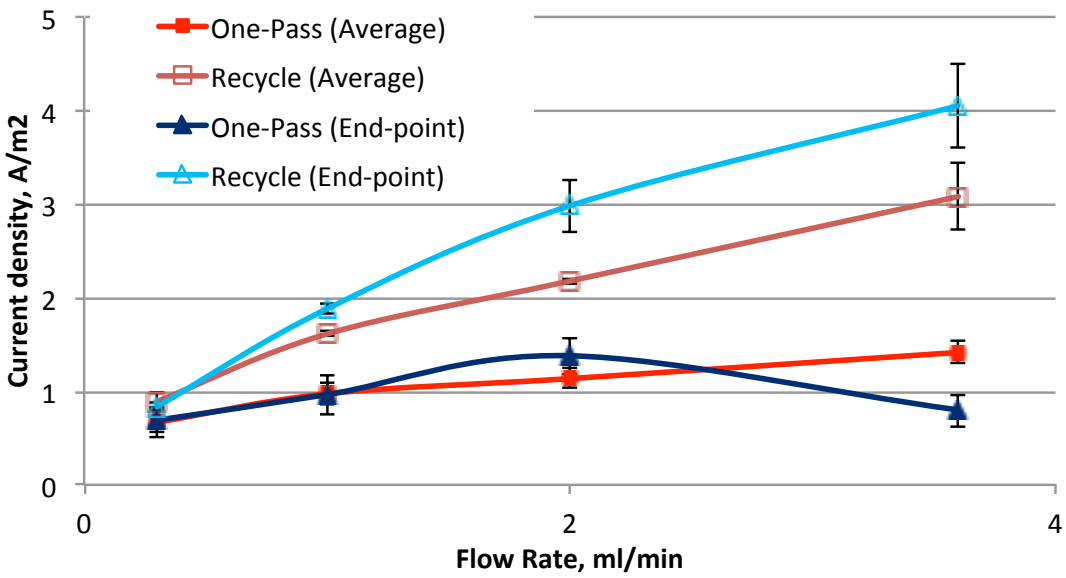

Figure 18: Comparison of average and end-point current densities during one-pass and recycle operation. The error bars represent standard deviation of data obtained for duplicate MEC reactors.

Thus, the benefits of faster flow rate and higher OLR can be better captured through the use of recycle, evidenced by the doubling of the end-point current observed at a loading rate of 3 g/L-day and 1 mL/min flow rate, and a five-fold increase at 10 g/L-day and 3.6 mL/min. While the time required for conversion of the BOAP compounds to electrons is an obvious factor limiting current production at higher flow rates under one-pass condition, other factors such as inhibition, mass transfer and/or pH gradients in biofilm may also be playing a role. The concentration of the substrate used was maintained at 0.026 g/L, which is relatively low, therefore, substrate inhibition is unlikely to be a factor limiting current production with increased loading. Much higher concentrations of organic acids, furanic and phenolic compounds have been used in bioanode without evidence of inhibition in previous reports [19,20]. Inhibition due to product may be a possibility since production of protons generated in the anode biofilm generally increases with increasing OLR. Formation of proton gradients within a biofilm in an anode operated under batch conditions has been reported in the literature [21], however, since the MECs

used in this study were operated under continuous flow conditions, mass transfer due to proton accumulation within the biofilm is likely negligible as pH values did not drop below 7.1 in the bulk. Furthermore, the increasing flow rate used in the experiments, corresponding to increasing OLRs, helped to ensure this. Mass transfer issues in general would be more of a limitation at the lower flow rates, but low OLRs at these levels helps prevent this. Likewise, higher OLRs where proton accumulation could be more of an issue is prevented by using faster flow rates, thus the low HRT for a complex substrate in one-pass conditions is likely the main culprit for the reduction in current output at the highest flow rate despite enhanced mass transfer conditions. The effect of flow rate on mass transfer is further addressed in section 3.6. The recycle operation had a significant impact on the conversion efficiencies as well. Figure 19 shows the efficiency parameters for the recycle operation in comparison to the one-pass operation. The ACE increased by 22.4% at the lowest flow rate of 0.3 mL/min, when the operation was changed from one-pass to recycle. At the highest flow rate of 3.6 mL/min, the ACE increased 2.8-fold from 9.9 ± 0.7% to 28.1± 2.8%. This demonstrates that recycle of the anode fluid enabled much higher conversion of the BOAP substrate to current as flow rate increased. The HE followed a similar trend, with an increase of 18.4% at 0.3 mL/min and 146% at 3.6 mL/min. The average maximum ACE achieved for the MECs combining the results from the replicate reactors was 70.9 ± 7.9% and the average maximum HE was 48.7 ± 13%. The cathode conversion efficiency was 94.5 ± 0.7% at 3.6 mL/min, which decreased to 68.0 ± 11.1% at 0.3 mL/min. This behavior can be explained in a way similar to that given earlier for the one-pass condition. A decrease in cathode half-cell potential was also observed for the recycle experiments with decreasing flow rate and OLR, similar to the one-pass condition, thus reducing the potential difference enabling the cathodic reaction, and limiting cathode efficiency.

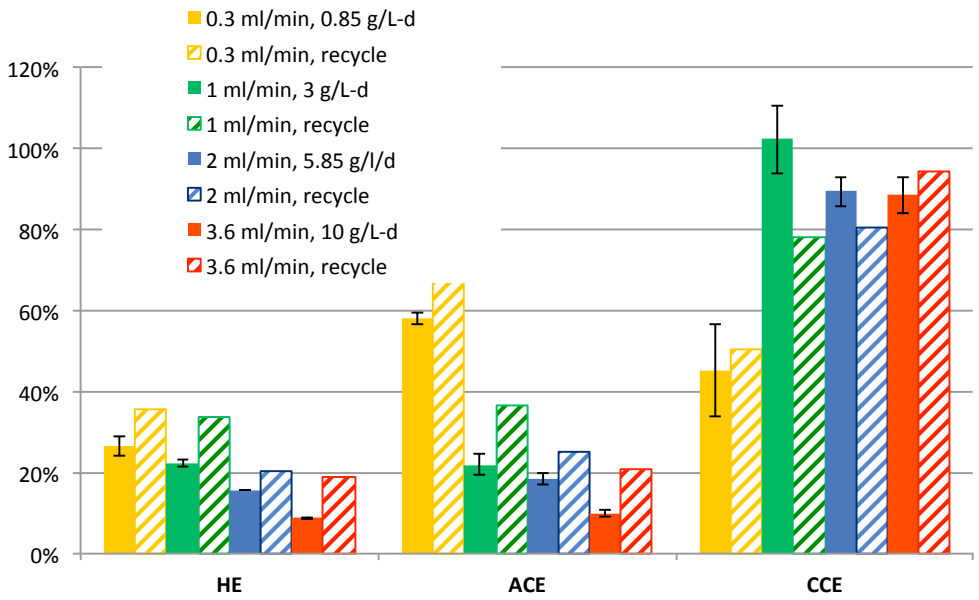

Figure 19: Comparison of anode and cathode conversion efficiencies and hydrogen recovery during recycle operation vs one-pass operation. The results shown are for one of the two MECs with error bars representing standard deviation of two replicate runs.

Furthermore, we have observed in additional experiments (data not shown) that when currents fall below ~1 mA, cathode efficiencies and hydrogen production tend to drop-off significantly regardless of the applied potential, indicating additional factors may be impacting these values.

COD removal under recycle conditions

The recycle operation enabled accumulation of unused substrate in the system, increasing the substrate concentration and COD in the anode liquid with time, until a steady state was reached. Analysis of the COD at the end of the recycle experiments thus allowed calculation of COD removal over the duration of the experiment whereas this was not possible for the one-pass conditions given the low concentration used. Table 4 shows the COD removal under recycle conditions. The COD removal was relatively high ranging from 52.3% to 74.2% in the flow rate

range of 1 to 3.6 mL/min. The overall trend of increasing COD removal with flow rate is reverse to that obtained for Coulombic efficiency (CE). At a flow rate of 1 mL/min and OLR of 3 g/L-d, the CE was 57.63% ± 6.73%, while at 3.6 mL/min and 10 g/L-d, CE was 28.12% ± 2.84%. This indicates that as the flow rate increased, the relative conversion by exoelectrogenesis decreased.

Table 4: MEC performance under recycle conditions.

	MEC-A 1 ml/min 3 g/L-d	MEC-B 1 ml/min 3 g/L-d	MEC-A 2 ml/min 5.85 g/L-d	MEC-B 2 ml/min 5.85 g/L-d	MEC-A 3.6 ml/min 10 g/L-d	MEC-B 3.6 ml/min 10 g/L-d
COD	69.92%	57.65%	62.79%	52.34%	75.03%	73.55%
CE	52.87%	62.39%	39.86%	48.69%	30.12%	26.11%
CCE	79.20%	77.09%	84.27%	77.26%	94.04%	95.03%
HRE	39.48%	27.72%	21.09%	19.47%	21.25%	16.56%

This may be due to increase in side reactions such as methanogenesis and/or limitation due to mass transfer. The occurrence of methanogenesis is feasible given the reports on methanogenesis in the literature even at lower concentrations and OLRs [5,8,22]. Furthermore, the continued removal of COD at high OLRs indicates that fermentation of compounds within BOAP continued, which would then continue to produce acetic acid as a byproduct. While current output did increase with flow rate indicating that electroactive bacteria were utilizing more acetic acid at each level, the increasing drop in CE indicates that a greater proportion of acetic acid was lost (as it was not found to accumulate), or the additional COD did produce acetic acid as efficiently. This could be the result of side reactions such as methanogenesis or biomass growth with increasing flow rate/OLR. Prior to initiation of the continuous operation

studies reported here, the MECs were operated under batch conditions intermittently prior to this study as reported in the Methods section. This may have resulted in the growth of methanogens. Growth of methanogens in the bioanode has been demonstrated by many researchers [23-25] and remains a persistent problem. Additionally, with increased substrate supply diversion of carbon and reducing equivalents for growth could also be contributing to the lower CE. This would support the increased COD removal observed, while diverting less toward current generation to allow growth. Another factor may also be mass transfer/pH limitations due to insufficient proton transfer out of the biofilm. Measurement of the pH in the bulk anode liquid at the end of recycle operation indicated the pH to vary between 7.07 and 6.69, respectively for OLRs between 3 to 10 g/L-day. Calculation of proton accumulation from anodic reaction and accounting for proton consumption in the cathode, it was estimated that the anode pH would change to 6.6 at the highest OLR. Since the observed pH was 6.69, it suggests that proton accumulation is likely not responsible for the limited current production or the loss in CE at higher flow rates (Calculations in Appendix). It is clear that the biofilm was capable of exoelectrogenesis and was not likely limited by substrate or pH. Thus, the most likely reason for the widening gap between COD removal and CE at higher OLR/flow rates may be microbial growth or side reactions such as methanogensis. The measurement of methane in a continuous flow system such as ours was difficult due to the lack of headspace in the anode. However, given the fact that acetic acid was not found to be accumulating at the highest flow rate and OLR despite the low CE, we can say that alternate microbial processes were contributing to the observed electrochemical efficiency loss. Future work will focus on overcoming limitation of our set up in measuring the contributions of methanogenesis and/or other side reactions to COD removal, as well as quantifying possible growth under higher loading.

Understanding the mass transfer implications of setting OLR

As outlined in the introduction, there are two methods for achieving an increase in OLR (1) increased concentration of substrate, or (2) increased flow rate (reduced HRT). We chose the latter for our main set of experiments keeping concentration constant, but to clearly demonstrate the mass transfer implications of our choice, we carried out additional experiments at 10 g/L-d achieved by changing the concentration instead. At 0.3 mL/min, a concentration of 0.3 g/L is required to achieve an OLR of 10 g/L-d, which is ~ 12x greater than the concentration needed at a flow rate of 3.6 mL/min (0.026 g/L) to reach the same OLR. When comparing these two flow rates under one-pass conditions, the end point current density is much lower at the higher flow rate: (0.76 vs. 3.34A/m^2, Figure 20). This may appear to be an effect of concentration, since the higher concentration is expected to give a higher current. However, comparison of the current density at the two concentrations under recycle conditions indicates that this may not be the case. The mass transfer effects are masked under one-pass conditions due to the complex nature of the substrate as detailed in previous sections. Under recycle conditions, the end point current density at the higher concentration was 2.9 A/m^2 vs. 4.6 A/m^2 at the lower concentration and higher flow rate. This implies that the flow rate is influencing the current production. Compared to the one-pass condition, the recycle condition improves the end point current density 5.7-fold, at the higher flow rate. The observation that higher concentration does not result in higher current implies that mass transfer limitations exist in the MEC. When the flow rate is increased, these limitations are alleviated, resulting in higher current densities, in the case of recycle operation. The same increase in current density is not realized under one-pass condition, because the higher flow rate results in rapid removal of the unconverted BOAP and any intermediates that may be

produced by the anodic reaction, which are substrates for exoelectrogenesis. An alternate explanation could be substrate inhibition as the lower flow rate has 10x greater concentration. However, substrate inhibition is unlikely to be the reason for reduced current as recent studies have shown much higher concentrations are required for the type of compounds present in BOAP to be inhibitory [19,20]. Furthermore, our previous work used 0.1 to 0.3 g/L BOAP in batch studies and did not see losses in current compared to the lower concentrations tested.

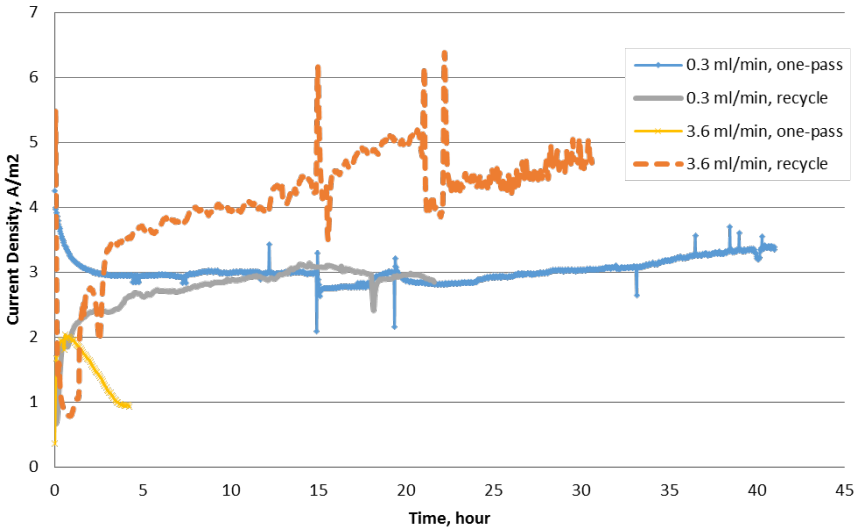

Figure 20: Comparison of current output across different flow rates during one-pass and recycle operation at 10 g/L-d.

Mass transfer is thus the likely reason for lower current output at higher concentration and low flow rate. The recycle experiment demonstrates that mass transfer plays a large role in conversion of BOAP, and that the higher flow rate alleviates this limitation. If mass transfer was not an issue, the higher concentration and lower flow rate would have resulted in a higher current in the recycle experiment as well. This also confirms and expands our conclusions made in section 3.3, that the use of recycle can better take advantage of the mass transfer benefits of faster flow rates, and enable better conversion of complex substrates present in BOAP to current.

The rate of hydrogen production from complex substrates can thus be influenced more so by introducing recycle than increasing the HRTs. Increasing HRT could increase the hydrogen productivity to a certain extent. Our results indicate that improvements in productivity at higher loading rates (5-20 g/L-day) required for commercial application of MECs [26] would require a combination of recycle with higher flow rates or lower HRTs, especially for complex wastewaters which contain fermentable substrates. A study by Gil-Carrera et al. using municipal wastewater showed that two MECs in series were needed for sufficient removal of COD [6]. In our experiments, a single MEC was used with recycle of the effluent to achieve a similar effect. Use of a two-chamber MEC design allowed higher hydrogen productivity, which was not realized in their study due to use of a membraneless MEC.

Influence of complex fermentable feed stream on MEC performance

Conversion of fermentable substrates in the bioanode requires careful consideration of process conditions, which influence mass transfer and kinetics. The BOAP substrate used in this study contains 15% of the COD as acetic acid, while the remaining compounds represent fermentable substrates of varying recalcitrance. Thus, the ability to catalyze the additional steps from fermentable substrate to acetic acid may be hindered by higher flow rates with less time for conversion under one-pass conditions as outlined in section 3.3. Increased ACE at lower flow rates (and OLRs) indicates a higher proportion of compounds passing through the anode were diverted to current generation, likely through better utilization of easily accessible VFA's like acetic acid, as well as production of acetic acid from other fermentable compounds in BOAP. At higher flow rates, utilization of even the easily accessible volatile fatty acids (VFAs) were low, and use of the other fermentable substrates for current production were likely non-existent as

ACE was only ~9% under one-pass. The introduction of recycle was shown to improve this, however efficiency was low as described in section 3.4, likely due to microbial growth or side reactions such as methanogenesis that consumed additional acetic acid produced from recycle compounds. Byproducts generated from the breakdown process were analyzed by HPLC to understand their fate during the recycle operation. The analysis revealed that the anode consortium was capable of consuming the major substrates identified by HPLC in the BOAP feedstock, such as levoglucosan, acetic acid, propionic acid, furfural and hydroxymethylfurfural (HMF). Two intermediates were found to accumulate, but only at higher OLRs. These were phenol and catechol. A recent study investigating furan and phenolic model compounds, such as those present in BOAP, have reported these same compounds to be generated during the degradation of phenolic compounds [20]. In our previous studies, these compounds were found to gradually disappear, over longer term experiments [4] . Zeng et al. (2015) reported that acetate was the primary product of degradation of the model furanic and phenolic compounds [20]. Absence of acetate accumulation in our studies indicates that it was consumed by the members of the anode community, producing current and potentially other products such as methane by methanogenesis as previously stated.

When developing microbial biocatalytic anodes for complex organic streams such as BOAP, there are important structural features and relationships between community members that need to be established in order to efficiently convert the substrates present. Focusing on the two general groups of fermentative and exoelectrogenic bacteria, these functional groups depend on each other and develop syntrophic interactions, with fermenters requiring relief from feedback inhibition due to accumulation of organic acid end products [20], and electrogens requiring acetic acid for electrode respiration [5]. Thus, these two groups work together to link

fermentation to electricity generation. However, these two groups are not the only functional members that can develop in anode communities. Methanogenic archaea are detrimental organisms in the context of microbial electrolysis that can compete with the exoelectrogenic bacteria for substrate and space in the anode. Operational conditions and variables can significantly impact the conversion and hydrogen production in MECs employing complex fermentable substrates as demonstrated in this study.

Implications of MEC integration into biorefinery

The bio-oil aqueous phase used as a substrate for MEC in this work is a waste product in the pyrolytic biorefinery process, since it cannot be effectively converted into biofuel. It is also a problem for disposal because it has low pH of about 3.0 and causes instability in the bio-oil intermediate within which it is emulsified. Use of BOAP for hydrogen production solves many problems for the thermochemical biorefinery such as preventing loss of carbon and energy via the aqueous phase, reduction in greenhouse gas emissions via reduced need for natural gas to produce the hydrogen and eliminating wastewater treatment required to remove phenolic and other toxic compounds present in BOAP. MEC can be considered as a process intensification measure as well, since it can reduce the number of unit operations needed in the biorefinery for hydrogen production. A conventional process would require a steam reformer to convert natural gas into hydrogen and a wastewater treatment step to clean the biorefinery effluent. Use of MEC reduces the unit operations, potentially reducing capital costs as well as GHG emissions and energy losses from the thermochemical reforming steps. Implementation of MECs in biorefineries requires continuous operation, which was shown to be feasible in this study. However, the need for recycle raises additional questions regarding costs of pumping, which

need to be evaluated and compared with existing alternatives to determine the feasibility of the MEC-based biorefinery process.

Conclusion

Operational parameters impacting a continuous MEC process for hydrogen production in the biorefinery were investigated. Biomass-derived bio-oil aqueous phase was used as the feedstock. Two operational conditions: one-pass and recycle were investigated at varying flow rates (OLR and HRT) with constant substrate concentration. Higher flow rates increased hydrogen productivity by 3-fold under one-pass conditions, but at the expense of ACE and current output. Both, mass transfer and kinetic limitations were important depending on the operating conditions. One-pass operation masked the mass transfer benefits of faster flow rates since conversion of the complex substrate BOAP, required a longer HRT for multiple conversion steps to generate electrons via synergistic fermentative and exoelectrogenic path, before current production could be realized. Recycle of anode liquid helped alleviate the kinetic issues and improved ACE by 184%, hydrogen productivity by an additional 116%, and end point current by 468%. Additional experiments with a 10x difference in concentration confirmed that the significant increase in endpoint current was a result of a combination of better mass transfer coupled to improved kinetics achieved via recycling, which increased conversion of unconverted substrates and intermediates to electrons, allowing the benefits of faster flow rate to be realized. However, a 51% loss in CE was observed at higher loading rates despite increased COD removal. This suggests that potential losses via microbial growth and/or methanogenesis may still be occurring. Furthermore, low applied voltages can result in losses in cathode efficiency, and reduction in CCE when current is < 1mA. This study demonstrated that use of high flow

rates with recycle can improve conversion of fermentable substrates present in BOAP, improving rate of hydrogen production in MECs.

References

1. Jones S, Meyer P, Snowden-Swan L, et al. *Process design and economics for conversion of lignocellulosic biomass to hydrocarbon fuels*: PNNL;2013. PNNL-23053, NREL/TP-5100-61178.
2. Borole AP. Microbial Electrochemical Cells and Biorefinery Energy Efficiency. In: Cong T, Eckert C, eds. *Biotechnology for Biofuel Production and Optimization, Edition 1*. New York: Elsevier; 2016:449-472.
3. Borole AP. Improving energy efficiency and enabling water recycle in biorefineries using bioelectrochemical cells. *Biofuels, Bioproducts & Biorefining.* 2011-09-29 2011;5(1):28-36.
4. Lewis AJ, Ren S, Ye X, Kim P, Labbe N, Borole AP. Hydrogen production from switchgrass via a hybrid pyrolysis-microbial electrolysis process. *Bior. Technol.* 2015;195:231-241.
5. Gil-Carrera L, Escapa A, Carracedo B, Moran A, Gomez X. Performance of a semi-pilot tubular microbial electrolysis cell (MEC) under several hydraulic retention times and applied voltages. *Bioresource Technology.* Oct 2013;146:63-69.
6. Gil-Carrera L, Escapa A, Moreno R, Moran A. Reduced energy consumption during low strength domestic wastewater treatment in a semi-pilot tubular microbial electrolysis cell. *Journal of Environmental Management.* Jun 2013;122:1-7.
7. Escapa A, San-Martin MI, Mateos R, Moran A. Scaling-up of membraneless microbial electrolysis cells (MECs) for domestic wastewater treatment: Bottlenecks and limitations. *Bioresource Technology.* Mar 2015;180:72-78.
8. Cusick RD, Bryan B, Parker DS, et al. Performance of a pilot-scale continuous flow microbial electrolysis cell fed winery wastewater. *Applied Microbiology and Biotechnology.* Mar 2011;89(6):2053-2063.
9. Ditzig J, Liu H, Logan BE. Production of hydrogen from domestic wastewater using a bioelectrochemically assisted microbial reactor (BEAMR). *International Journal of Hydrogen Energy.* Sep 2007;32(13):2296-2304.
10. Logan BE, Call D, Cheng S, et al. Microbial electrolysis cells for high yield hydrogen gas production from organic matter. *Environ. Sci. Technol.* Dec 2008;42(23):8630-8640.
11. Tartakovsky B, Manuel MF, Wang H, Guiot SR. High rate membrane-less microbial electrolysis cell for continuous hydrogen production. *International Journal of Hydrogen Energy.* Jan 2009;34(2):672-677.
12. Escapa A, Lobato A, Garcia DM, Moran A. Hydrogen production and COD elimination rate in a continuous microbial electrolysis cell: The influence of hydraulic retention time and applied voltage. *Environmental Progress & Sustainable Energy.* Jul 2013;32(2):263-268.
13. Escapa A, Gil-Carrera L, Garcia V, Moran A. Performance of a continuous flow microbial electrolysis cell (MEC) fed with domestic wastewater. *Bioresource Technology.* Aug 2012;117:55-62.
14. He Z, Wagner N, Minteer SD, Angenent LT. An upflow microbial fuel cell with an interior cathode: Assessment of the internal resistance by impedance Spectroscopy. *Environ. Sci. Technol.* Sep 2006;40(17):5212-5217.

15. Aelterman P, Versichele M, Marzorati M, Boon N, Verstraete W. Loading rate and external resistance control the electricity generation of microbial fuel cells with different three-dimensional anodes. *Bioresource Technology.* 2008;99(18):8895-8902.
16. Freguia S, Rabaey K, Yuan ZG, Keller J. Sequential anode-cathode configuration improves cathodic oxygen reduction and effluent quality of microbial fuel cells. *Water Research.* Mar 2008;42(6-7):1387-1396.
17. Borole AP, Hamilton CY, Vishnivetskaya TA. Enhancement in energy conversion efficiency and current density of 3-dimensional MFC anodes using pre-enriched consortium and continuous supply of electron donors. . *Bioresour. Technol.* 2011;102(8):5098-5104.
18. Harnisch F, Schröder U. Selectivity versus mobility: separation of anode and cathode in microbial bioelectrochemical systems. *Chemsuschem.* 2009;2(10):921-926.
19. Borole AP, Mielenz J, Vishnivetskaya TA, Hamilton CY. Controlling accumulation of fermentation inhibitors in biorefinery water recycle using microbial fuel cells. *Biotechnol. Biofuels.* 2009;2(1):7.
20. Zeng X, Borole AP, Pavlostathis SG. Biotransformation of furanic and phenolic compounds with hydrogen gas production in a microbial electrolysis cell. *Environ. Sci. & Technol.* 2015;49(22):13667-13675.
21. Babauta JT, Nguyen HD, Harrington TD, Renslow R, Beyenal H. pH, redox potential and local biofilm potential microenvironments within Geobacter sulfurreducens biofilms and their roles in electron transfer. *Biotechnology and Bioengineering.* Oct 2012;109(10):2651-2662.
22. Gil-Carrera L, Mehta P, Escapa A, et al. Optimizing the electrode size and arrangement in a microbial electrolysis cell. *Bioresource Technology.* Oct 2011;102(20):9593-9598.
23. Freguia S, Rabaey K, Yuan ZG, Keller J. Syntrophic Processes Drive the Conversion of Glucose in Microbial Fuel Cell Anodes. *Environ Sci Technol.* Nov 2008;42(21):7937-7943.
24. Parameswaran P, Zhang HS, Torres CI, Rittmann BE, Krajmalnik-Brown R. Microbial Community Structure in a Biofilm Anode Fed With a Fermentable Substrate: The Significance of Hydrogen Scavengers. *Biotechnology and Bioengineering.* Jan 2010;105(1):69-78.
25. Sleutels T, Darus L, Hamelers HVM, Buisman CJN. Effect of operational parameters on Coulombic efficiency in bioelectrochemical systems. *Bioresource Technology.* Dec 2011;102(24):11172-11176.
26. Sleutels T, Ter Heijne A, Buisman CJN, Hamelers HVM. Bioelectrochemical Systems: An Outlook for Practical Applications. *Chemsuschem.* Jun 2012;5(6):1012-1019.

Appendix

Analysis of pH changes in anode during MEC operation.

Based on pH changes in anode and cathode, changes in proton concentration were calculated using the Henderson-Hasselbalch equation: $pH = pKa + \log([A^-]/[HA])$ …..1

The anode contained sodium phosphate as buffer [20] and the cathode contained 0.1 M potassium phosphate buffer. The effect of production and consumption of protons on pH was calculated using the following equations, respectively:

$pH = 6.82 + \log(([A^-]-[H^+])/([HA]+[H^+]))$ ….2

$pH = 6.82 + \log(([A^-]+[H^+])/([HA]-[H^+]))$ ….3

The A- and HA were represented by HPO_4^{-} - and $H_2PO_4^-$, respectively and were calculated separately for the two chambers.

Example calculation: The anode pH changed from 7.2 to 6.71 for MEC-A for the experiment with 10 g/L-day OLR. In 23.6 hours, 4.2 mA of current was produced. This corresponded to a proton production of 0.00369 moles, which was equivalent to proton production at anode. Hydrogen production in cathode was 38.5 mL. This consumed 3.12 mmoles of protons. The pH of the cathode changed from 6.9 to 12.1, which corresponds to proton consumption of 1.09 mmoles. The residual protons required for hydrogen production, therefore came from anode. This was calculated to be 2.028 mmoles. Subtracting the protons transferred to cathode from anode from the total protons produced in the anode, the pH in the anode is calculated to be 6.66. The observed pH of 6.71, therefore matches quite well with this estimated value, indicating that all protons produced in the anode biofilm came out of the biofilm. This was potentially due to the high flow rate employed in the MEC.

Table 5: Concentrations of major chemical compounds in bio-oil aqueous phase quantified by HPLC-PDA and GC-FID.

Quantification method	Major chemicals	Concentration based on aqueous phase (g/L)
HPLC-PDA	Furfural	1.01
	1,2-benzendiol	1.77
	Phenol	1.8
	Levoglucosan	15.33
	Acetic acid	11.96
	Proponic acid	1.89
	Vanillic acid	2.69
	HMF	0.54
	Total	36.99
GC-FID	Phenol, 2-methoxy-	0.25
	2-methyl-4-methyphenol	0.07
	Cyclohexanone	0.07
	3-methyl-1,2-cyclophetandiol	0.46
	2,6-Dimethoxyphenol	0.26
	1,3-propanediol	1.84
	3-ethylphenol	0.56
	2(5H)-Furanone	1.17
	1-hydroxybutanone	1.35
	Total	6.02
	Sum	43.01

CHAPTER III

ORGANIC LOADING RATE SHIFTS ELECTRON BALANCE AND MICROBIAL COMMUNITY STRUCTURE DURING CONVERSION OF BIOMASS-DERIVED STREAM

This chapter is derived from a manuscript currently in preparation.

AJL designed and carried out batch experiments, electrochemical analyses, HPLC analysis, COD analysis, GC analysis, data interpretation and manuscript preparation. APB provided guidance in experimental designed and manuscript preparation. We acknowledge Professor Xiaofei Ye, Pyoungchung Kim and Shouji Ren for their work in producing the bio-oil aqueous phase.

Abstract

In order for MEC performance to reach commercial levels, a better understanding of the interrelationship between microbial community structure and operational parameters is needed. This can allow for the identification of environmental conditions that enhance or or inhibit positive interactions with community for substrate conversion and syntrophic current production. This study investigates the effect of OLR at two different flow-rates for a biomass-fed microbial electrolysis cell. The results revealed a strong correlation between substrate loading and the microbial composition. Increase in population of Firmicutes was observed at high substrate concentration or loading. Additionally, multiple exoelectrogenic strains from the *Geobacteraceae* family were found at different conditions. The substrate loading affected which Geobacter strains was dominant in the anode implying that a certain trait related to higher concentration such as inhibition tolerance, etc. may be at play. The results provide a basis for optimization of the MEC performance by manipulating the growth or feeding regimes during MEC start-up or initial biofilm development. Alternately, specific exoelectrogenic strains can be isolated, separately grown and introduced to bioaugment the community for achieving higher

performance.

Introduction

Microbial electrolysis is a promising technology for the production of renewable hydrogen from biomass waste streams. Integral to this technology is a robust microbial community capable of converting the wide spectrum of compounds found within complex streams. It is well established that even for simple substrates, syntrophic interactions among fermenters and exoelectrogens as well as hydrogen scavengers are required to produce current in the anode[1–4]. For more complex substrates these needs are compounded and additional strategies including division of labor are likely required[5]. In order to continue making improvements in performance of MEC systems, a better understanding of how operating conditions may impact the necessary synergistic interactions required for conversion of biomass streams is needed. This will allow development of methods to effectively manage the community for enhancing performance and long-term stability of hydrogen production.

This study takes an integrated approach tracking system performance and uses it to optimize process parameters. The performance variables monitored include electrochemical performance, metabolite profiles, off-gas production, and microbial community structure. The coordinated assessment of electrochemical and biochemical data has potential to provide a full picture of the anode community function as well as identification of the pathways recruited for conversion of substrate to electrons. The effect of organic loading rate (OLR) and flow-rate on performance was scrutinized in order to understand the substrate uptake, electron and carbon flow and product distribution among current, methane, cellular biomass and other sinks. Furthermore, interactions between various functional groups within the community were investigated to understand the

impact on hydrogen productivity.

Methods

The electrochemical methods used for the work described in this chapter are the same as that used in Chapter 3. The microbial characterization methods used in this chapter are similar to that in Chapter 2.

Results and Discussion

MEC performance under differential OLR and flow-rate

The effect of OLR and flow-rate was investigated by comparing MEC performance within a 2x2 matrix of OLR and flow rate. The OLRs tested were of 2 and 20 g/L-d at flow-rates of 4.0 and 0.4 mL/min. The productivities and efficiencies obtained under these conditions are displayed in Figure 21. Typical OLRs reported in literature range from very low to about 5 g/L-day. The higher OLR we examined was based on the target needed for commercial application. Based on our analysis, an OLR of 20 g/L-day will be necessary to achieve hydrogen productivities above 10 L/L-day. Furthermore, stability of MEC performance is also an important criteria for application feasibility. Therefore, each condition was tested for a period of 3 weeks. At an OLR of 2 g/L-d, average H_2 productivity and current density remained fairly stable around 1.0 L/L-d and 1.3 A/m^2 at both flow-rates. 4.0 to 0.4. The differences between the two reactors were within one standard deviation, essentially indicating negligible difference. Looking at efficiencies, a small reduction in CE, and an increase in CCE was observed upon changing flow-rate from 4.0 mL/min to 0.4 mL/min.

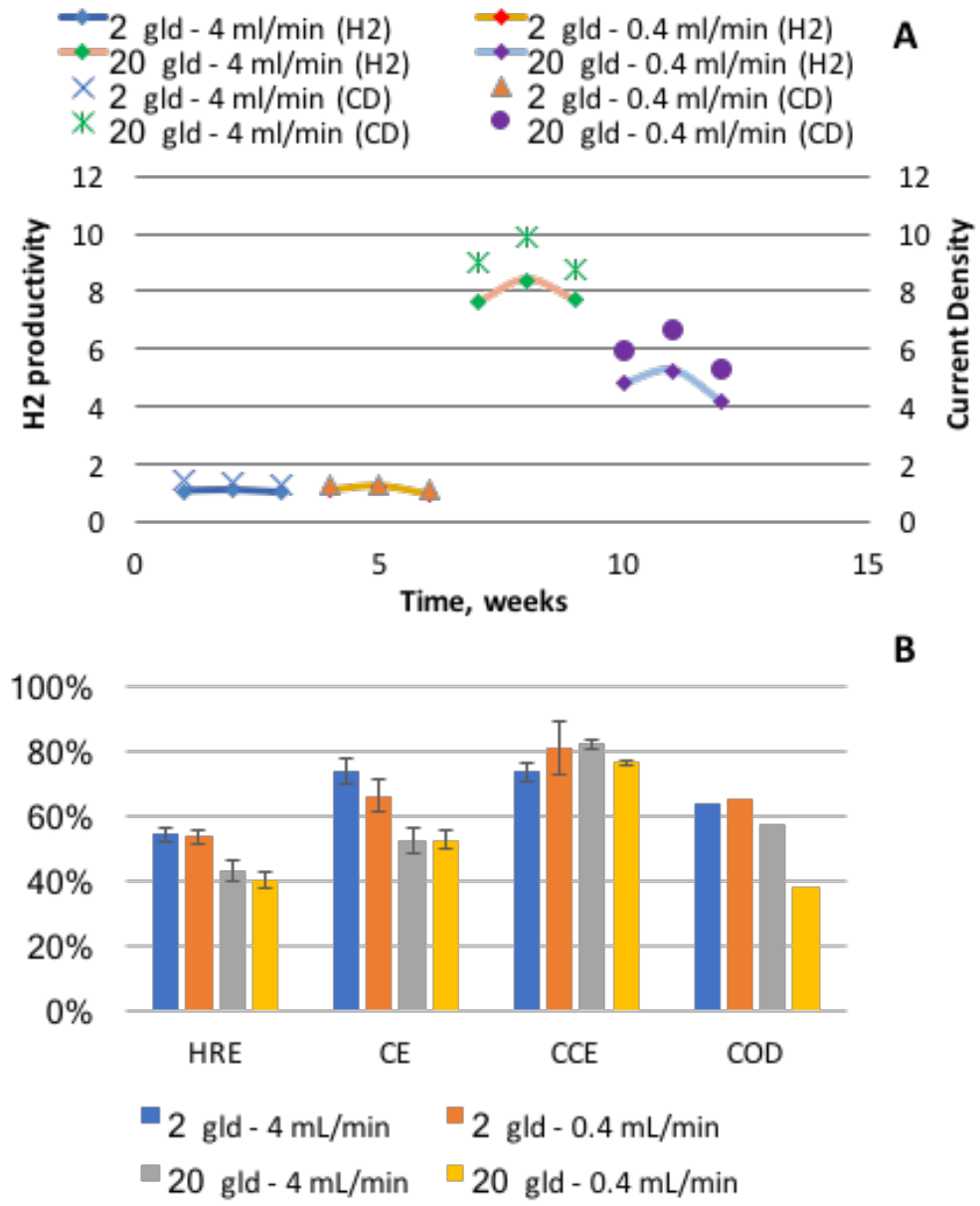

Figure 21: MEC productivities and efficiencies across OLR and flow-rate.

At the high flow-rate, CE reached 73.8 ± 3.9% but decreased to 66.25 ± 4.7% at the low flow-rate. Conversely, CCE was 73.6 ± 2.9% at the high flow-rate and 81.0 ± 8.1% at the lower flow-rate. These differences also fall within one standard deviation, and results from a second reactor operated under same conditions also displayed similar efficiency values at the OLR of 2 g/L-d.

Increasing the OLR to 20 g/L-d, however, showed clear differences between the two flow-rates (Figure 21). Additionally, the higher OLR itself resulted in significantly higher hydrogen production. At the flow rate of 4.0 mL/min, increasing OLR to 20 g/L-d resulted in a ~8-fold increase in H_2 productivity and current density, reaching 7.91 ± 0.42 L/L-d and 9.22 ± 0.59 A/m^2, respectively. On the efficiency side, a substantial reduction in CE was observed, which decreased from 73.8% to 52.3 ± 3.7%. COD removal also decreased by 6.8% to 57.1 ± 3.9%. Interestingly, CCE increased only slightly to 82.1 ± 1.4%, falling within one standard deviation of the CCE at 2 g/L-d. In our previous work, a clear increase in CCE was observed with OLR, which was due to a more negative cathode potential and increased production of protons in the anode[6].The lack of trend observed here is likely due to longer experimental run time during which cathode pH was not controlled. This allowed the cathode pH to rise and experience levels >12 pH units for extended periods of time. Reduced availability of protons at the cathode over the long run times is likely to have depressed CCE values. Recent work investigating proton transfer rates and proton availability in the cathode in MECs has shown that hydrogen productivity is a function of proton transfer rate from anode to cathode[7]. Inability to generate hydrogen obviously affects the CCE, thus, explaining the observations made during this study. As a result of the lower CCE, which combined with lower anode CE values, also reduced HRE from 54.3 ± 2.1% to 43.0 ± 2.9%. Similar trends were observed at the flow rate of 0.4

mL/min, however, the changes were much less pronounced compared to those at 4.0 mL/min. The higher productivities achieved upon increasing loading from 2 to 20 g/L-d could not be sustained when the flow-rate was reduced back to 0.4 mL/min. H_2 productivity and current density decreased 1.7 and 1.6-fold to 4.73 ± 0.55 L/L-d and 5.94 ± 0.70 A/m^2, respectively. CCE also decreased by 5.8% to 76.3 ± 0.88%, but CE remained relatively stable. The explanation for similar CE values between flow-rates at 20 g/L-d despite marked decreases in H_2 productivity and current density can be found by comparing the COD removal. At 4.0 mL/min, COD removal was 57.1 ± 3.9% but it was only 38.1 ± 3.7% at 0.4 mL/min. This lowers the value of (n_s), the amount of the intermediate substrate available for current production, allowing a similar CE to be maintained with lower current output.

Our previous work assessing baseline MEC performance as a function of OLR covered a smaller range of BOAP loadings from 2-10 g/L-d, and at only one flow-rate (4.0 mL/min), but produced similar trends with respect to CE, current density and hydrogen productivity[8]. A maximum hydrogen productivity of 4.3 L/L-d was achieved at a loading of 10 g/L-d. The H_2 productivity increased to 7.91 ± 0.42 L/L-d, when the OLR was increased to 20 g/L-d. One observed difference from the previous study was the trend in COD removal, which decreased with OLR in the present study, whereas the opposite was true in the previous work. The higher loading rate used in this study may have saturated the capacity of the microbial community for substrate uptake or product formation, leading to lower substrate removal. The latter hypothesis is examined further in Sections 3.2 and 3.3, where the analysis of the intermediates is reported along with an electron balance. Escapa et al. also saw a trend similar to that observed in our current work, with lowering of percent COD removal with increase in OLR. The COD removal was reported to drop from 65% at OLR of 0.25 g/L-d to 38% at 3.13 g/L-d using domestic

wastewater. Nonetheless, the COD removal obtained at higher loading and flow-rate was maintained above 50%, exceeding the values previously achieved at lower loadings, while maintaining a high hydrogen productivity.

Biotransformation of individual compounds within BOAP

As detailed above, COD removal decreased upon increasing OLR from to 2 to 20 g/L-d and decreased further at this OLR when the flow-rate was decreased to 0.4 mL/min. Outside of furfural, the other 9 compounds analyzed followed the same trend but to different degrees (Figure 22). Three of the largest changes were seen for acetate, catechol and propionic acid. Acetate removal remained >90% during the first 3 conditions but dropped to 40.1% during 20 g/L-d and 0.4 mL/min operation. Catechol displayed a similar trend, dropping to 22.4% at the final level. Propionic acid displayed the starkest differences as a function of OLR, dropping from 100% biotransformation at the lower loadings to substantial accumulation at the higher loadings, reaching -241.8% after shifting to 20 g/L-d, and then accumulating further to -469.3% at the flow rate of 0.4 mL/min. Compared to previous work at 10 g/L-d[8], HMF removal improved but removal of propionic acid and acetic acid dropped substantially. Miceli et al. demonstrated across multiple substrates that higher initial concentrations led to higher production of short-chain fatty acids[9]. Thus, the higher loading level of 20 g/L-d in this study may have led to substantial increase in the production of these compounds, leading to concentrations that exceeded the capacity of the microbial consortium to degrade them compared to the lower loadings. Additionally, Zeng et al. have reported on the synergistic toxicity of mixed solutions of furanic and phenolic compounds, whose fermentation can impact exoelectrogenesis[10,11]. Thus, given the complex nature of BOA, the loading of 20 g/L-d may have approached these limits.

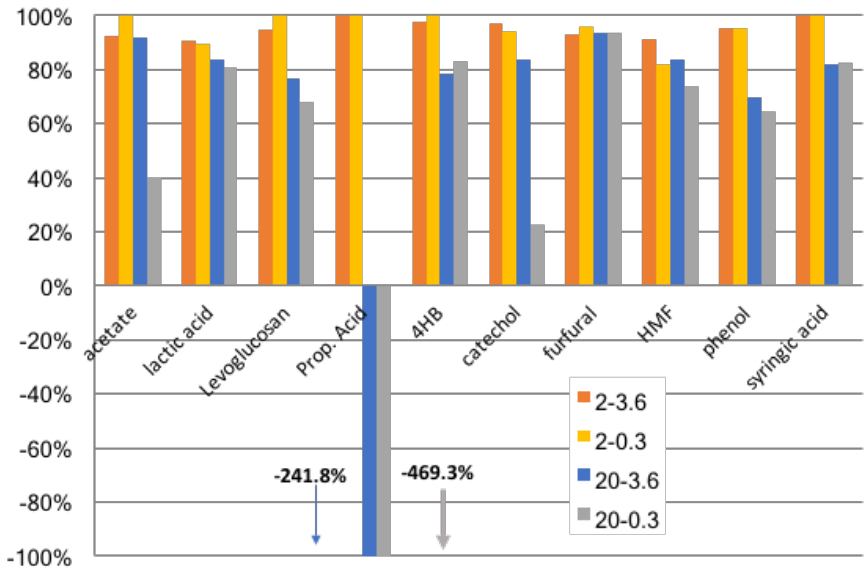

Figure 22 : Biotransformation of compounds within BOAP during differing OLR and flow-rates. Legend notation is 'OLR - flow-rate'.

The observed trends indicate a potential shift in the microbial community metabolism and possible changes in community structure as a response to OLR and concentration at higher loadings, resulting from possible inhibition or saturation, leading to a depressed ability to convert the intermediates as well as some parent compounds.

Distribution of electrons from BOAP conversion

Electron distribution into anode products of current, methane, and undefined sinks were tracked over each week of the 3-week cycle for each condition and averaged to determine the fate of electrons derived from BOAP conversion. The proportion of electrons directed to current production was highest at the lowest loadings corresponding to the CE values reported in the previous section, but the proportion diverted to methane was also highest at the lower levels, reaching ~30% (Figure 23). Diversion of electrons to additional sinks did not occur, but this changed substantially when the loading rate was increased to 20 g/L-d. A reduction in the

electrons directed to current was observed at the higher loadings, dropping to 52.3 ± 3.7% and 52.6 ± 3.1%, respectively. Additionally, the proportion of electrons diverted to methane also decreased to 8.0 ± 1.1% and 9.0 ± 1.5%, respectively. Thus, with a decrease in electrons captured as current and methane, a large increase in electron diversion to undefined sinks was observed, reaching 39.5 ± 2.4% and 37.9 ± 2.3% at the higher loadings.

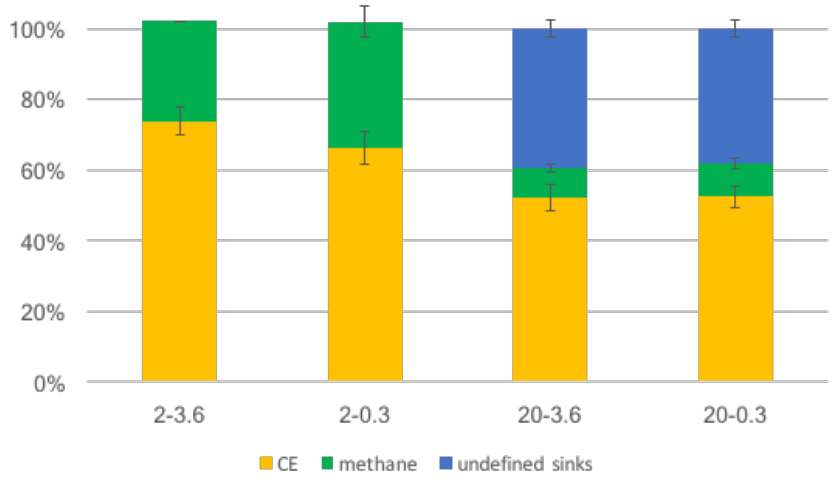

Figure 23: Electron balance across different operating conditions.

As mentioned above, Miceli et al. also observed an increase in electron flow to short-chain fatty acids with increased substrate concentrations, with a corresponding reduction in the proportion of electrons diverted to methane, which also observed in this study. Additionally, Freguia et al. demonstrated in a microbial fuel cell that pulsed carbon addition can result in intracellular storage, which is then consumed during starvation producing current after external depletion of substrate[12]. This was also observed in our recent work[16], where CE was found to temporarily exceed 100% once substrate depletion slowed down. It is therefore quite likely that in the current study, the high continuous rate of substrate addition and accumulated concentration during the experiment did not allow the microbial community to tap into intracellular stores, resulting in the

observed increase of electron diversion to undefined sinks.

Microbial community structure

Changes in MEC operation resulted in structural changes to the anode microbial community. A clear trend was observed for *Deltaproteobacteria*, comprised mainly of *Geobacteraceae*, increasing steadily from 17.1 to 51.82% over the conditions tested (Figure 24a). Additionally, *Betaproteobacteria* decreased slightly upon reducing the flow-rate during 2 g/L-d from 22.5 to 14.0%, but dropped substantially at both higher loading conditions to <1.0%. The Firmicutes population was fairly stable between 27-28% at the lower levels but jumped to 47.0% upon increasing the loading to 20 g/L-d. However, this population could not be maintained and declined to 32.9% upon dropping to 0.4 mL/min at 20 g/L-d. Bacteroidetes dropped initially from 12.1 to 7.7% after decreasing the flow-rate at 2 g/L-d, but then remained fairly stable across the other levels. The methanogen population remained at low levels throughout, never exceeding 4%, but higher loading did reduce its population density. This corresponded well with the lower methane yields observed at the higher loading (Figure 3). Members of the Clostridia class within Firmicutes are known to be strong fermenters and were present at high levels at all levels but increased further at higher loadings. The family *Ruminococcaceae*, which contains known anaerobic cellulolytic organisms[13,14] was found to increase considerably from 6.7 to 23.5% at 20 g/L-d. Conversely, the family *Lachnospiraceae* remained at high levels during the first 3 conditions but decreased to 1.8% upon decreasing the flow-rate at 20 g/L-d. Organisms within this family also have fermenting abilities as well as acetogenic abilities through the use of H_2 and CO_2[15]. Thus, the possible shift to volatile fatty acid production resulting in decreased methane production may have also impacted the population of

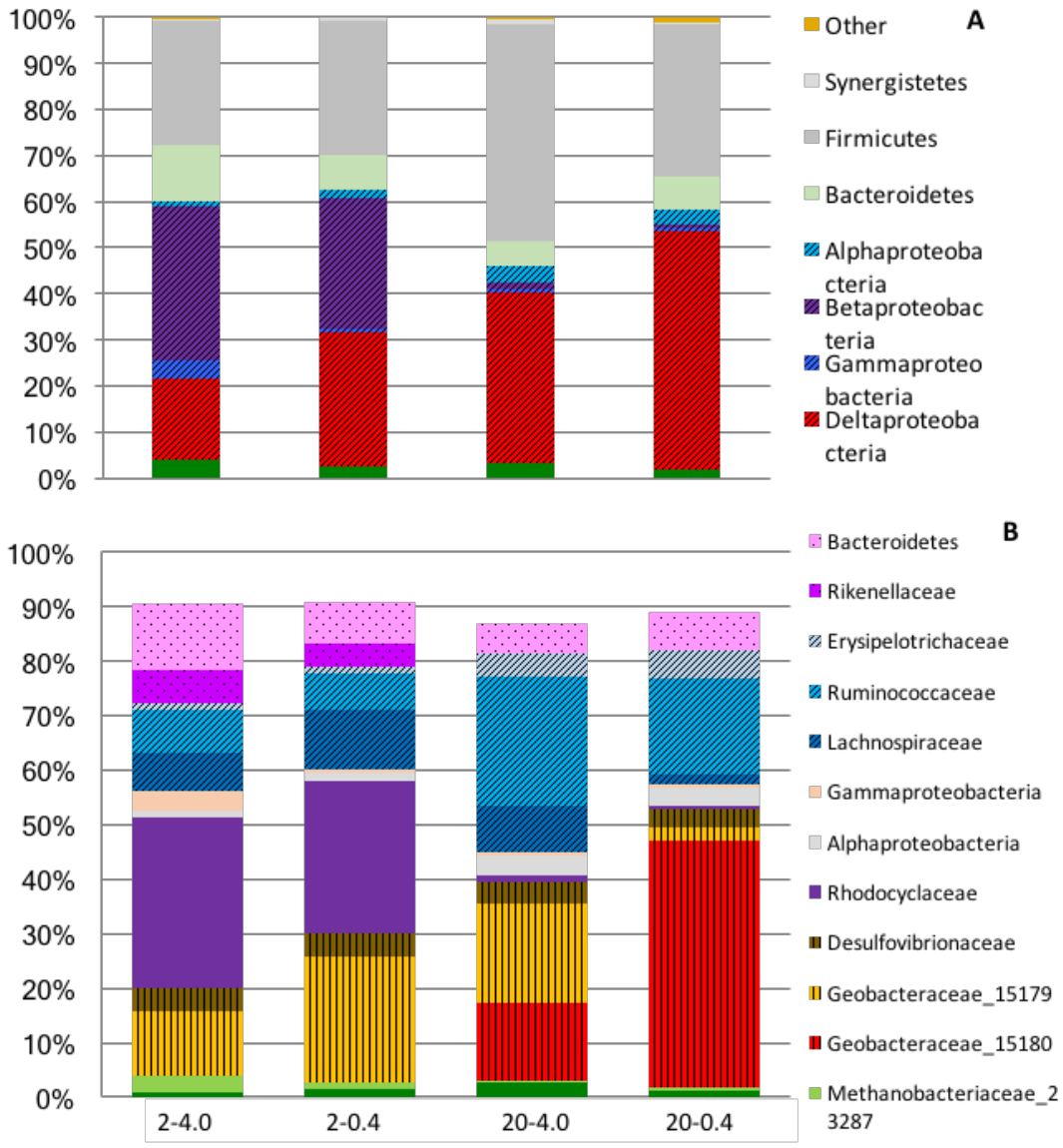

Figure 24: Microbial community structure across the tested OLR and flow-rate combinations.

this family, while allowing other volatile fatty acid producers such as those within *Ruminococcaceae* to proliferate. The observed decrease at higher loading for *Betaproteobacteria* was traced to the family *Rhodocyclaceae*, which decreased from 31.5 to 0.57%. This family is known for its versatile abilities and wide substrate range, and was found to remain at high levels both with BOAP and pure acetic acid[16]. Thus, its strong decrease with OLR is somewhat surprising given the wide substrate availability and increasing acetic acid concentrations. It is possible that the toxic environment reduced the population density of this organism within the community. An example of this can be seen in looking closer at the trends for *Geobacteraceae*, which increased overall, likely due to increased acetate concentration at each condition. However, looking at specific OTUs within this family (Figure 24b) we can see that Geobacter_15179 was dominant at the lower loadings reaching 23.0% while Geobacter_15180 was <0.2%. However, after increasing OLR rate and continuing further to the lower flow-rate, Geobacter_15179 dominated the low loading MEC decreasing to 2.4% while Geobacter_15180 increased drastically to 45.3% of the population. These results indicate that higher concentrations of BOAP provide different selective advantages that reduced the fitness of the one dominant Geobacter strain and allowing another strain to proliferate.

Conclusions

Investigations in this chapter were targeted to understand the microbial basis for the effects observed at low and high OLR on electrochemical performance. A 2x2 matrix of OLR and flow rate was employed using flow rate of 0.4 and 4.0 mL/min and OLR of 2 and 20 g/L-d. An increase in the population of Firmicutes was observed at the higher organic loading rate. Ruminococcaceae and Lachnospiraceae were the dominant members within Firmicutes which

increased with availability of more substrate. The exoelectrogen population showed an interesting change in that the overall population of Deltaproteobacteria increased, but the specific strains within Geobacteraceae which was dominant at lower OLR decreased significantly, but another species partially replaced it at the higher substrate loading. The results show a clear effect of the substrate loading and flow rate on the performance of the MEC, which can be used to optimize the growth of the community for high performance during MEC operation for hydrogen production.

References

1. Parameswaran P, Torres CI, Lee HS, Krajmalnik-Brown R, Rittmann BE. Syntrophic interactions among anode respiring bacteria (ARB) and non-ARB in a biofilm anode: Electron balances. *Biotechnol Bioeng*. 2009;103(3):513-523. doi:10.1002/bit.22267.
2. Gao Y, Ryu H, Santo Domingo JW, Lee H-S. Syntrophic interactions between H2-scavenging and anode-respiring bacteria can improve current density in microbial electrochemical cells. *Bioresour Technol*. 2014;153:245-253. doi:10.1016/j.biortech.2013.11.077.
3. Hari AR, Katuri KP, Gorron E, Logan BE, Saikaly PE. Multiple paths of electron flow to current in microbial electrolysis cells fed with low and high concentrations of propionate. *Appl Microbiol Biotechnol*. 2016;100(13):5999-6011. doi:10.1007/s00253-016-7402-2.
4. Miceli JF, Garcia-Peña I, Parameswaran P, Torres CI, Krajmalnik-Brown R. Combining microbial cultures for efficient production of electricity from butyrate in a microbial electrochemical cell. *Bioresour Technol*. 2014;169:169-174. doi:10.1016/j.biortech.2014.06.090.
5. Thygesen A, Marzorati M, Boon N, Thomsen AB, Verstraete W. Upgrading of straw hydrolysate for production of hydrogen and phenols in a microbial electrolysis cell (MEC). *Appl Microbiol Biotechnol*. 2011;89(3):855-865. doi:10.1007/s00253-010-3068-3.
6. Lewis AJ, Borole AP. Understanding the impact of flow rate and recycle on the conversion of a complex biorefinery stream using a flow-through microbial electrolysis cell. *Biochem Eng J*. 2016;116:95-104. doi:10.1016/j.bej.2016.06.008.
7. Borole AP, Lewis AJ. Proton transfer in microbial electrolysis cells. *Sustain Energy Fuels*. 2017;0:1-12. doi:10.1039/C7SE00034K.
8. Lewis AJ, Ren S, Ye X, Kim P, Labbe N, Borole AP. Hydrogen production from switchgrass via an integrated pyrolysis-microbial electrolysis process. *Bioresour Technol*. 2015;195:231-241. doi:10.1016/j.biortech.2015.06.085.
9. Miceli III JF, Torres CI, Krajmalnik-Brown R. Shifting the balance of fermentation products between hydrogen and volatile fatty acids: microbial community structure and function. *FEMS Microbiol Ecol*. 2016;92(September 2016):1-8. doi:10.1093/femsec/fiw195.
10. Zeng X, Borole AP, Pavlostathis SG. Inhibitory Effect of Furanic and Phenolic Compounds on Exoelectrogenesis in a Microbial Electrolysis Cell Bioanode. *Environ Sci Technol*. September 2016. doi:10.1021/acs.est.6b01505.
11. Zeng X, Collins MA, Borole AP, Pavlostathis SG. The extent of fermentative transformation of phenolic compounds in the bioanode controls exoelectrogenic activity in a microbial electrolysis cell. *Water Res*. 2017;109:299-309. doi:10.1016/j.watres.2016.11.057.
12. Freguia S, Rabaey K, Yuan Z, Keller J. Electron and carbon balances in microbial fuel cells reveal temporary bacterial storage behavior during electricity generation. *Environ Sci Technol*. 2007;41(8):2915-2921. doi:10.1021/es062611i.
13. Kouzuma A, Kasai T, Nakagawa G, et al. Comparative Metagenomics of Anode-Associated Microbiomes Developed in Rice Paddy-Field Microbial Fuel Cells. Moreno-Hagelsieb G, ed. *PLoS One*. 2013;8(11):e77443. doi:10.1371/journal.pone.0077443.

14. Rismani-Yazdi H, Christy AD, Dehority BA, Morrison M, Yu Z, Tuovinen OH. Electricity generation from cellulose by rumen microorganisms in microbial fuel cells. *Biotechnol Bioeng*. 2007;97(6):1398-1407. doi:10.1002/bit.21366.
15. Rieu-Lesme F, Morvan B, Collins MD, Fonty G, Willems A. A new H2 / CO2-using acetogenic bacterium from the rumen: Description of Ruminococcus schinkii sp. nov. *FEMS Microbiol Lett*. 1996;140(2-3):281-286. doi:10.1111/j.1574-6968.1996.tb08350.x.
16. Lewis AJ, Campa MF, Hazen TC, Borole AP. Unravelling biocomplexity of electroactive biofilms for producing hydrogen from biomass. *Microb Biotechnol*. July 2017. doi:10.1111/1751-7915.12756.

CHAPTER IV

UNRAVELING BIOCOMPLEXITY OF ELECTROACTIVE BIOFILMS FOR PRODUCING HYDROGEN FROM BIOMASS

This chapter was originally published by:

Lewis AJ, Campa MF, Hazen TC, Borole AP. Unravelling biocomplexity of electroactive biofilms for producing hydrogen from biomass. *Microb Biotechnol*. July 2017. doi:10.1111/1751-7915.12756.

No alterations were made to the published article for inclusion in the dissertation. AJL designed and carried out batch experiments, electrochemical analyses, HPLC analysis, COD analysis, GC analysis, data interpretation and manuscript preparation. MFC assisted in community sample preparation and analyses. TCH and APB provided guidance on manuscript preparation We acknowledge Professor Xiaofei Ye, Pyoungchung Kim and Shouji Ren for their work in producing the bio-oil aqueous phase.

Abstract

Leveraging nature's biocomplexity for solving human problems requires better understanding of the syntrophic relationships in engineered microbiomes developed in bioreactor systems. Understanding the interactions between microbial players within the community will be key to enhancing conversion and production rates from biomass streams. Here we investigate a bioelectrochemical system employing an enriched microbial consortium for conversion of a switchgrass-derived bio-oil aqueous phase (BOAP) into hydrogen via microbial electrolysis (MEC). MECs offer the potential to produce hydrogen in an integrated fashion in biorefinery platforms and as a means of energy storage through decentralized production to supply hydrogen to fueling stations, as the world strives to move toward cleaner fuels and electricity-mediated transportation. A unique approach combining differential substrate and redox conditions revealed

efficient but rate-limiting fermentation of the compounds within BOAP by the anode microbial community through a division of labor strategy combined with multiple levels of syntrophy. Despite the fermentation limitation, the adapted abilities of the microbial community resulted in a high hydrogen productivity of 9.35 L/L-d. Using pure acetic acid as the substrates instead of the biomass-derived stream resulted in a 3-fold improvement in productivity. This high rate of exoelectrogenesis signifies the potential commercial feasibility of MEC technology for integration in biorefineries.

Introduction

Many conversion technologies that could comprise the future bio-economy are still under development and rapid progress is needed in order to meet the growing need for renewable and carbon-neutral energy sources. Renewable hydrogen supply and water management are among important issues facing sustainable development of biorefineries, due to the high hydrogen demand for deoxygenation and potential for water limitations in areas with intensive agriculture [1]. Additionally, hydrogen in and of itself is being pursued as a renewable fuel source due to the significant reductions in tail-pipe emissions that are possible via fuel cell technologies and can also serve as an energy storage mechanism for off-peak power [2]. Hydrogen production from renewable sources such as biomass, however, has been lagging [3]. Strategies such as dark fermentation have made progress but experience low yields and carbon losses to side products and can struggle with more complex streams, while photofermentation poses operational and design challenges [4] . Bioelectrochemical systems offer a novel way to solve these problems by recruiting biocatalysis and electrocatalysis for efficient conversion of complex biomass resources [5-7]. Engineering model organisms to convert biomass into usable bioenergy products can be

challenging via synthetic biology [8,9] due to the complex nature of lignocellulosic biomass and the large spectrum of compounds that result from hydrolytic or thermochemical depolymerization [10]. The complexity of nature can be harvested to develop efficient conversion systems for energy production by repurposing the biology to solve specific human needs. In natural anoxic environments, microbial communities have evolved to degrade biomass and recycle the energy present in complex organic carbon through interactions of two main factions: fermentative and respiring bacteria. The fermentative organisms break down larger carbon compounds resulting in end products that are utilized by respiring bacteria to reduce nitrate, sulfate, iron, or solid metals; storing the energy in cellular biomass or reduced inorganic end products [11,12]. Bioelectrochemical systems provide a controlled environment where these processes continue to take place, but couple the electron transfer to a solid electrode, providing a means to harvest the energy as electrons and subsequently as hydrogen or other products.

While recent studies have expanded the understanding of anode microbial communities using simple fermentable substrates or domestic wastewater [13-16] , few studies have focused on investigating the biocomplexity of engineered BESs utilizing more complex, biomass-derived streams. There have been several studies utilizing biomass-derived streams such as fermentation effluent or other agro/industrial waste, but have separated the fermentation from the MEC and did not focus on developing a mixed microbial community combining the fermentation and exoelectrogenesis steps [13,17-19]. Mahmoud et al. [14] demonstrated the limitation of fermentation in treating more recalcitrant streams like raw landfill leachate directly in the MEC, requiring Fenton oxidation to improve biodegradability to enhance performance. Additional agro-wastes like molasses and hydrolysates such as those from straw and corn stover conversion have been investigated directly in MECs [20-22]. Of these, only Thygesen et al. tracked compound levels with

time and were able to identify microbial roles for xylan degradation and propionate and acetate production, but observed low performance. Additionally, recent studies using intermediates and end-products generated during fermentation such as carboxylic acids and alcohols have investigated their role as substrates in bioanode. Use of propionate as a substrate in MEC has revealed that it goes through a two-step process to produce current. Hari et al., have delineated the pathways of propionate conversion in MEC and reported that it is first transformed into acetate and formate/hydrogen, followed by exoelectrogenesis to produce current [23]. Similarly for butyrate, acetate has been reported to serve as a primary branching point for uptake by exoelectrogens [15]. Lastly, Parameswaran et al. demonstrated that using ethanol as the substrate, three interacting groups including fermentative bacteria, H_2-scavenging bacteria, and exoelectrogenic bacteria, were needed for successful conversion of the substrate into electrons [16].

Conversion of an aqueous fraction of biomass-derived pyrolysate to electrons was recently demonstrated in a bioanode with high efficiency and productivity for renewable hydrogen production in a microbial electrolysis cell (MEC) [24,25]. In order to reach levels for commercial considerations, un raveling the biocomplexity of such a system will be key to unlocking the potential of MEC technology and its application to produce hydrogen and advanced biofuels using the billion-ton biomass resource [26]. Thus far, studies in the literature investigating complex streams have been lacking in biocatalyst development and community interrogation. The first step in this process is to understand the multi-step conversion process and the interactions among various functional groups to enable complete degradation. In order to accomplish this, an integrated approach utilizing shifts in electrochemical and substrate conditions as well as time course metabolite tracking are needed to provide insights into the resulting interactions that develop for conversion of complex substrates. Delineating the

bioelectrochemical interactions and influence of process conditions on community composition can help establish the relationship between biocomplexity and system performance including yield, efficiency and rate of production of the desired products.

In this study, we report on the interaction between multiple microbial groups including fermentative and exoelectrogenic groups within a high-performing anode community processing switchgrass-derived bio-oil aqueous phase (BOAP) into hydrogen via a bioelectrochemical route. Experiments were conducted to study the behavior of the bioanode community under two different control regimes, one focused on changing the substrate from a complex feedstock to a substrate ideal for exoelectrogens, and the other on changing the poised potential. The latter substrate was acetic acid, which is an intermediate generated from the complex substrate BOAP, thus interrelating the two parameters. The following coupled investigations were conducted to parse the effects of the interacting parameters:

1. Conversion of BOAP under poised conditions,
2. Conversion of acetic acid under poised conditions
3. Conversion of BOAP under open-circuit conditions to assess fermentative conversion, while restricting exoelectrogenesis

The underlying hypothesis we investigate is that the formation of acetic acid from the complex BOAP substrate is rate limiting. Sequential operation of MEC at poised and open circuit (un-poised) conditions provides insights into the rate at which the carbon from BOAP is directed to intermediates for exoelectrogenesis such as acetic acid and subsequently into current. Hydrogen productivity and current density as well as efficiencies of the anode, cathode and hydrogen recovery were determined. Lastly, microbial community characterization was conducted to gain insights into the relative changes in fermentative, methanogenic and exoelectrogenic populations

during these experiments to understand biocomplexity.

Methods

MEC construction and experimental setup

Two replicate MECs were constructed with anode and cathode volumes of 16 ml each with a projected area 12.56 cm^2. A porous carbon felt was used as anode material with a thickness of 13 mm, and 40 mm in diameter. A membrane electrode assembly (MEA) was used as a membrane separator and cathode catalyst. The cathode consisted of Pt-deposited carbon matching the diameter of the anode at 40 mm. Nafion 115 was used as a membrane separator between the anode and cathode chambers, and a carbon rod and stainless steel wire were used as current collectors in the two chambers, respectively. Additional details of the MEC construction are reported elsewhere [25].

Bioanode enrichment

As described and characterized previously, [24,25] bio-oil aqueous phase (BOAP) generated from pyrolysis of switchgrass was used as substrate for enrichment of the microbial community in this study to develop a microbial community for application in biorefinery. Anode media consisted a minimal salt medium containing Wolf's mineral and vitamin solutions as reported previously. The cathode solution used was 100 mM potassium phosphate buffer.

Batch operation

The MEC anodes utilized a flow-through design, with the anolyte continuously recycled to and from a feed reservoir (Appendix Figure Figure 31) [25]. A batch concentration of 0.5 g

COD/L was used for testing BOAP and acetic acid. Additionally, a concentration of 0.1 g COD/L was also used for acetic acid as this approximately corresponds to the amount of acetic acid present at time zero in 0.5 g COD/L BOAP. The total recirculation volume for the anode including external reservoir was 200 ml with a flow rate of 3.6 ml/min. Poised conditions were maintained at -0.2 V vs Ag/AgCl via a Reference 3000 potentiostat/galvanostat/zero resistance ammeter (Gamry Instruments, Warminster PA) in all experiments. Prior to the start of each experiment, circulation of media and substrate were stopped to allow current output to decrease to the baseline level. This was done to minimize contribution of stored carbon present in biofilm cells during previous feeding. The feed reservoir was then replaced with fresh media and the circulation lines and anode chamber were flushed so that all substrate remaining from the previous experiment is removed from the whole system. The cathode buffer was not circulated and was replaced before each experiment and again after 8-10 hours when pH was >11 during the 0.5 g COD/L experiments. Additionally, the anode reservoir pH was adjusted at this time from 6.6 to 7.0. BOAP conversion was slower compared to acetic acid, so experimental run times were extended for BOAP experiments to 72 hours, while acetic acid experiments at a concentration of 0.1 g/L and 0.5 g/L were run for 6 and 24 hours, respectively. The results from first 24 hours of the BOAP conversion experiment were compared with acetic acid experiments, but results for the BOAP substrate beyond 24 hours are also discussed.

Community Sampling

Microbial samples were taken from the MEC anode in an anaerobic glovebox utilizing a coring tool to remove a piece of the carbon felt [25]. Core samples were taken prior to the start of each experiment and replaced with a fresh sterile core of the same size. The core was then

removed at the end of each experiment to assess how exposure to the experimental conditions impacted the composition of the community. DNA was extracted from each core using a MoBio Power Biofilm DNA extraction kit, following manufacturer's protocol (Qiagen). Library prep was then carried out on the extracted DNA for 16S analysis on Illumina MiSeq following the methods of Caporaso et al. [59]. PCR products were checked via gel electrophoresis, and then were pooled and run through Zymo DNA Clean and Concentrator. Samples were then checked using a Bioanalyzer and final concentration determined by Qubit. Kapa qPCR was also carried out for quality control. Sequencing was carried out with Illumina MiSeq 250 bp PE run, and sequence data analyzed via Qiime.

Analysis and calculations

HPLC samples were taken every 2 hours for the first 8-10 hours, and then at each 24-hour mark thereafter. H_2 production was measured at these times by volume displacement. At the end of each run gas samples for GC analysis were taken from the cathode outlet to confirm hydrogen production. Liquid samples from the anode were taken from a T-valve placed in the recirculation line prior to entering the reactor. HPLC and COD analysis were conducted to measure the extent of conversion of the substrates in BOAP. All sampling procedures were carried out as previously described [25].

Performance and conversion efficiency were characterized by Coulombic efficiency (CE), cathodic conversion efficiency (CCE), hydrogen recovery (HRE), and were calculated as previously described [25,60]. Calculation of the removal rates for individual compounds and overall COD were done on the basis of each time block and were not cumulative, subtracting the mass of compound/COD measured via HPLC/COD from time point to time point. From these values, the

following method was used for generating the theoretical contribution of each compound to H_2 production:

$$Electron\ equivalents = \frac{concentration * liquid\ volume}{Molecular\ weight\ of\ compound} * moles\ e^{-}per\ mole\ of\ compound$$

The electron moles for each compound are calculated from the complete oxidation of 1 mol of compound to CO_2, protons, and electrons (Additional File 1: Table S1). The electron equivalents can then be converted into theoretical volume of H_2 through the use of two electrons per mole of H_2 with the ideal gas law, which can then be subsequently converted to a production rate using a specified time frame within the experiment. This calculation makes the assumption that any decrease in compound concentration during batch conversion results in 100% conversion to intermediates such as acetic acid and on to electrons. To calculate the efficiency at which intermediates are produced from the compounds identified by HPLC during open circuit conditions, the following equation is used:

$$I_{eff} = {(I\ electron\ equiv.)}\Big/{(Total\ electron\ equiv.)}$$

With "I" = intermediate, such as acetic acid, and the total electron equivalents includes all compounds that were removed during the given time frame.

Results and Discussion

H_2 Production from BOAP vs Acetic Acid in MEC

Current and hydrogen production from two different substrates, BOAP and acetic acid was investigated to understand the transformation of BOAP in a bioanode. Acetic acid was

chosen as a second substrate for investigations because this is a known intermediate for exoelectrogens and a common end-product of fermentation reactions, although not the only one. A comparison of the current production from the two substrates has potential to reveal the relative rates of fermentation vs. exoelectrogenesis in the MEC. While BOAP experiments were extended for 72 hours, the results from BOAP for the first 24 hours are also compared as acetic acid experiments did not run beyond this time. Total hydrogen productivity from BOAP at a concentration of 0.5 g COD/L was 4.44 ± 0.68 L/L-day over the first 24 hours. Over the same period, the hydrogen productivity using 0.5 g COD/L acetate was 9.05 ± 0.71 L/l-day. At this concentration, the maximum H_2 production rate and current density for BOAP were 9.35 ± 1.73 L/L-d and 8.76 ± 1.54 A/m^2, respectively (Figure 25). In comparison, the maximum productivity and current density reached a higher peak for 0.1 g COD/L acetic acid. They were 1.4 and 1.3-fold higher than that of BOAP, reaching 13.33 ± 0.96 L/L-d and 11.48 ± 2.94 A/m^2, respectively. The overall amount of H_2 produced over the entire run was 3-fold higher with 0.5 g COD/L BOAP compared to 0.1 g COD/L acetic acid (Appendix Table 8). This is not unexpected, since the BOAP experiment was fed with 5-fold more total COD. A comparison of the experiments with 0.5 g COD/L acetic acid and 0.5 g COD/L BOAP (Figure 1) shows that the maximum H_2 productivity and current density increased to 2.9-fold and 2.8-fold, reaching 27.6 ± 5.29 L/L-d and 24.7 ± 3.64 A/m^2, respectively. The cumulative H_2 production from acetic acid over the duration of the experiment was 1.9-fold higher compared to BOAP.

Looking at efficiencies during the first 24 hours, BOAP produced lower hydrogen recovery (HRE), anode Coulombic efficiency (CE) and cathode conversion efficiency (CCE) (Figure 25). The anode CE, HRE and CCE for BOAP were 71.22 ± 15.08%, 66.90 ± 12.69% and 94.16 ± 2.12%, respectively.

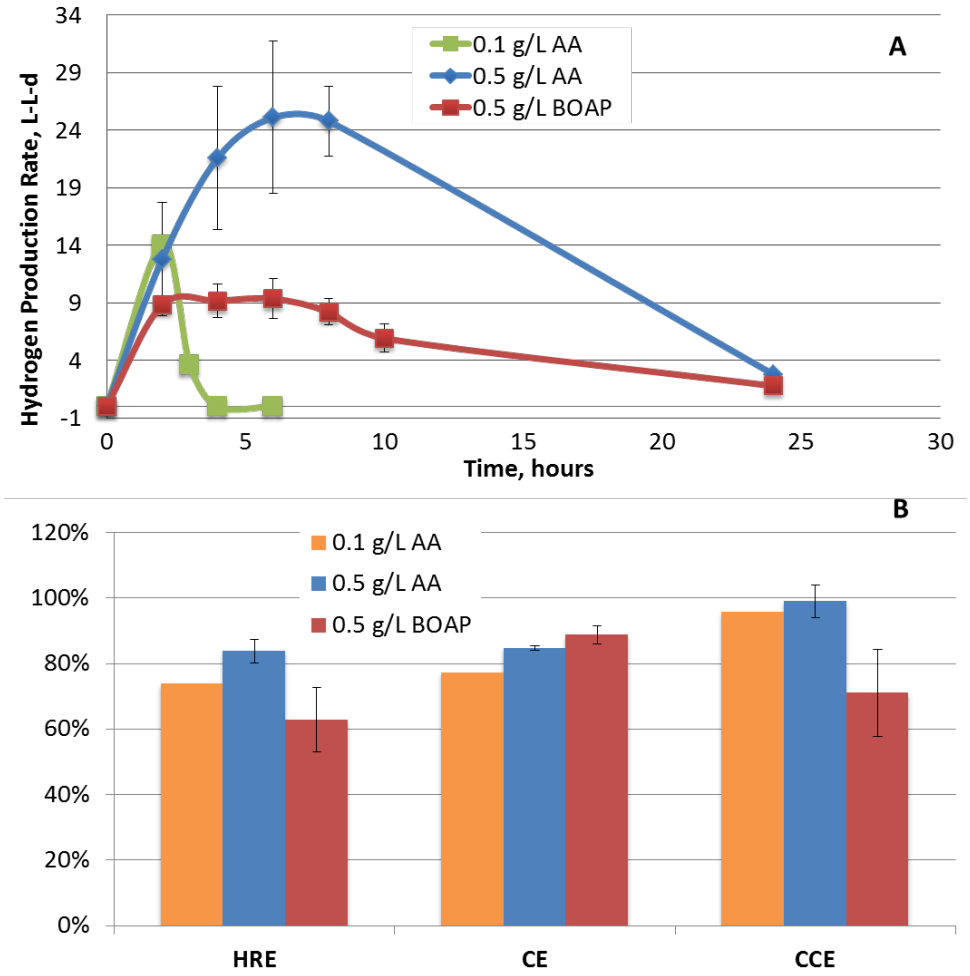

Figure 25: (A) Hydrogen productivity and (B) efficiency during batch experiments with BOAP and acetic acid as substrate.

For 0.1 and 0.5 g COD/L acetic acid, CE improved by 6.8 and 13.4% while HRE increased by 6.5 and 16.9%, respectively. However, as mentioned above, BOAP conversion was slower than for acetic acid, so experimental run time was continued beyond 24 hours to 72 hours. This increased overall CE by 17.5% to 88.77% ± 2.7% (Additional File 1: Figure S2). However, HRE and CCE were reduced to 62.81 ± 9.84% and 70.96 ± 13.25%, respectively. The improvement in CE for BOAP with extended run time is discussed in subsequent sections, and could be result of intracellular uptake/storage during the first 24 hours of BOAP conversion. The reduction in CCE and HRE for BOAP is likely the main reason for a lower total volume of H_2 compared to 0.5 g COD/L acetic acid, despite similar anode efficiencies. This outcome results from a lower and more prolonged current output from BOAP, resulting in a lower average cell voltage for the run with BOAP, which reduces the efficiency of H_2 production at the cathode. A similar observation has been reported in the literature [24,27]. The differences in current production from the two substrates, BOAP and acetic acid at the same concentration (0.5 g COD/L) indicate that the bioanode community was limited by fermentation of BOAP. Secondly, the observation that 0.5 g COD/L BOAP could produce 3-fold more H_2 compared to 0.1 g COD/L acetic acid at high anode efficiency indicates that the microbial community is capable of breaking down BOAP into intermediates, which serve as substrates for exoelectrogens. Another potential cause for lower current output with BOAP may be perceived to be inhibition by toxic furanic and phenolic compounds present in BOAP. However, our previous work in collaboration with Georgia Institute of Technology using the same microbial inoculum has shown that inhibition by these individual compounds and mixture of these compounds begins to occur only at a concentration two orders of magnitude higher than those used in this study. Thus, it is unlikely that inhibition is playing a significant role in limiting the BOAP conversion. Further evidence is provided in

subsequent sections. These results provide the first evidence that fermentative processes in conversion of biomass-derived liquids may be the limiting step in this process.

Comparing hydrogen productivity and Coulombic efficiency with those in the literature, Wang et al. were able to achieve a hydrogen production rate of 2.27 L/L-d and CE of 95% using molasses wastewater in a single chamber MEC. Lu et al. reached a hydrogen production rate of 1.41 L/L-d with a CE of 80% with fermentation effluent, which was further improved to 87% using lower applied voltage [19]. Additionally, Li et al. 2014 achieved a production rate of 3.43 L/L-d by coupling to a first step of dark fermentation to produce VFA's, and reached 72% CE [28]. So despite the fermentation limitation identified in this study, the maximum productivities and efficiencies reached of 9.3 L/L-d and 88.7% using the more recalcitrant BOAP stream compared to fermentation effluents and molasses wastewater. This demonstrates that fermentation step need not be separated from the exoelectrogenic step, and that higher performance and efficiency can be achieved in a single MEC using a specifically enriched biocatalyst.

BOAP intermediates generated during open-circuit stimulus

In order to determine and quantify the intermediates generated during fermentation of BOAP and to further test the hypothesis of fermentative limitations, another experiment with 0.5 g COD/L BOAP was carried out utilizing an open-circuit stimulus-response. This condition allows the system to reach open circuit voltage, preventing the carbon felt from acting as an electron acceptor, which halts exoelectrogenesis while enabling fermentation to proceed. During the interruption from 0-4 hours, acetic acid accumulation was observed at a steady rate of 8.63 ± 0.13 mg/h (Figure 26). The rate of acetic acid production may be slightly underestimated since part of it may be simultaneously consumed by exoelectrogens which have the ability to store

charge[29]. To assess the efficiency of acetic acid production from the compounds identified by HPLC, an electron equivalence analysis was conducted as described in the Experimental section. Approximately 43.20% of the electron equivalents present in the substrate were converted to acetic acid during the first two hours of open-circuit stimulus, which increased to 68.3% by the end of 4 hours. These results demonstrate that acetic acid is the major collective fermentation end product from the community during the conversion of BOAP.

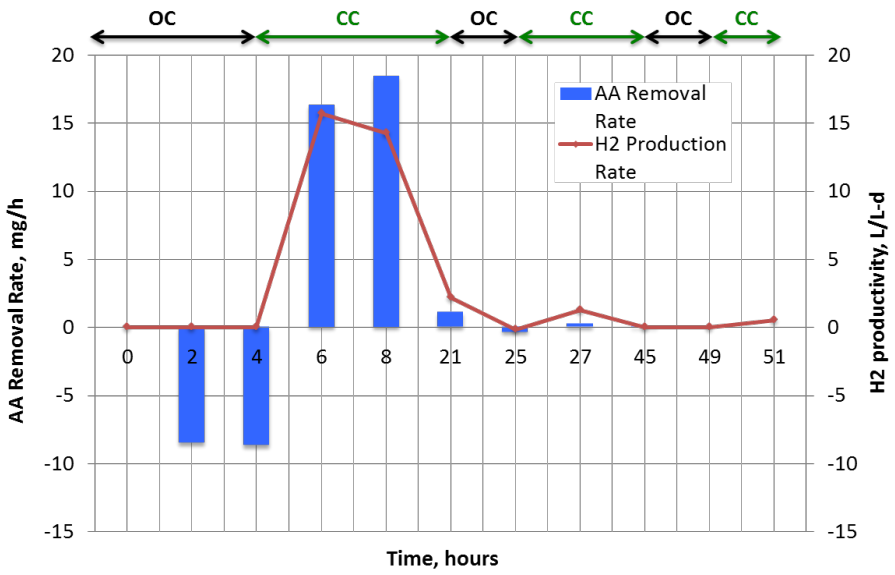

Figure 26: Acetic acid (AA) removal rates and hydrogen productivity during anode potential interruption experiment. OC: open circuit voltage, CC: set anode potential of -0.2 V vs Ag/AgCl reference electrode.

The remaining electrons not recovered at the end of 4 hours in the aqueous effluent, were likely taken up by the cells to form cellular biomass or stored internally as polyhydroxyalkanoates or intracellular metabolites. The electrochemical data collected post-4 hours was evidence for the latter since the coulombic efficiency obtained after poising the electrode was greater than 100%. Analysis of the aqueous effluent by HPLC showed that although additional fermentation byproducts were present, they were generated during closed circuit experiments as well. Only

acetate showed the trend representative of an exoelectrogenesis substrate via heavy accumulation during open circuit condition, and fast removal once re-poised, further suggesting that the other intermediates are not dominant fermentation end-products in our system. Additionally, their concentration was an order of magnitude lower than acetic acid, indicating that acetic acid was the dominant branching point to exoelectrogenesis. While it is possible that some of these compounds could serve as substrates for unknown exoelectrogens, many fermentation intermediates such as propionate, butyrate, ethanol and butanol have been shown to be directly used for exoelectrogenesis [15,23,30]. Additionally, as described in the community analysis section, some δ-*Proteobacteria* were found to persist during pure acetic acid experiments and thus could be diverting a small portion of acetic acid during open-circuit stimulus.

Considering the acetic acid production rate of 8.6 mg/h during open circuit conditions compared to the acetic acid removal rate of 58.7 mg/h achieved using 0.5 g COD/L of pure acetic acid (Appendix Table 9), it is clear that the exoelectrogenic microbial subpopulation is capable of converting acetic acid at higher rates than it is being produced from BOAP. Furthermore, after the circuit was closed following open-circuit stimulus, the current production reached a higher level than what was achieved without any interruption of circuit, further indicating the exoelectrogenic subpopulation is capable of higher current output, and that compounds within BOAP were not inhibitory to either of the subpopulation. Some intermediates produced from BOAP such as formate and lactate are likely substrates for exoelectrogenesis, however, they were not dominant products during the open circuit condition. The rate of exoelectrogenesis would be higher if they also serve as substrates for exoelectrogenesis. The observed results during open-circuit stimulus, compared to the closed-circuit experiment thus demonstrate that the rate of fermentation was the limiting step in conversion of BOAP to current.

Biotransformation of individual BOAP substrates under poised conditions

While previous work has demonstrated significant removal of the main compounds within BOAP by the end of the run and at high efficiency [25], the relative rates and order of conversion over time of the various components of the complex mixture BOAP have not been reported previously. The implications of this are significant, since pure microbial cultures can struggle with many of the lignin-derived compounds present in BOAP [31], while microbial communities can convert complex biomass streams containing these compounds via emerging synergistic capabilities within the consortium. The composition of BOAP is outlined in Appendix Table 10. The main compounds within BOAP were all transformed simultaneously within 48 hours, although at different rates (Figure 27). Overall COD removal reached 58.4% by 24 hours, and further increased to 74.8% by 72 hours. For the fermentable substrates, levoglucosan had the highest initial removal rate of 16.59 ± 0.59 mg/h over the first 2 hours of the batch run, followed by furfural with a rate of 1.35 ± 0.23 mg/h (Table 6). However, relative to starting concentrations, furfural had the highest initial removal percentage of 87.74 ± 1.33%, with levoglucosan reaching 58.93 ± 2.63%. HMF is another major fermentable compound present in BOAP, which was utilized at a lower rate initially with 28.88 ± 13.47% removal after two hours, but increased to 54.49 ± 6.46% after 10 hours. This may be due to lower microbial density or intrinsic reaction rates. For the fermentation byproducts acetic acid and propionic acid, their initial removal rates were 6.55 ± 4.36 and 2.83 ± 0.80 mg/h, respectively. However, because acetic acid is being produced through fermentation of the other compounds within BOAP simultaneously, it's true removal rate is underestimated. Nevertheless, the observation that concentration of acetic acid never increased with time demonstrates that its removal

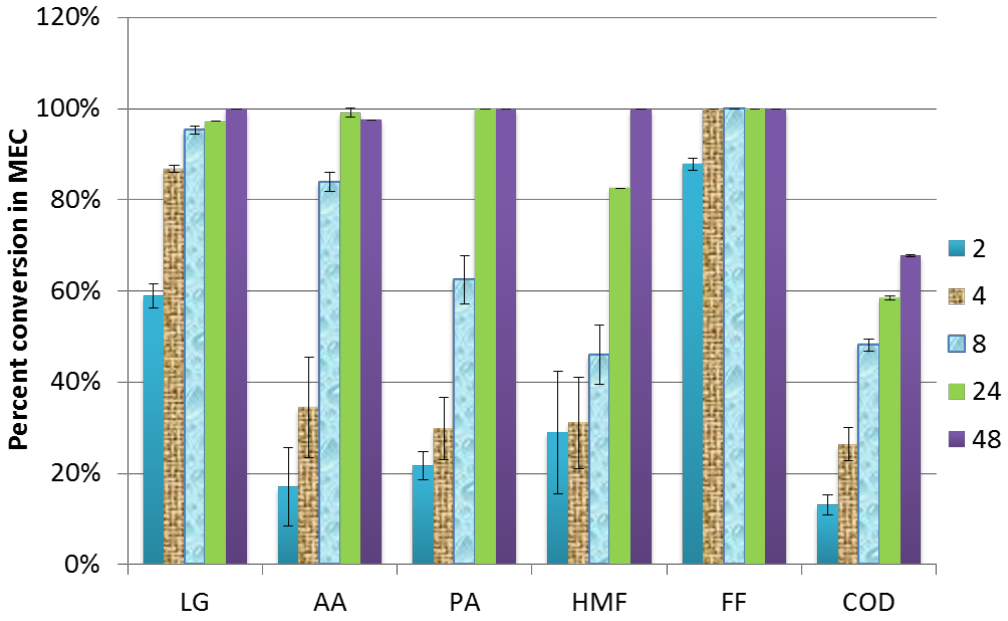

Figure 27: Percent removal of individual model compounds within BOAP as measured by HPLC. The legend refers to the hours at which samples were collected.

outpaced production. This can also be the case for additional intermediate compounds produced during the conversion of BOAP as phenol and catechol have been identified intermediates from larger phenolic compounds in the literature[33] and their concentrations were found to fluctuate during our experiments. However, their concentration at the end of the experiment was lower than the starting concentration, indicating that they were still utilized by the anode consortium, ablbeit to a more limited extent.

To further understand the productivity, efficiency, and biotransformation trends observed during the conversion of BOAP, the theoretical contributions from each compound identified by HPLC toward H_2 production were calculated via an electron equivalence calculation similar to that described in the previous section (Figure 28). This calculation relies on the assumption that removal of the parent compounds results in their complete conversion to CO_2, electrons, and protons. The bars on the y-axis show equivalent rate of hydrogen production if all electrons were

Table 6: Removal rates of individual compounds in mg/h during batch experiment with BOAP as substrate.

Time	2	4	6	8	10	24
levoglucosan	16.59 ± 0.59	7.83 ± 0.59	2.36 ± 0.04	0.04 ± 0.18	-0.01 ± 0.24	0.08 ± 0.06
acetic acid	6.55 ± 4.36	6.48 ± 2.11	9.62 ± 0.85	8.38 ± 1.06	3.66 ± 1.05	0.24 ± 0.03
propionic acid	2.83 ± 0.8	1.07 ± 0.63	2.97 ± 0.14	1.30 ± 1.37	1.45 ± 0.88	0.47 ± 0.03
HMF	0.55 ± 0.44	-0.05 ± 0.39	0.17 ± 0.28	0.14 ± 0.03	0.17 ± 0.15	0.08 ± 0.03
2(5H)-furanone	0.39 ± 0.1	0.02 ± 0.02	0.00	0.00	0.00	0.00
Catechol	0.07 ± 0.07	0.03 ± 0.01	-0.03 ± 0.02	0.02 ± 0.01	-0.01 ± 0.03	-0.02 ± 0.02
furfural	1.35 ± 0.23	0.19 ± 0.01	0.00	0.00	0.00	0.00
phenol	-0.01 ± 0.13	0.04 ± 0.04	0.01 ± 0.04	0.01 ± 0.06	0.00 ± 0.04	0.01± 0.01
COD	32.43	33.01	43.43	10.42	N/A	3.19

recovered as hydrogen at the cathode. While assuming 100% conversion is not possible, visualization in this manner allows us to estimate the extent to which the observed results deviate from this condition in discrete time frames. The results show a lag in hydrogen production compared to the rate of substrate removal. This is not unexpected since the substrate concentrations measured at the various time points are indicative of disappearance of substrate and not necessarily complete conversion. Furthermore, comparing Figure 4a and b, we can see an inverse trend in the first 6 hours, with contributions attributed to individual compound removal starting high and dropping off, while overall COD-based contribution starts lower and increases with time. This is indicative of production of biotransformation intermediates or cellular storage, contributing to increasing COD removal from 0-6 hours, followed by a decreasing trend thereafter. Coulombic efficiency from to 6-24 hours exceeded 100% during normal poised conditions, indicating that intracellular storage was being tapped in addition to the substrate present.

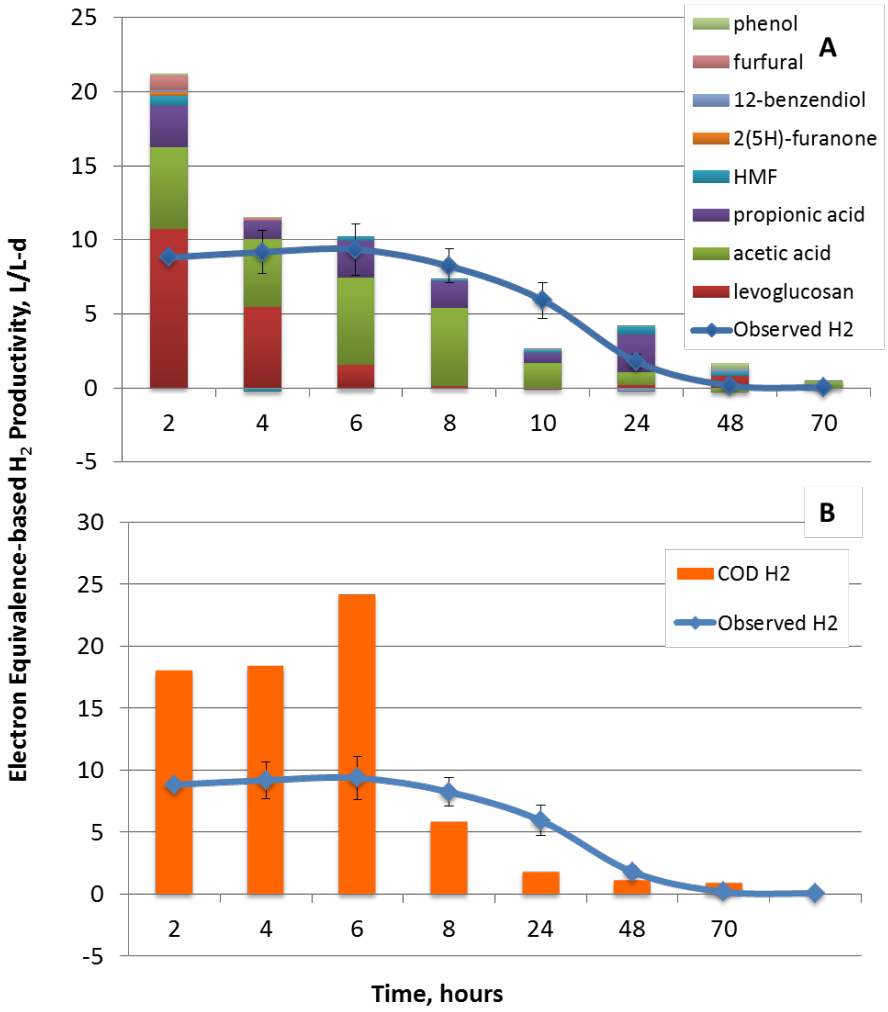

Figure 28: (A) Comparison of hydrogen productivity obtained experimentally with that estimated via electron equivalence calculation for conversion of individual compounds within BOAP. (B) COD contributions to hydrogen productivity based on electron equivalence compared to observed hydrogen productivity.

Community Analysis

The bioanodes used in these experiments had been exposed to BOAP and adapted to this substrate for >2 years, and have evolved and enriched for BOAP conversion and acetate oxidation [6]. Focusing first on two important groups in the microbial community, exoelectrogens and methanogens, the results show different trends depending on the substrate used (Figure 29b). Exoelectrogens, represented by the family *Geobacteraceae* increased from 1.9% to 33.0%, when BOAP was used as the substrate. A similar trend was seen when pure acetic acid was used as the substrate, increasing the population density of the exoelectrogens from 15.6% to 54.0%. On the contrary, the population of methanogens showed an opposite trend. With BOAP as the substrate, the methanogenic *Euryarchaeota* increased from 2.2% to 17.2%, while their population decreased from 13.1% to 1.8% with acetic acid as the substrate. Two inferences can be derived from these results. First, batch additions of acetic acid as well as BOAP provide a large amount of acetate, which is preferred by *Geobacter* for growth and exoelectrogenesis, thus explaining their growth with both substrates. Secondly, the fact that the population of methanogens was only observed to increase when using the complex fermentable substrate and decreased with pure acetic acid indicates the methanogens present in the anode are not acetoclastic and are likely hydrogenotrophic. Thus, the methanogen population is mainly feeding on intermediates produced during the fermentation process such as H_2 and CO_2 rather than the end product acetate, which is predominantly used by the exoelectrogenic fraction[29,32]. The growth of methanogens is a well-documented issue in bioelectrochemical systems even at low organic loading rates, and thus poses a significant challenge for controlling their growth at higher, industrially relevant levels [33,34]. The difference in exoelectrogen population at the start

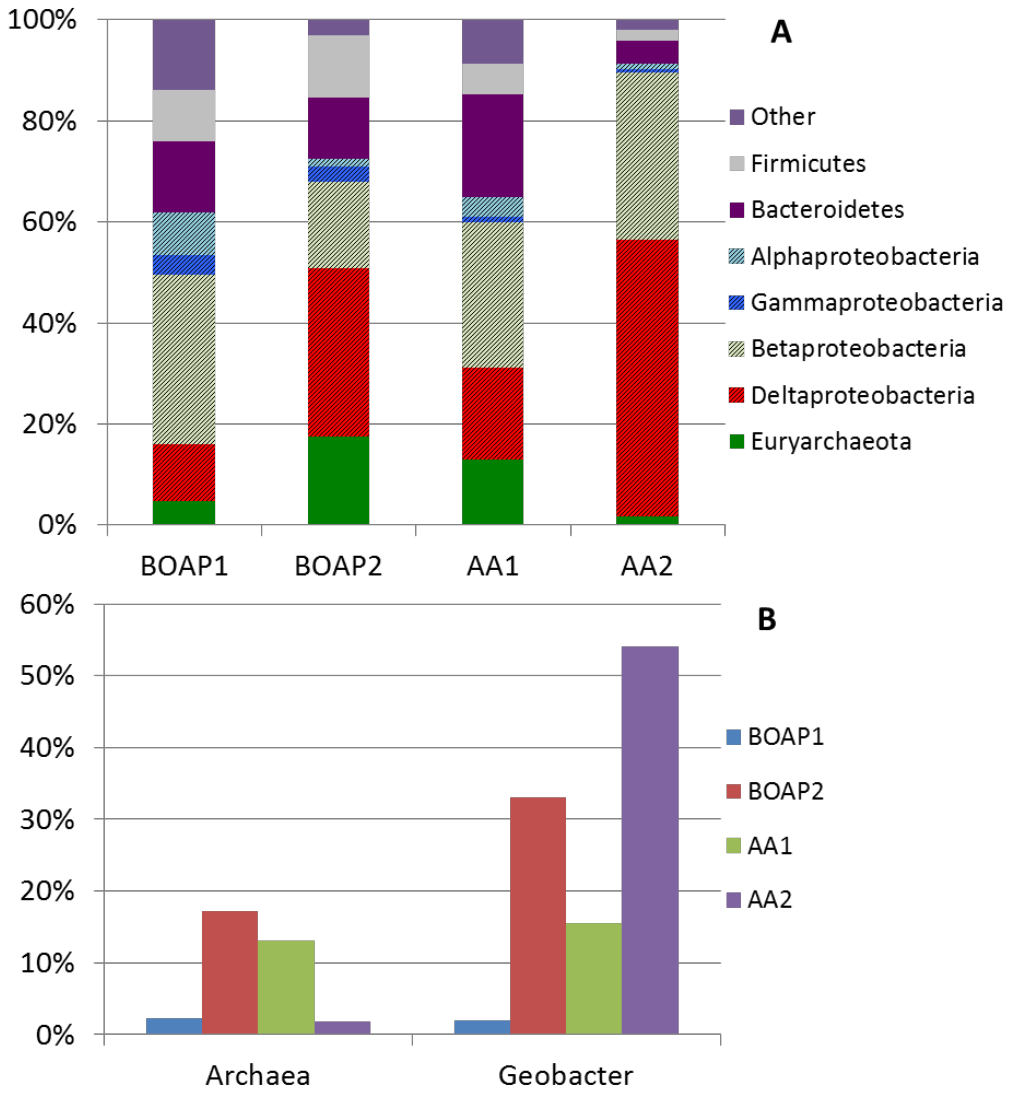

Figure 29: 16S rRNA-based taxonomical classification of the MEC community for batch BOAP vs acetic acid experiments. Numbers 1 &2 indicate samples collected at the beginning (1) and the end (2) of each batch series. (A) Bar chart showing taxonomy of the MEC anode community at the phylum level with sub-classification of the Proteobacteria at class level. (B) Trends in Archaea vs Geobacter subpopulations observed with the two substrates.

and end of BOAP and acetic acid experiments differed greatly, which highlights the effect of substrate and fermentation limitation. Performance in terms of efficiency and current output did not improve as the *Geobacter* population increased with BOAP as the substrate during this study. This is because the amount of *Geobacter* is not the main determining factor for performance in the BOAP-fed system, but rather a consequence of the use of BOAP in the anode. An experiment conducted post-acetic acid run using BOAP as the substrate showed similar current as that produced prior to the use of acetic acid as substrate in the MEC (Appendix Figure 33). As demonstrated in previous section, fermentation of BOAP to end products like acetate is a limiting factor in the bioanode conversion process. Once the substrate was switched to pure acetate, the exoelectrogens no longer relied on fermentation to produce the substrates they need and current production increased 3-fold and the *Geobacter* population increased further to 54%. Thus, limited availability of acetic acid limits *Geobacter* growth and affects its population in the anode. This was clearly illustrated by the experiment which was conducted post the acetic acid run (Appendix Figure 33). This indicates that the current production in MEC is not necessarily determined by the *Geobacter* population, but by the substrate used in the MEC.

In addition to the changes in *Geobacter* and methanogen population, additional taxonomic groups including Firmicutes, Bacteroidetes and multiple classes of *Proteobacteria* also demonstrated trends as a function of substrate Figure 29a). Firmicutes, and Bacteroidetes persisted during BOAP experiments at >10% of the population, but were reduced significantly when acetic acid was used as the substrate. *Gamma*p*roteobacteria* also showed this trend but to a lower extent. This indicates that these microbes are active in the fermentation of parent or intermediate compounds from BOAP, and cannot be sustained on acetate alone. Firmicutes have been found frequently in bioelectrochemical anodes when fermentable substrates have been used

[35,36] and this phylum houses many biomass degraders and glucose fermenters in *Clostridia*. Additionally, certain microbes within *Gammaproteobacteria* and Bacteroidetes have also been found to only persist when fed with fermentable sugars [37]. In contrast, *Betaroteobacteria* declined during BOAP experiments but persisted during pure acetic acid, although it should be noted that this class did still remain at high levels during BOAP feeding despite the overall reduction (Figure 5B). Looking closer at the family level of *Betaoteobacteria* (Additional File 1: Figure S4) *Rhodocyclaceae*, and *Comamonadaceae* have been identified in our previous work and house a wide metabolic range of microbes [25,36,38-41]. While these families have been implicated in degradation of complex carbon compounds they have also been found to have abilities in acetate utilization [42] and some members of *Comamonadaceae* have also been found to be capable of electricity generation [40], which would explain both of their abilities to persist during pure acetic acid feeding.

Emergent functionality in engineered community

The conversion of phenolic and furanic compounds provides a significant challenge to fermentation of BOAP, as these classes of compounds are known to be inhibitory to many microbes [31]. Fermentation of the furanic compounds furfural and HMF have been found to produce intermediates such furoic acid, furfuryl alcohol, 2,5-bis(hydroxymethyl)furan, requiring further biotransformation to be converted to acetic acid [43,44]. Additionally, phenolic compounds such as phenol and catechol are even more recalcitrant, with fermentation proceeding most slowly for these types of compounds in the experiments presented in this study. Many of these intermediates including phenol, catechol and furoic acid were found in MEC effluent when BOAP served as the substrate. The comparative studies with BOAP and acetic acid show that the

microbial groups were established and enriched in the anode to collectively participate in a fermentative chain that is capable of oxidizing the complex carbon compounds within BOAP progressively to acetic acid. The evidence presented in this study suggests that the microbial community utilize a synergistic strategy through mutually beneficial division of labor and syntrophic exchange as depicted in Figure 30 that results in emergent functionality in converting the wide array of compounds within BOAP. Division of labor was evident through the simultaneous conversion of identifiable compounds, which allows for parallel processing and allocation of compounds to various microbes with different functionality and metabolic capabilities. This type of cooperative interaction within microbial communities is seen in natural environments and in engineered settings, manifesting into various ways of enhancing overall substrate utilization [45 46-49]. This may also help prevent the toxic effects of many of these compounds on other community members Downstream from this initial division of labor, the co-conversions of the fermentable substrates converge to acetic acid as demonstrated by open-circuit stimulus-response. This leads to syntrophic cross-feeding from fermentative groups to exoelectrogenic groups for the generation of current, and is the foundation for electricity generation from fermentable substrates [16,29,30]. Compounds such as levoglucosan were strongly preferred within the BOAP mixture by the microbial community, which is not unexpected as it is a sugar derivative, leading to the fastest removal rate. One of the pathways through which levoglucosan can be degraded is using levoglucosan kinase to convert it to glucose-6 phosphate [50-53]. This pathway generates acetic acid and thus the conversion of levoglucosan to acetic acid can occur in a single organism. Conversely, conversion of the phenolic and furanic compounds may require multiple steps. Catechol, phenol, and furoic acid were found in the MEC effluent and were found to fluctuate with time during the experimental run, indicating their production

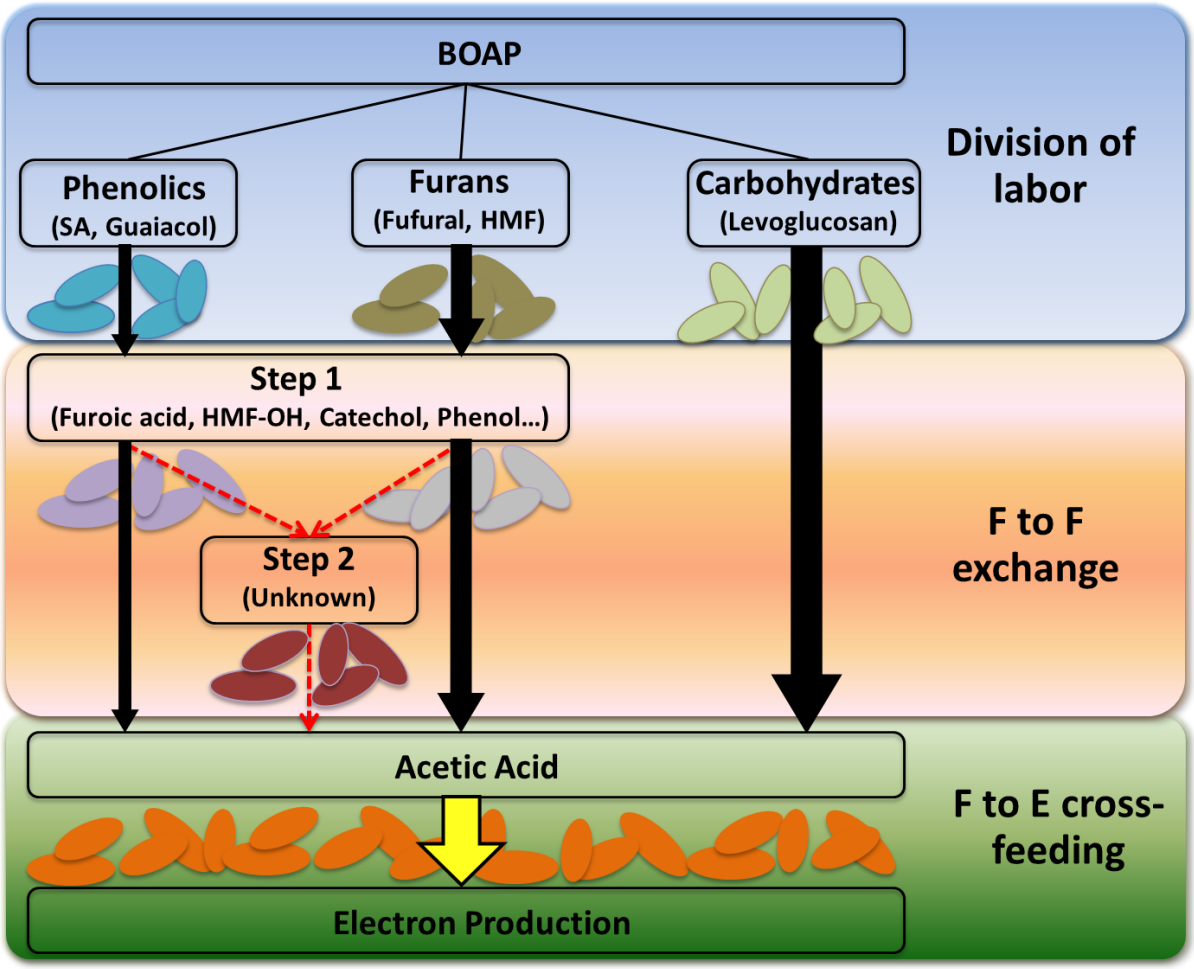

Figure 30: Schematic of possible pathways active in anode microbiome for conversion of fermentable compounds within BOAP. "F" corresponds to fermentative bacteria, "E" corresponds to exoelectrogenic bacteria. Intermediate level 1 includes compounds such as phenol, catechol, furoic-acid, which were observed experimentally. VA: Vanillic acid, SA: Syringic Acid, HBA: Hydroxybenzoic acid, HMF: Hydroxymethylfurfural.

from other compounds present in BOAP. These compounds have been identified as intermediates in the conversion of methoxy phenols and furanic compounds in a MEC which used the same source of enrichment used in these studies [43]. Thus, exchange of carbon between community members may be occurring at several levels for multiple compounds during biotransformation of the lignin and hemicellulose-derived intermediates. Syntrophies that direct electrons away from the electrode were also evident. An increase in the population of *Euryarchaeota* which functions to re-direct fermentation intermediates through methanogenesis, was found. Nonetheless, CE for the BOAP batch runs reached >80% demonstrating an efficient and robust community that can convert cellulose, hemicellulose and lignin-derived pyrolytic intermediates including inhibitory compounds at appreciable rates, providing a foundation for further improvements to reach commercial targets.

Bioelectrochemical systems for biorefining applications

The need for integrated solutions to the current renewable challenges facing the world continues to grow, and new innovative approaches to fully utilize lignocellulosic feedstocks will be essential. Bioelectrochemical systems have the potential for integration into variety of bioenergy platforms to help meet this goal [5,6]. MECs offer the potential to produce hydrogen in an integrated fashion in biorefinery platforms and as a means of energy storage through decentralized production to supply hydrogen to fueling stations, as the world strives to move toward cleaner fuels and electricity-mediated transportation. This study integrates a number of novel features into one to address practical applications such as use of MECs in biorefineries. These include:

1. Approach of comparing complex substrate, BOAP vs Acetate, using open and closed

circuit conditions to understand fermentation vs. exoelectrogenesis relevant to biorefinery streams

2. Community focus to understand the interactions within functional microbial groups. This can allow identifications of conditions to promote positive interactions and ways to minimize negative interactions
3. Overall integrative/systems approach, looking at metabolites (individual compounds within mixture), genomics, and electrochemical data
4. Use of high performing MEC design capable of achieving high productivity and CE without using high concentration of substrates

The demonstrated maximum rates with BOAP in this study are nearing the targets needed for practical application[54], and almost 30-fold higher than that identified by US DOE Fuel Cell Technology Office as state of the art [55]. Alternate technologies such as *in vitro* synthetic enzyme systems have achieved comparatively high yields and productivities of 29 L/L-day (54 mmol H_2/L-h) utilizing both xylose and glucose from corn stover hydrolysate[44]. The study presented here is a big step towards realizing the use of renewable waste biomass as a feedstock vs. sugars or natural gas for hydrogen production.

As shown in this study, developing an emergent microbial community capable of efficiently producing hydrogen from all constituents of biomass can be accomplished, but further work is necessary to increase the productivity to 20 L/L-day or more to enable commercial consideration. This can be achieved via targeted increase in fermentative population. The generation of electrons from waste biomass has significant implications for the production of high-value chemicals as well. This can be done via integration of electrosynthesis at the cathode

[56,57] with the bioanode developed in this study. Future work will focus on utilizing deep sequencing techniques to better understand the interactions among active groups within the microbial community and additional environmental factors impacting performance. Building on methods previously established such as those using operational "shocks" coupled to metatranscriptomic analysis identification of functional roles of different community members is possible [58]. Providing the right environment for improving fermentation, while reducing competing pathways such as methanogenesis can enhance the production of acetic acid from BOAP. Continued efforts in these areas can lead to the development of an optimal microbial community management strategy for developing stable and high performing electroactive biofilms while contributing to overall strategies for engineering microbial communities for additional industrial applications.

Conclusions

Renewable H_2 production from biomass-derived streams is approaching targets for practical application utilizing bioelectrochemical systems that leverage the emergent capabilities of microbial communities. A maximum productivity of 9.35 ± 1.73 L/L-d with BOAP was achieved with a switchgrass-derived pyrolysate. The productivity was increased 3-fold to 27.6 ± 5.29 L/L-d using pure acetic acid, demonstrating the potential capability of this system. The enriched microbial community demonstrated efficient and simultaneous conversion of a wide range of compounds through synergistic division of labor strategy and multi-substrate syntrophy demonstrated by open-circuit stimulus-response, effectively directing the biomass electrons to intermediates such as acetic acid at an efficiency of 68.3%. However, the rate of fermentation and production of intermediates which could serve as substrates for exoelectrogenesis limited the

system productivity. This study serves to provide a foundation from which to build on for understanding biocomplexity in bioelectrochemical systems for conversion of biomass-derived streams and toward the development of community management and engineering strategies for enabling renewable hydrogen production.

References

1. Jones S, Meyer P, Snowden-Swan L, et al. *Process design and economics for conversion of lignocellulosic biomass to hydrocarbon fuels*: PNNL;2013. PNNL-23053, NREL/TP-5100-61178.
2. FCTO. *State of the States: Fuel Cells in America*: Fuel Cell Technologies Office; November 2016 2016.
3. Rahman S, Masdar M, Rosli MI, et al. Overview biohydrogen technologies and application in fuel cell technology. *Renewable and Sustainable Energy Reviews.* 2016;66:137-162.
4. Singh A, Sevda S, Abu Reesh IM, Vanbroekhoven K, Rathore D, Pant D. Biohydrogen production from lignocellulosic biomass: technology and sustainability. *Energies.* 2015;8(11):13062-13080.
5. Borole AP. Improving energy efficiency and enabling water recycle in biorefineries using bioelectrochemical cells. *Biofuels, Bioproducts & Biorefining.* 2011-09-29 2011;5(1):28-36.
6. Borole AP. Microbial Electrochemical Cells and Biorefinery Energy Efficiency. In: Cong T, Eckert C, eds. *Biotechnology for Biofuel Production and Optimization, Edition 1*. New York: Elsevier; 2016:449-472.
7. Borole AP. Microbial Fuel Cells and Microbial Electrolyzers. *The Electrochemical Society - Interface.* Fall 2015 2015;24(3):55-59.
8. Zuroff TR, Curtis WR. Developing symbiotic consortia for lignocellulosic biofuel production. *Applied Microbiology and Biotechnology.* 2012;93(4):1423-1435.
9. Cardinale S, Arkin AP. Contextualizing context for synthetic biology–identifying causes of failure of synthetic biological systems. *Biotechnology journal.* 2012;7(7):856-866.
10. Kumar P, Barrett DM, Delwiche MJ, Stroeve P. Methods for pretreatment of lignocellulosic biomass for efficient hydrolysis and biofuel production. *Industrial & engineering chemistry research.* 2009;48(8):3713-3729.
11. Lovley DR. Dissimilatory metal reduction. *Annual Reviews in Microbiology.* 1993;47(1):263-290.
12. Nealson KH, Saffarini D. Iron and manganese in anaerobic respiration: environmental significance, physiology, and regulation. *Annual Reviews in Microbiology.* 1994;48(1):311-343.
13. Lalaurette E, Thammannagowda S, Mohagheghi A, Maness PC, Logan BE. Hydrogen production from cellulose in a two-stage process combining fermentation and electrohydrogenesis. *International Journal of Hydrogen Energy.* Aug 2009;34(15):6201-6210.
14. Mahmoud M, Parameswaran P, Torres CI, Rittmann BE. Relieving the fermentation inhibition enables high electron recovery from landfill leachate in a microbial electrolysis cell. *Rsc Advances.* 2016;6(8):6658-6664.
15. Miceli JF, Garcia-Peña I, Parameswaran P, Torres CI, Krajmalnik-Brown R. Combining microbial cultures for efficient production of electricity from butyrate in a microbial electrochemical cell. *Bioresource Technology.* 2014;169:169-174.
16. Parameswaran P, Torres CI, Lee HS, Krajmalnik-Brown R, Rittmann BE. Syntrophic

Interactions Among Anode Respiring Bacteria (ARB) and Non-ARB in a Biofilm Anode: Electron Balances. *Biotechnology and Bioengineering.* Jun 2009;103(3):513-523.
17. Wang A, Sun D, Cao G, et al. Integrated hydrogen production process from cellulose by combining dark fermentation, microbial fuel cells, and a microbial electrolysis cell. *Bioresource Technology.* 2011;102(5):4137-4143.
18. Marone A, Ayala-Campos OR, Trably E, et al. Coupling dark fermentation and microbial electrolysis to enhance bio-hydrogen production from agro-industrial wastewaters and by-products in a bio-refinery framework. *International Journal of Hydrogen Energy.* 2017;42(3):1609-1621.
19. Lu L, Ren NQ, Xing DF, Logan BE. Hydrogen production with effluent from an ethanol-H-2-coproducing fermentation reactor using a single-chamber microbial electrolysis cell. *Biosensors & Bioelectronics.* Jun 2009;24(10):3055-3060.
20. Wang Y, Guo W-Q, Xing D-F, Chang J-S, Ren N-Q. Hydrogen production using biocathode single-chamber microbial electrolysis cells fed by molasses wastewater at low temperature. *International Journal of Hydrogen Energy.* Nov 11 2014;39(33):19369-19375.
21. Thygesen A, Marzorati M, Boon N, Thomsen AB, Verstraete W. Upgrading of straw hydrolysate for production of hydrogen and phenols in a microbial electrolysis cell (MEC). *Applied Microbiology and Biotechnology.* 2011;89(3):855-865.
22. Shen R, Liu Z, He Y, et al. Microbial electrolysis cell to treat hydrothermal liquefied wastewater from cornstalk and recover hydrogen: Degradation of organic compounds and characterization of microbial community. *International Journal of Hydrogen Energy.* 2016;41(7):4132-4142.
23. Hari AR, Katuri KP, Gorron E, Logan BE, Saikaly PE. Multiple paths of electron flow to current in microbial electrolysis cells fed with low and high concentrations of propionate. *Applied Microbiology and Biotechnology.* 2016;100(13):5999-6011.
24. Lewis AJ, Borole AP. Understanding the Impact of Flow Rate and Recycle on the Conversion of a Complex Biorefinery Stream Using a Flow-Through Microbial Electrolysis Cell. *Biochem. Eng. J.* 2016;in press(Special Issue: Advances in Biorefinery Engineering).
25. Lewis AJ, Ren S, Ye X, Kim P, Labbe N, Borole AP. Hydrogen production from switchgrass via a hybrid pyrolysis-microbial electrolysis process. *Bior. Technol.* 2015;195:231-241.
26. Ghimire A, Frunzo L, Pirozzi F, et al. A review on dark fermentative biohydrogen production from organic biomass: process parameters and use of by-products. *Applied Energy.* 2015;144:73-95.
27. Gil-Carrera L, Escapa A, Carracedo B, Moran A, Gomez X. Performance of a semi-pilot tubular microbial electrolysis cell (MEC) under several hydraulic retention times and applied voltages. *Bioresource Technology.* Oct 2013;146:63-69.
28. Li X-H, Liang D-W, Bai Y-X, Fan Y-T, Hou H-W. Enhanced H-2 production from corn stalk by integrating dark fermentation and single chamber microbial electrolysis cells with double anode arrangement. *International Journal of Hydrogen Energy.* Jun 5 2014;39(17):8977-8982.
29. Freguia S, Rabaey K, Yuan ZG, Keller J. Syntrophic Processes Drive the Conversion of Glucose in Microbial Fuel Cell Anodes. *Environ Sci Technol.* Nov 2008;42(21):7937-

7943.
30. Kiely PD, Regan JM, Logan BE. The electric picnic: synergistic requirements for exoelectrogenic microbial communities. *Current Opinion in Biotechnology.* 2011;22(3):378-385.
31. Jarboe LR, Liu P, Royce LA. Engineering inhibitor tolerance for the production of biorenewable fuels and chemicals. *Current Opinion in Chemical Engineering.* 2011;1(1):38-42.
32. Ishii S, Hotta Y, Watanabe K. Methanogenesis versus electrogenesis: Morphological and phylogenetic comparisons of microbial communities. *Biosci Biotechnol Biochem.* Feb 2008;72(2):286-294.
33. Cusick RD, Bryan B, Parker DS, et al. Performance of a pilot-scale continuous flow microbial electrolysis cell fed winery wastewater. *Applied Microbiology and Biotechnology.* Mar 2011;89(6):2053-2063.
34. Escapa A, Lobato A, Garcia DM, Moran A. Hydrogen production and COD elimination rate in a continuous microbial electrolysis cell: The influence of hydraulic retention time and applied voltage. *Environmental Progress & Sustainable Energy.* Jul 2013;32(2):263-268.
35. Jung S, Regan JM. Comparison of anode bacterial communities and performance in microbial fuel cells with different electron donors. *Appl. Microbiol. Biotechnol.* Nov 2007;77(2):393-402.
36. Rismani-Yazdi H, Christy AD, Dehority BA, Morrison M, Yu Z, Tuovinen OH. Electricity generation from cellulose by rumen microorganisms in microbial fuel cells. *Biotechnol Bioeng.* Aug 2007;97(6):1398-1407.
37. Ishii Si, Suzuki S, Norden-Krichmar TM, et al. Microbial population and functional dynamics associated with surface potential and carbon metabolism. *The ISME journal.* 2014;8(5):963-978.
38. Borole AP, Hamilton CY, Vishnivetskaya TA, Leak D, Andras C. Improving power production from acetate-fed microbial fuel cells via enrichment of exoelectrogenic organisms in continuous flow systems. *Biochem. Eng. J.* 2009;48:71-80.
39. Hesselsoe M, Füreder S, Schloter M, et al. Isotope array analysis of Rhodocyclales uncovers functional redundancy and versatility in an activated sludge. *The ISME journal.* 2009;3(12):1349-1364.
40. Xing DF, Cheng SA, Logan BE, Regan JM. Isolation of the exoelectrogenic denitrifying bacterium Comamonas denitrificans based on dilution to extinction. *Applied Microbiology and Biotechnology.* Feb 2010;85(5):1575-1587.
41. Oren A. The Family Rhodocyclaceae. In: DeLong EF, Lory S, Stackebrandt E, Thompson FL, eds. *The Prokaryotes: Alphaproteobacteria and Betaproteobacteria* Berlin, Heidelberg: Springer Berlin Heidelberg; 2014.
42. Ginige MP, Keller J, Blackall LL. Investigation of an acetate-fed denitrifying microbial community by stable isotope probing, full-cycle rRNA analysis, and fluorescent in situ hybridization-microautoradiography. *Applied and Environmental Microbiology.* 2005;71(12):8683-8691.
43. Wierckx N, Koopman F, Ruijssenaars HJ, de Winde JH. Microbial degradation of furanic compounds: biochemistry, genetics, and impact. *Applied Microbiology and Biotechnology.* 2011;92(6):1095-1105.

44. Zeng X, Borole AP, Pavlostathis SG. Biotransformation of furanic and phenolic compounds with hydrogen gas production in a microbial electrolysis cell. *Environ. Sci. & Technol.* 2015;49(22):13667-13675.
45. Hays SG, Patrick WG, Ziesack M, Oxman N, Silver PA. Better together: engineering and application of microbial symbioses. *Current opinion in biotechnology.* 2015;36:40-49.
46. Eiteman MA, Lee SA, Altman E. A co-fermentation strategy to consume sugar mixtures effectively. *Journal of biological engineering.* 2008;2(1):1.
47. Briones A, Raskin L. Diversity and dynamics of microbial communities in engineered environments and their implications for process stability. *Current Opinion in Biotechnology.* 2003;14(3):270-276.
48. Crespi BJ. The evolution of social behavior in microorganisms. *Trends in ecology & evolution.* 2001;16(4):178-183.
49. Fröstl JM, Overmann J. Physiology and tactic response of the phototrophic consortium "Chlorochromatium aggregatum". *Archives of Microbiology.* 1998;169(2):129-135.
50. Layton DS, Ajjarapu A, Choi DW, Jarboe LR. Engineering ethanologenic Escherichia coli for levoglucosan utilization. *Bioresource Technology.* 2011;102(17):8318-8322.
51. Dai J, Yu Z, He Y, et al. Cloning of a novel levoglucosan kinase gene from Lipomyces starkeyi and its expression in Escherichia coli. *World Journal of Microbiology and Biotechnology.* 2009;25(9):1589-1595.
52. Zhuang X, Zhang H. Identification, characterization of levoglucosan kinase, and cloning and expression of levoglucosan kinase cDNA from Aspergillus niger CBX-209 in Escherichia coli. *Protein expression and purification.* 2002;26(1):71-81.
53. Kitamura Y, Abe Y, Yasui T. Metabolism of Levoglucosan (1, 6-Anhydro-α-d-glucopyranose) in Microorganisms. *Agricultural and Biological Chemistry.* 1991;55(2):515-521.
54. Sleutels T, Ter Heijne A, Buisman CJN, Hamelers HVM. Bioelectrochemical Systems: An Outlook for Practical Applications. *Chemsuschem.* Jun 2012;5(6):1012-1019.
55. EERE. Hydrogen production: Fuel Cell Technologies Program Multi-Year Research, Development and Demonstration Plan. 2015; http://energy.gov/eere/fuelcells/downloads/fuel-cell-technologies-office-multi-year-research-development-and-22.
56. Borole AP. Bioelectrochemical Systems, Energy Production and Electrosynthesis. *J. Microbial & Biochemical Technology.* 2012;4(7):xv-xvi.
57. Rabaey K, Girguis P, Nielsen LK. Metabolic and practical considerations on microbial electrosynthesis. *Current Opinion in Biotechnology.* Jun 2011;22(3):371-377.
58. Ishii Si, Suzuki S, Norden-Krichmar TM, et al. A novel metatranscriptomic approach to identify gene expression dynamics during extracellular electron transfer. *Nature Communications.* 2013;4:1601.
59. Caporaso JG, Lauber CL, Walters WA, et al. Ultra-high-throughput microbial community analysis on the Illumina HiSeq and MiSeq platforms. *The ISME journal.* 2012;6(8):1621-1624.
60. Logan BE, Call D, Cheng S, et al. Microbial electrolysis cells for high yield hydrogen gas production from organic matter. *Environ. Sci. Technol.* Dec 2008;42(23):8630-8640.

Appendix

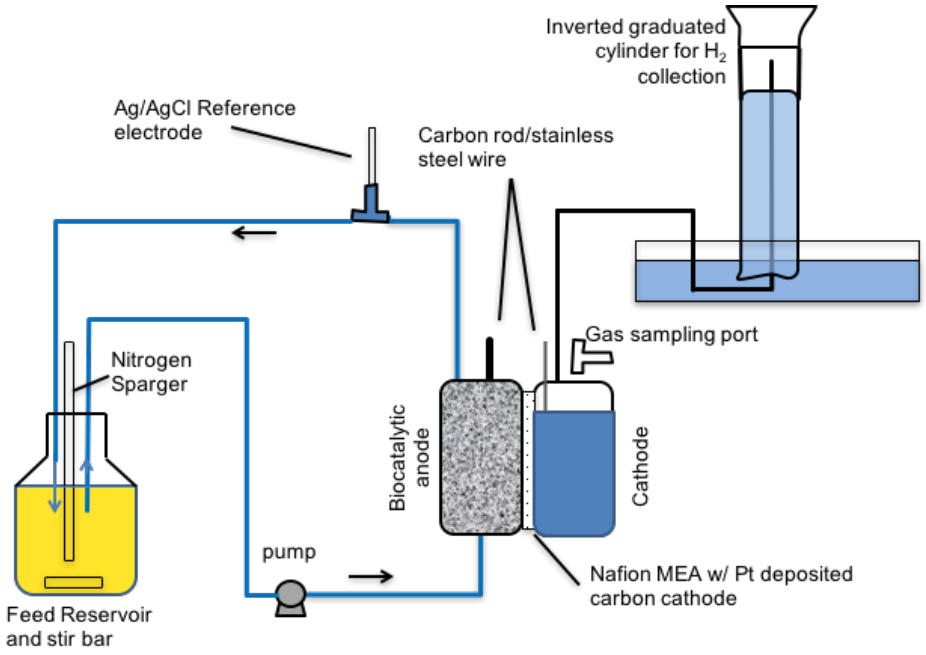

Figure 31: Schematic of MEC system investigating hydrogen production under batch conditions.

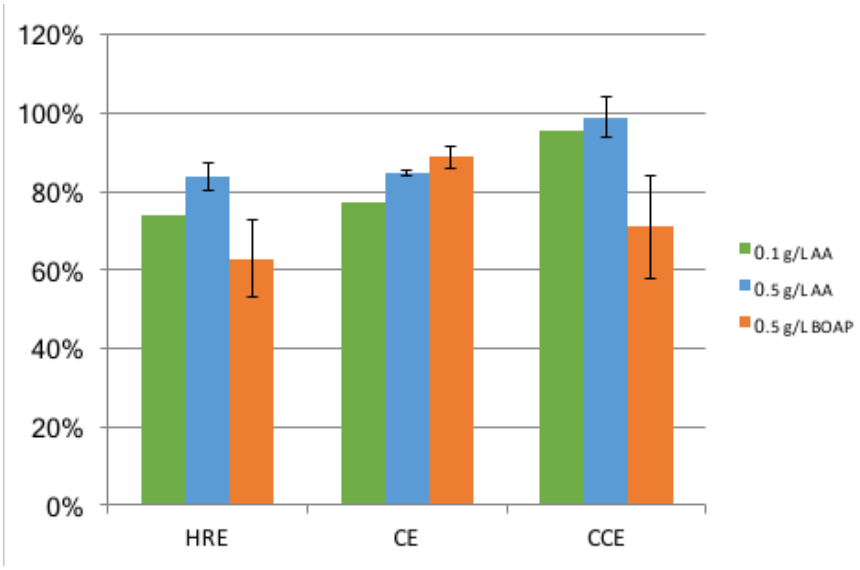

Figure 32: Efficiency during batch experiments with BOAP and acetic acid as substrate for entire runs.

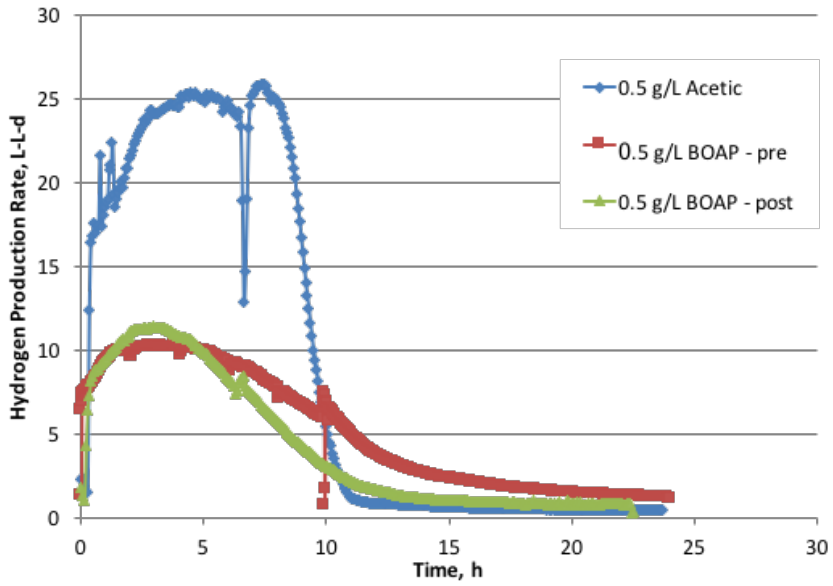

Figure 33: Fig. S3: Hydrogen productivity during comparing run before and after acetic acid use.

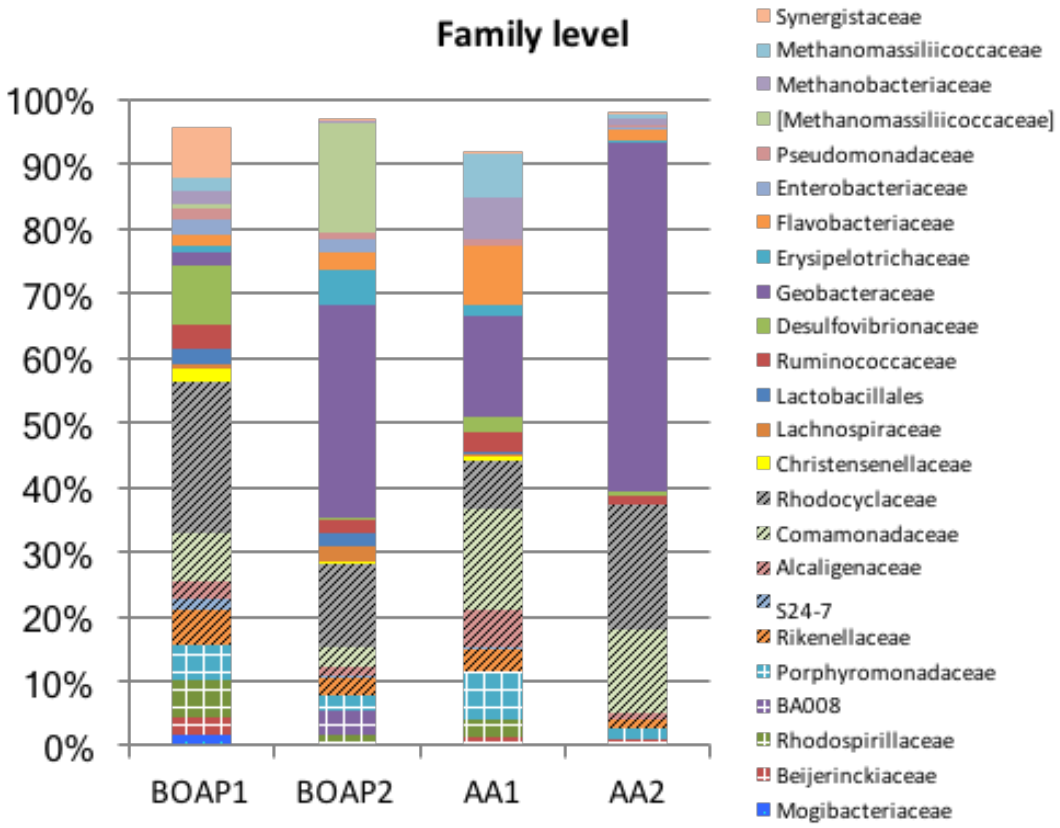

Figure 34: 16S r RNA-based taxanomical classification to the family level for batch BOAP vs acetic acid. Numbers 1,2 indicate samples from beginning (1) and end (2) of each batch series.

Table 7: Table S1: Calculation of the electrons liberated through the theoretical conversion of 1 mol of compound/COD to 1 mol of acetic acid.

Compound	**Conversion**
Levoglucosan	$C_6H_{10}O_5 + 7H_2O = 6CO_2 + 24H^+ + 24e^-$
Acetic acid	C2H4O2 + 2H2O = 2CO2 + 8H + 8e
Propionic acid	$C_3H_6O2 + 4H_2O = 3CO_2 + 14H^+ + 14e^-$
HMF	$C_6H_6O_3 + 9H_2O = 6CO_2 + 24H^+ + 24e^-$
2(5H)-Furanone	$C_4H_4O_2 + 6H_2O = 4CO_2 + 16H^+ + 16e^-$
Catechol	$C_6H_6O_2 + 10H_2O = 6CO_2 + 26H^+ + 26e^-$
Furfural	$C_5H_4O_2 + 8H_2O = 5CO_2 + 20H^+ + 20e^-$
Phenol	$C_6H_6O + 11H_2O = 6CO_2 + 27H^+ + 27e^-$
COD	$CH_2O + H_2O = CO_2 + 4H^+ + 4e^-$

Table 8: Table S2: Cumulative hydrogen production from each batch experiment.

Time	**MEC-A**	**MEC-B**
0.1 g/L AA	19.00	17.50
0.5 g/L AA	128.25 ± 5.73	118.80 ± 7.35
0.5 g/L BOAP	48 ± 4.95	62.85 ± 11.81

Table 9: Table S3: Acetic acid and COD removal rates for each batch experiment.

Time	**2**	**4**	**6**	**8**	**24**
0.1 g/L AA	33.89	6.60	0.00		
0.5 g/L AA	37.32 ±8.11	53.01 ±8.10	48.62 ±1.15	53.10 ±2.02	4.34 ±0.96
0.5 g/L BOAP	32.43	33.01	43.43	10.42	3.19

Table 10: Table S4. Concentrations of major chemical compounds in bio-oil aqueous phase quantified by HPLC-PDA and GC-FID.

Quantification method	Major chemicals	Concentration based on aqueous phase (g/L)
HPLC-PDA	Furfural	1.01
	1,2-benzendiol	1.77
	Phenol	1.8
	Levoglucosan	15.33
	Acetic acid	11.96
	Proponic acid	1.89
	Vanillic acid	2.69
	HMF	0.54
	Total	36.99
GC-FID	Phenol, 2-methoxy-	0.25
	2-methyl-4-methyphenol	0.07
	Cyclohexanone	0.07
	3-methyl-1,2-cyclophetandiol	0.46
	2,6-Dimethoxyphenol	0.26
	1,3-propanediol	1.84
	3-ethylphenol	0.56
	2(5H)-Furanone	1.17
	1-hydroxybutanone	1.35
	Total	6.02
	Sum	43.01

CHAPTER V

EFFECT OF FEEDING REGIME ON MEC PERFORMANCE AND MICROBIAL COMMUNITY STRUCTURE FOR BIOREFINERY APPLICATIONS

This chapter is derived from a manuscript currently in preparation.

AJL designed and carried out batch experiments, electrochemical analyses, HPLC analysis, COD analysis, GC analysis, data interpretation and manuscript preparation. APB provided guidance in experimental designed and manuscript preparation. We acknowledge Professor Xiaofei Ye, Pyoungchung Kim and Shouji Ren for their work in producing the bio-oil aqueous phase.

Abstract

In order for bioelectrochemical systems to reach their commercial potential, a better understanding of the reactors perform under different operating conditions and resulting impact on the microbial community need to be better understood. Continuous operation was carried out at 2 and 20 g/L-d, and directly compared to fed-batch operation with same total of substrate added. Changes in electrochemical performance, metabolite profiles, electron flux and microbial community structure were tracked across the different conditions. At the lower level, similar microbial communities and electrochemical performance resulted. At the high loading conditions tested, continuous operation resulted in better performance and more stable output compared to fed-batch operation. Average H_2 productivity and current density at 20 g/L-d reached 7.9 ± 0.4 L/L-d and 9.2 ± 0.6 A/m^2 while fed-batch operation produced average values of 4.27 ± 3.2 L/L-d and 5.1 ± 3.3 A/m^2, respectively dropping drastically in the 2nd week of performance to current densities below 1 A/m^2. This high concentration environment resulted in different selective pressures, increasing the proportion of fermenting organisms such as *Firmicutes,* including the family *Ruminococcaceae,* while selecting for different strains of *Geobacter*, which may have contributed to reduced performance. Additionally, electron diversion to undefined sinks

increased to 69.7% ± 5.6% during fed-batch operation at a concentration of 2.5 g/L. Continuous operation was able to mitigate these effects better compared to fed-batch operation, but further insights into the mechanistic details of the process are needed to uncover specific structure-function dynamics and how to maintain these positive interactions.

Introduction

Opportunities to enhance the viability of advanced biofuel technologies lie with the ability to fully utilize the entire feedstock and co-produce high-value commodities in addition to fuel[1]. Many proposed technologies such as pyrolysis, hydrothermal liquefaction of algae, and lignocellulosic fermentations produce waste streams that must be valorized. Focusing on the production of biofuel from lignocellulosic feedstocks via pyrolysis, a significant amount of hydrogen is needed for upgrading of the produced bio-oil for generating drop-in fuel hydrocarbons[2]. The ability to produce hydrogen from process waste stream from pyrolysis, or other conversion technologies, can significantly reduce treatment costs as well as reduce expenditures on external sources of hydrogen. Microbial electrolysis is an emerging technology capable of handling robust waste streams with high efficiency and is thus a prime candidate for biorefinery integration.

While crops can be typically harvested in large batches, fuel demands are constant and thus many potential biorefineries may strive for continuous operation[3], which means a continuous production of waste streams. While this does not fundamentally preclude batch operations from functioning economically, it does pose additional challenges such as the need for storage tanks etc. However, many biochemical companies rely on batch or fed-batch operations as their means of production, and reactor designs and operation for this type of fermentation are well developed.

Thus, with MEC development in it's infancy, understanding the impact of different feeding regimes on performance will be important for reaching commercial applications. Recent studies have made strides in understanding the impact of operating conditions and bottlenecks[4–8] , but additional work is required for reaching commercial applications. While trends of increasing H_2 productivity with loading rate and flow-rate were demonstrated in the above examples, studies comparing the impact of specific feeding regimes are sparse. Using a corn stover-derived waste stream, Pannell et al. found that MECs fed continuously maintained a more stable Coulombic efficiency (CE) while fed-batch operation dropped over time with increasing concentration[9]. Additionally, they found hydrogen productivity to increase with OLR while output decreased with fed-batch as the concentration increased. However, disparate working concentration levels between batch vs continuous mode in this study may have impacted the results. Additional studies have sought to design high-performing continuous systems using a CSTR-adapted MFC system to achieve high COD removal and power density with brewery wastewater[10] while another utilized carbon nanotubes to achieve high COD removal and good productivity using corn-stover wastewater derived from hydrothermal liquefaction[11]. A fed-batch study using straw hydrolysate observed accumulation of phenols over time with low productivity[12]. Zeng et al. also found that model compounds within BOAP can be inhibitory to the key microbial process of exoelectrogenesis, and the toxicity is raised with compounds in combination[13]. Thus, lignocellosic-derived streams must consider this into operational design.

In this study, we set out to create truly comparable conditions for batch vs continuous operation by using the same experimental run time with the same amount of total substrate added over that period. This allows for a more realistic comparison of the differences between the two feeding regimes, and any resulting differences in performance that may impact commercial

applications. We utilized a previously described switchgrass-derived bio-oil aqueous phase(BOAP)[14], and two different sets of replicate reactors enriched on BOAP. Biotransformation of individual compounds within BOAP as well as overall COD removal were measured for each condition. Additionally, changes to the microbial community of each reactor were characterized via 16s rRNA analysis after each test to investigate the impact on community structure and determine the relationship between mode of operation, community structure and MEC performance.

Methods

MEC construction and enrichment

The two-chambered MEC system utilized has equal anode and cathode volumes of 16 ml each with a projected area 12.56 cm^2. A porous carbon felt was used as anode material and a membrane electrode assembly consisting of Nafion-115 and Pt-deposited carbon cathode between the two chambers. A carbon rod and stainless steel wire served as current collectors in the two chambers, respectively. The anode chamber utilizes an up-flow design with an external media reservoir for recirculation of unconverted compounds with a flow-rate of 3.6 mL/min. Two replicate MEC anode communities developed in previous studies were split to create a 2nd pair of replicate reactors[7,8].

MEC operation

In all reactors, continuous vs fed-batch operation was carried out in succession. Each condition was tested for a period of 3 weeks, with weekly media changes. However, for the

highest batch level tested, a period of 2 week was utilized due to degradation in reactor performance. The first set of replicate reactors began with 4 g/L-d OLR followed by fed-batch operation with 0.5 g/L BOAP feeding every 40 hours, to achieve the same total substrate added. In the 2nd set of replicate reactors, the initial OLR was 20 g/L-d BOAP, followed by fed-batch operation of 2.5 g/L BOAP added every 40 hours. Additionally, this second set of reactors was allowed to have a longer growth period to develop a higher biomass density for operating at higher loading and fed-batch conditions prior to testing. Following the 20 g/L-d period, a recovery period was employed to recover performance back to starting levels prior to initiating fed-batch operation. During the recovery period, a lower loading of 2 g/L-d was utilized for 4-7 days as a precautionary measure to alleviate any possible inhibition that may have occurred during long-term exposure to high loading and return current densities to those obtained at beginning of continuous operation. A constant anode potential of -0.2 V vs Ag/AgCl was used throughout and the resulting cell potentials were tracked as well. Anode and cathode pH were not strictly controlled but were adjusted on a daily basis, with the 20 g/L-d and 2.5 g/L fed-batch conditions receiving continuous NaOH addition to minimize pH fluctuations. Anode pH values ranged between 7.1-6.5, and cathode pH ranged from 6.9-13.5 during the daily operation.

Metabolite analysis

Biotransformation of individual compounds as well as overall COD removal were measured from effluent samples collected from anode effluent at the end of each week-long run for each condition tested. Additionally, anode and cathode off-gas measurements were also made at this time. COD analysis was carried out using Hach HR COD (20–1500 mg/L COD) vials and were digested in a Hach DRB 200 reactor at 150°C for 2 hours. Samples were then cooled to

room temperature before measuring absorbance at 620 nm on Spectronic 20 Genesys. For HPLC analysis, a Jasco 2000Plus (Jasco analytical instruments) equipped with PU-2089S Plus pump, a MD-2018 Plus Photodiode Array detector (PDA), a RI-2031 Plus intelligent RI detector was utilized with 5 mM H_2SO_4 mobile phase at flow-rate of 0.6 ml/min. Gas samples were collected via air-tight syringe and analyzed by gas chromatography (GC).

Microbial community analysis

Microbial community samples were taken at the end of each condition through a sampling port on the back of the anode chamber [3]. The core sample was placed in a sterile centrifuge tube or freezer vial and stored at -80 °C. DNA was extracted from each sample using a MoBio Power Biofilm DNA extraction kit, following manufacturer's protocol (Qiagen, Germantown, MD). Library prep was then carried out on the extracted DNA for 16S analysis on Illumina MiSeq following the methods of Caporaso et al.[15] PCR products cleaned and concentrated using Zymo DNA Clean and Concentrator and then quality checked via Bioanalyzer and Kapa qPCR. Sequencing was carried out with Illumina MiSeq 250 bp PE run, and sequence data analyzed via Qiime [4].

Calculations

Performance and conversion efficiency were characterized by Coulombic efficiency (CE), cathodic conversion efficiency (CCE), hydrogen recovery (HRE), and were calculated as previously described[14,16].

Results and Discussion

Hydrogen productivities and efficiencies

H_2 productivity and current density for 4 g/L-d averaged 2.19 ± 0.02 L/L-d and 2.65 A/m^2, which increased by 30.1% and 20.0% upon shifting to fed-batch, reaching 2.85 ±0.27 L/L-d and 3.18 A/m^2, respectively. The results in Figure 35 indicate that fed-batch operation resulted in additional growth of the microbial community with current and hydrogen output increasing over time, and this can be seen clearer from the raw data of current output after each feeding (Appendix Figure 39). The max current density increased steadily from 8.8 to 15.4 A/m^2 over the 3-week period tested while a noticeable increase in current for the reactor operated with continuous feeding did not occur. Additionally, all efficiency values increased for fed-batch operation. The anode CE and CCE increased by ~6% each, reaching 74.1 ± 3.9% and 85.5 ± 3.3%, respectively. The HRE increased by 10% to 63.3 ± 4.6%. COD removal, however, did not follow this trend and decreased from 67.8 ± 4.8% to 59.8 ± 2.7% during fed-batch operation, which is interesting given the increase in current over this period.

Continuous operation of the MECs at 20 g/L-d increased hydrogen productivity and current output to 7.9 ± 0.4 L/L-d, while the current density reached 9.2 ± 0.6 A/m^2. At the higher loading, the higher availability of acetate provided via the substrate as well as that produced from the other compounds in BOAP was the likely reason for continued increase in output. However, CE could not be maintained under this condition and dropped to 52.3 ± 3.7%. Additionally, CCE was slightly lower at 82.1 ± 1.4%, which may be due to proton limitation in the cathode [5].

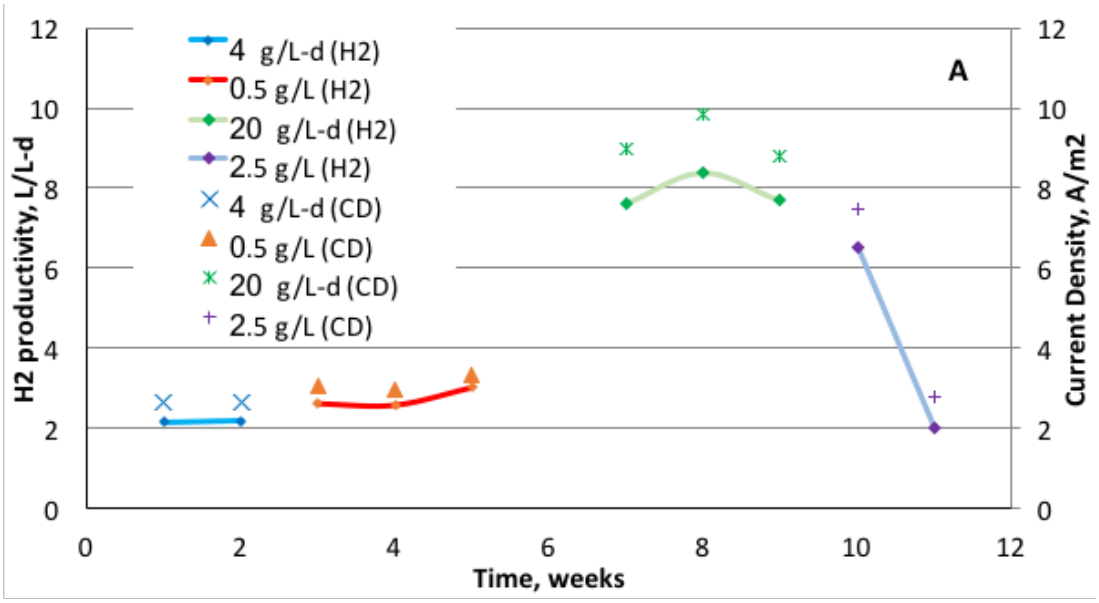

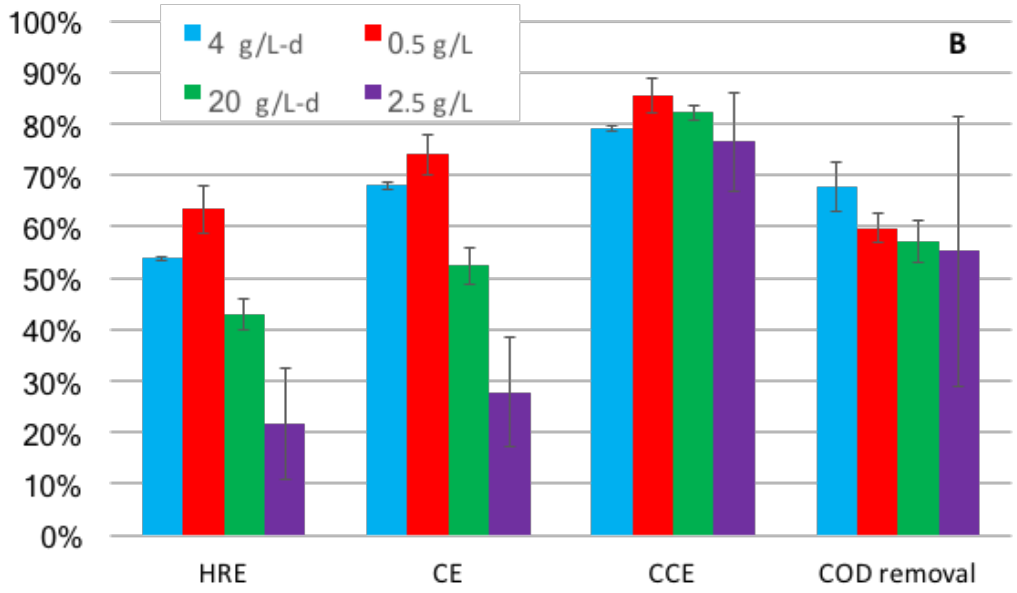

Figure 35: (A) MEC performance obtained under continuous and fed-batch mode of operation at various loading conditions. The units g/L-d in the legend refer to continuous mode of operation, while g/L refers to fed-batch mode of operation. (B) MEC efficiency and COD removal during continuous and fed-batch mode of operation. HRE: Hydrogen Recovery, CE: Anode Coulombic Efficiency, CCE: Cathode Conversion Efficiency.

Shifting to fed-batch mode at this higher level of substrate supply resulted in a substantial reduction in performance. Fed-batch operation initially resulted in high current and H_2, reaching max levels of 14 A/m^2 after each of the first two feedings, but declined rapidly thereafter. Output decreased to below 1 A/m^2 within two weeks. The fed-batch experiment was discontinued for the 3rd week due to the degradation in performance. The average CE and COD removal over this period was 27.8 ± 10.6% and 55.2 ± 26.3%. Cathode efficiency was able to remain relatively high at 76.5 ± 9.6%. This is a surprising result given the significant decrease in current over the two week period. The cathode voltage was found to decrease significantly resulting in average cell voltage of -0.55 V for this condition. In comparison, the 20 g/L-d run had an average cell voltage of -1.1 V, twice that of the fed-batch condition while only a 5.6% increase in CCE was observed. The low voltage of -0.55 V is still sufficient to generate hydrogen, and since the hydrogen production rate was low, the cathode was likely to not be limited by protons either, thus resulting in high CCE.

Microbial community Analysis

Changes in the microbial community structure were observed during both fed-batch and continuous operating conditions. The Figure 36a shows the progression of the community under the four conditions tested, analyzed at the end of each operation period. The population density of *Deltaproteobacteria* comprising mainly of *Geobacteraceae* increased slightly between continuous and fed-batch mode of operation at the lower loading condition. However, it decreased at the higher loading conditions. Comparing the fed-batch experiments at the two loading conditions, despite the higher acetic acid concentrations present at the higher loading level, the *Deltaproteobacteria* population declined from 47.0% to 28.4% at 2.5 g/L (Figure2a).

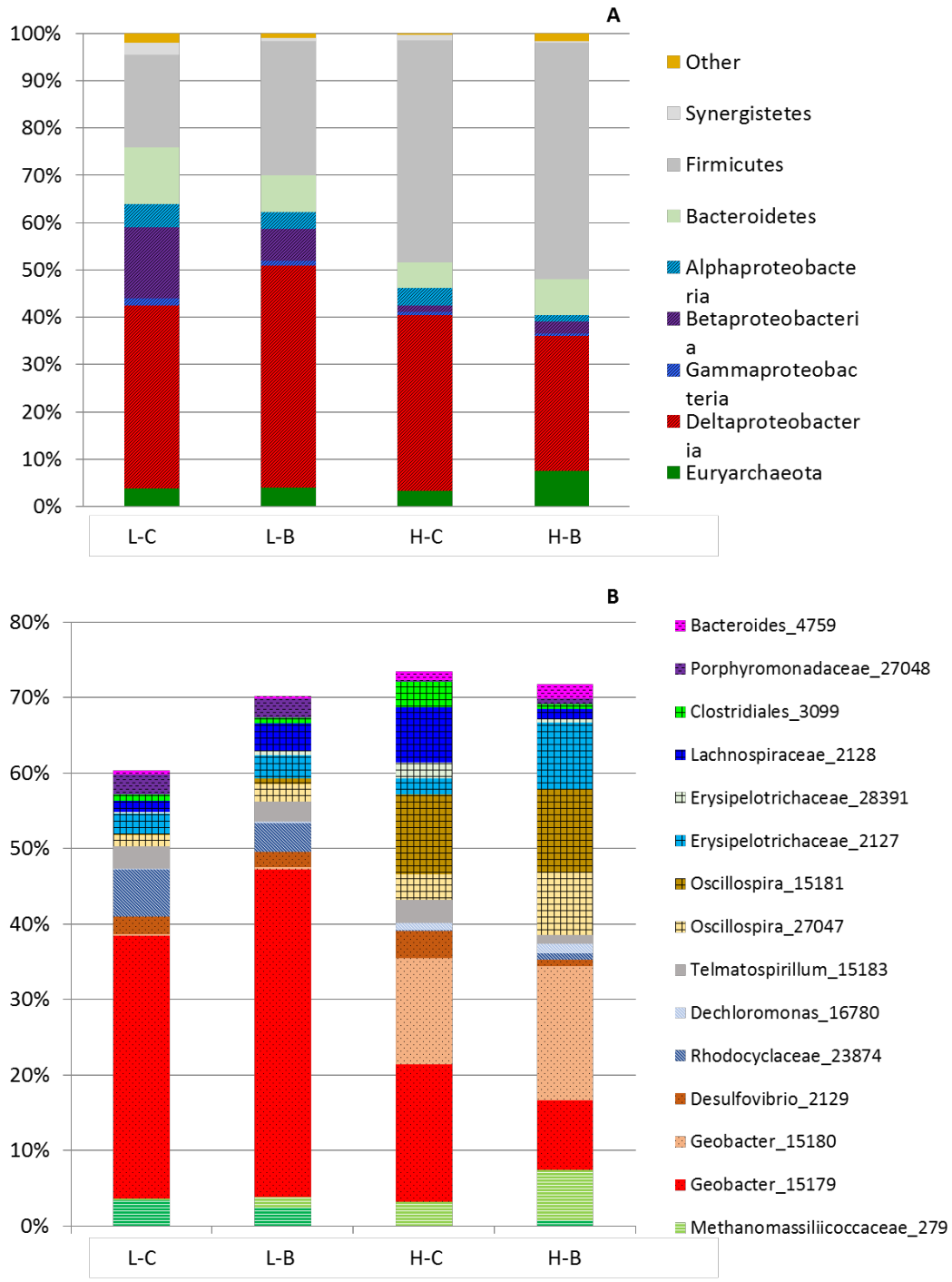

Figure 36: Characterization of microbial community in MEC under different conditions. A. Analysis at the phylum level. B. Analysis at the family and genus level.

This drop was even more significant in the 2nd replicate reactor (data not shown). Additionally, *Betaproteobacteria* declined rapidly after the first condition (L-C), decreasing from 15.1% at 4 g/L-d, to 1.5% at 20 g/L-d (H-C). The Bacteroidetes and Euryarchaeota populations remained fairly stable throughout, while the Firmicutes population rose rapidly from 19.5% at 4 g/L-d, to 50.1% at 2.5 g/L (H-B). Looking deeper into the changes in the community structure, individual OTUs within the groups above were analyzed in the context of the observations at the phylum and class level. While the overall *Deltaproteobacteria* and *Geobacteraceae* population decreased overall at the higher loading levels, we can see that two different Geobacter OTUs had differing preferences for the conditions investigated. Geobacter_15179 dominated the lower loading conditions reaching 43.4% at 0.5 g/L (Figure 36b); however, this was overtaken rapidly by another Geobacter (15180) at the higher loadings dropping to 9.2% at 2.5 g/L (H-B), in line with the overall trend for the parent family, *Deltaproteobacteria*. However, Geobacter_15180 was observed to take its place increasing to 14.2% (H-C) and 17.8% (H-B) from a lower population density of ~0.2-0.3% at the lower levels. The total population of *Deltaproteobacteria*, however, was much lower than that under low loading conditions. This indicates that the different loading/concentration conditions resulted in differing competitive advantages between these two Geobacter strains, resulting in a strong reversal in relative proportions. It appears thatGeobacter_15180 is better suited to survive in the high BOAP environment. Within the phylum *Firmicutes*, the families *Ruminococcaceae* and *Erysipelotrichaceae* have been implicated in acidogenesis and displayed a strong preference for the higher substrate conditions including *Oscillospira* OTUs, with the overall family increasing from 4.2 and 6.7% to 23.5 and 27.8%. The family *Ruminococcaceae* also has known cellulolytic as well and acetogenic abilities[17–19], while the *Oscillospira* genus has been found in the rumen of cattle and other

animals[17] and have been identified as butyrate producer[20]. Lachnospiraceae_2128 increased in proportion up to 7.4% at 20 g/L-d (H-C), but was not sustained and dropped to 1.4% at 2.5 g/L (H-B). *Lachnospiraceae* has been shown to contain H_2 consumers[19] appears likely that upon shifting toward volatile fatty acid production, reduced its proportion in the community while allowing organisms within *Ruminococcaceae* to proliferate.

Electron balance

The flow of electrons into different anode products of current, methane, and undefined sinks were tracked over the length of each operational condition and averaged to determine the fate of electrons derived from BOAP (Figure 37). The proportion of electrons directed to current production was highest at the lower conditions averaging ~70%, with methane accounting for the remaining 30% with flow to undefined sinks mostly minimal. Diversion of electrons to undefined sinks increased drastically with the increase in working concentration that accompanies the 20 g/L-d and 2.5 g/L fed-batch operation, increasing to 39.5 ± 2.4% and 69.7% ± 5.6% while progressively decreasing the flow of electrons to current and methane. Miceli et al. also observed a reduction in the proportion of electrons diverted to methane as substrate concentration increased[21], similar to observations in this study. However, the decrease in electrons to methane were captured in the production of VFAs. However, the electron balance calculations in this study are based only on the COD analysis of the effluent. The undefined sinks are likely to consist of cellular biomass and intracellular storage. Community analysis above showed strong growth of *Firmicutes* during the high loading conditions, which must have diverted a considerable portion of electrons extracted from BOAP towards is growth. Freguia et al. have reported intracellular storage to occur during pulsed carbon addition in a microbial fuel

cell. [22]. During continuous operation at 20 g/L-d and 2.5 g/L fed-batch operation, it is likely that substrate concentration levels remained high enough to promote intracellular storage, likely contributing to the observed increase of electron diversion to undefined sinks. Additionally, Esteve-Nunez et al. observed evidence for the ability of exoelectrogens to over-express cytochromes for charge storage[23]. Inhibition of exolectrogens during high loading conditions as well as protons limitations in the cathode could result in a restriction of current flow, leading to charge storage and a depression of observed electrons captured as current.

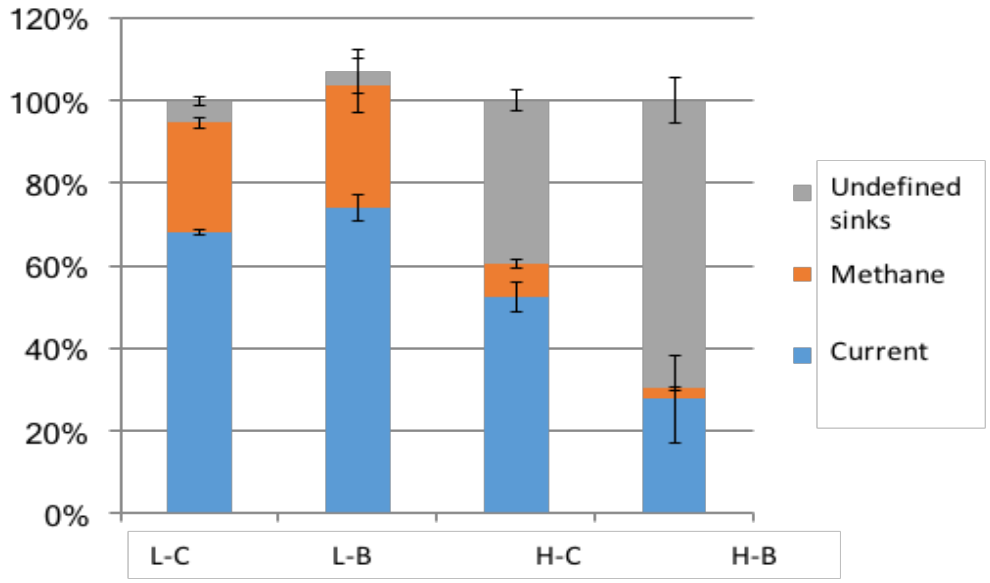

Figure 37: Distribution of electrons in the products at the end of the MEC experiments. L-C: Continuous operation at 4 g/L-d, L-B: Fed-batch operation at 0.5 g/L, H-C: Continuous operation at 20 g/L-d, H-B: Fed-batch operation at 2.5 g/L.

Biotransformation of compounds within BOAP

The extent of biotransformation across the 10 compounds analyzed was similar between the two lower level conditions except for the phenolic compounds of catechol, phenol and syringic acid (Figure 38). Accumulation of catechol to -124.8% was seen during fed-batch operation, while 42.4% removal was observed during continuous operation. Almost 80%

reduction in phenol and syringic acid was observed during continuous feeding at 4 g/L-d, however, it dropped to ~15% during fed-batch operation. Under the higher loading condition of 20 g/L-d, catechol removal increased compared to the lower loading condition. This may be due to an increase in population of the microbes consuming catechol. Its accumulation was not observed under fed-batch operation at the 2.5 g/L loading condition, but compared to the continuous operation, its removal dropped substantially from 83.6% to 36.4%.

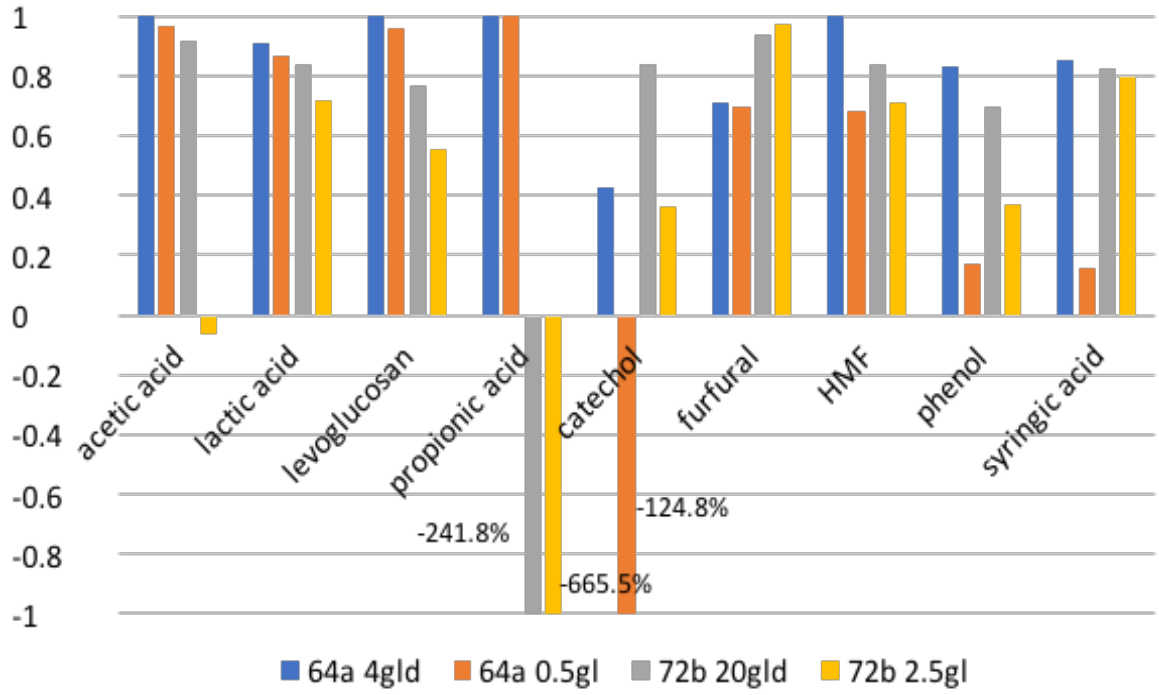

Figure 38: Percent removal of major components of BOAP in MEC under different conditions.

This indicates that batch operating conditions are not good for removal of catechol. Syringic acid removal was very similar in fed-batch and continuous operation, while phenol removal dropped from 69.6% (H-C) to 37.2% (H-B) under the higher loading conditions. Additionally, a large shift in propionic acid and acetate metabolism was observed between the low and high levels. At both low conditions, propionic acid was removed at 100%, but that was

reversed and accumulation was observed at the higher loading levels, reaching -241.8 (H-C) and 665.5% (H-B), respectively. For acetic acid, biotransformation at the lower levels and 20 g/L-d remained >90%, but shifting to fed-batch at 2.5 g/L drastically decreased removal resulting in slight accumulation to -6.1%. The high starting concentration of substrate during 2.5 g/L feedings likely saturated the capacity of the community for converting certain intermediates, which include propionic acid and acetic acid [21]. An additional observation that appears contradictory to trends for other compounds is the observation of higher removal of catechol and syringic acid at 2.5 g/L vs 0.5 g/L. A longer enrichment period progressively increasing BOAP loading may have resulted in a high density of microbes needed to remove these compounds, evidenced by good conversion during 20 g/L- loading. However, despite the good % removal of phenolics at the higher levels, the working concentrations of phenolic compounds remained much higher and overall COD removal dropped substantially to 36.6% during the final week of fed-batch operation at 2.5 g/L. Zeng et al. has reported inhibition of exoelectrogens due to the individual phenolic and furanic compounds within BOAP. The concentration of individual phenolic compounds at which this occurred was an order magnitude higher than that used in this study[13], however, the combined effect of all the phenolic compounds present in BOAP, characterized and uncharacterized, may have resulted in a stronger inhibition.

Conclusions

At the high loading conditions tested, continuous operation resulted in better performance and more stable output compared to fed-batch operation. Average H_2 productivity and current density at 20 g/L-d reached 7.9 ± 0.4 L/L-d and 9.2 ± 0.6 A/m^2 while fed-batch operation produced average values of 4.27 ± 3.2 L/L-d and 5.1 ± 3.3 A/m^2, respectively dropping

drastically in the 2nd week of performance to current densities below 1 A/m^2, preventing a 3rd week of operation at this level. The collective results indicate that high loading conditions can result in metabolic and microbial community shifts, resulting in the accumulation of propionic acid and substantial reduction in acetic acid conversion. This high concentration environment resulted in different selective pressures, increasing the proportion of fermenting organisms such as Firmicutes*,* including the family *Ruminococcaceae,* while selecting for different strains of Geobacter OTUs, which may have contributed to reduced performance. Additionally, electron diversion to undefined sinks increased to 69.7% ± 5.6% during fed-batch operation at a concentration of 2.5 g/L. Continuous operation was able to mitigate these effects better compared to fed-batch operation, but further insights into the mechanistic details of the process are needed to uncover specific structure-function dynamics and how to maintain these positive interactions. Further analysis of the community via omics techniques can link individual community members to various functional roles at the high loading conditions. This can help in isolating the negative interactions resulting from accumulation of intermediates such as propionic acid, etc. and allow development of strategies to further promote an increase in productivity.

References

1. da Silva TL, Gouveia L, Reis A. Integrated microbial processes for biofuels and high value-added products: the way to improve the cost effectiveness of biofuel production. *Appl Microbiol Biotechnol*. 2014;98(3):1043-1053. doi:10.1007/s00253-013-5389-5.
2. Jones S, Meyer P, Snowden-Swan L, et al. Process design and economics for the conversion of lignocellulosic biomass to hydrocarbon fuels: Fast pyrolysis and hydrotreating bio-oil pathway. *Energy*. 2013;(November):97. doi:PNNL - 23053 NREL/TP - 5100 - 61178.
3. Yue D, You F, Snyder SW. Biomass-to-bioenergy and biofuel supply chain optimization: Overview, key issues and challenges. *Comput Chem Eng*. 2014;66:36-56. doi:10.1016/j.compchemeng.2013.11.016.
4. Pham HT, Boon N, Aelterman P, et al. High shear enrichment improves the performance of the anodophilic microbial consortium in a microbial fuel cell. *Microb Biotechnol*. 2008;1(6):487-496. doi:10.1111/j.1751-7915.2008.00049.x.
5. Gil-Carrera L, Escapa a., Carracedo B, Morán a., Gómez X. Performance of a semi-pilot tubular microbial electrolysis cell (MEC) under several hydraulic retention times and applied voltages. *Bioresour Technol*. 2013;146:63-69. doi:10.1016/j.biortech.2013.07.020.
6. Escapa A, Lobato A, García DM, Morán A. Hydrogen production and COD elimination rate in a continuous microbial electrolysis cell: The influence of hydraulic retention time and applied voltage. *Environ Prog Sustain Energy*. 2013;32(2):263-268. doi:10.1002/ep.11619.
7. Lewis AJ, Borole AP. Understanding the impact of flow rate and recycle on the conversion of a complex biorefinery stream using a flow-through microbial electrolysis cell. *Biochem Eng J*. 2016;116:95-104. doi:10.1016/j.bej.2016.06.008.
8. Borole AP, Lewis AJ. Proton transfer in microbial electrolysis cells. *Sustain Energy Fuels*. 2017;0:1-12. doi:10.1039/C7SE00034K.
9. Pannell TC, Goud RK, Schell DJ, Borole AP. Effect of fed-batch vs. continuous mode of operation on microbial fuel cell performance treating biorefinery wastewater. *Biochem Eng J*. May 2016. doi:10.1016/j.bej.2016.04.029.
10. Wang H, Qu Y, Li D, et al. Cascade degradation of organic matters in brewery wastewater using a continuous stirred microbial electrochemical reactor and analysis of microbial communities. *Sci Rep*. 2016;6:27023. doi:10.1038/srep27023.
11. Shen R, Liu Z, He Y, et al. Microbial electrolysis cell to treat hydrothermal liquefied wastewater from cornstalk and recover hydrogen: Degradation of organic compounds and characterization of microbial community. *Int J Hydrogen Energy*. 2016;41(7):4132-4142. doi:10.1016/j.ijhydene.2016.01.032.
12. Thygesen A, Marzorati M, Boon N, Thomsen AB, Verstraete W. Upgrading of straw hydrolysate for production of hydrogen and phenols in a microbial electrolysis cell (MEC). *Appl Microbiol Biotechnol*. 2011;89(3):855-865. doi:10.1007/s00253-010-3068-3.
13. Zeng X, Borole AP, Pavlostathis SG. Inhibitory Effect of Furanic and Phenolic Compounds on Exoelectrogenesis in a Microbial Electrolysis Cell Bioanode. *Environ Sci Technol*. September 2016. doi:10.1021/acs.est.6b01505.
14. Lewis AJ, Ren S, Ye X, Kim P, Labbe N, Borole AP. Hydrogen production from

switchgrass via an integrated pyrolysis-microbial electrolysis process. *Bioresour Technol*. 2015;195:231-241. doi:10.1016/j.biortech.2015.06.085.
15. Caporaso JG, Lauber CL, Walters W a, et al. Ultra-high-throughput microbial community analysis on the Illumina HiSeq and MiSeq platforms. *ISME J*. 2012;6(8):1621-1624. doi:10.1038/ismej.2012.8.
16. Logan BE, Call D, Cheng S, et al. Microbial electrolysis cells for high yield hydrogen gas production from organic matter. *Environ Sci Technol*. 2008;42:8630-8640. doi:10.1021/es801553z.
17. Ye T, Cai H, Liu X, Jiang H-L. Dominance of Oscillospira and Bacteroides in the bacterial community associated with the degradation of high-concentration dimethyl sulfide under iron-reducing condition. *Ann Microbiol*. 2016;66(3):1199-1206. doi:10.1007/s13213-016-1207-5.
18. Kouzuma A, Kasai T, Nakagawa G, et al. Comparative Metagenomics of Anode-Associated Microbiomes Developed in Rice Paddy-Field Microbial Fuel Cells. Moreno-Hagelsieb G, ed. *PLoS One*. 2013;8(11):e77443. doi:10.1371/journal.pone.0077443.
19. Gagen EJ, Padmanabha J, Denman SE, McSweeney CS. Hydrogenotrophic culture enrichment reveals rumen *Lachnospiraceae* and *Ruminococcaceae* acetogens and hydrogen-responsive *Bacteroidetes* from pasture-fed cattle. Imperial J, ed. *FEMS Microbiol Lett*. 2015;362(14):fnv104. doi:10.1093/femsle/fnv104.
20. Gophna U, Konikoff T, Nielsen HB. *Oscillospira* and related bacteria - From metagenomic species to metabolic features. *Environ Microbiol*. 2017;19(3):835-841. doi:10.1111/1462-2920.13658.
21. Miceli III JF, Torres CI, Krajmalnik-Brown R. Shifting the balance of fermentation products between hydrogen and volatile fatty acids: microbial community structure and function. *FEMS Microbiol Ecol*. 2016;92(September 2016):1-8. doi:10.1093/femsec/fiw195.
22. Freguia S, Rabaey K, Yuan Z, Keller J. Electron and carbon balances in microbial fuel cells reveal temporary bacterial storage behavior during electricity generation. *Environ Sci Technol*. 2007;41(8):2915-2921. doi:10.1021/es062611i.
23. Esteve-Núñez A, Sosnik J, Visconti P, Lovley DR. Fluorescent properties of c-type cytochromes reveal their potential role as an extracytoplasmic electron sink in Geobacter sulfurreducens. *Environ Microbiol*. 2008;10(2):497-505. doi:10.1111/j.1462-2920.2007.01470.x.

Appendix

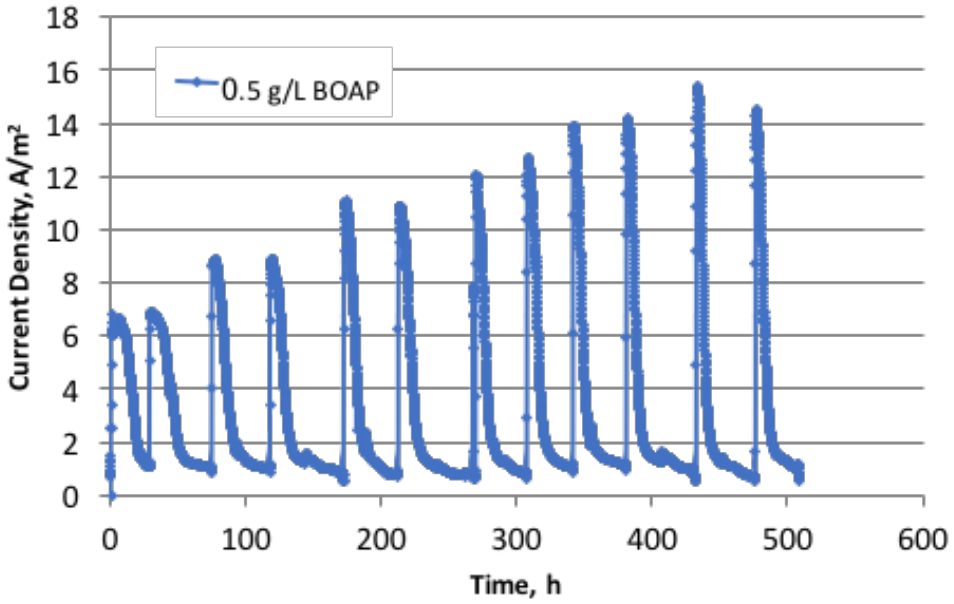

Figure 39: Current output over 3 week period of fed-batch conditions at 0.5 g/L BOAP.

CHAPTER VI

ADAPTING MICROBIAL COMMUNITIES TO LOW ANODE POTENTIALS IMPROVES PERFORMANCE OF MECS AT NEGATIVE POTENTIALS PERFORMANCE

This chapter is derived from a manuscript currently in preparation.

AJL designed and carried out batch experiments, electrochemical analyses, HPLC analysis, COD analysis, GC analysis, data interpretation and manuscript preparation. APB provided guidance in experimental designed and manuscript preparation. We acknowledge Professor Xiaofei Ye, Pyoungchung Kim and Shouji Ren for their work in producing the bio-oil aqueous phase.

Abstract

A unique aspect of microbial electrolysis cells is the use of an applied voltage for H_2 production. A variation on this parameter is the use of a controlled anode potential rather than controlled cell voltage, which can result in a more stable redox environment for the anode microbes. In this study, long-term exposure of anode consortia at -400 mV and 0 mV vs. Ag/AgCl resulted in a gradual divergence of the resulting bioanode midpoint potentials by >100 mV over a 6-month period. Cyclic voltammetry revealed a shift in peak current production to more negative potentials for the reactor poised at -400 mV. Furthermore, chronopotentiometry indicated very different profiles, showing a difference of 500 mV in the potential required to achieve a current of 15 mA (equivalent to 12 A/m^2). A 3-fold higher current was observed at a poised potential of -400 mV for the anode enriched at a poised potential of -400 mV, compared to that enriched at 0 mV. The substrate used was a bio-oil aqueous phase (BOAP) derived from switchgrass, making this study unique with potential for biorefinery application in producing hydrogen, fuels or chemicals. Operation at -400 mV resulted in a 1.5-fold higher electrical efficiency reaching 164.9%, while marginally reducing hydrogen recovery by 1.0%. The results provide evidence for adaptation of complex communities to optimize applied potential, while

reducing energy input for electrolysis. The community developed here has potential to be explored further to understand complex community-function relationships.

Introduction

Bioelectrochemical systems (BESs) are an emerging technology for the treatment of wastewater [1-4] as well as the production of fuels and chemicals [5-8]. The unique aspect of these systems is a solid electron acceptor for microbial processes, imparting a path to oxidize or reduce compounds without adding specific electron donor or acceptor chemicals. This is done via control of redox potential to enable more complete substrate conversion or promote conversion pathways that would normally be thermodynamically unfavorable. Microbial electrolysis is one type of BES, capable of producing renewable hydrogen and recovering energy from organic waste streams [9]. In these systems, organic compounds are converted to electrons, protons, and CO_2 by an electroactive microbial community capable of transferring these electrons to a solid anode electrode. Hydrogen is produced from these electrons and the protons diffusing from the anode to the cathode with the help of a small applied voltage [10,11]. An applied voltage of ~0.14 V is required to produce hydrogen with acetate as the substrate, however, in practice this value is typically greater than 0.6 V and can reach as high as 1.0 V. This value refers to the difference in potential between the anode and cathode, and typically this difference is controlled via a power source or potentiostat. However, the anode potential can move freely as a function of the substrate concentration, rate of conversion and electron production by the microbial community; resulting in a dynamic redox environment at the anode. An alternative method is to control the anode potential, which allows the cell voltage to change as cathode voltage drops with the rate of electron transfer from the anode. While both methods have pros and cons, controlling the cell

voltage can risk exposing the microbial community to a range of potentials, and thus does not provide an optimal redox environment for the anode community [12]. The anode potential which determines the energy gained by the anode microbes is a function of the free energy change for the reaction given as [13]:

$$\Delta G^{\circ\prime} = -n.F.(E^{\circ\prime}_{donor} - E^{\circ\prime}_{acceptor})$$

The potential is further related to the Nernst equation as follows:

$$E = E^{\circ} + RT/nF \ln ox/red$$

The primary substrate for exoelectrogenesis is typically acetate, which has a standard biological potential of -496 mV vs Ag/AgCl [51]. Thus, set anode potentials more positive than -496 mV result in the cells gaining energy for cell growth. However, this increase is not linear for biological systems and potentials above a certain threshold (~ 0 mV) may not increase energy gain for anaerobic microbes[13], nor improve performance of BESs operating under anaerobic conditions. The typical range of set anode potentials investigated has been between -400 mV to +200 mV vs Ag/AgCl. Several studies have shown higher activity per unit biomass as well as higher current output at more negative potentials while more positive potentials yielded thicker but less efficient biofilms [14,15]. In other studies, a more positive potential, up to a certain point, has been reported to result in a faster colonization process and better current output [16-18]. Of the studies that have investigated more negative anode potentials [12,14-18 19], only 5 were conducted in microbial electrolysis cells, and almost all used pure acetate as the substrate, with a few using a simple fermentable substrate. Ishii et al. have demonstrated that different microbial pairs form depending on substrate (using simple fermentable substrates) and electrode potential [20], and thus complex streams need to be investigated as they likely result in additional complexities compared to the above studies using pure acetate. Lastly, all of the mentioned studies exposed the reactors to negative potential levels for < 2 months and those with output >2 mA showed

maximum current output at the most positive end of the voltage range scanned during cyclic voltammetry on the return path, despite their enrichment at negative potentials. This demonstrates the enrichment of these reactors at negative potentials did not select for microbes with ability to operate at lower potentials than typically seen with *Geobacter* sp. Proper biocatalyst enrichment is often overlooked in bioelectrochemical systems across all areas of investigation and the data from this study demonstrates that longer-term enrichment is needed to substantially shift the midpoint potentials of the reactors to achieve high current output at negative potentials.

The complexity of community-structure relationships in BESs is significant and further development of these systems requires more insightful studies highlighting the inter-relationships between the biology and electrochemistry using real-world substrates. Using a biomass-derived stream [21,22], we hypothesize that a directed, long-term enrichment of anode microbial community can result in more permanent and active redox species at negative potentials in microbial electrolysis cells. Two reactors were enriched under identical MFC conditions using pyrolysis-derived bio-oil aqueous phase (BOAP) [21,22], and then were shifted to MEC operation at anode voltages of -400 mV and 0 mV vs Ag/AgCl for the 6 month enrichment period. Cyclic voltammetry was used to track shifts in the redox activity of the community over time. Additionally, chronopotentiometry was utilized to gauge the equilibrium anode potential reached by each community for a set current output, to better understand the natural preferences of each enriched community. Changes in the anode community were examined via 16S rRNA sequencing method to understand the long-term effects of anode poised potential. The ability to operate at more negative potentials has important practical implications for electrical efficiency, stability and electricity costs for MEC applications.

Methods

MEC Construction and Set-up

A dual-chamber bioelectrochemical cell convertible between MFC and MEC was constructed for bioanode development. The anode chamber was 16 ml in volume and contained a porous carbon felt (projected surface area = 12.56 cm^2, specific surface area = 454 cm^2cm^{-3}) that was plasma treated to increase hydrophilicity [21,23]. An Ag/AgCl reference electrode was used and connected to the anode chamber through a port in the wall of the chamber. The reactor has a flow-through design with the anode and cathode chambers separated by a Nafion-115 membrane pressed with a platinum-deposited carbon (0.5 mg/cm^2; 10% Pt; E-TEC, FuelCellsEtc., Bryan, TX) on the cathode side. An external anode reservoir was used to recirculate media. A schematic of the system can be found in the Appendix Figure 46. The MECs were primarily operated under continuous mode of substrate addition, however batch experiments were also conducted as described in Section 2.5. A minimal nutrient salt medium including Wolf's mineral and vitamin solutions was used and circulated through the anode chamber at a flow rate of 3.6 mL/min [21,23]. A syringe pump was used to inject BOAP in-line during the enrichment and operational periods described below. The substrate BOAP consisted of a wide range of organic compounds including carboxylic acids, anhydrosugars, alcohols, aldehydes, ketones, furanic and phenolic compounds with a full list in the Appendix Table 14 [22]. Its use as a substrate in MEC and the conversion of the individual components as well as effect of process conditions on performance has been reported previously [7,21]. The cathode chamber was also 16 ml in volume, which was filled with a 100 mM potassium phosphate buffer without recirculation when the system was used as MEC.

The cathode buffer was replenished periodically when pH exceeded 11. The current collector was a 12 cm^2 piece of stainless steel mesh interfaced with the Pt-deposited carbon cathode.

Anode Microbial Community Development

Two reactors were used in this study, and the anode was inoculated with two cores from a previously developed MEC grown using switchgrass-derived BOAP [7]. The core was a 5 mm diameter x 12.5 mm length piece removed from the anode along with the microbial biofilm. After inoculation, 0.2 g/L of glucose was added in batch to supplement growth while BOAP was fed continuously at a rate of 2 g/L-d under MFC conditions with air-cathode and an external resistance of 250 ohms. After 24 hours, the substrate was switched to 1 g/L-d of 1:1 mixture of glucose and BOAP to facilitate biofilm growth during start-up. The glucose served as a supplemental carbon source and its concentration was gradually reduced from 50% to 0% over the first 3 months of operation, while the BOAP loading was increased from 1 to 2 g/L-d. The external resistance was also reduced from 250 ohms to 22 ohms over this time frame. After the 3 month growth period as MFC, similar redox profiles were observed and confirmed through cyclic voltammetry (CV). At this point, the reactors were shifted from MFC to MEC operation by removing the external resistors and applying potentiostatic control at set anode potentials of -400 mV and 0 mV. The oxygen was completely removed from the cathode via nitrogen sparging and sealing the cathode inlet while the outlet was connected to a hydrogen collection system (Figure 1). During this re-acclimation period to the new potential levels, glucose was used periodically as a supplement for growth of new microbes under the altered redox conditions. All experiments investigating effect of redox potential on performance of MECs were done using BOAP as the sole carbon source.

Community Sampling

For sampling of the anode community, the reactors were taken into an anaerobic glovebox where core samples were taken using a sterile coring tool and a 5mm diameter x 12.5 mm sample of the anode carbon felt was removed [27]. Cores were taken approximately every month during the 6 month enrichment period and each core was replaced with a fresh sterile core of the same size. DNA was extracted using a MoBio Power Biofilm DNA extraction kit, following manufacturer's protocol (Qiagen). Library prep was carried out for paired-end 16S analysis on Illumina MiSeq following the methods of Caporaso et al. using primers 515f-806r targeting the V4 region [24]. PCR products were checked via gel electrophoresis, and then were pooled and run through Zymo DNA Clean and Concentrator. Samples were then checked using Bioanalyzer and final concentration determined by Qubit. Kapa qPCR was also carried out for quality control. Sequencing was carried out with Illumina MiSeq 250 bp PE run, and sequence data analyzed via Qiime.

Cyclic Voltammetry

Cyclic voltammetry (CV) was carried out approximately every 2 weeks to assess growth, and maximum current output. A scan rate of 1 mV/s was used with a range of -500 mV to 100 mV vs Ag/AgCl, with 3 cycles carried out for each condition. The last cycle and the return path was used for determination of electrochemical parameters. Fresh media was utilized for each CV, with a batch addition of 0.1 g/l BOAP as the substrate. The anode chamber and recirculation lines were flushed to remove residual media and any planktonic cells [23]. A 10 minute "charging" period was used after flushing to equilibrate the system and reach a stable current prior to

initiating CV. Additionally, non-turnover CV was also utilized to assess redox active species within the microbial community. The reactors were starved for ~24 hours, followed by a change of the nutrient medium and flushing out of the anode to remove residual nutrient medium and planktonic cells. Parameters for non-turnover CV were the same as those described above. First derivative analysis was carried out on turnover CV's to determine the midpoint potential for each reactor. This was done by plotting the difference between current output during the return path against anode potential. Thus the midpoint potential value, which corresponds to the steepest part of the slope of the catalytic wave, can be identified as a peak through the first-derivative analysis.

Chronoamperometry

After 6 months of operation at the two anode potentials, the performance of the MECs was investigated via a batch experiment. The reactors were poised at their respective anode potentials of -400 and 0 mV vs Ag/AgCl and fed with a batch addition of 0.3 g/L of BOAP. The experiment was monitored for a total of 20 hours. Hydrogen was collected using an external gas displacement system [7]. The volume displaced was measured every 2 hours for the first 8 hours, and then again at the end of 20 hour period, with gas samples taken through septum placed near the cathode outlet in the gas displacement line. Anode effluent samples were collected after 20 hours for COD analysis.

Chronopotentiometry

The reactors were also investigated using chronopotentiometry. A batch concentration of 0.5 g/L BOAP was used, and set current levels spanned a range of 1-20 mA. Each current level

was held for 600 seconds, with the exception of 1 mA which was carried out for 300 seconds, to demonstrate stability of current output before shifting to the next current level. Maximum voltage allowed was +100 mV, at which point the experiment would terminate to avoid exposure to more positive potentials.

Analysis and Calculations

Liquid samples were taken from the anode reservoir and COD analysis was conducted to measure the extent of overall BOAP conversion. 2 mL samples were added to Hach HR COD (20–1500 mg/L COD) vials and were digested in a Hach DRB 200 reactor at 150◦C for 2 h. Digested samples were then cooled at room temperature and analyzed on Spectronic 20 Genesys with absorbance readings taken at 620 nm. Gas samples taken from the cathode outlet were analyzed via gas chromatography to confirm hydrogen production and to subtract any gases transferred from the anode (very small methane fraction detected). Performance and conversion efficiencies were characterized by current density, hydrogen productivity, Coulombic efficiency (CE), cathodic conversion efficiency (CCE), hydrogen recovery (HRE), electrical efficiency (EE) and calculated as described in the supplementary information [9,21].

Results

Effect of poised potential on midpoint potential

To understand the impact of set anode potential on microbial communities fed with a biomass-derived stream, CV analysis was utilized to track the midpoint potentials of each reactor over a 6-month period. The midpoint potential depends on the extracellular electron transfer

machinery utilized by exoelectrogenic organisms within the anode community, and is defined as the potential required to produce half the maximum current [25]. Thus, shifting of this midpoint potential would indicate a change in the dominant redox machinery deployed by the microbial community for transferring electrons to the electrode. This value was calculated by performing a first-derivative analysis of the cyclic voltammograms. When anode potential control was first implemented, the midpoint potentials of the two reactors were nearly identical at -416 and -418 mV vs Ag/AgCl, respectively (Figure 40A). After one month the potentials began to diverge, but at this stage, a shift had only occurred for the reactor poised at -400 mV. The midpoint for this reactor dropped to -450 mV, while the other remained essentially unchanged at -416 mV. The 0 mV reactor did not change significantly, however, the average potential during the 6th month was slightly more positive at -390 mV. The final midpoint potential for the -400 mV reactor plateaued at -490 mV. There was some variation during the course of the 6 month enrichment, but overall the trends held for each reactor.

The 100 mV divergence in midpoint potentials between the two reactors provides evidence that the anode potential does impact the redox behavior of the microbial community. . Figure 40B shows a full CV scan at the end of the enrichment period to highlight the impact on redox behavior. Comparison of the resulting current profiles shows that the shift in midpoint potentials has enhanced ability of the reactor poised at -400 mV to produce higher current at more negative potentials, achieving its maximum output near its poised potential, while both reactors reached similar current in the positive potential range. This large peak near -400 mV was reproducible and appeared during both forward and reverse scans. The peak was observed every time a CV was done following the 6-month enrichment period, investigated over a follow-up period of 8 weeks.

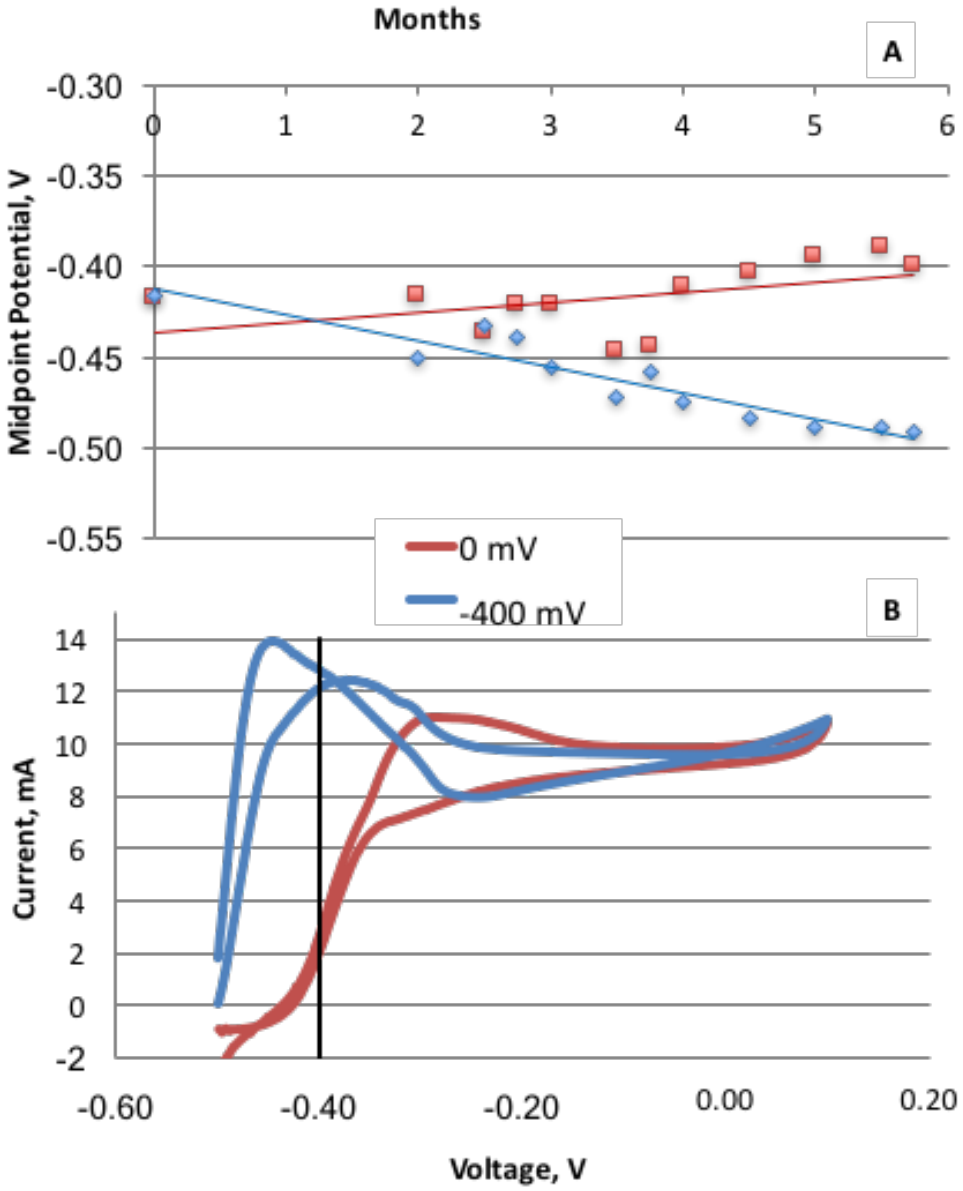

Figure 40: (A) Tracking of anode midpoint potential over time. (B) Overlaid CV's from the two reactors poised at 0 and -400 mV at the end of the 6 month period.

Furthermore, since a low scan-rate of 1 mV/s was used, the observed feature is indicative of a truly unique redox machinery present in the microbial community. While some differences were observed between the forward and reverse scans, the differences between the two reactors were clear. The redox-active peak and the microbial composition of the two reactors had changed. Some asymmetries between the scans can be due to sub-saturated supply of substrate (BOAP concentration of 0.1 g/L), which was utilized to avoid excess growth. Additionally, overpotentials due to buried redox centers can also cause the asymmetry [26].

Impact of poised potential on active redox species

To look closer at the changes in the relative redox profiles of the two reactors, non-turnover CV analysis was also carried out. As opposed to catalytic CV's, in which substrate is provided and multiple turnovers of all redox proteins occurs, non-turnover CV's starve the microbes of electron donors and allow only one oxidation/reduction event [26,27]. As can be seen in Figure 41A, both reactors shared the same discernible anodic peaks (P1-P2) prior to a shift in set anode potential. After long-term exposure to different potentials, the reactors produced different redox peaks, indicating changes in active redox proteins. The dominant peak P1 present for both reactors grew initially and shifted from -0.38 to -0.36 for the 0 mV reactor. Conversely, the P1 peak was significantly reduced for the -400 mV reactor (Figure 41B, peak B2) and shifted to the same voltage of -0.36 V as the 0 mV reactor, while a new dominant peak (B1) appeared at -0.48 V. The smaller original P2 peak also shifted more positive for the 0 mV reactor from -0.31 V to -0.29 V, while this peak was removed altogether for the - 400 mV reactor. Peak B1 for the -400 mV reactor with a midpoint potential of -0.48 V vs Ag/AgCl is more negative than what has been reported previously in the literature for active redox proteins in these systems.

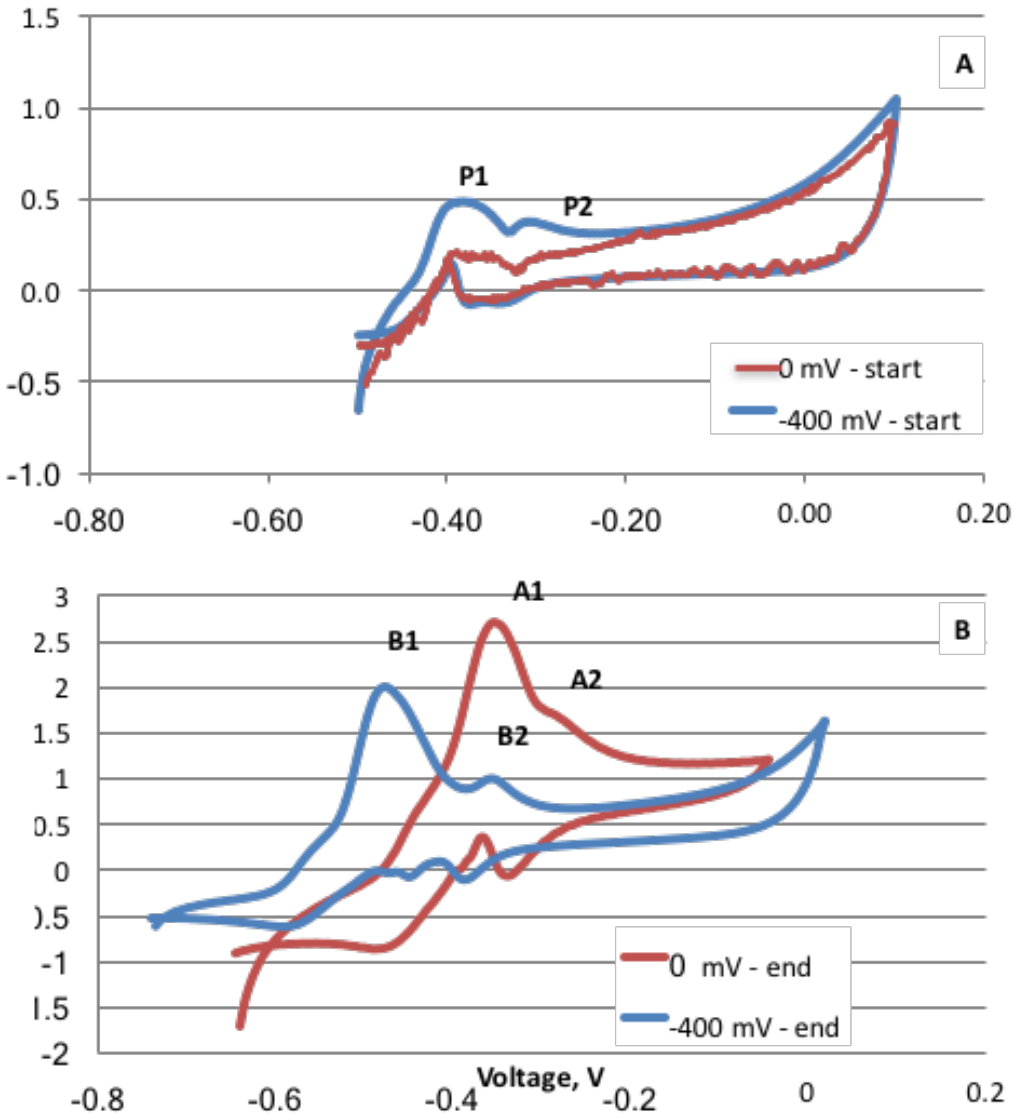

Figure 41: Non-turnover cyclic voltammetry (CV) analysis of MEC reactors at the beginning and end of set anode potential experiments. (A) CV analysis of reactors prior to shift to different anode poising potentials. P1-P2 represent the shared peak features. (B) CV analysis after 5 months of exposure to different poised conditions. A1-2 peaks refer to peaks for 0 mV reactor, and B1-2 refer to peaks for -400 mV reactor.

The nearest candidates are multiheme cytochromes OmcB and OmcZ with midpoint potentials of -0.39 and -0.42 V vs Ag/AgCl [28] [29]. For peak A1 and B2, OmcB is also a candidate while a PpcA type protein is most likely, which is a periplasmic c-type cytochrome that has been purified from *G. sulferreducens* with a midpoint potential of -0.37 V [30]. While it has been demonstrated that cytochromes such as OmcZ have a wide potential range due to multi-heme structure [28], current output is not equivalent over this range and their characteristic peaks have not been shown to deviate from their midpoint potential during non-turnover CV [31]. The observed changes in non-turnover CV profiles provide evidence that different redox active machinery was expressed by the consortium as a result of long-term exposure to a lower anode potential.

Microbial Community Analysis

During the enrichment period of 6 months, several differences in community structure arose between the reactors (Figure 42). A steady increase in *Geobacteraceae* was seen for the 0 mV community, reaching 50.5% by the end of the enrichment period. However, such a clear trend for this family did not occur for the -400 mV reactor, although this proportion did increase significantly by the end of enrichment to 21.0%. Additionally, *Lactobacillus* and an uncharacterized family (*BA008)* also increased gradually but to a lower degree, reaching 8.8% and 7.9%, respectively in the 0 mV reactor, while only reaching 0.1% and 3.8% in the -400 mV reactor. *Lactobacillus* species have been implicated in complex carbon degradation as well as participating in direct electron transfer for power generation in microbial fuel cells [32-34]. For the -400 mV community, *Lachnospiraceae* steadily increased to 44.7%, while this group did not increase in the 0 mV reactor remaining around 1%. This family has been found in BESs [35], and certain isolates have been implicated in extracellular electron transfer [36].

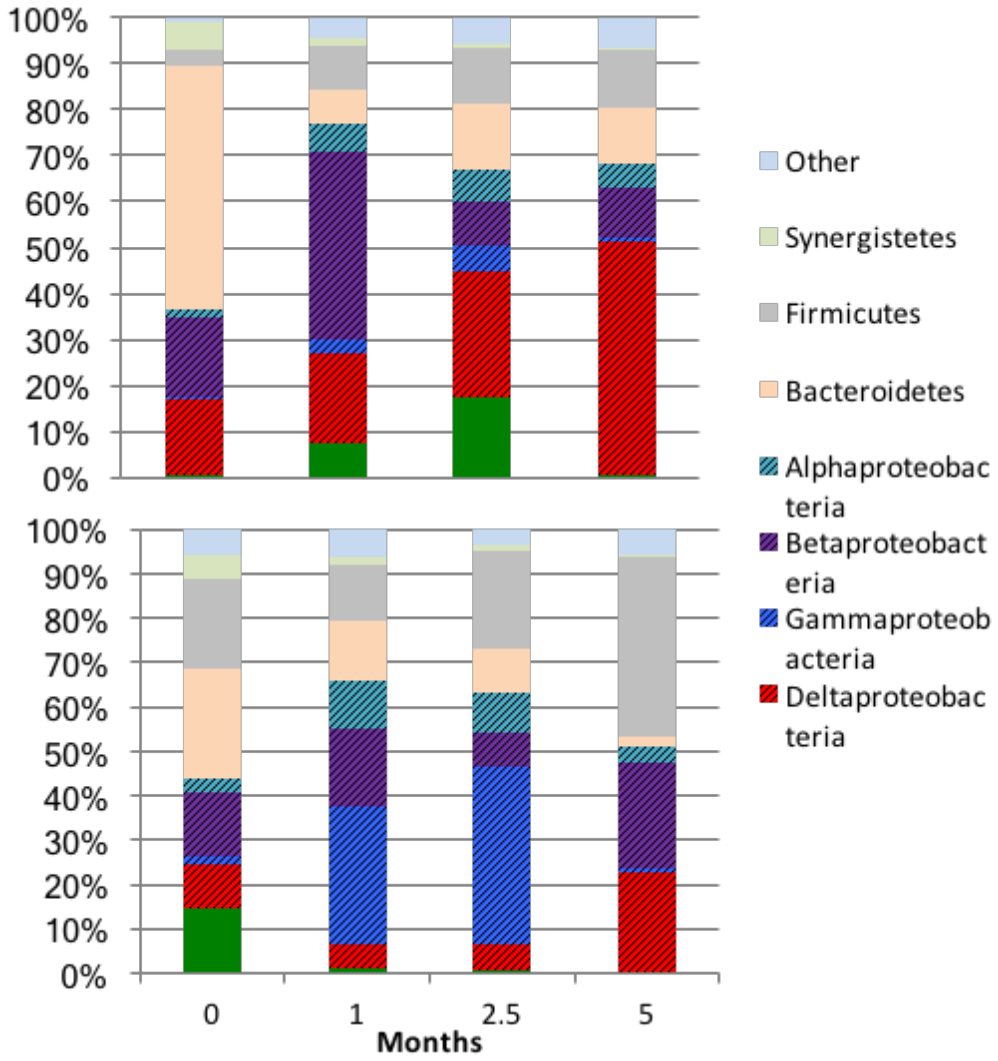

Figure 42: 16S rRNA sequencing-based microbial community characterization of bioanode samples grown at 0 mV and -400 mV vs Ag/AgCl. Dominance of *Geobacteraceae* was observed at set anode potential of 0 mV, however, *Lachnospiraceae* and *Rhodocyclaceae* dominated in the MEC poised at -400 mV.

Additionally, members of *Rhodocyclaceae* family increased to 19.9% by the end of enrichment period, but did not display a steadily increasing trend. Microbes from the *Rhodocyclaceae* family have been found in a variety of bioelectrochemical systems using short-chain fatty acids as substrates. [37,38]. Certain members of this family have also been found to carry out extracellular electron transfer [39]. While specific trends were observed for certain community members, there was also a level of instability and inconsistency for other groups that varied significantly and could result from community sampling or slight variations in loading and co-substrate use over the enrichment period. Sampling of cores of differing age from different areas of anode could possibly introduce a level of heterogeneity, which has been reported in the literature for bioelectrochemical systems [40-42]. Additionally, ecological issues such as founder effects during re-colonization can be impacted by slight variations in substrate loading/co-substrates and skew the community composition on the new cores, which were introduced each time a felt sample was taken. It should also be noted that different microbial groups can carry out similar functions in complex communities, so determining causes of structural changes can pose significant challenges in these systems and require deeper sequencing techniques to fully resolve active community member function. Nonetheless, the same media/operating conditions, except the poised potential, were used in both reactors for growth with similar community sampling procedures to minimize any potential differentiating effects.

Enhanced current production at negative potentials

While CV results demonstrated changes in the redox profiles over time, chronopotentiometry (CP) was carried out to further investigate the impact of these changes in the two reactors. CP, in contrast to chronoamperometry (CA), consists of setting the current

output rather than applied potential, and measures changes in the anode potential. This allows the anode community to naturally reach an equilibrium voltage for a given current based on it's redox capabilities. As the set current was increased beyond the 5 mA level, the anode voltage increased more drastically for the 0 mV reactor, compared to the -400 mV reactor (Figure 43). Upon reaching 15 mA, the 0 mV reactor was unable to sustain the current, and reached the upper limit of +100 mV and terminated. In contrast, for the -400 mV reactor, the anode voltage did not rise as rapidly, sustaining a 3-fold higher current at -400 mV. Additionally, this reactor was able to sustain overall higher currents reaching 20 mA before the anode voltage could no longer hold and reached the +100 mV limit. It must be noted that CV analysis was carried out directly preceding CP, and showed that the -400 mV reactor's maximum current exceeded that of the 0 mV reactor by ~3 mA. This is suggestive of a greater biomass density in the reactor poised at -400 mV or a higher specific activity. Evidence for a higher specific activity (activity per unit biomass) at more negative potentials has been reported in literature for other systems [14,15]. Further work is needed to determine the exact cause for the differences. Nevertheless, these results indicate that long-term exposure to more negative anode potentials can drive adaptation by the microbial community to the new redox environment, leading to altered redox functionality.

Impact on MEC performance

To assess the practical implications of using more negative set anode potentials during MEC operation, a continuous experiment at higher loading of 10 g/L-d was carried out to compare BOAP conversion, electrochemical efficiency, and hydrogen output between the 0 and -400 mV reactors.

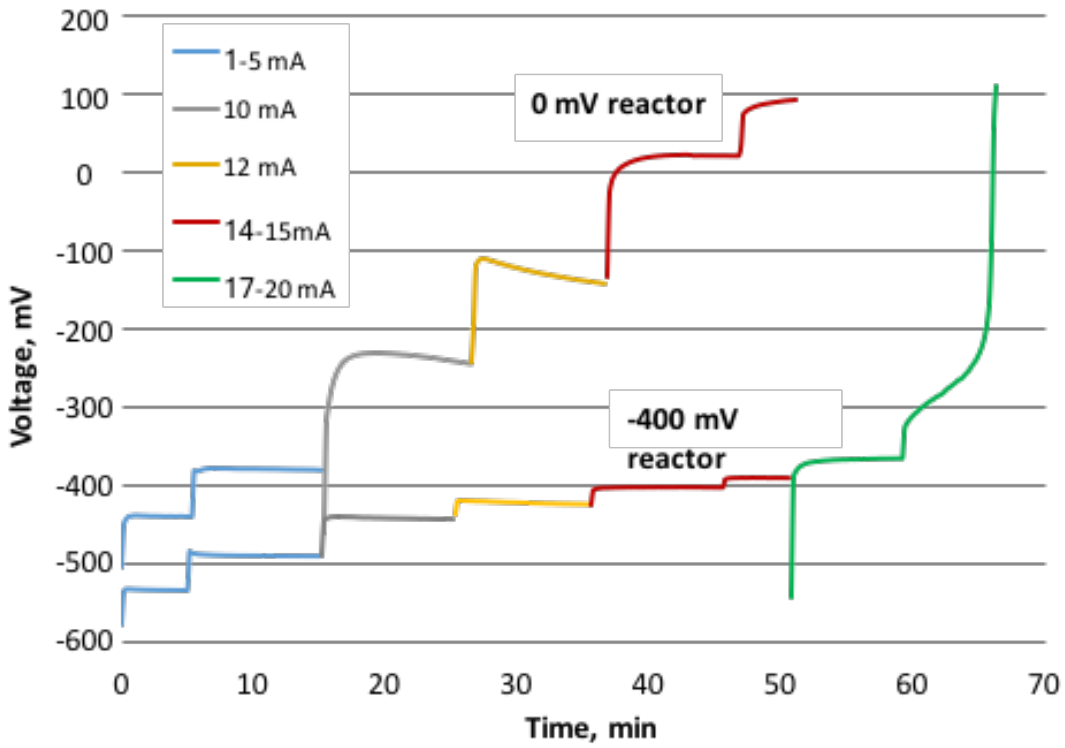

Figure 43: Chronopotentiometric comparison of reactors poised at 0 mV vs -400 mV. Anode potential required to reach a current from 1-20 mA is plotted on the y-axis.

Under continuous mode of substrate addition, the 0 mV reactor performed better in terms of current and hydrogen output as well as Coulombic efficiency (CE) and hydrogen recovery (HRE) as shown in Table 11, however, the -400 mV reactor still outperformed with respect to the electrical efficiency. Average current densities for the continuous experiment reached 6.01 ± 0.07 and 5.00 ± 0.20 A/m^2, for the two reactors poised at 0 and -400 mV respectively. Similarly, hydrogen productivities reached 6.15 ± 0.15 and 5.00 ± 0.55 L-H_2/L-anode/day, respectively. The 0 mV reactor achieved a higher Coulombic efficiency (CE) of 73.28 ± 0.25% and correspondingly higher hydrogen recovery (HRE) of 71.8 ± 2.88%, approximately 12% higher than the -400 mV reactor. In addition to the continuous experiments, a batch experiment was also conducted at a loading of 0.3 g/L BOAP to further assess the performance of the reactors.

Table 11: MEC performance and efficiencies for 10 g/L-d continuous experiment with BOAP as the substrate.

Anode potential	HRE	CE	CCE	COD removal	H2 rate (L/L-d)	CD (A/m^2)	Cell potential (V)	Cathode potential (V)	Electrical efficiency
0 mV	71.80%	73.28%	97.98%	54.63%	6.15	6.01	-1.21	-1.21	119.61%
STD	2.88%	0.25%	3.60%	1.60%	0.15	0.07	0.05	0.05	8.91%
-400 mV	59.10%	61.85%	95.49%	53.89%	5.00	5.00	-0.77	-1.17	182.64%
STD	5.19%	1.19%	6.56%	0.43%	0.55	0.20	0.04	0.04	3.53%

The performance of the reactor poised at -400 mV was higher than the 0 mV reactor in terms of the current density and hydrogen productivity as well, in addition to the electrical efficiency. The maximum current densities reached for the two reactors poised at 0 and -400 mV were 8.21and 10.8 A/m^2, respectively (Figure 44). Similarly, maximum hydrogen productivities reached 7.73 and 10.93 L-H_2/L-anode/day, respectively. These observations under batch conditions indicate each reactor community has a higher maximum capacity than that observed during continuous operation. However, CE and CCE and HRE were reduced under batch conditions (Table 12), likely attributable in part to shorter experimental run time, but were more similar between the reactors than during continuous operation. The results show that using a more negative anode potential does not have a negative effect on current output. Interestingly

cathode conversion efficiency (CCE) was similar between the two reactors under both feeding conditions despite a difference of approximately -440 mV in cell voltage.

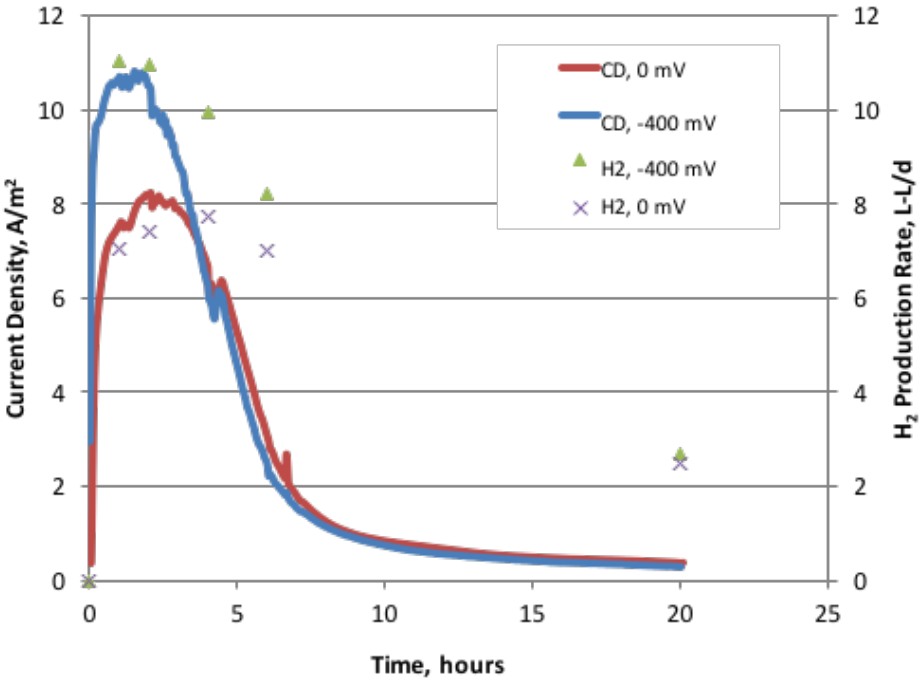

Figure 44: Current output and hydrogen productivity for 0.3 g/L batch run with the BOAP substrate.

Higher cell voltage has typically been associated with better cathode efficiencies and hydrogen production [43]. Our previous work has shown that performance limitations can occur at high loading rates due to proton transfer limitations [44]. Consequently, the anode efficiency and current output drops, which impacts more at lower anode potentials. The pH observations during this study support this explanation (data not shown). The pH was not strictly controlled in these studies and was adjusted only once a day. The -400 mV reactor showed a higher sensitivity to pH changes, as observed from the higher current obtained after pH adjustment compared to the 0 mV reactor and thus average current/hydrogen output and CE for the -400 mV reactor may have been more affected by the lack of strict pH control. Nonetheless, despite slightly lower output

and half-cell efficiencies, the electrical efficiency for the -400 mV reactor reached 182.64 ± 3.53%, a >60% improvement over the 0 mV reactor.

Table 12: MEC performance and efficiencies for 0.3 g/L batch run using BOAP as the substrate.

Anode potential	HRE	CE	CCE	COD removal	H2 rate (L/L-d)	CD (A/m^2)	Cell potential (V)	Cathode potential (V)	Electrical efficiency
0 mV	40.36%	50.15%	80.48%	62.50%	2.47	2.93	1.06	-1.06	112.39%
-400 mV	39.32%	51.20%	76.79%	65.63%	2.66	3.32	0.69	-1.09	164.87%

These results indicate the potential benefits of operating MEC reactors at more negative anode potentials. The ability to reduce electrical energy input has potential to improve the economics of hydrogen production if the productivity and efficiencies can be maintained, as was demonstrated here.

Discussion

Positive anode voltages are commonly viewed as a needed driving force to allow sufficient energy gain to exoelectrogenic microbes and to achieve satisfactory electron transfer rates [45]. However, for practical applications, providing excess energy for microbes is not necessarily desirable. As BESs are continuing to be pursued for commercial applications, large-scale systems will require significant electrical input for microbial electrolysis and other microbial

electrochemical systems [46] and thus the reduction in electrical input observed in this study could contribute to enhancing commercial viability. Two main factors should be considered when choosing a set anode potential:

1. Formal potential of substrate
2. Midpoint potential of the community

As previously mentioned, the anode set potential must be more positive than the formal potential of the substrate being used to allow sufficient energy gain for the microbes. Acetate, the most common substrate for exoelectrogens, and the main intermediate through which the present community produces current [37,41,47], has a formal potential of -496 mV vs Ag/AgCl. Acetate is present in BOAP at a level of 15 wt.% of the total COD in BOAP and it is also the main intermediate produced from the conversion of the compounds within BOAP for consumption by exoelectrogens in this system. The midpoint potential of the community indicates the voltage at which half the maximum current is produced. This is mainly determined via the final extracellular bacterial electron acceptor, i.e. cytochromes, nanowires, etc. [16]. Thus, the anode set potential typically is set at least 50 mV more positive than this point in the region where current output has plateaued. The most common acetate-utilizing organism in BESs is *Geobacter Sulfurreducens*, which has a typical midpoint potential of -0.36 to -0.37 V vs Ag/AgCl reference electrode. Given this midpoint potential, a minimum theoretical anode potential of ~ -375 mV (vs. Ag/AgCl) would be required for MEC operation. The set anode potential essentially determines the anode overpotential, when the MEC is operated under set anode potential conditions. Thus, the question that arises is: What is the optimal set potential for the anode to minimize overpotential and maximize hydrogen production? Growing the anode community by setting the cell potential rather than anode potential can lead to anode operating potentials much

higher than -375 mV causing high anode overpotentials. While some excess energy may be required to enhance initial growth rates, operation of these systems during hydrogen production may not require the high anode potentials. Since the substrate used in this study is BOAP, it is likely to result in a higher energy gain compared to acetate. However, a comparison between the 0 mV and the -400 mV reactor using the same substrate is appropriate and is discussed below. Operation of the bioanode at -400 mV was shown to shift the midpoint potential from the typical *Geobacter* range of -360 mV [27,48] to -490 mV, approaching the acetate reaction potential in the anode. If an MEC can be operated at a set anode potential of -400 mV, the anode overpotential would be considerably lower. Under these circumstances, the majority of the overpotential for hydrogen production will result from the cathode side (Figure 45). As shown from our results, operating the anode at the low poised potential did not have adverse effects on the MEC performance due to low energy gain, as the current output actually reached higher levels during chronopotentiometry for the -400 mV reactor. The *Geobacter* population was higher in the 0 mV reactor, which seems contrary to expectations. Some studies have reported a higher activity per unit biomass at more negative potentials [14,15], which may explain how a community with a lower proportion of *Geobacter* can produce more current. Additionally, as described in the community analysis, additional non-model exoelectrogens may be present and operational at more negative potentials. The results demonstrate that only ~100 mV difference (or possibly less) between the acetate potential and anode potential is necessary to maintain performance if the microbial community is sufficiently evolved for this function.

While anode electrode potential has been investigated substantially in the literature, less have focused on more negative anode potentials, and even less with complex streams. Table 13 highlights studies across bioelectrochemical systems investigating more negative anode

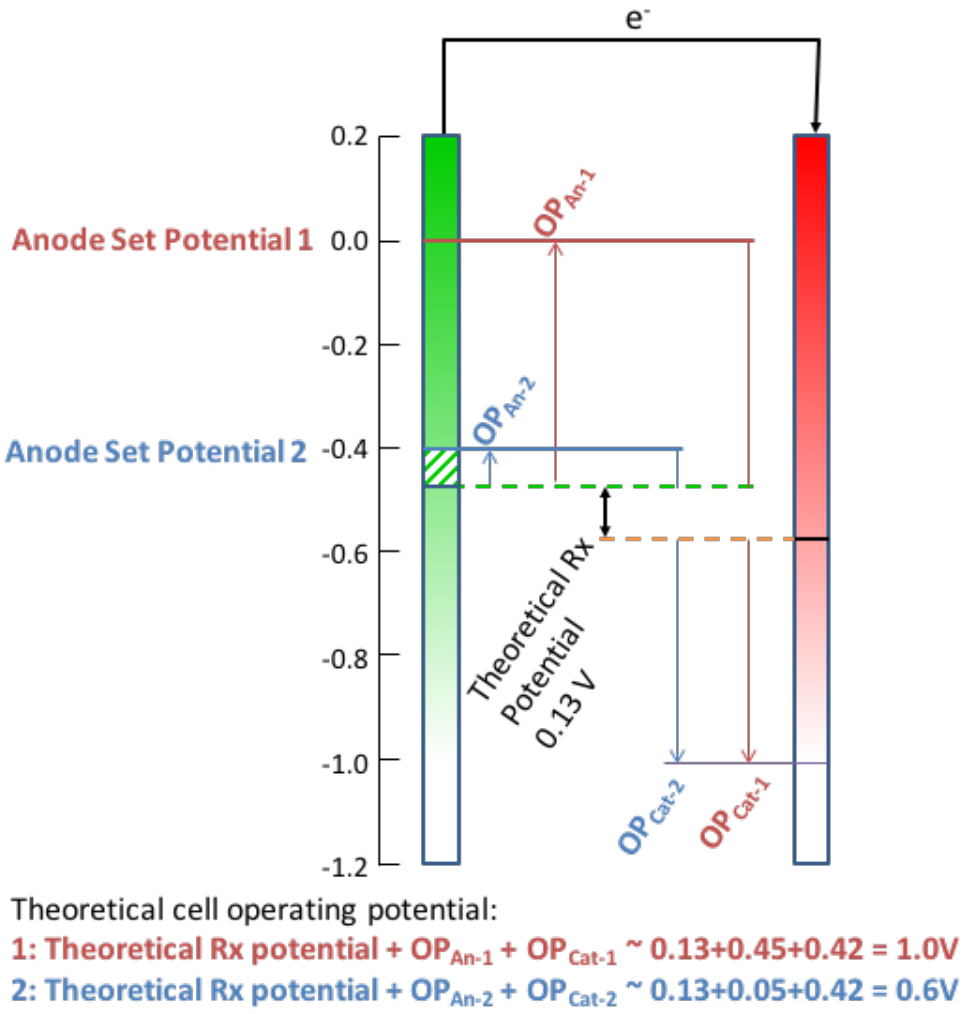

Figure 45: Theoretical overpotentials for 0 and -400 mV reactors operated with acetate as the substrate. (OP) indicates operating potential, (An) indicates anode, (Cat) indicates cathode. Voltage values are relative to Ag/AgCl reference electrode.

potentials. Many of these studies produced low current densities at the most negative potentials, with CV analysis still showing better performance at the more positive potentials. Of those that reached good performance similar to that observed for this study, a high current output of 8.8 A/m^2 was reached for one of the studies at an electrode potential of ~ -420mV vs Ag/AgCl [15]. However; CV profiles still produced an oxidation peak of -214 mV, much more positive than the set potential used and only slightly more negative than that typically seen for *Geobacter* species, which dominated their acetate-fed community [15]. Ketep et al. were able to achieve high current densities at more negative potentials by a 'scratching and re-inoculation' method with progressively lowering of the anode potential, reaching 6.8 A/m^2 at an equivalent electrode potential of ~ -370 mV vs Ag/AgCl [19]. This enrichment method displayed a shift in the midpoint potential from secondary to tertiary biofilms, reaching an estimated -440 mV vs Ag/AgCl. It should be noted that this study was carried out under MFC conditions and under alkaline pH, producing a different environment than the other studies mentioned here. Using a slightly more negative potential in our study and a longer enrichment period of ~240 days in an optimized reactor design, this study for the first time shows a peak maximum at very negative potentials (-490 mV) along the anodic curve or the return path of a CV scan (i.e., during positive to negative potential scan of CV curve). A peak maximum at such negative potentials indicates more active and permanent redox abilities requiring longer-term adaptation as that observed here. This has resulted in producing the most negative midpoint potential for a reactor reported to date, which was additionally characterized by chronopotentiometry, which highlighted the different redox abilities of the two communities developed at different potentials in this study.

The enrichment carried out in this study allowed our negatively poised reactor to achieve high current densities, hydrogen productivity, and CE compared to that reported in the literature

Table 13: Studies in literature review using more negative anode potentials in bioelectrochemical systems.

Anode Potential (Ag/AgCl)	Substrate	Enrichment Period (days)	Inoculum Source	Configuration (MFC/MEC)	Current Output	CE	Community	References
-400, -200 mV	0.5 g/L acetate	33	acetate-fed MFCs	MFC	170, 142 A/m^3	~80%	NA	[14]
-420, -360 mV	15 mM acetate	50	WAS	MEC	10.3 A/m^2	NA	>90% Geobacter	[15]
-370, -200 mV[1]	20 mM acetate	NA	pure Geobacter	MFC	1.3, 2 A/m^2	NA	NA	[16]
-510, -270 mV[1]	1 g/L formic acid	70	primary clarifier effluent	MFC	0, 80 A/m^3	NA	NA, 58% Geobacter	
-300, -200 mV	20 mM acetate	<30	anaerobic sludge	MFC	4, 6 A/m^2	NA	NA	
-200 mV	6.7 mM xylose	<30	enriched anaerobic digester culture	MFC	0.08 A/m^2	0.70%	diverse, low to no Geobacter detected	
-460, -329 mV[1]	1 g/L acetate	60	primary clarifier effluent	MFC	< 1 A/m^2	17,75%	~50% Geobacter	
-460, -300 mV[1]	.82 g/L acetate	>30	primary clarifier effluent	MEC	3, 10 A/m^{2*}	>90%	>90% Geobacter	[50]
-420, -360, -250 mV	15 mM acetate	<30	50:50 mixture of soil and activated sludge	MEC	NA, 1.7, 2.4 A/m^{2*}	NA	Different Geobacter strains	
-400, -200 mV	1.5 g/L acetate	5	pre-acclimated watewater, acetate	MEC	79, 365 A/m^3	80-90%	NA	[12]
-360, -210 mV[1]	36 mM propionate	155	Synthetic WWM + starch, milk, yeast	MEC	77,103 A/m^3	49, 71%	<60% Geobacter	[51]
-410, -260 mV[1]	2.5 mM sucrose	160	Lagoon sediment	MFC	.24 A/m^2	35, 43%	Diverse, low Geobacter	[20]
-370 mV[1]	5 mM acetate	70	paper mill / primary clarifier effluent	MFC	6.6 A/m2	22%	No Geobacter detected	[19]
-400 mV	0.5 g/L BOAP	240	BOAP enriched MEC community	MEC	12 A/m^2	50-70%	<25% Geobacter	This study

[1]Used conversion of +210 mV to convert SHE to Ag/AgCl
*Calculated using projected surface area of anode reported in referenced study
Current density based on that observed at the set anode potential

using pure acetate and positive anode potentials or applied voltages [12,15,49]. Observations from this study and those in the literature indicate that a long-term exposure at more negative potentials is necessary to achieve a significant improvement in catalytic performance. Multiple studies [16,50,52] have shown the ability of *Geobacter* species to alter its dominant redox machinery in response to different anode potentials. Zhu et al. reported different redox species to be active over a potential range of -0.36 to 0.3 V [50], however; the mid-point potential of a given redox peak did not change with applied potential. The more positively poised reactors produced significantly higher current than the more negatively poised reactors, indicating a different behavior compared to what we observed in this study. The results suggest that exoelectrogens within the -400 mV reactor community may be expressing different proteins active at very low potentials, allowing for more negative set anode potentials to produce similar or better electron transfer rates compared to those reported previously in the literature. Documentation of different cytochromes producing different currents certainly exists in the literature [53,54], although not at potentials below -400 mV.

Community analysis indicates families such as *Lachnospiraceae* and *Rhodoyclaceae* that were present in higher proportion in the -400 mV reactor may be playing a role. However, the analysis of electrogenically active populations is complicated with the use of BOAP as a substrate, as it contains fermentable compounds that result in growth of additional microbial groups. Using deep sequencing techniques, Ishii et al. found that different fermenter-exoelectrogen pairs arose depending on the anode potential and the substrate used [20]. Thus, the observed differences in families outside of *Geobacteraeace* between the -400 and 0 mV reactors may be due to the formation of different fermenter-exoelectrogen pairs that form for conversion of BOAP at different potentials. Conversely, as outlined in Section 3.3, these additional groups

may represent exoelectrogenic members, which perform both fermentative and electron transfer functions single-handedly.

Additionally, studies have also indicated that even within the *Geobacteraceae* family, different species can populate the anode depending on applied potential [20,55]. Thus, in addition to changes in community composition, we cannot rule out the possibility that changes in gene expression or evolution of proteins existing within known or unknown exoelectrogens in the -400 mV reactor lead to the observed changes in current producing abilities at more negative potentials. The 16S rRNA sequence analysis alone is insufficient to distinguish between these different functional associations. Further studies utilizing deeper sequencing techniques such as metagenomcis and metatranscriptomics are needed to provide further insights into differences in the specific functionality between communities enriched at 0 mV and -400 mV conditions in MECs.

Conclusion

Enrichment of reactors at -400 and 0 mV resulted in a gradual divergence in midpoint potential reaching a difference of 100 mV, with non-turnover CV's indicating changes in the active redox species. *Geobacteraceace* were prominent in both reactors but to a higher degree in the 0 mV reactor, reaching population density of 50.5%, while additional groups of *Lachnospiraceae* and *Rhodocyclaceae* increased in the -400 mV reactor, to 44.7 and 19.9%, respectively. Changes in groups besides *Geobacteraceace* may be the result of different fermenter-exoelectrogen pairing or from the increase in electroactive members within these groups that are better suited for negative anode potentials. Long-term enrichment at -400 mV resulted in a 500 mV difference in the anode voltage required to produce 15 mA, with a current

density of 11.15 A/m^2 sustained at the enrichment level of -400 mV during chronopotentiometry. This study for this first time to our knowledge shows a peak maximum at very negative potentials along the return path of a CV scan indicating more active and permanent redox abilities at more negative potentials that require long-term adaptation and possibly different exoelectrogens utilizing cytochromes with more negative midpoint redox potentials. Continuous experiments at 10 g/L-d BOAP also resulted in a >60% increase in electrical efficiency for the -400 mV reactor, reaching 182.64 ± 3.53%, The collective results provide evidence that long-term enrichment of exoelectrogens can result in significant improvement in catalytic performance and current output at negative anode potentials through biological changes in the anode, that cannot be achieved through short-term experiments. This can lead to lower anode overpotentials, while increasing electron transfer rates to levels typically seen for positive anode set potentials. The study provides a foundation for investigating community composition-function relationships and genomic vs. transcriptomic changes in biomass-fed anode communities as a function of redox potential.

References

1. Escapa A, San-Martin MI, Mateos R, Moran A. Scaling-up of membraneless microbial electrolysis cells (MECs) for domestic wastewater treatment: Bottlenecks and limitations. *Bioresource Technology.* Mar 2015;180:72-78.
2. Liu W-f, Cheng S-a. Microbial fuel cells for energy production from wastewaters: the way toward practical application. *Journal of Zhejiang University SCIENCE A.* 2014;15(11):841-861.
3. Sleutels T, Ter Heijne A, Buisman CJN, Hamelers HVM. Bioelectrochemical Systems: An Outlook for Practical Applications. *Chemsuschem.* Jun 2012;5(6):1012-1019.
4. Pant D, Singh A, Van Bogaert G, et al. Bioelectrochemical systems (BES) for sustainable energy production and product recovery from organic wastes and industrial wastewaters. *Rsc Advances.* 2012;2(4):1248-1263.
5. Borole AP, Hamilton C, Schell D. Conversion of residual organics in corn stover-derived biorefinery stream to bioenergy via microbial fuel cells. *Environ Sci Technol.* 2013;47(1):642-648.
6. Borole AP, Mielenz J, Vishnivetskaya TA, Hamilton CY. Controlling accumulation of fermentation inhibitors in biorefinery water recycle using microbial fuel cells. *Biotechnol. Biofuels.* 2009;2(1):7.
7. Lewis AJ, Borole AP. Understanding the impact of flow rate and recycle on the conversion of a complex biorefinery stream using a flow-through microbial electrolysis cell. *Biochemical Engineering Journal.* 2016;116(Special Issue: Advances in Biorefinery Engineering):95-104.
8. Pannell C, Goud R, Schell D, Borole AP. Effect of fed-batch vs. continuous mode of operation on microbial fuel cell performance treating biorefinery wastewater. *Biochem. Eng. J.* 2016;in press.
9. Logan BE, Call D, Cheng S, et al. Microbial electrolysis cells for high yield hydrogen gas production from organic matter. *Environ. Sci. Technol.* Dec 2008;42(23):8630-8640.
10. Liu H, Grot S, Logan BE. Electrochemically assisted microbial production of hydrogen from acetate. *Environ. Sci. Technol.* Jun 2005;39(11):4317-4320.
11. Rozendal RA, Hamelers HV, Euverink GJ, Metz SJ, Buisman CJ. Principle and perspectives of hydrogen production through biocatalyzed electrolysis. *International Journal of Hydrogen Energy.* 2006;31(12):1632-1640.
12. Nam J-Y, Tokash JC, Logan BE. Comparison of microbial electrolysis cells operated with added voltage or by setting the anode potential. *International Journal of Hydrogen Energy.* 2011;36(17):10550-10556.
13. Logan BE. Exoelectrogenic bacteria that power microbial fuel cells. *Nat. Rev. Microbiol.* May 2009;7(5):375-381.
14. Aelterman P, Freguia S, Keller J, Verstraete W, Rabaey K. The anode potential regulates bacterial activity in microbial fuel cells. *Applied Microbiology and Biotechnology.* Mar 2008;78(3):409-418.
15. Torres CI, Krajmalnik-Brown R, Parameswaran P, et al. Selecting Anode-Respiring Bacteria Based on Anode Potential: Phylogenetic, Electrochemical, and Microscopic Characterization. *Environmental Science & Technology.* Dec 2009;43(24):9519-9524.

16. Wei J, Liang P, Cao X, Huang X. A new insight into potential regulation on growth and power generation of Geobacter sulfurreducens in microbial fuel cells based on energy viewpoint. *Environmental Science & Technology.* 2010;44(8):3187-3191.
17. Wang X, Feng Y, Ren N, et al. Accelerated start-up of two-chambered microbial fuel cells: effect of anodic positive poised potential. *Electrochimica Acta.* 2009;54(3):1109-1114.
18. Finkelstein DA, Tender LM, Zeikus JG. Effect of electrode potential on electrode-reducing microbiota. *Environmental Science & Technology.* 2006;40(22):6990-6995.
19. Ketep SF, Bergel A, Bertrand M, Achouak W, Fourest E. Lowering the applied potential during successive scratching/re-inoculation improves the performance of microbial anodes for microbial fuel cells. *Bioresource Technology.* 2013;127:448-455.
20. Ishii Si, Suzuki S, Norden-Krichmar TM, et al. Microbial population and functional dynamics associated with surface potential and carbon metabolism. *The ISME journal.* 2014;8(5):963-978.
21. Lewis AJ, Ren S, Ye X, Kim P, Labbe N, Borole AP. Hydrogen production from switchgrass via a hybrid pyrolysis-microbial electrolysis process. *Bior. Technol.* 2015;195:231-241.
22. Ren S, Ye P, Borole AP, Kim P, Labbe N. Analysis of switchgrass-derived bio-oil and associated aqueous phase generated in a pilot-scale auger pyrolyzer. *J. Appl. & Anal. Pyrolysis.* 2015;119:97-103.
23. Borole AP, Hamilton CY, Vishnivetskaya TA, et al. Integrating engineering design improvements with exoelectrogen enrichment process to increase power output from microbial fuel cells *J. Power. Sources.* June 15, 2009 2009;191(2):520-527.
24. Caporaso JG, Lauber CL, Walters WA, et al. Ultra-high-throughput microbial community analysis on the Illumina HiSeq and MiSeq platforms. *The ISME journal.* 2012;6(8):1621-1624.
25. Miceli III JF, Parameswaran P, Kang D-W, Krajmalnik-Brown R, Torres CsI. Enrichment and analysis of anode-respiring bacteria from diverse anaerobic inocula. *Environmental Science & Technology.* 2012;46(18):10349-10355.
26. LaBelle E, Bond DR. Cyclic voltammetry for the study of microbial electron transfer at electrodes. In: Rabaey K, Angenent LT, Schroder U, Keller J, eds. *Bioelectrochemical Systems, From Extracellular Electron Transfer to Biotechnological Application*: IWA Publishing; 2010.
27. Marsili E, Sun J, Bond DR. Voltammetry and Growth Physiology of Geobacter sulfurreducens Biofilms as a Function of Growth Stage and Imposed Electrode Potential. *Electroanalysis.* Apr 2010;22(7-8):865-874.
28. Inoue K, Qian X, Morgado L, et al. Purification and characterization of OmcZ, an outer-surface, octaheme *c*-type cytochrome essential for optimal current production by *Geobacter sulfurreducens*. *Appl. Environ. Microbiol.* Jun 2010;76(12):3999-4007.
29. Katuri KP, Kavanagh P, Rengaraj S, Leech D. Geobacter sulfurreducens biofilms developed under different growth conditions on glassy carbon electrodes: insights using cyclic voltammetry. *Chemical Communications.* 2010;46(26):4758-4760.
30. Ewing T, Ha PT, Beyenal H. Evaluation of long-term performance of sediment microbial fuel cells and the role of natural resources. *Applied Energy.* 2016.

31. Hartshorne RS, Jepson BN, Clarke TA, et al. Characterization of Shewanella oneidensis MtrC: a cell-surface decaheme cytochrome involved in respiratory electron transport to extracellular electron acceptors. *JBIC Journal of Biological Inorganic Chemistry.* 2007;12(7):1083-1094.
32. Pannell TC, Goud RK, Schell DJ, Borole AP. Effect of fed-batch vs. continuous mode of operation on microbial fuel cell performance treating biorefinery wastewater. *Biochemical Engineering Journal.* 2016;116:85-94.
33. Shen R, Liu Z, He Y, et al. Microbial electrolysis cell to treat hydrothermal liquefied wastewater from cornstalk and recover hydrogen: Degradation of organic compounds and characterization of microbial community. *International Journal of Hydrogen Energy.* 2016;41(7):4132-4142.
34. Liu W, Huang S, Zhou A, et al. Hydrogen generation in microbial electrolysis cell feeding with fermentation liquid of waste activated sludge. *International Journal of Hydrogen Energy.* 2012;37(18):13859-13864.
35. Rismani-Yazdi H, Carver SM, Christy AD, et al. Suppression of methanogenesis in cellulose-fed microbial fuel cells in relation to performance, metabolite formation, and microbial population. *Bioresource Technology.* 2013;129:281-288.
36. Jiang Y-B, Zhong W-H, Han C, Deng H. Characterization of Electricity Generated by Soil in Microbial Fuel Cells and the Isolation of Soil Source Exoelectrogenic Bacteria. *Frontiers in Microbiology.* 2016;7.
37. Borole AP, Hamilton CY, Vishnivetskaya TA, Leak D, Andras C. Improving power production from acetate-fed microbial fuel cells via enrichment of exoelectrogenic organisms in continuous flow systems. *Biochem. Eng. J.* 2009;48:71-80.
38. Hesselsoe M, Füreder S, Schloter M, et al. Isotope array analysis of Rhodocyclales uncovers functional redundancy and versatility in an activated sludge. *The ISME journal.* 2009;3(12):1349-1364.
39. Hori T, Müller A, Igarashi Y, Conrad R, Friedrich MW. Identification of iron-reducing microorganisms in anoxic rice paddy soil by 13C-acetate probing. *The ISME journal.* 2010;4(2):267-278.
40. Percival SL, Walker JT, Hunter PR. *Microbiological aspects of biofilms and drinking water*: CRC Press; 2000.
41. Borole AP, Reguera G, Ringeisen B, Wang Z-W, Feng Y, Kim BH. Electroactive biofilms: Current status and future research needs. *Energy Environ. Sci.* 2011;4:4813-4834.
42. Jung S, Regan JM. Comparison of anode bacterial communities and performance in microbial fuel cells with different electron donors. *Appl. Microbiol. Biotechnol.* Nov 2007;77(2):393-402.
43. Call D, Logan BE. Hydrogen production in a single chamber microbial electrolysis cell lacking a membrane. *Environ Sci Technol.* May 2008;42(9):3401-3406.
44. Borole AP, Lewis AJ. Proton transfer in microbial electrolysis cells. *Sustainable Energy & Fuels.* 2017;1:725.
45. Wagner RC, Call DF, Logan BE. Optimal set anode potentials vary in bioelectrochemical systems. *Environmental Science & Technology.* 2010;44(16):6036-6041.

46. Bajracharya S, ter Heijne A, Benetton XD, et al. Carbon dioxide reduction by mixed and pure cultures in microbial electrosynthesis using an assembly of graphite felt and stainless steel as a cathode. *Bioresource Technology.* 2015;195:14-24.
47. Logan BE, Rabaey K. Conversion of wastes into bioelectricity and chemicals by using microbial electrochemical technologies. *Science.* 2012;337(6095):686-690.
48. Marsili E, Rollefson JB, Baron DB, Hozalski RM, Bond DR. Microbial Biofilm Voltammetry: Direct Electrochemical Characterization of Catalytic Electrode-Attached Biofilms. *Appl. Environ. Microbiol.* Dec 2008;74(23):7329-7337.
49. Sleutels TH, Ter Heijne A, Buisman CJ, Hamelers HV. Steady-state performance and chemical efficiency of Microbial Electrolysis Cells. *International Journal of Hydrogen Energy.* 2013;38(18):7201-7208.
50. Zhu X, Yates MD, Hatzell MC, Ananda Rao H, Saikaly PE, Logan BE. Microbial community composition is unaffected by anode potential. *Environmental Science & Technology.* 2014;48(2):1352-1358.
51. Hari AR, Katuri KP, Gorron E, Logan BE, Saikaly PE. Multiple paths of electron flow to current in microbial electrolysis cells fed with low and high concentrations of propionate. *Applied Microbiology and Biotechnology.* 2016;100(13):5999-6011.
52. Busalmen JP, Esteve-Nunez A, Feliu JM. Whole cell electrochemistry of electricity-producing microorganisms evidence an adaptation for optimal exocellular electron transport. *Environmental Science & Technology.* Apr 2008;42(7):2445-2450.
53. Zacharoff L, Chan CH, Bond DR. Reduction of low potential electron acceptors requires the CbcL inner membrane cytochrome of Geobacter sulfurreducens. *Bioelectrochemistry.* 2016;107:7-13.
54. Levar CE, Chan CH, Mehta-Kolte MG, Bond DR. An inner membrane cytochrome required only for reduction of high redox potential extracellular electron acceptors. *Mbio.* 2014;5(6):e02034-02014.
55. Cardinale S, Arkin AP. Contextualizing context for synthetic biology–identifying causes of failure of synthetic biological systems. *Biotechnology journal.* 2012;7(7):856-866.

Appendix

Calculations utilized for performance values:

- Coulomic Efficiency: $CE_{anode} = \frac{I_{obs}t}{n_s n_e F}$
- Hydrogen recovery (HRE): $Y_{H2} = \frac{PV_{H2}/RT}{2\Delta nCOD}$
- Hydrogen production rate: $Q_{H2} = \frac{V_{H2}/V_{anode}}{t}$
- Cathode conversion efficiency: $CE_{cat} = \left(\frac{V_{H2}}{\frac{I_{obs}tRT}{2FP}}\right)$
- Electrical efficiency: $\eta_E = \frac{-W_{H2}}{W_E}$

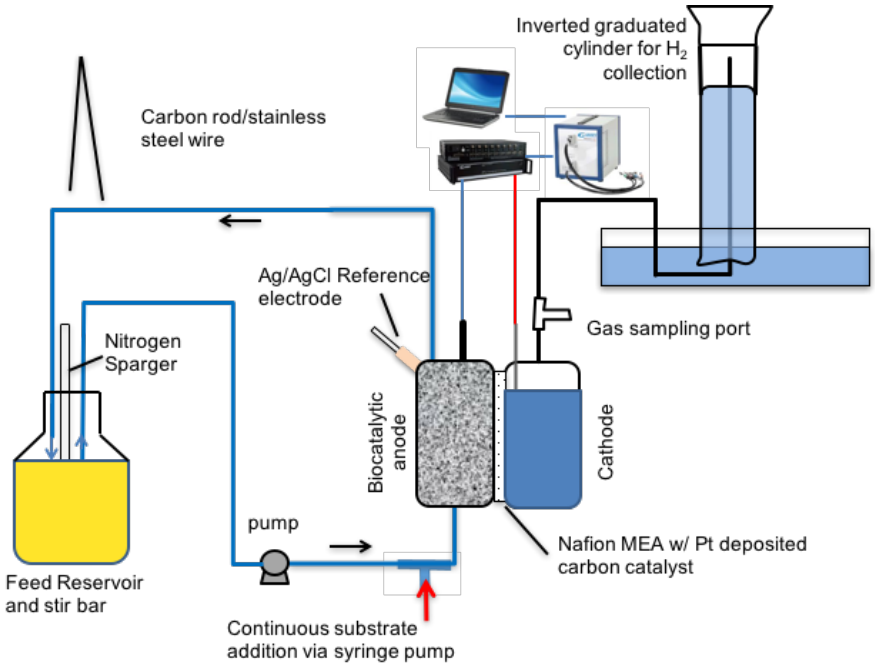

Figure 46: Schematic of MEC system

Table 14: Concentrations of major chemical compounds in bio-oil aqueous phase quantified by HPLC-PDA and GC-FID

Quantification method	Major chemicals	Concentration based on aqueous phase (g/L)
HPLC-PDA	Furfural	1.01
	1,2-benzendiol	1.77
	Phenol	1.8
	Levoglucosan	15.33
	Acetic acid	11.96
	Proponic acid	1.89
	Vanillic acid	2.69
	HMF	0.54
	Total	36.99
GC-FID	Phenol, 2-methoxy-	0.25
	2-methyl-4-methyphenol	0.07
	Cyclohexanone	0.07
	3-methyl-1,2-cyclophetandiol	0.46
	2,6-Dimethoxyphenol	0.26
	1,3-propanediol	1.84
	3-ethylphenol	0.56
	2(5H)-Furanone	1.17
	1-hydroxybutanone	1.35
	Total	6.02
	Sum	43.01

CHAPTER VII

UNCOVERING THE STRATEGIES DEPLOYED BY MICROBIAL COMMUNITIES TO CHANGING REDOX ENVIRONMENTS

This chapter is derived from a manuscript currently in preparation.

AJL designed and carried out batch experiments, electrochemical analyses, HPLC analysis, COD analysis, GC analysis, data interpretation and manuscript preparation. APB provided guidance in experimental designed and manuscript preparation. We acknowledge Professor Xiaofei Ye, Pyoungchung Kim and Shouji Ren for their work in producing the bio-oil aqueous phase.

Abstract

The anode potential determines the energy available to the exoelectrogenic microbes within microbial electrolysis cells and is thus an important parameter for controlling energy input and output. While many studies have investigated the impact of anode potential, the current study investigates the short-term and long-term responses to shifts in redox conditions, and how microbes adapt to more or less energy availability in the near-term and long-term. To accomplish this, reactors were enriched at opposite potential levels of -400 mV and 0 mV vs Ag/AgCl for 8 months to establish different redox profiles as confirmed by cyclic voltammetry and chronopotentiometry and were then shifted to opposite potential levels to assess short-term and long-term responses. It was found that the reactor enriched at 0 mV showed lower current density after being exposed to -400 mV over the short-term as well as the long-term. This corresponded to a decrease in the population of Deltaproteobacteria in the community after the 3-week exposure period at -400 mV and an increase in Rhodocyclaceae. The reactor enriched at -400 mV, when poised at 0 mV, resulted in a very short term increase in current, but the average current density over the 48-hour and 3-week exposure period did not show much change. Community analysis indicated that population of Geobactereaceae and Comamonadaceae

increased 12-22% after the long-term exposure to 0 mV. Chronopotentiometric analysis showed that up to 16 A/m^2 could be generated at a poised potential of -400 mV in the reactor enriched at -400 mV, however, only 8 A/m^2 could be generated in the reactor enriched at 0 mV. The results demonstrate that shifting the operation of anodes enriched at 0 mV to -400 mV does not improve electrochemical performance due to the inability of the community to adapt to the change.

Introduction

Bacteria capable of respiring solid electron acceptors are specifically enriched in bioelectrochemical systems due to the use of solid anode materials. Many exoelectrogenic species have been identified, mainly belonging to the phylum *Proteobacteria* and are represented by the model species *Geobacter sulfurreducens* and *Shewanella oneidensis*. Bacteria in other phyla including *Firmicutes* and *Bacteroidetes* have been found to populate bioelectrochemical systems fed with complex carbon substrates[1]. These systems provide the opportunity to study the interactions of different community members during carbon degradation and the relationship between microbial extracellular electron transfer (EET) processes and solid surface potentials[1–3]. Model electrogenic organisms such as *Geobacter sulfurreducens* and *Shewanella ondeidesis* have been heavily investigated utilizing simple substrates to identify components of the extracellular electron transfer chain, resulting in characterization of c-type cytochromes and pili proteins that have been linked to current generation[4,5]. The extracellular components interact with the terminal electron acceptor, the anode electrode, and the potential of which controls the energy available to these microbes[6]. Within microbial communities, Zhu et al. observed that Geobacter species dominated acetate-fed communities regardless of anode potential, but active redox species present differed[7]. Looking closer at the redox machinery of Geobacter species, it

was identified through mutant Geobacter strains that different cytochromes are involved depending on external electrode potential[8–10]. Thus, the potential exists that certain microbes may be able to alter their redox machinery as mechanism for adaptation to changing redox environments. However, the majority of studies investigating more negative redox potentials have not achieved similar output as positive anode potentials, which would indicate protein shifts within microbes already present may not be sufficient to drive equivalent output. Genetic and molecular level investigations into these mechanisms has been under-investigated in bioanode communities utilizing complex substrates. Uncharacterized microbes can often make up a significant portion of anode communities in complex waste streams, and thus the pathways for electricity generation deployed by these microbes and their component mechanisms are largely unknown. Ishii et al. have utilized modern sequencing approaches with operational "shocks" and different substrates to elucidate functional roles and interactions of community members[11]. In a separate study, they also found that different microbial pairs formed as functional of substrate and anode potential[12].

This study set out to investigate the hypothesis that shifts in gene expression are not sufficient to maintain performance at more negative potentials.. Separate reactor communities were enriched for ~8 months at opposite potential levels of -400 and 0 mV vs Ag/AgCl to develop distinctly different redox profiles, and then were shifted to opposite levels to measure the response. A suite of electrochemical tools were used to interrogate this as well as the use of shotgun metagenomics investigate differences in genes present resulting from enrichment at opposite potential levels.

Methods

Methods used in this chapter are the same as those from previous chapter.

Results and Discussion

Short-term response to anode potential shift

Now that functional divergence was clearly established after enrichment, each reactor was shifted to the opposite potential level to assess short-term as well as long-term responses to changing redox conditions. The hypothesis was that if the change in electrochemical performance is due to changes in gene expression, then a short-term exposure to a different potential would change the performance to reflect the new condition. However, if the electrochemical performance is due to inherent differences in the microbial community, then long term exposure to the new redox condition will be necessary to effect the change in electrochemical performance, which will be accompanied by change in the community composition itself. To assess short-term responses, the reactors were operated for 48 hours at their normal potential levels at a loading of10 g/L-d loading BOAP, at which point they were shifted to the opposite potential for an additional 48 hours. The results of the experiment are shown in Figure 47A. For the reactor enriched at 0 mV, the potential shift resulted in an immediate drop in current output by 80%, however the community was able to adapt and regain 60% of it's previous productivity after 5 hours. Overall, the current density fell from a plateau of ~6.3 A/m^2, obtained at 0 mV operation to a relatively stable output of ~3.9 A/m^2 over the 48 hours period after being poised at -400 mV. The average H_2 productivity did not decrease proportionally and remained high at 5.1 L/L-d.

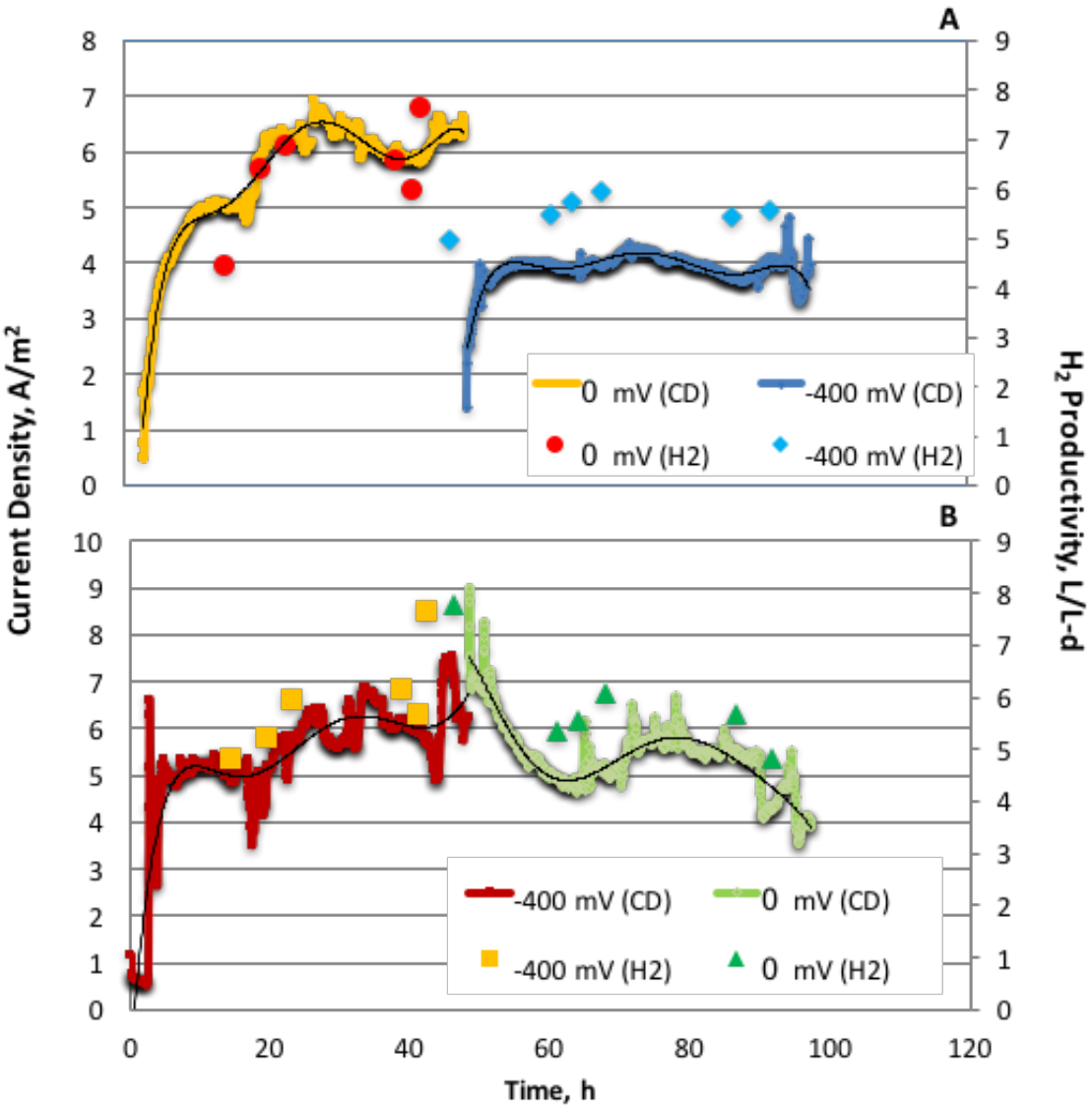

Figure 47: Potential shift experiment at 10 g/L-d BOAP for (A) 0 mV reactor shifted to -400 mV and (B) -400 mV reactor shift to 0 mV.

For the reactor enriched at -400 mV, the initial change in current output after shifting to 0 mV was opposite to that observed for the one enriched at 0 mV. Current output increased slightly after the shift, but decreased thereafter. Furthermore, output was somewhat unstable over the next 48 hours, but average values were similar to those prior to the shift, remaining around 5.4 A/m^2 and 5.25 L/L-d before and after the shift. Looking at the corresponding efficiency values, some interesting trends arise (Figure 48). For the 0 mV reactor, the CE decreased from 53.2 to 45.5%, while COD removal also dropped from 65.3 to 58.2%, which is not unexpected given the drop in current output after the shift described above. Interestingly, HRE increased from 51.5 to 61.0% due to a large jump in CCE from 97.0% to 125.6%. This subsequently led to a surge in electrical efficiency, increasing from 110.8 to 199.7%. Moving to the -400 mV reactor, a different pattern was observed. Shifting to 0 mV resulted in a slight decrease in CE from 54.6 to 53.0%, however COD removal increased, rather than decreased, from 63.3% to 68.0%. One explanation for the increase in COD removal and slight reduction in CE is that the sudden change in available energy gain from a more positive electrode could have resulted in growth as well as diversion electrons to undefined sinks, which has been observed recently at more positive potentials[13]. Electrical efficiency values shifted as a result as well, decreasing from 157.8 to 108.0% due to the higher electrical input at the anode while not gaining in performance. HRE and CCE only nominally changed, with HRE decreasing from 51.0 to 49.9%, while CCE increased slightly from 93.4 to 94.1%.

The stable CCE and HRE values for the -400 mV reactor are puzzling given the large increase in CCE upon shifting to negative potential for the 0 mV reactor, as this effect would have been expected for the -400 mV reactor moving to positive potential, which should increase efficiency/rate of hydrogen evolution reaction at the cathode due to a higher cell voltage.

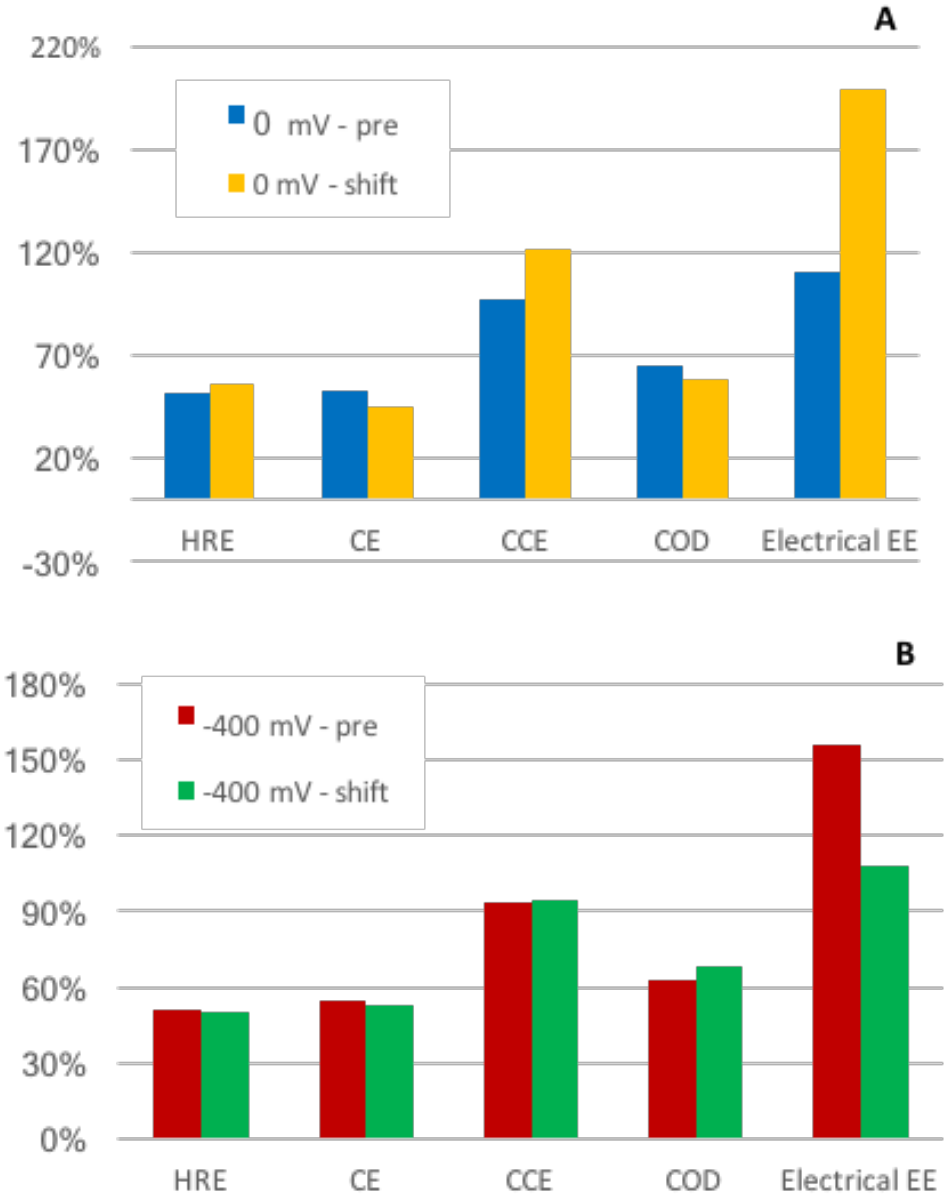

Figure 48: Efficiency values for pre and post potential (A) 0 mV reactor shifted to -400 mV and (B) -400 mV reactor shift to 0 MV.

The reduction in anode potential after the shift for the 0 mV reactor resulted in decrease of ~400 mV in cell potential, but the cathode voltage remained at the same pre-shift level ~1.3 V (data not shown). For the -400 mV reactor, the same trend was observed with cell voltage increasing by ~400 mV upon shifting to 0 mV, and again the cathode voltage remained unaffected and was stable at the same level of ~1.3 V. The sustained negative cathode potential for both reactors allowed for sustained high reaction efficiency at the cathodes to continue and produce an equivalent amount of H2 compared to before the shift. Thus, it appears that cathode voltage is a stronger determiner of cathode efficiency and the reasons for enhanced CCE for the 0 mV reactor upon shifting to more negative potentials and reduced HRE and CE for the -400 mV reactor upon shifting to more positive potentials is linked the difference in COD removal and energy availability. For the -400 mV reactor, the hydrogen evolution reaction proceeded with same efficiency as cathode voltage remained stable but upon shifting to a more positive potential, COD removal increased rather than decreased, increasing the theoretical amount of H2 that should be produced after the shift. However, as the increase in energy available to the microbes at the more positive potential allowed for diversion of more electrons to growth or undefined sinks, HRE and CE decreased. Conversely, COD removal decreased for the 0 mV reactor upon shifting to more negative potential, lowering the amount of hydrogen that should be observed. However, due to the high current production prior to the shift, which in return produces a high amount of protons, which in the immediate aftermath decreased current 6-fold, the protons produced at the anode prior to the shift may have inflated the hydrogen collection post-shift, as transport can be rate limiting for the process[14]. Additionally, while a negative cathode voltage allows high efficiency, the rate can also be limiting, with electrons produced prior to the shift also not reacting immediately, and thus combined with proton transport, likely

contributed to increased hydrogen production post-shift, resulting in a spike in CCE and HRE.

Biotransformation of compounds during short-term response

To further elucidate the impacts of anode potential shift on performance, changes to individual compound removal of main compounds within BOAP were analyzed. Overall COD removal decreased after shifting the reactor enriched at 0 mV to -400 mV, while it increased after shifting the reactor enriched at -400 mV to 0 mV. The former is referred to as 0 mV reactor, while the latter is referred to as -400 mV reactor, henceforth (based on their enrichment potential). The COD removal result is supported by the total removal rate obtained by addition of the removal rates of individual compounds measured via HPLC (Figure 49). Looking more closely, acetic acid removal rates decreased from 2.12 to 2.04 mg/h for the 0 mV reactor upon shifting to -400 mV. As acetic acid has been demonstrated to be the main fermentation end product and substrate for exoelectrogenesis, this reduction in metabolic uptake is likely the main driver for reduced current after shifting the 0 mV reactor. On the other hand, acetic acid removal rates were enhanced upon shifting the -400 mV reactor to 0 mV, increasing from 1.92 to 2.35 mg/h. While the average current output did not substantially increase after this shift, the initial hours did see a large rise in current. The results obtained suggest that extra electrons were likely diverted to growth and undefined sinks as described above. Looking at additional compounds, removal rates remained fairly steady for the 0 mV reactor with some slight increases. For the reactor shifted from -400 mV to 0 mV, an increase in the total removal rate was observed, which was primarily a result of increased acetate removal rate.

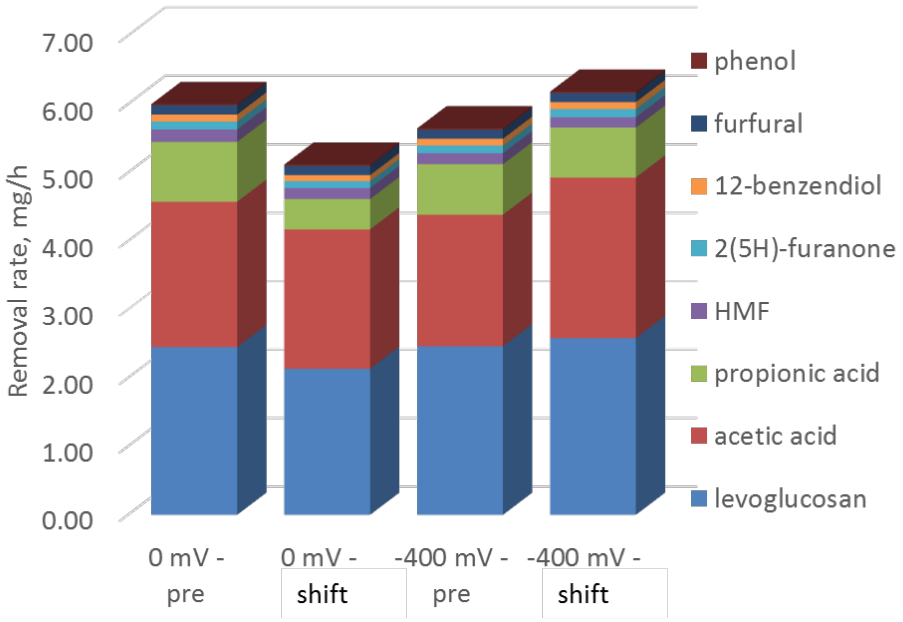

Figure 49: Individual compound removal during BOAP conversion before and after 48 hours of potential shift experiments.

Impact of Long-term anode potential shift of MEC performance

The reactors were kept at the opposite potential level for an additional 3 weeks beyond the initial short-term responses and same 10 g/L-d experiment was conducted to observe changes in performance after prolonged exposure to opposite potential levels. For the 0 mV reactor, average current density and H_2 productivity did not improve beyond the short-term response, and H_2 productivity actually decreased from 5.14 to 3.91 L/L-d (Figure 50). This dip in hydrogen productivity is due to CCE returning to a more expected value than that of post-shift performance, which was inflated due to a lag in proton and electron reaction at the cathode prior to the shift, resulting in a higher than expected CCE. For the -400 mV reactor, current density also slightly decreased compared to the short-term response remaining > 5 A/m^2, however, H_2 productivity dropped from 5.3 to 3.37 L/L-d, similar to that observed in 0 mV reactor.

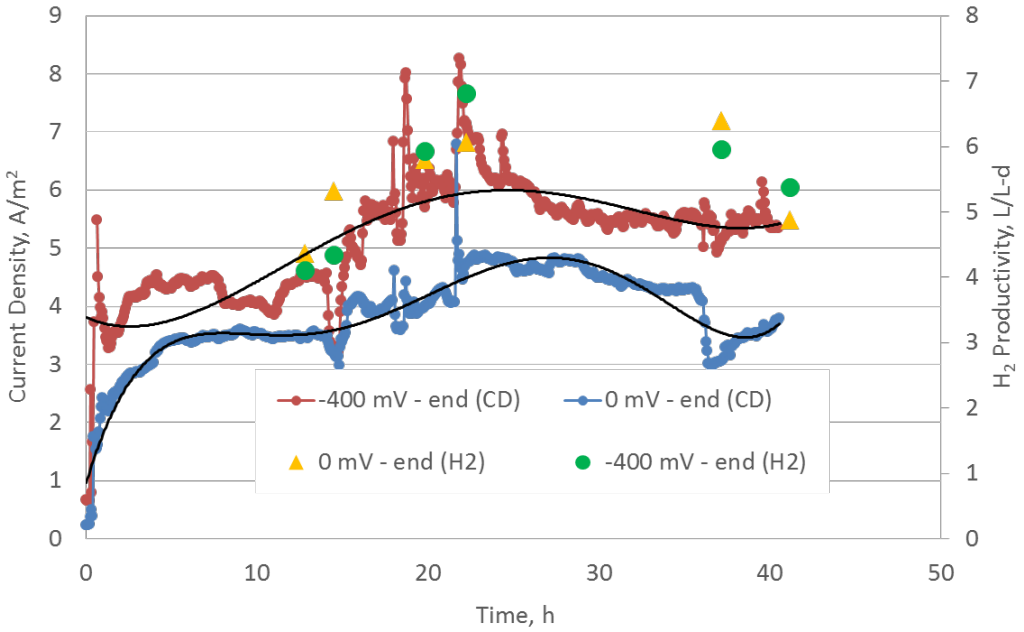

Figure 50: Current and hydrogen productivity at 10 g//L-d after long-term enrichment at opposite potential levels. The notation '-400 mV – end' corresponds to the -400 mV reactor poised at opposite level of 0 mV and vice versa.

This unproportioned drop in H_2 productivity compared to current density is unexpected for -400 mV, and is the result of a lower than expected CCE as described below. Efficiency values followed the trends observed for current density and H_2 productivity (Figure 51). However, the 0 mV reactor saw more substantial decreases in performance. CE declined further after the short-term response, dropping from 45.5 to 36.6%. HRE also decreased from 56.2 to 32.1%. This is due to large reduction in CCE, which had spiked during the short-term response increasing from 97.0 to 121.5%, but after long-term exposure CCE had declined to 88.0%. Electrical efficiency also dropped substantial compared to the short-term response, declining to 141.8%, but remained higher than pre-shift levels. The -400 mV reactor saw less of a decline in anode performance, with CE staying close to 50%, however HRE declines were greater for this reactor, dropping to 31.0% with corresponding decrease in CCE to 62.6%. Likewise, with the higher energy input and reduced cathode performance, electrical efficiency declined further to 73.4%.

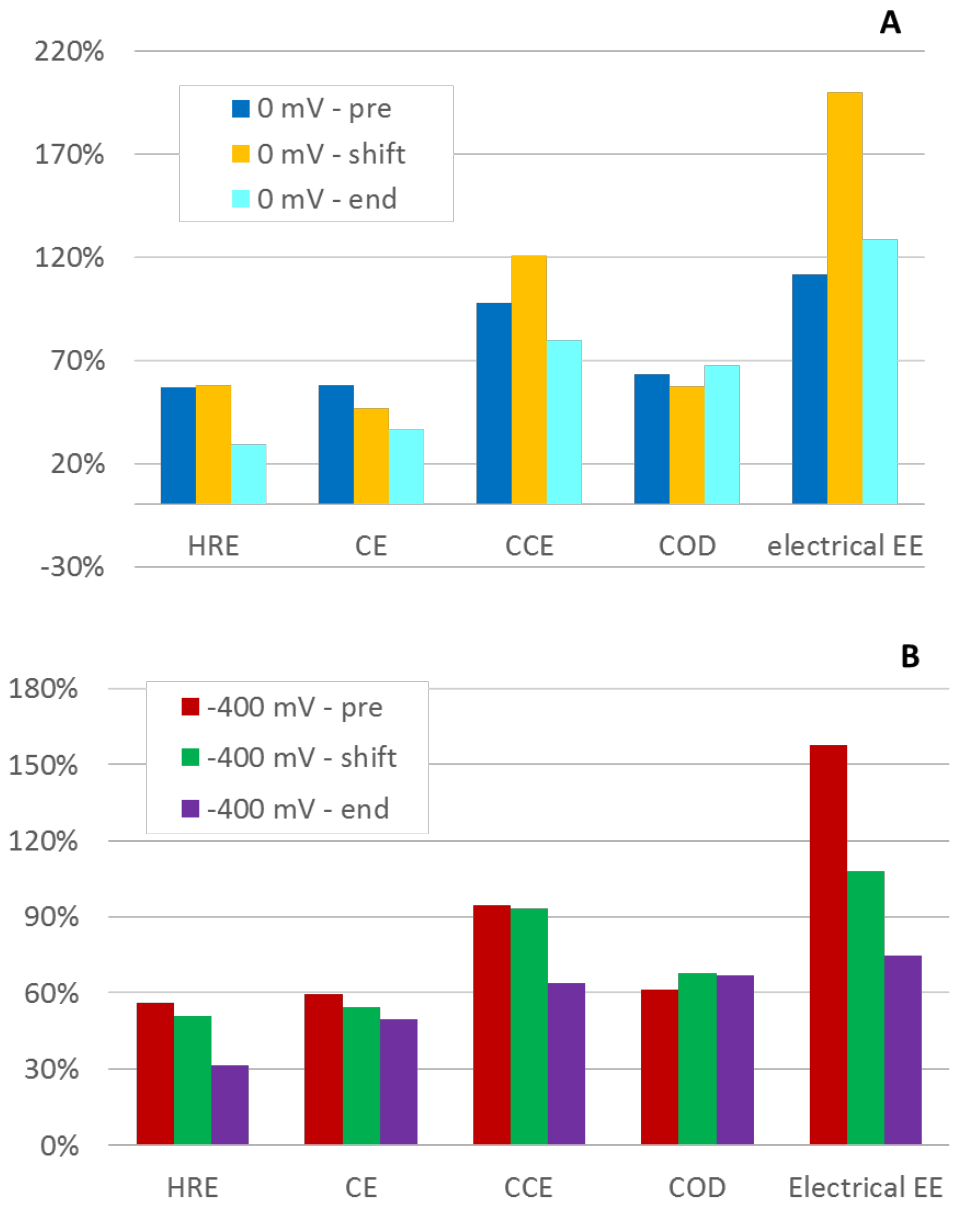

Figure 51: Efficiency values comparing pre-shift, post-shift, and end after long-term exposure to opposite potential levels.

The substantial decline in H_2 productivity and CCE compared to anode performance is perplexing, as the more positive anode and more negative cathode potential should maintain CCE as current output remained high, so it is possible that degradation of the cathode may have occurred, leading to lower than expected hydrogen production.

Long-term impact anode potential shift on redox profiles

In order to assess the ability of the community to further adapt beyond initial short-term response, the potential shift was continued for 3 weeks to assess long-term adaptation to permanent changes in external redox conditions. Cyclic voltammetry was used to track changes in the redox profile of the two reactors prior to the shift, after short-term response and after long-term exposure. In Figure 52, we can see interesting trends that develops for the two reactors. Starting with the 0 mV reactor, the short-term response after 48 hours of anode potential shift was a noticeable reduction in onset potential, while the midpoint potential only marginally decreased. After long-term exposure for 3 weeks, the midpoint potential returns to it's original value prior to shifting, while the trajectory of the onset potential levels off and does not decrease any further. In contrast, the short-term response for -400 mV resulted in larger shift in the positive direction for both the onset and midpoint potentials. Additionally, both onset and midpoint potentials continued in the positive direction after long-term exposure. The overall result was a convergence of the two reactors' onset and midpoint potentials, however, after 3 weeks of exposure to opposite potential levels, the -400 mV reactor still maintained more negative onset and midpoint potentials than the 0 mV reactor. This indicates that the differences observed in electrochemical performance are due to differences in the community and not just a change in gene expression resulting from change in poised potential.

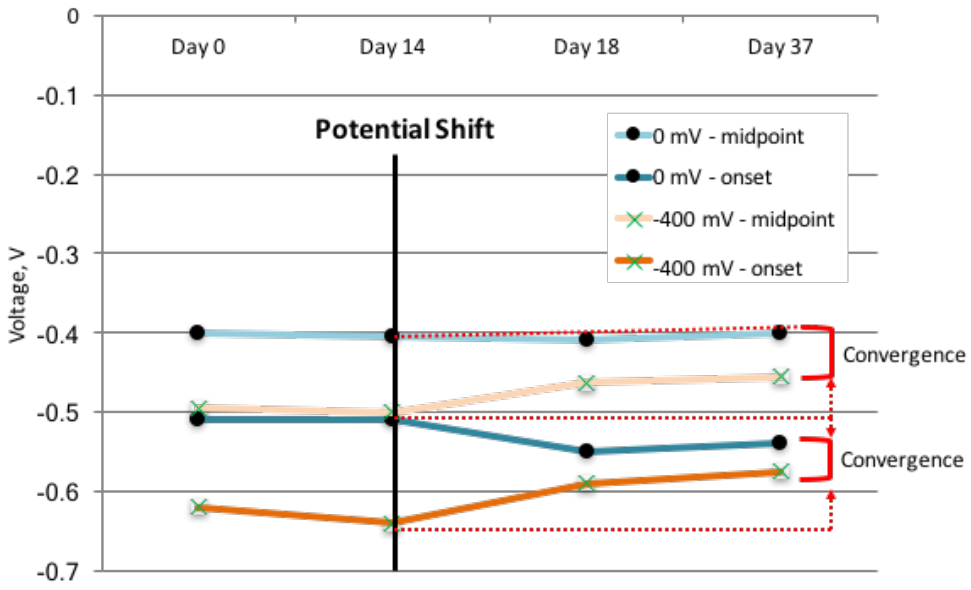

Figure 52: Tracking of anode midpoint and onset potentials over prior to and after potential shift.

This observation was investigated further through the use of chronopotetiometry. The results clearly show the -400 mV reactor has maintained it's abilities to generate current at more negative potentials despite exposure to positive potentials for a period of 3 weeks (Figure 53). While the 0 mV reactor is able to maintain similar anode potentials below 5 mA, upon moving to high currents, the divergence grows, with the -400 mV reactor is able to maintain a current of 20 mA at its original potential level, while the 0 mV reactor anode voltage did not reach stable level at this voltage, and likely would have reached the upper limit of +0.1 V had the run time been extended for that level. The collective results demonstrate much longer time scales may be necessary to shift the redox profiles of mature biofilms, and thus may require enrichment at the desired level of anode operation.

The trends in onset and midpoint potential changes after short-term and long-term exposure offer insights into the adaptive strategies that the microbial community may employ for changing redox conditions.

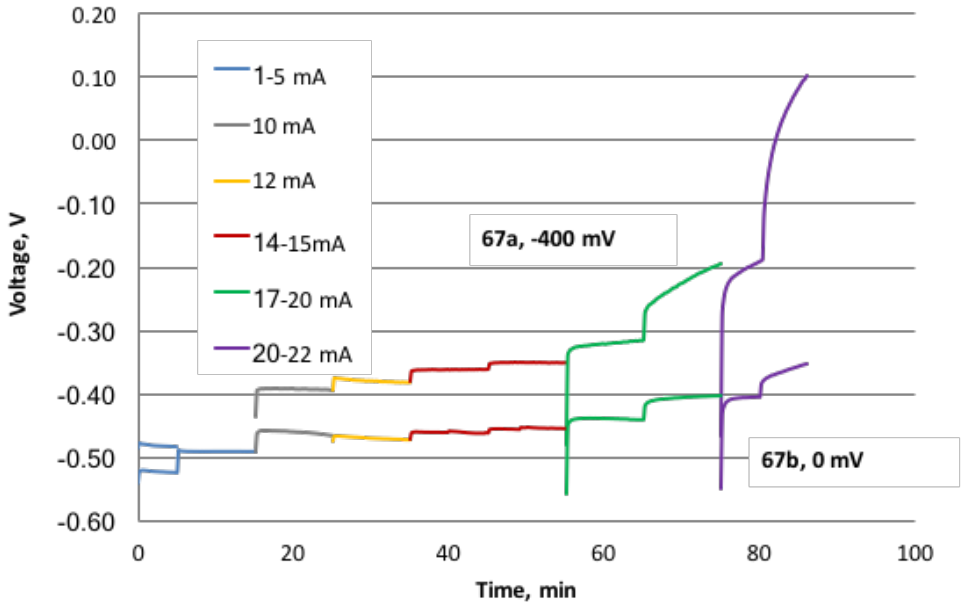

Figure 53: Chronopotentiometric comparison of reactors after potential shift to opposite level poised at 0 mV vs -400 mV.

The observation of an initial decrease in onset potential but only slight decrease in midpoint potential for the 0 mV reactor may indicate a shift in gene expression as short-term response to reduced anode potential. The effective result of reducing anode potential is a reduction in the terminal electron acceptor availability to the microbes. As a response, the community may have increased expression of extracellular cytochromes to serve as a capacitive outlet for excess electron production with respect to terminal electron acceptor availability, which would have been likely during 0 mV reactor shift, which also resulted in a decrease in acetic acid metabolism as result. It has been demonstrated that overexpression of extracellular cytochromes can occur as a result of electron acceptor limiting conditions including OmcB[15–17]. Additionally, another short-term, as well as long-term adaption strategy that may be used by microorganisms in response to different redox environments can be a shift in expression of cytochrome-type proteins that preferentially work at more positive or negative potential levels[8,9]. However, the

observed results from onset/midpoint potential analysis as well as chronopotentiometry indicate that such strategies are insufficient to fully impart the ability for high performance at more negative potentials.

Long-term changes in microbial community structure

Microbial community analysis was carried out for pre-shift and after long-term exposure to the opposite potential level. The energy available to exoelectrogens is substantially reduced at -400 mV compared to 0 mV, which is reflected in the trends observed for *Deltaproteobacteria*. A decrease in their population was observed in the 0 mV reactor from 33.0 to 23.7%, while for the -400 mV reactor, an increase was observed from 24.7 to 29.9% (Figure 54). On the other hand, *Euryarchaeota* remained at very low levels throughout, but appeared to show preference for negative potentials, increasing after long-term exposure to more negative potentials for 0 mV reactor. *Gammaproteobacteria* also appeared to show this preference while *Alphaproteobacteria, Betaproteobacteria,* and *Bacteroidetes* remained fairly consistent between the 'pre-shift' and 'end-point' samples. The pre-shift condition is defined as the one prior to changing the potential, while the end-point condition refers to the 48 hour test period after the 3 week period of poising at opposite potential, which was the same potential as that maintained for the 3 week period. Studies in the literature have seen varying results in terms of the impact of anode potential on community structure[18,7,19]. It is likely that the strength of selection based on anode potential is more subtle in terms of community changes, especially for mature biofilms compared to stronger selective pressures such as substrate changes[20,21]. Additionally, in the current study it is likely that the selective pressures are not equal between the shifting potentials levels of each reactor.

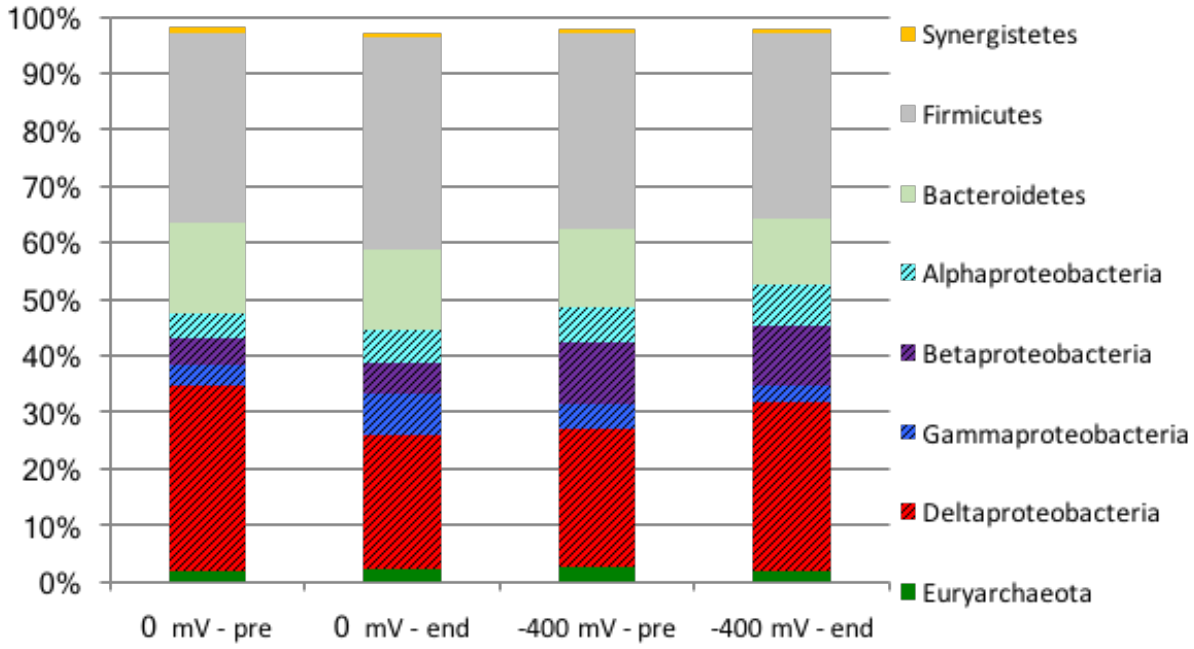

Figure 54: 16s rRNA analysis of microbial community pre-shift and after long-term exposure to opposite potential levels. (A) Phylum and Class level. (B) Individual OTUs displaying potential redox preferences.

Focusing on energy gain and electron transport, a microbial community adapted to 0 mV is likely to utilize more positive terminal electron transfer machinery in its transport chain as result of positive electrode enrichment. Thus, shifting to a substantially more negative potential would severely impact the ability of those terminal cytochromes to donate electrons to electrode, necessitating a shift in gene expression, if such genes are available, or requiring different exoelectrogenic microbes that deploy electron transfer proteins functional at more negative potentials. Conversely, shifting the -400 mV reactor to 0 mV does not impair the ability of the terminal cytochromes to donate to the electrodes, and thus the selective pressure on the community to change is likely to be stronger in the 0 mV reactor, which was shifted to -400 mV. Looking closer at individual OTUs in Table 15, community members highlighted in green show the highest preference for negative potentials, while rows highlighted in orange show stronger

preference for positive potentials. Geobacter_NR10308 decreased drastically after long-term exposure to more negative potentials, declining 4.9-fold, while displaying a reciprocal increase in the -400 mV reactor. Meanwhile, Geobacter_NR10426 and Geobacter_NR3759 increased after shifting to more negative potentials, indicating these OTUs may deploy a wider redox range of cytochromes. Additionally, Comamonadaceae_838837 declined 2-fold at more negative potentials, while increasing slighting in the -400 mV reactor after shifting. Strong preference for negative potentials was also seen for two *Peptococcaceae* OTUs. This family has been shown to be an iron-reducing family capable of exoelectrogenesis[22] and thus may have a selective advantage at more negative redox potentials. Outside of typical exoelectrogen families, Rhodocyclaceae_NR11127 showed a strong preference for negative redox potentials, increasing 4.3-fold after long-term exposure to negative potentials, decreasing 3.25-fold at positive potentials. Microbes within *Rhodocyclaceae* have commonly been found in BES systems with versatile metabolic abilities and potential exoelectrogenic abilities[23–25]. While substantial reductions in certain OTUs in the 0 mV reactor after long-term exposure to more negative potentials provides evidence for positive potential preference, increase in certain OTUs for the -400 mV reactor may not preclude them from having strong negative redox abilities as outlined above due to differing strengths of selective pressures between the two conditions. Structural changes to exoelectrogens in the -400 mV reactor, which resulted from an enrichment which lasted >6 months at the -400 mV potential did not occur within the 3-week exposure to higher potential. The observation that previously demonstrated abilities to perform at more negative potentials did not change despite exposure to positive potentials for 3 weeks provides additional evidence to support the lower selective pressure on that community.

Table 15: Individual OTUs showing high differential counts between conditions. Rows highlight in green indicate preference for negative potential, while rows in orange indicate preferences for positive potential.

OTU	0 mV - pre	0 mV - end	Differential	-400 mV - pre	-400 mV - end	Differential
Rhodocyclaceae_NR11127	5458	23656	4.33	14230	4374	-3.25
Erysipelotrichaceae_356760	6124	17345	2.83	11911	8266	-1.44
Pseudomonadaceae_239924	32929	90060	2.73	46968	25531	-1.84
Rhodocyclaceae_4357289	8535	19866	2.33	26130	22337	-1.17
Peptococcaceae_NR10598	1733	3749	2.16	3634	668	-5.44
Peptococcaceae_NR7022	4801	9679	2.02	10136	1862	-5.44
Enterococcaceae_766768	22615	36062	1.59	45353	71338	1.57
Rhodospirillaceae_524625	41748	63620	1.52	62444	48565	-1.29
Porphyromonadaceae_4305693	27072	39430	1.46	51892	35317	-1.47
Lachnospiraceae_4325509	118445	167413	1.41	92000	104171	1.13
Methanobacteriaceae_547463	11064	14900	1.35	12422	10356	-1.20
Geobacteraceae_NR10426	76474	90637	1.19	90574	103361	1.14
Geobacteraceae_NR3759	62705	73377	1.17	74793	83454	1.12
Porphyromonadaceae_675063	53229	57442	1.08	25724	18006	-1.43
Rhodocyclaceae_NR3977	9815	7503	-1.31	50558	17545	-2.88
Synergistaceae_3121406	13039	6995	-1.86	11275	6793	-1.66
Comamonadaceae_838837	19221	9271	-2.07	24255	27604	1.14
Geobacteraceae_NR10308	137513	27820	-4.94	35615	43335	1.22

Conclusions

Two MEC reactors enriched at -400 mV and 0 mV were investigated by reversing the potential to 0 and -400 mV, respectively, over short-term (48 hours) and long-term (3 weeks) periods to assess the changes in microbial community and the corresponding electrochemical performance. It was found that the reactor enriched at 0 mV showed lower current density after being exposed to -400 mV over the short-term as well as the long-term. This corresponded to a decrease in the population of Deltaproteobacteria in the community after the 3-week exposure period at -400 mV and an increase in Rhodocyclaceae. The reactor enriched at -400 mV, when poised at 0 mV, resulted in a very short term increase in current, but the average current density over the 48-hour and 3-week exposure period did not show much change. Community analysis indicated that population of Geobactereaceae and Comamonadaceae increased 12-22% after the long-term exposure to 0 mV. Chronopotentiometric analysis showed that up to 16 A/m^2 could be generated at a poised potential of -400 mV in the reactor enriched at -400 mV, however, only 8 A/m^2 could be generated in the reactor enriched at 0 mV. The results demonstrate that shifting the operation of anodes enriched at 0 mV to -400 mV does not improve electrochemical performance due to the inability of the community to adapt to the change.

References

1. Logan BE, Regan JM. Electricity-producing bacterial communities in microbial fuel cells. *Trends Microbiol*. 2006;14(12):512-518. doi:10.1016/j.tim.2006.10.003.
2. Rabaey K, Verstraete W. Microbial fuel cells: novel biotechnology for energy generation. *Trends Biotechnol*. 2005;23(6):291-298. doi:10.1016/j.tibtech.2005.04.008.
3. Lovley DR. Microbial fuel cells: novel microbial physiologies and engineering approaches. *Curr Opin Biotechnol*. 2006;17(3):327-332. doi:10.1016/j.copbio.2006.04.006.
4. Reguera G, McCarthy KD, Mehta T, Nicoll JS, Tuominen MT, Lovley DR. Extracellular electron transfer via microbial nanowires. *Nature*. 2005;435(7045):1098-1101. doi:10.1038/nature03661.
5. Gorby YA, Yanina S, McLean JS, et al. Electrically conductive bacterial nanowires produced by Shewanella oneidensis strain MR-1 and other microorganisms. *Proc Natl Acad Sci U S A*. 2006;103(30):11358-11363. doi:10.1073/pnas.0604517103.
6. Logan BE. Exoelectrogenic bacteria that power microbial fuel cells. *Nat Rev Microbiol*. 2009;7(5):375-381. doi:10.1038/nrmicro2113.
7. Zhu X, Yates MD, Hatzell MC, Ananda Rao H, Saikaly PE, Logan BE. Microbial community composition is unaffected by anode potential. *Environ Sci Technol*. 2014;48:1352-1358. doi:10.1021/es404690q.
8. Levar CE, Chan CH, Mehta-Kolte MG, Bond DR. An inner membrane cytochrome required only for reduction of high redox potential extracellular electron acceptors. *MBio*. 2014;5(6):e02034. doi:10.1128/mBio.02034-14.
9. Zacharoff L, Chan CH, Bond DR. Reduction of low potential electron acceptors requires the CbcL inner membrane cytochrome of Geobacter sulfurreducens. *Bioelectrochemistry*. 2016;107:7-13. doi:10.1016/j.bioelechem.2015.08.003.
10. Levar CE, Hoffman CL, Dunshee AJ, Toner BM, Bond DR. Redox potential as a master variable controlling pathways of metal reduction by Geobacter sulfurreducens. *ISME J*. 2017;11(3):741-752. doi:10.1038/ismej.2016.146.
11. Ishii S, Suzuki S, Norden-Krichmar TM, et al. A novel metatranscriptomic approach to identify gene expression dynamics during extracellular electron transfer. *Nat Commun*. 2013;4:1601. doi:10.1038/ncomms2615.
12. Ishii S, Suzuki S, Norden-Krichmar TM, et al. Microbial population and functional dynamics associated with surface potential and carbon metabolism. *ISME J*. 2014;8(5):963-978. doi:10.1038/ismej.2013.217.
13. Hari AR, Katuri KP, Logan BE, Saikaly PE. Set anode potentials affect the electron fluxes and microbial community structure in propionate-fed microbial electrolysis cells. *Sci Rep*. 2016;6:38690. doi:10.1038/srep38690.
14. Borole AP, Lewis AJ. Proton transfer in microbial electrolysis cells. *Sustain Energy Fuels*. 2017;0:1-12. doi:10.1039/C7SE00034K.
15. Chin K-J, Esteve-Núñez A, Leang C, Lovley DR. Direct correlation between rates of anaerobic respiration and levels of mRNA for key respiratory genes in Geobacter sulfurreducens. *Appl Environ Microbiol*. 2004;70(9):5183-5189. doi:10.1128/AEM.70.9.5183-5189.2004.

16. Esteve-Núñez A, Sosnik J, Visconti P, Lovley DR. Fluorescent properties of c-type cytochromes reveal their potential role as an extracytoplasmic electron sink in Geobacter sulfurreducens. *Environ Microbiol*. 2008;10(2):497-505. doi:10.1111/j.1462-2920.2007.01470.x.
17. Stephen CS, LaBelle E V., Brantley SL, Bond DR, Clarke T. Abundance of the Multiheme c-Type Cytochrome OmcB Increases in Outer Biofilm Layers of Electrode-Grown Geobacter sulfurreducens. Smidt H, ed. *PLoS One*. 2014;9(8):e104336. doi:10.1371/journal.pone.0104336.
18. Torres CI, Krajmalnik-Brown R, Parameswaran P, et al. Selecting anode-respiring bacteria based on anode potential: Phylogenetic, electrochemical, and microscopic characterization. *Environ Sci Technol*. 2009;43(24):9519-9524. doi:10.1021/es902165y.
19. Dennis PG, Virdis B, Vanwonterghem I, et al. Anode potential influences the structure and function of anodic electrode and electrolyte-associated microbiomes. *Sci Rep*. 2016;6:39114. doi:10.1038/srep39114.
20. Pant D, Van Bogaert G, Diels L, Vanbroekhoven K. A review of the substrates used in microbial fuel cells (MFCs) for sustainable energy production. *Bioresour Technol*. 2010;101(6):1533-1543. doi:10.1016/j.biortech.2009.10.017.
21. Borole AP, Reguera G, Ringeisen B, Wang Z-W, Feng Y, Kim BH. Electroactive biofilms: Current status and future research needs. *Energy Environ Sci*. 2011;4(12):4813. doi:10.1039/c1ee02511b.
22. Kunapuli U, Lueders T, Meckenstock RU. The use of stable isotope probing to identify key iron-reducing microorganisms involved in anaerobic benzene degradation. *ISME J*. 2007;1(7):643-653. doi:10.1038/ismej.2007.73.
23. Borole AP, Hamilton CY, Vishnivetskaya T, Leak D, Andras C. Improving power production in acetate-fed microbial fuel cells via enrichment of exoelectrogenic organisms in flow-through systems. *Biochem Eng J*. 2009;48(1):71-80. doi:10.1016/j.bej.2009.08.008.
24. Hesselsoe M, Füreder S, Schloter M, et al. Isotope array analysis of Rhodocyclales uncovers functional redundancy and versatility in an activated sludge. *ISME J*. 2009;3(12):1349-1364. doi:10.1038/ismej.2009.78.
25. Lewis AJ, Ren S, Ye X, Kim P, Labbe N, Borole AP. Hydrogen production from switchgrass via an integrated pyrolysis-microbial electrolysis process. *Bioresour Technol*. 2015;195:231-241. doi:10.1016/j.biortech.2015.06.085.

CHAPTER VIII

CHARACTERIZATION OF ENRICHED MICROBIAL COMMUNITY REVEALS NOVEL PLAYERS FUNNELING COMPLEX BIOMASS STREAM TO ELECTRONS FOR RENEWABLE HYDROGEN PRODUCTION

This chapter is derived from a manuscript currently in preparation.

AJL designed and carried out batch experiments, electrochemical analyses, HPLC analysis, COD analysis, GC analysis, DNA/RNA sequencing analysis, data interpretation and manuscript preparation. Assistance with training in DNA/RNA analyses was provided by Dr. Shunichi Ishii. APB provided guidance in experimental designed and manuscript preparation. We acknowledge Professor Xiaofei Ye, Pyoungchung Kim and Shouji Ren for their work in producing the bio-oil aqueous phase.

Abstract

Microbial communities have great potential as an alternative biocatalyst for conversion of lignocellulosic streams. Microbial communities have evolved to collectively carry out these functions for biomass-derived streams and this functionality can be deployed in systems such a microbial electrolysis cells to convert biorefinery streams into useful hydrogen. In the present study, an enriched high-performing community fed with a pyrolysis-derived aqueous phase was analyzed via metagenomics and transcriptomics to characterize the genetic potential of the community for biomass degradation, as well as uncover the active players involved in linking degradation to electron transfer to elucidate functional roles within the community and ecological interactions that drive high performance. An optimized assembly process resulted in the generation of 21 high-quality genomes form the microbial community. *Pelobacter propionicus* and *Robinsoniella peoriensis* were found to be the dominant strains in the community, making up nearly 50%. The former was demonstrated to possess novel exoelectrogenic behavior for its taxonomy, containing similar numbers of c-type cytochromes

with expression of the essential OmcZ, in addition to a pilA sequence that was similar to the ultra-conductive *Geobacter metallireducens* pilA. *Robinsoniella peoriensis* strain contained a substantial number of biomass-degrading genes, with a total of 425 CDS for CAZy related genes. The large amount of Firmicutes in the population totaling 42.5%, and the community as whole containing 2735 CAZy CDs spread across different roles in lignocellulosic degradation highlights selective forces of biomass-derived streams, requiring robust fermenters and cellulolytic microbes to convert the biomass to electrons, which the community demonstrated with high efficiency.

Introduction

The microbial communities that nature evolves to couple the degradation of organic carbon to anaerobic respiration of solid metals/minerals are an important part of the global carbon cycle occurring in soil and marine sediments. Three general steps are commonly found to occur: hydrolysis, fermentation, and anaerobic respiration. In addition to evolving specific functional abilities within individual microbes, the microbial community as a whole must develop strategies to achieve complete conversion of biomass. Syntrophic interactions have been demonstrated even for simple fermentable substrates [1–4]. However, additional strategies of division of labor and more complicated syntrophic partnerships are likely required for conversion of more complex biomass-derived streams[5]. Bioelectrochemical systems provide a pseudo-controlled environment where these steps can be studied with the substitution of a solid carbon electrode as final electron acceptor.

Many exoelectrogenic species that can respire solid electrodes have been identified, mainly belonging to the phylum Proteobacteria and are represented by the model species *Geobacter*

sulfurreducens and *Shewanella oneidensis*. These model exoelectrogenic organisms have been heavily investigated utilizing simple substrates to identify components of the extracellular electron transfer chain, resulting in characterization of c-type cytochromes and pili proteins that have been linked to current generation[6,7]. Despite continued growth of this field, little progress has been made in understanding microbial communities and the structure-function dynamics that allow for conversion of more complex, recalcitrant biomass-derived streams. Additionally, genetic and molecular investigation of exoelectrogens within bioanode communities utilizing real-world complex substrates has been under-investigated. Many different microbial taxa outside of model exoelectrogens and uncharacterized microbes can make up a substantial portion of anode communities while *Geobacter* species populations can be reduced[8,9]. Thus, it is likely that additional exoelectrogenic microbes can develop competitive advantages when pure substrates are not used.

A deeper investigation is needed in order to understand the community structure and resulting interactions that develop with more complex substrates in order to enhance conversion and electricity generation. In order to effectively manage these communities and increase productivity for commercial applications, the community members needed for conversion of individual compounds within complex streams, as well as their exoelectrogen partners, need to be characterized. This information can lead to identifying the positive interactions linking bioconversion to electroactivity, as well as negative interactions and environmental conditions that decrease productivity.

Our previous work has demonstrated that the complex nature of this stream requires multiple fermenting groups capable of converting anhydrosugars, acids, aldehydes, ketones, furanic and phenolic compounds to be efficiently converted by the microbial community generating

exoelectrogenic intermediates such as acetic acid to produce electrons which will enable hydrogen production at the cathode. It was discovered that fermentative processes can be limiting in BOAP conversion to hydrogen in MEC[5]. Our hypothesis was that if the fermentative members of the community can be identified, then strategies could be developed to increase their population to overcome the limitation in conversion of BOAP. In order to gain a better understanding of the active community members and their function roles in this system, an integrated 'omics approach was utilized to identify individual microbes present in the community, and assess active expression coupled with metabolite information. Initial processing of the generated DNA and RNA data was carried out following the framework design by Albertson et al. and expanded by Ishii et al.[10–12] as described in the methods. A metagenomic and metatranscriptomic analysis was conducted to assess the community structure and assess the functional ability of the consortium.

Methods

MEC operation and sampling

Replicate MEC reactors that have been in operation for >1.5 years under both continuous and batch conditions for conversion of a pyrolysis-derived bio-oil aqueous phase (BOAP) were used in this study[8,13]. The reactors were operated at a continuous organic loading rate of 20 g/L-d BOAP for a period of 3 weeks, with media changes once per week. The anodes were constantly poised at an anode set potential of -0.2 V vs Ag/AgCl. A recirculation loop from an external media reservoir was utilized to recycle unconverted compounds at a rate of 3.6 mL/min. The anode recirculation volume totaled 200 mL, with actual anode chamber making up 16 mL. A

sampling port was constructed on side of the anode compartment to sample the microbial community growing on the carbon felt electrode as shown in Appendix Figure 61. A 1.5 cm diameter hole was drilled into the back of the anode plate for each reactor, and a serum bottle rubber stopper was used to seal the hole. Metal plates were used to hold the stopper in place. This port could then be opened and closed rapidly as needed to remove anode felt cores for microbial sampling.

Reactor sampling

After 3 weeks of operation at 20 g/L-d BOAP loading to stabilize the microbial community, a media change was carried out and the reactor was operated for 46 hours, after which the 1st media sample was taken for metabolite analysis. After an additional 2 hours, a 2nd media sample was taken for metabolite analysis and the 1st community sample was taken. Both planktonic as well as biofilm samples were taken. This was done by first flushing 5 ml from the anode to sample the planktonic microbes, which was then followed by sampling of the biofilm via the port described above. A core of the carbon felt was cut out using a coring tool. The core sample was placed in a 1.5 ml sterile centrifuge tube containing RNAlater© and was flash frozen in liquid nitrogen. The liquid sample was briefly pelleted and resuspended in RNAlater© and flash frozen in liquid nitrogen.

Metagenomic and transcriptomic sequencing and assembly

DNA and RNA were co-extract using a MObio PowerBiofilm RNA Isolation Kit (Qiagen) with modification of the manufacturer's instructions to allow co-extraction. The co-extracted DNA and RNA were then separated using the AllPrep DNA/ RNA Mini Kit (Qiagen).

The prepared DNA and DNAse treated RNA were sequenced via paired-end sequencing on Illumina HiSeq by Macrogen-Japan (ADD MORE DETAILS). Additionally, separate amplicon 16S rRNA sequencing using V3-V4 region was also carried out on the DNA samples by Macrogen-Japan. The de-novo assembly of raw metagenomic sequences was conducted using a process as previously described[11]. Briefly, paired-end sequences from planktonic and biofilm community samples from the same reactor were co-assembled in CLC-genomics Workbench (Qiagen) using a bubble size of 700 and kmer size of 33. Contigs were filtered to include those sizes >500 bp. Contigs were then taxonomically assigned using PhyloPythiaS. Additionally, GC content was determined using methods fromAlbertson et al. [10] Next, predicted gene sequences within the contigs were determined via MetaGeneMark to generate predicted gene sequences and corresponding amino acid files. All predicted amino acid sequences were functionally annotated based on KEGG orthologous (KO) groups using the KEGG Automatic Annotation Server[14]. Proteins were also annotated to c-type cytochromes based on a CXXCH motif search[12], and those containing two or more occurrences of the motif may indicate multi-heme c-type cytochromes (MH-cytCs). Conserved protein orthologous groups of c-type cytochromes were used for family assignment[15].

Bin-genome and annotation

Bin-genome generation was carried out as previously described[12], with some additional steps. Read-mapping was carried out separately for planktonic and biofilm paired-end reads back to the co-assembled contigs, with the following parameters: mismatch cost = 2, insertion cost = 3, deletion cost = 3, length fraction = 0.7, and similarity = 0.95. Initial clusters were generated by plotting the average coverage of planktonic vs biofilm from read-mapping and then were refined

using Cytoscape® and tetra nucleotide frequency method[10]. The genome "completeness" of bin-genomes was also carried out as previously described[11], using 107 marker genes for bacteria and 137 marker genes for archaea.

Metabolite analysis

Anode and cathode off-gas measurements were made up to the 1st media sample at 46 hours, after which only cathode off-gas was measured. Gas collections were sampled via air-tight syringe on analyzed via gas chromatography (GC). Media samples taken for metabolite analysis were process for COD conversion and individual compounds as previously described[8]. COD samples were added to Hach HR COD (20–1500 mg/L COD) vials and digested in a Hach DRB 200 reactor at 150◦C for 2 h. Digested samples were allowed to cool to room temperature and analyzed on Spectronic 20 Genesys with absorbance readings taken at 620 nm. For HPLC, a Jasco 2000Plus (Jasco analytical instruments) equipped with PU-2089S Plus pump, a MD-2018 Plus Photodiode Array detector (PDA), a RI-2031 Plus intelligent RI detector was utilized with 5 mM H2SO4 mobile phase at flow-rate of 0.6 ml/min.

Calculations

Performance and conversion efficiency were characterized by Coulombic efficiency (CE), cathodic conversion efficiency (CCE), hydrogen recovery (HRE), and were calculated as previously described[8,16].

Results and Discussion

Microbial Community Structure

The microbial community analyzed in the present study was obtained from MEC reactors that have been in operation for >1.5 years using a pyrolysis-derived bio-oil aqueous phase (BOAP)[8,13] as the substrate. The reactors were operated under continuous feeding mode at an OLR of 20 g/L-d BOAP for 3 weeks prior to the microbial sampling. BOAP is a complex mixture containing various biomass degradation products including levoglucosan, furfural, HMF, and acetic acid among others. Enhanced recovery of bins was achieved through a combined approach of initial clustering based on average coverage and GC-content (Appendix Figure 62, differential coverage binning, tetranucleotide frequencies and finally utilizing connection mapping through Cytoscape®[17]. The optimized assembly and bin-genome process resulted in the generation of 23 complete genomes >90% and 15 high-quality genomes determined by HMP criteria[12,18], with total bins accounting for 90% of reads generated while only requiring 6,844 contigs (Table 16) The microbial community contained two dominant bin-genomes referred to as Delta1 and Clost2, which were identified as strains of *Pelobacter propionicus* and *Robinsoniella peoriensis*. These two bins accounted for nearly half of the population at 23.4 and 21.8%, respectively. The 3rd highest bin-genome was identified as *Propioniciella superfundia* at 4.8%. A host of additional Firmicutes led by Clostridia related organisms as well as Desulfovibrio, Bacteroidetes, were also present but to a lower degree <3%. Despite relatively high levels of acetate, a strain of *Geobacter Sulfurreducens* was found to be present at only ~1.2%. Additionally, methanogens were relatively suppressed at <2%. Separate 16S rRNA sequencing analysis was also carried out using V3-V4 region 16S rRNA sequence.

Table 16: Summary of results from bin-genome assembly

Read frequency (Bin-genome)	Length	Contigs	Reads	Abundance (%)	GC% ave	No of ORF	No of KO	No of CytC	No of MHCyt C	Genome Comp (%)	%	recA closest relatives
Delta1	4,640,266	42	2403640 2	**23.4%**	53.8	4067	1911	**108**	**71**	**96**	98	Pelobacter propionicus
Clost2	7,482,335	172	2926266 4	**21.8%**	41.1	6120	3373	15	2	**93**	97	Robinsoniella peoriensis
Act3	3,145,829	20	2919486	**4.8%**	66.8	2873	1566	8	2	**99**	92	Propionicicella superfundia
Delta4	4,998,079	75	3816141	**3.6%**	57.5	4485	2230	37	17	**95**	96	Desulfovibrio fructosivorans
Clost5	2,707,889	83	1333044	**2.1%**	44.5	2623	1513	15	1	**97**	82	Eubacterium limosum
Clost6	3,104,592	62	1711001	**2.5%**	50.3	2961	1653	10	1	**98**	98	Christensenella minuta
Bact7	4,975,196	37	2607322	**2.5%**	44.3	3887	1693	16	6	**98**	99	Proteiniphilum acetatigenes
Ery8	3,398,368	53	1448485	**2.2%**	35.7	3248	1856	9	0	**96**	100	Erysipelatoclostridium ramosum DSM 1402
Unc9	1,004,858	19	632133	**3.0%**	49.0	1036	485	3	0	89	89	Candidatus Saccharibacteria oral taxon TM7x

Table 16 Continued

Read frequency (Bin-genome)	Length	Contigs	Reads	Abundance (%)	GC% ave	No of ORF	No of KO	No of CytC	No of MHCyt C	Genome Comp (%)	%	recA closest relatives
Clost10	3,367,573	61	1366239	**2.0%**	53.1	3316	1593	18	1	**97**	84	Oscillibacter valericigenes
Met11	2,606,360	34	1145263	**2.4%**	58.5	2652	1319	12	0	**92**	99	Methanomassiliicoccus luminyensis
Alpha12	3,005,181	44	1191141	**2.0%**	60.5	2756	1793	10	3	**99**	85	Rhodospirillum rubrum
Firm13	3,035,822	30	1246689	**2.1%**	55.6	2878	1604	10	0	**98**	74	Anaerotruncus colihominis
Baci14	2,457,828	86	481781	**1.0%**	38.6	2333	1431	6	1	**97**	96	Enterococcus saccharolyticus
Act15	2,793,810	25	975255	**1.9%**	63.8	2551	1378	10	0	**96**	87	Propionicicella superfundia
Delta16	3,651,860	71	1102641	**1.4%**	58.8	3360	1703	**97**	**62**	**99**	99	Geobacter soli/Sulferreducens
Firm17	2,836,838	59	621328	**1.1%**	53.0	2735	1407	16	1	**96**	74	Pelotomaculum thermopropionicum
Clost18	3,340,583	60	726912	**1.1%**	52.6	3300	1534	12	0	**97**	92	Oscillibacter valericigenes

Table 16 Continued

Read frequency (Bin-genome)	Length	Contigs	Reads	Abundance (%)	GC% ave	No of ORF	No of KO	No of CytC	No of MHCyt C	Genome Comp (%)	%	recA closest relatives
Clost19	2,977,316	34	661811	**1.0%**	48.1	2907	1653	13	0	**95**	99	Catabacter hongkongensis
Clost20	2,581,910	66	614378	**1.2%**	35.4	2377	1401	16	1	**98**	80	Clostridium neopropionicum
Bact21	2,718,749	27	617358	**1.1%**	36.7	2265	1135	8	0	**100**	83	Prevotella bryantii
Clost22	5,887,669	66	1153288	**1.0%**	40.0	5303	3216	27	4	**92**	93	Clostridium cellobioparum
Clost23	3,059,276	16	675443	**1.1%**	54.1	2879	1638	9	0	**98**	88	Ruminococcaceae bacterium AM2
Firm24	1,102,229	10	210573	**1.0%**	37.3	1024	570	7	0	**94**	72	Eggerthia catenaformis
Act25	3,154,996	153	451062	**0.7%**	65.6	3076	1700	12	4	84	86	Propionibacterium freudenreichii
Act26	3,142,645	448	418804	**0.6%**	70.0	3451	1767	9	1	P	94	Microlunatus phosphovorus
Firm27	3,437,189	147	400999	**0.4%**	38.6	3431	1888	12	0	P	81	Clostridium purinilyticum
Met28	1,050,980	145	123274	**0.4%**	25.7	980	589	7	0	P	86	Methanobrevibacter arboriphilus
Bact29	2,475,609	468	278126	**0.4%**	43.9	2552	1293	9	3	P	86	Proteiniphilum acetatigenes
Clost30	10,206,562	769	958476	**1.0%**	40.9	10686	5979	36	1	P	89	Ruminococcus torques
Beta31	5,707,321	1419	426723	**0.4%**	61.7	7234	3741	50	10	P	98	Comamonas testosteroni
Beta32	5,003,068	1401	340728	**0.3%**	66.6	7066	4025	42	6	P	100	Acidovorax caeni

Since full length 16S rRNA sequence was not determined, this method may not provide an accurate picture of the microbial community. The results showed that the data did not correspond well with the distribution observed via metagenomics analysis. For example, *Deltaproteobacteria* were determined to be 10.68% via 16s rRNA analysis, while core-gene analyses indicated a total of 26.95%. Additionally, the top organism identified via core-gene analyses: *Pelobacter propionicus,* was not successfully identified by 16S rRNA analysis. As reported previously[12],16S rRNA analysis has many additional issues such as: different gene copy numbers for ribosomal RNA, compatibility of universal primers in addition to others that can alter the relative proportions of the assigned taxonomy. The use of a core-gene analysis can provide a more accurate picture of the community and with less bias.

BOAP conversion and performance

The overall electrochemical performance of the MEC reactor harboring the microbial community was used to get a first look into the metabolic capability of the community. At an OLR of 20 g/L-d BOAP, an average current density of 9.1 A/m^2 and H_2 productivity of 7.6 L/L-d were obtained (Figure 55a). The microbial community showed very high efficiency for converting BOAP into current, reaching an anode CE of 81.4% (Figure 55b). A comparatively lower HRE of 65.3% and a CCE of 80.2% were obtained, which can be attributed to pH gradients across the anode and cathode. The pH was controlled only in the anode and not the cathode whereby it increased to >13. The proton limitation in the cathode has been reported to lower the CCE and HRE[19]. While conversion of substrate into electrons was high, overall COD removal was relatively low reaching 37.6% while electrical efficiency was 110.5%. GC analysis of off-gases indicated that 13.2% of the electrons were diverted to methane.

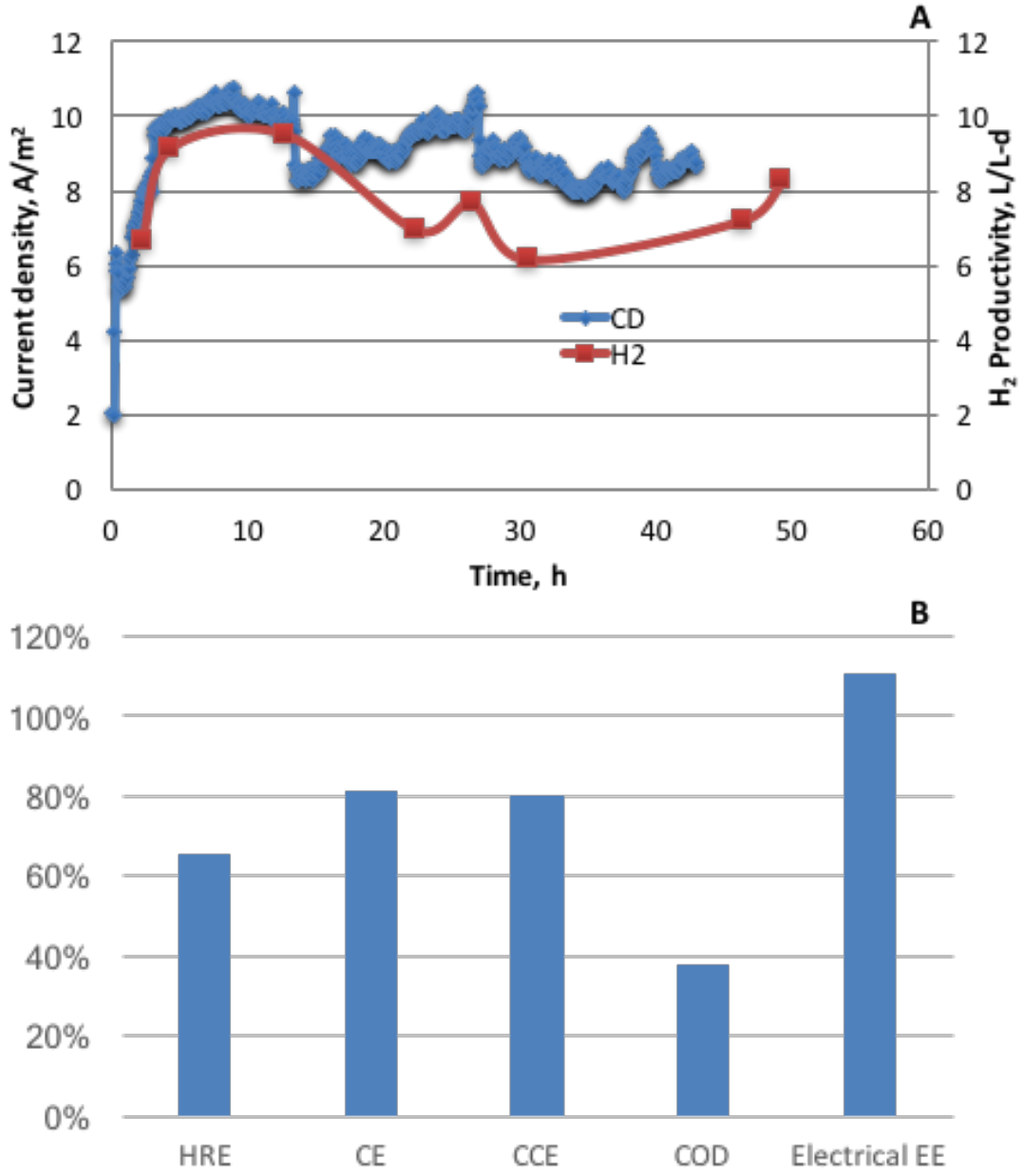

Figure 55: Electrochemical performance of microbial electrolysis cell at OLR of 20 g/L-d. CD: current density, HRE: Hydrogen recovery, CE: Coulombic efficiency, CCE: cathode conversion efficiency, EE: energy efficiency.

Thus, only 5.4% of electrons were lost to undefined sinks such as growth. It is likely that this resulted in the lower COD removal observed, allowing for the high efficiency of electrons directed to current.

Biotransformation of compounds with BOAP

A series of metabolite samples were taken from the effluent during BOAP conversion at 20 g/L-d and analyzed via HPLC. As outlined in the methods, a series of 3 samples were taken to assess conversion during normal poised conditions (Figure 56). Levoglucosan removal rate was the highest among all the substrates, since it was present at the highest concentration. Removal of acetic acid increased slightly prior to open-circuit stimulus, increasing from 5.3 to 7.34 mg/h. After apply open-circuit stimulus, which serves to halt acetate metabolism via exoelectrogenesis, acetate conversion decreased substantially and reversed to accumulation at -12.66 mg/h. Upon re-posing, acetate removal returned to 5.7 mg/h. The response of the exoelectrogen community to re-poising was not as strong as previously observed in terms acetate removal[5], and it is possible that the high BOAP concentrations result in a less favorable environment for the exoelectrogens, providing a higher level of stress. Propionic acid displayed a similar trend of increasing in conversion prior to open-circuit, which then resulted in accumulation at rate of -4.4 mg/h. However, upon re-poising propionic acid metabolism did not recover and accumulation persisted at -5.4 mg/h. It may be that propionic acid metabolism is tied more strongly to that of exoeelctrogenesis[20], or may possibly be used directly[21] but less preferentially by exoelectrogens, and thus the excess of acetic acid caused continued accumulation of propionic acid while acetate metabolism recovered. Additional compounds were removed at much lower rates did not display trends as a function of the electrode potential except for HMF, whose removal rate had been

slowly increasing up and through the open-circuit stimulus, but upon repoising, reduced 5-fold. It possible that upon re-poising, the re-engagement of acetate metabolism caused shifts in fermentative pathways that decreased flux through HMF conversion.

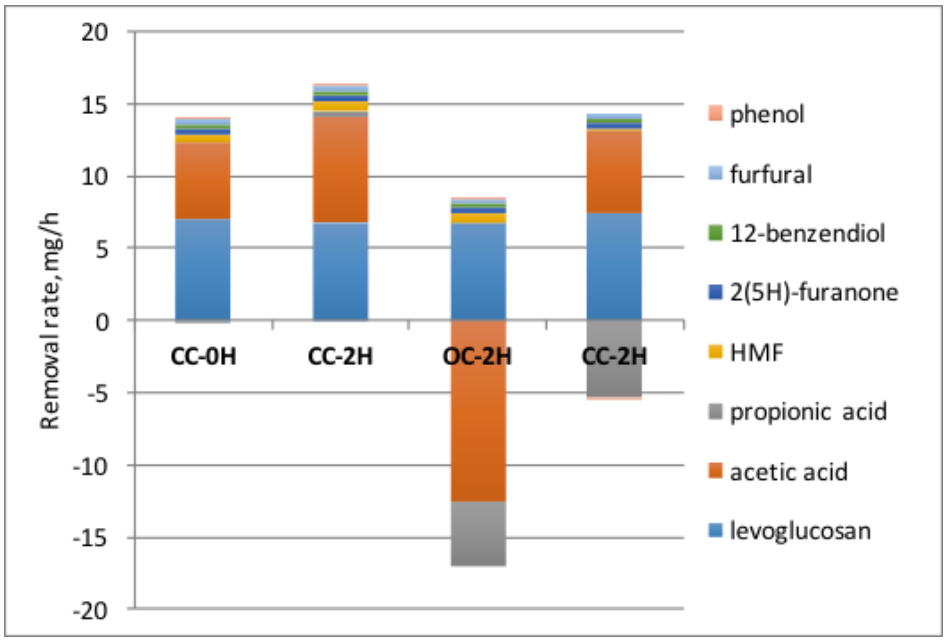

Figure 56: Individual compound conversion during BOAP conversion. (CC) closed-circuit, (OC) open-circuit.

Microbial community metabolism

To assess the broader metabolic activity of the assembled bin-genomes, marker genes associated with KEGG modules for metabolism related to respiration, specific substrates, glycolysis, and TCA cycle were selected[12,14]. Additionally, carbohydrate active enzymes from the Cazy database were also analyzed[22]. Gene expression levels based on mRNA-RPKM were normalized by DNA-RPKM for comparison among bin-genomes (Figure 57), and are discussed in the following sections.

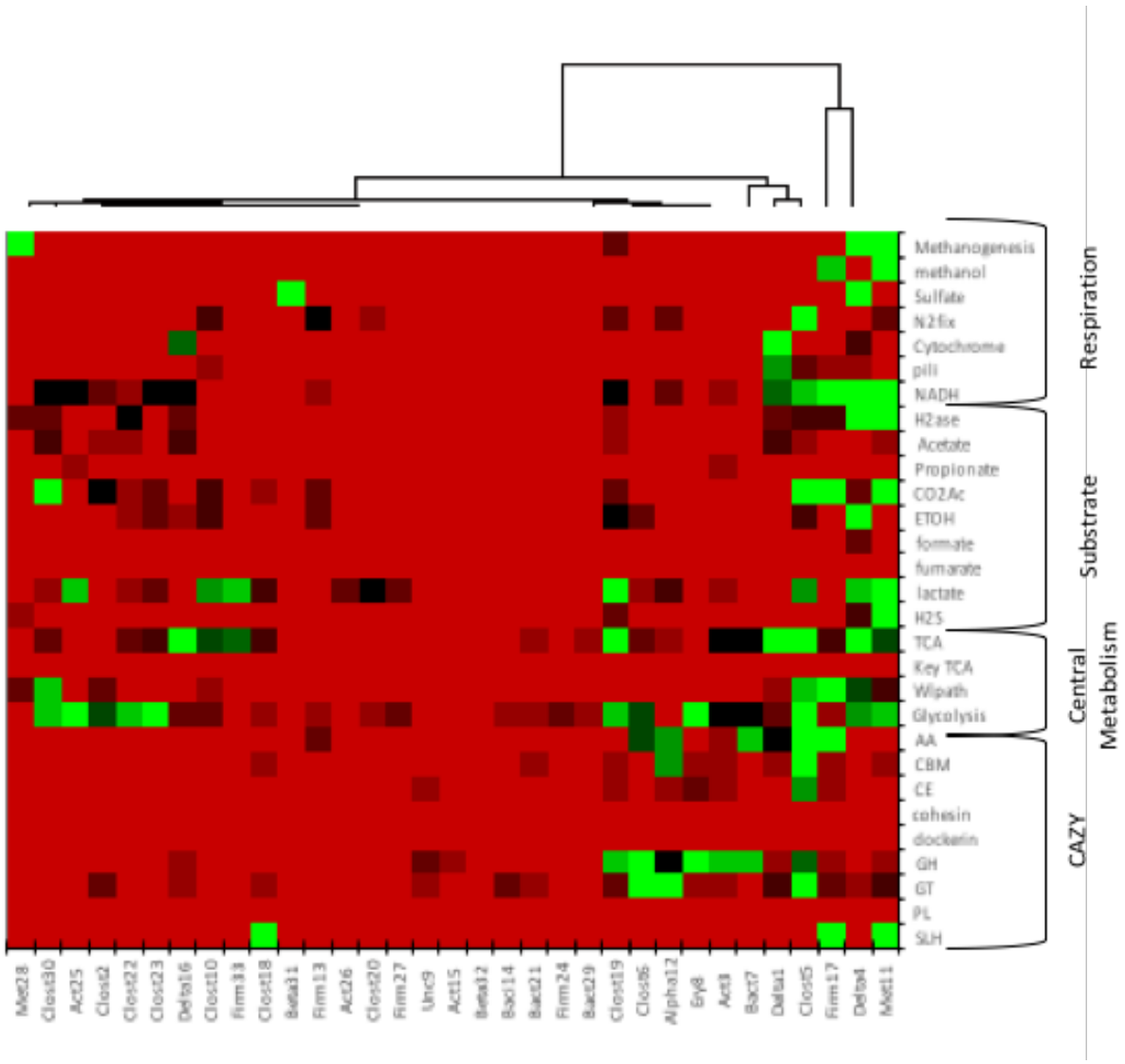

Figure 57: Heatmap of metabolic activity of bin-genomes.

Respiration activity

Methanogenesis, sulfate reduction, nitrogen fixation, and exoelectrogenesis were occurring simultaneously in the commnity Figure 57. While methanogen bin-genome Met11 was found to be active, off-gas analysis indicated that a significant portion of electrons were not diverted through this pathway. Delta4 was identified as *Desulfovibrio fructosivorans* and was sole active microbe in sulfate reduction, utilizing ethanol as carbon source. Clost5, identified as *Eubacterium limosum* displayed activity in nitrogen-fixation as well as NADH oxidoreductases and electron transfer flavoproteins. Delta16, identified as the well-known exoelectrogen *Geobacter Sulfurreducens*, and the top bin-genome Delta1, identified as *P. propionicus* were the only active exoelectrogenic and acetate consuming microbes in the community. While Delta1 consisted of 23.4% of the population, Delta16 was present at much lower levels (~1.4%). *P. propionicus* has not been reported as an exoelectrogen until now, nor has it been identified as an acetate utilizing microbe. The genome sequence reported previously was found to lack the necessary redox machinery for these two traits[23], however, it has lately been found to persist in some acetate fed BES systems[24]. Our study indicates an anomalous but novel feature of this organism, therefore a closer scrutiny is necessary. Furthermore, its phylogenetic proximity to *Geobacteraceae* also warrants a deeper investigation. Therefore, analysis of the core genes was carried out to confirm its identity. Using a method previously utilized for distinguishing between the Geobacteraceae and Pelobacteraceae familes[25], a blast alignment was done for the genes recA, gyrB, rpoB, and fusA (Appendix Table 17). *P. propionicus* was the highest %ID for all genes. Additionally, a phylogenetic tree was generated using KBase® based on a subset of COG domains, shown in Figure 58, further confirmation of the phylogenetic identity of Delta1.

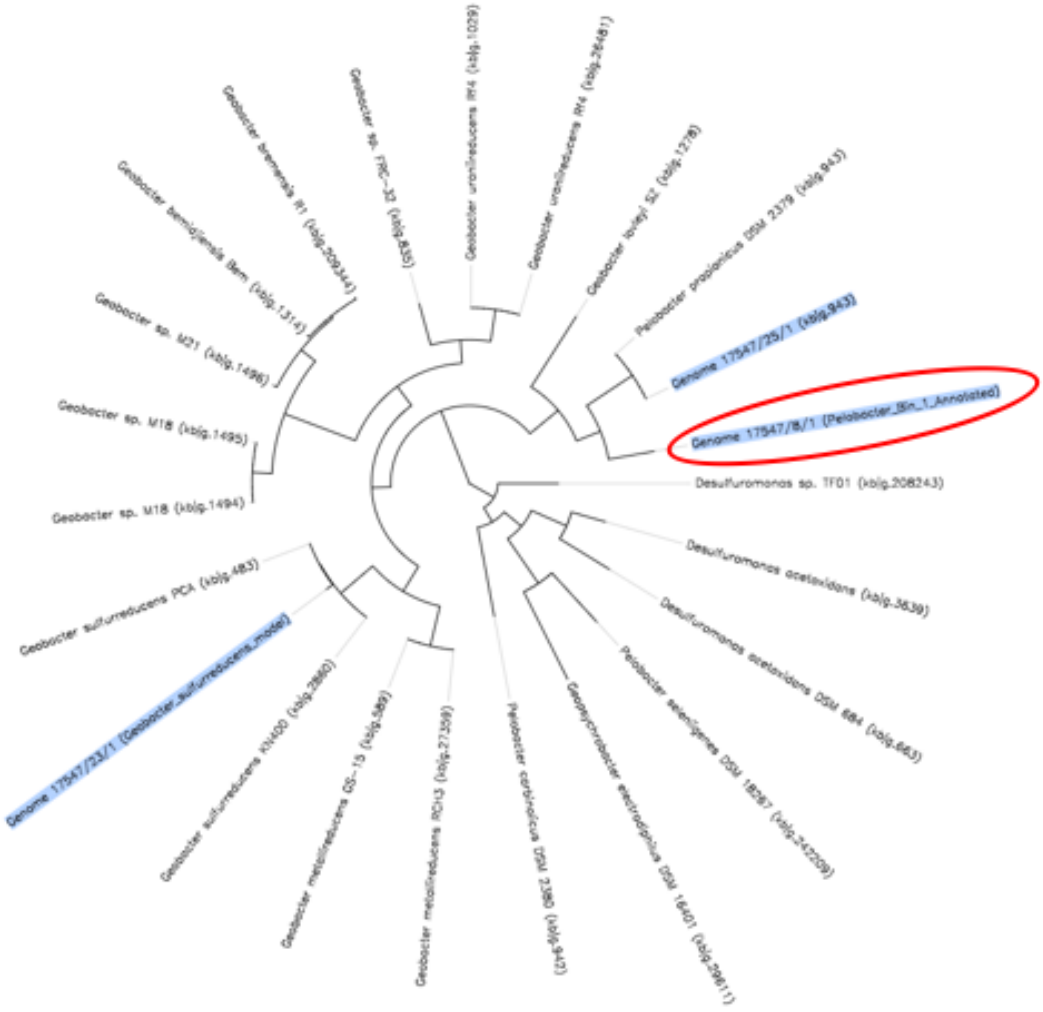

Figure 58: Phylogenetic tree for Delta1 bin-genome.

Comparison of Delta1 EET machinery

To investigate the novel exoelectrogenic ability of Delta1 further, a cytochrome analysis and alignment of the pilA gene, essential for pili formation in *Geobacter* strains, was carried out. Cytochrome analyses revealed Delta1 contained more total cytochromes (108) and multi-heme cytochromes (71) compared to Delta16, *G. sulfurreducens*. Furthermore, RNA analysis showed Delta1 had high expression of OmcX, Q, E and Z. OmcZ has been determined to be one of the most essential cytochromes for extracellular electron transfer (EET) [26–28]. Alignment of pilA against *P. propionicus* DSM as well as *G. sulfurreducens* and *G. metallireducens* also revealed some interesting results. Vargas et al. identified 5 aromatic residues in the pilA sequence that implicated in conductive abilities, which are highlighted in white in Figure 59.[29] The pilA sequence of Delta1 and the two Geobacter strains contain all 5 aromatic residues in the positions identified in that study. Additionally, expression of the pilA gene from *G. metallireducens* in *G. sulfurreducens* recently resulted in a 5000-fold improvement in conductivity, possibly due to a higher density of aromatic residues in the pilA gene *G. metallireducens*[30]. Looking closer at the pilA sequence alignment, Delta1 also contains additional aromatic residues similar to that of *G. metallireducens*, indicating the potential for enhance conductivity in this organism.

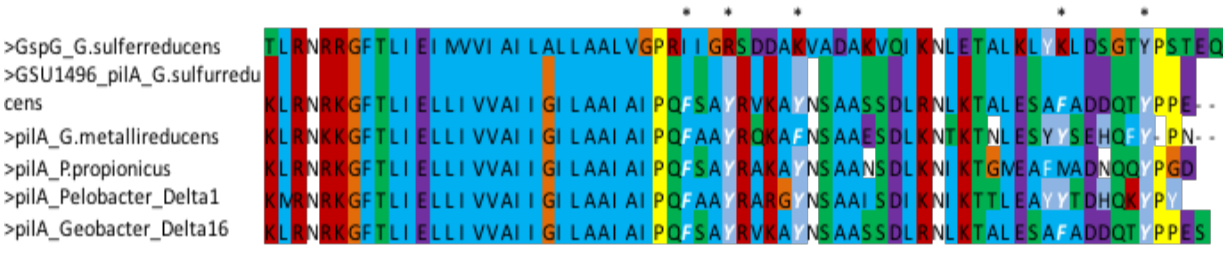

Figure 59: Alignment of pilA gene of Delta1 with other Pelobacter and Geobacter species. White letters highlight important aromatic residues.

Fermentative metabolism

Fermentative organisms within *Firmicutes* make up the largest portion of the population at 42.5%, displaying high activity for central metabolism via glycolysis. Firmicutes have been identified in the community as bin-genomes Clost2 and Clost6. These showed high expression of multiple sugar transport systems, as well as enzymes related to ribose, xylose, and xylulose metabolism. Thus, it is likely that this organism is heavily involved in the degradation of hemicellulose related compounds. Act3 and Clost5 bins and displayed high expression for propanediol dehydratases and ethanalomine utilization proteins as well as propanediol-acting alcohol dehydrogenases. These organisms are likely fermenting diols and with Act3 likely producing propionic acid in addition to acetic acid and other VFAs. Bin-genome Ey8 showed high activity for cellobiose specific enzymes, indicating a celluloytic role. Clost10 displayed high expression of genes uncharacterized in the KEGG database, and additional BLAST analysis could not pin down specific metabolisms, but propanediol as well as butanol related enzymes were found. To better characterize the ability of the fermentative organisms with many uncharacterized active genes likely related to biomass degradation, carbohydrate active enzymes were assessed through the CAZy database as described below.

Assessment of lignocelluosic active enzymes

BOAP is a complex mixture containing hundreds of biomass degradation products and requires a diverse and strong fermentative population. The predicted protein sequences from the assembled bin-genomes were aligned through the CAZy database[22] to identify lignocellulose-degrading enzymes likely needed to convert many of the compounds within BOAP. A total of

2735 CDSs for CAZy related genes were identified with e-value cut-off of 10^{-4}. Of those 1075 glycoside hydrolases (GH), 798 glycosyl transferases (GT), 308 carbohydrate esterases (CE), 219 carbohydrate-binding domains (CBM), 136 auxillary activities (AA), and 18 polysaccharide lyases (PL) (Figure 60A). By comparison, a recent study assessing CAZy genes from a thermophilc celluloytic community found 691 CDSs[31] ~4-fold less than that observed in this study. The Clost2 bin-genome, present at 21.8%, contained a substantial amount of CAZy related genes with 425 total CDSs. 26.8% of the glycoside hydrolases (288 CDs) found within this single bin, indicating a large role in the conversion of biomass-derivatives within BOAP. The largest number of CDSs were found for the families GH43, GH109, GH29, GH78 which contain, α-N-acetylgalactosaminidase, β-xylosidase, alpha-L-fucosidase and other enzymes related to hemicellulose degradation as well as enzymes involved in large polysaccharide hydrolysis such as alpha-L-fucosidase alpha-L-rhamnosidase. Clost2 also contains 55 glycosyl transferase and 36 carbohydrate esterase CDSs, including acetyl xylan esterses. The high number and diversity of CAZy related genes in this bin indicate a robust role. The 425 CAZY-related CDSs is higher than many top organisms identified from a thermophilic consortia adapted to degrade switchgrass[32]. Bact7 had the 2nd highest number of GH family CDSs with 233. Highly represented families included GH2, which contains cellulose-degrading enzymes such as beta-galactosidase. GH109 was also present in high amounts, encoding a α-N-acetylgalactosaminidase involved in hemicellulose degradation. Bact7 also contained a high amount of CE CDSs, including CE1 encoding an acetyl xylan esterase that helps solubilize xylan linkages for degradation. Bin-genome Act3 contains 42 GT CDSs including sucrose and cellulose synthase enzymes as well as 26 GH CDs, including GH13 alpha-amylases.

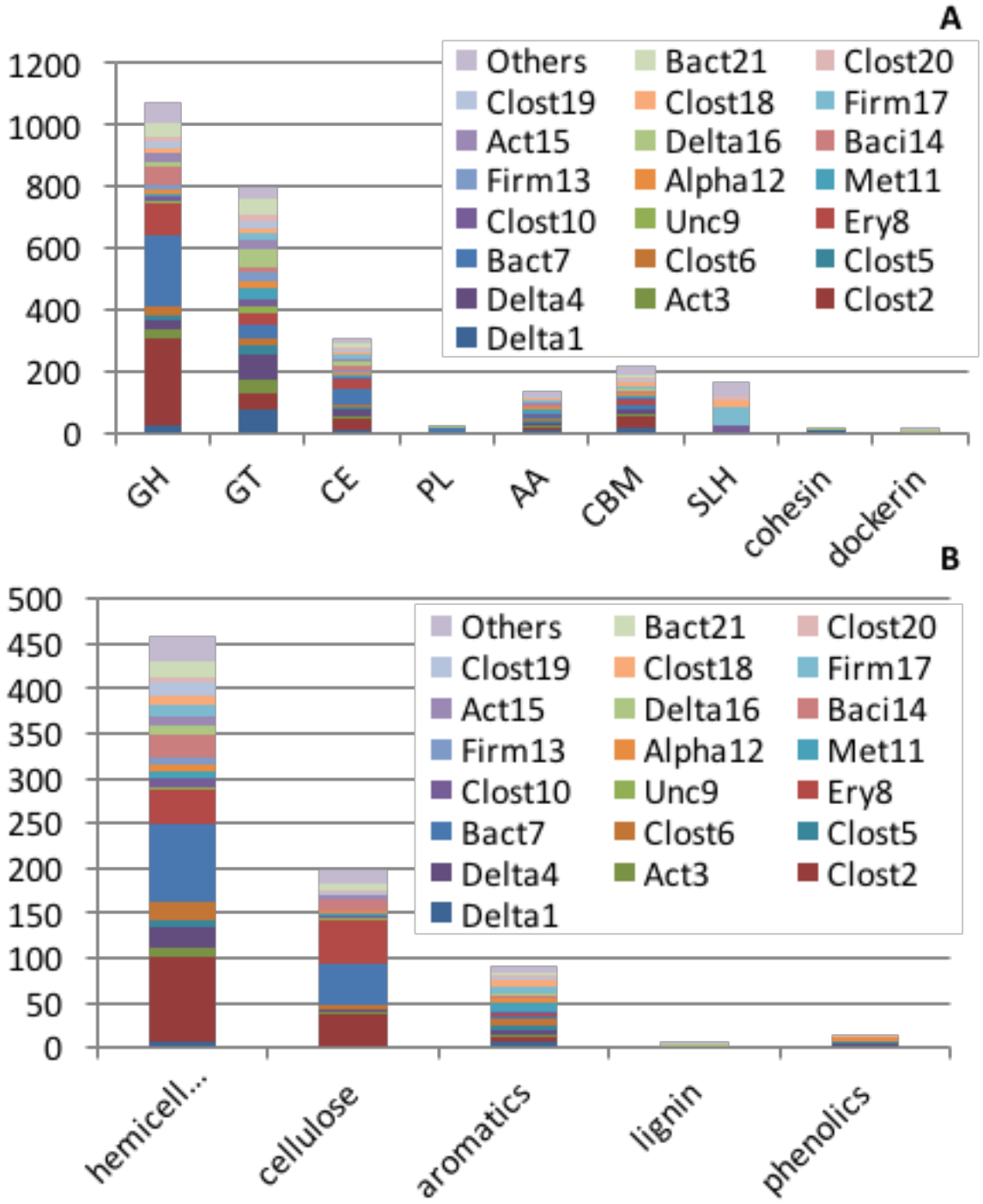

Figure 60: CDSs associated with carbohydrate-degrading enzymes.

Clost6 *Christensenella minuta* contains 31 GH and 24 GT CDSs, including GH109 alpha-N-acetylgalactosaminidase involved in hemiceullose degradation. Ery8 contained an additional 103 GH CDSs, including GH1 encoding enzymes such as beta-glucosidase and beta-galactosidase involved in cellulose degradation. Figure 60B depicts the identified CAZy genes in the community as the relate to the components of lignocellulosic biomass. Hemicellulose-related enzymes were the most prevalent with 459 CDS, followed by lignin with 199 CDSs. Additional classes of biomass derivatives such as phenolic and aromatic compounds were also delineated, with 92 and 14 CDS, respectively. Clost5, Clost6, and Firm17 all collectively deploy encoding 1,4-benzoquinone reductase for conversion of aromatic compounds. BOAP contains many compounds in these classes, including furfural, HMF, phenol, catechol, and vanillic acid. The CAZy results indicate the strong ability of this community for degradation of biomass-derived streams.

Conclusions

The optimized assembly process resulted in the capture of approximately 90% of the sequenced reads into bin-genomes producing, 21 high-quality genomes form the microbial community. The community was dominated by two strains related to *Pelobacter propionicus* and *Robinsoniella peoriensis*. The former was demonstrated to possess novel exoelectrogenic behavior for its taxonomy, containing similar numbers of c-type cytochromes with expression of the essential OmcZ, in addition to a pilA sequence which was similar to the ultra-conductive *Geobacter metallireducens* pilA. *Robinsoniella peoriensis* strain contained a substantial number of biomass-degrading genes, with a total of 425 CDS for CAZy related genes. The large amount of Firmicutes in the population totaling 42.5%, and the community as whole containing 2735

CAZy CDs spread across different roles in lignocellulosic degradation highlights selective forces of biomass-derived streams, requiring robust fermenters and cellulolytic microbes to convert the biomass to electrons, which the community demonstrated with high efficiency. The omics analysis thus identified key microbes responsible for the fermentative and exoelectrogenic function in the community, which can be manipulated to optimize MEC performance. To increase productivity further and increase removal rates without losing efficiency, further elucidation of functional roles of the active microbes may be necessary such that the positive interactions can be sustained leading to high performance.

References

1. Freguia S, Rabaey K, Yuan Z, Keller J. Syntrophic processes drive the conversion of glucose in microbial fuel cell anodes. *Environ Sci Technol*. 2008;42(21):7937-7943. doi:10.1021/es800482e.
2. Parameswaran P, Torres CI, Lee HS, Krajmalnik-Brown R, Rittmann BE. Syntrophic interactions among anode respiring bacteria (ARB) and non-ARB in a biofilm anode: Electron balances. *Biotechnol Bioeng*. 2009;103(3):513-523. doi:10.1002/bit.22267.
3. Miceli JF, Garcia-Peña I, Parameswaran P, Torres CI, Krajmalnik-Brown R. Combining microbial cultures for efficient production of electricity from butyrate in a microbial electrochemical cell. *Bioresour Technol*. 2014;169:169-174. doi:10.1016/j.biortech.2014.06.090.
4. Hari AR, Katuri KP, Gorron E, Logan BE, Saikaly PE. Multiple paths of electron flow to current in microbial electrolysis cells fed with low and high concentrations of propionate. *Appl Microbiol Biotechnol*. 2016;100(13):5999-6011. doi:10.1007/s00253-016-7402-2.
5. Lewis AJ, Campa MF, Hazen TC, Borole AP. Unravelling biocomplexity of electroactive biofilms for producing hydrogen from biomass. *Microb Biotechnol*. July 2017. doi:10.1111/1751-7915.12756.
6. Reguera G, McCarthy KD, Mehta T, Nicoll JS, Tuominen MT, Lovley DR. Extracellular electron transfer via microbial nanowires. *Nature*. 2005;435(7045):1098-1101. doi:10.1038/nature03661.
7. Gorby YA, Yanina S, McLean JS, et al. Electrically conductive bacterial nanowires produced by Shewanella oneidensis strain MR-1 and other microorganisms. *Proc Natl Acad Sci U S A*. 2006;103(30):11358-11363. doi:10.1073/pnas.0604517103.
8. Lewis AJ, Ren S, Ye X, Kim P, Labbe N, Borole AP. Hydrogen production from switchgrass via an integrated pyrolysis-microbial electrolysis process. *Bioresour Technol*. 2015;195:231-241. doi:10.1016/j.biortech.2015.06.085.
9. Montpart N, Rago L, Baeza JA, Guisasola A. Hydrogen production in single chamber microbial electrolysis cells with different complex substrates. *Water Res*. 2014;68C:601-615. doi:10.1016/j.watres.2014.10.026.
10. Albertsen M, Hugenholtz P, Skarshewski A, Nielsen KL, Tyson GW, Nielsen PH. Genome sequences of rare, uncultured bacteria obtained by differential coverage binning of multiple metagenomes. *Nat Biotechnol*. 2013;31(6):533-538. doi:10.1038/nbt.2579.
11. Ishii S, Suzuki S, Norden-Krichmar TM, et al. A novel metatranscriptomic approach to identify gene expression dynamics during extracellular electron transfer. *Nat Commun*. 2013;4:1601. doi:10.1038/ncomms2615.
12. Ishii S, Suzuki S, Tenney A, Norden-Krichmar TM, Nealson KH, Bretschger O. Microbial metabolic networks in a complex electrogenic biofilm recovered from a stimulus-induced metatranscriptomics approach. *Sci Rep*. 2015;5:14840. doi:10.1038/srep14840.
13. Lewis AJ, Borole AP. Understanding the impact of flow rate and recycle on the conversion of a complex biorefinery stream using a flow-through microbial electrolysis cell. *Biochem Eng J*. 2016;116:95-104. doi:10.1016/j.bej.2016.06.008.
14. Kanehisa M, Araki M, Goto S, et al. KEGG for linking genomes to life and the environment. *Nucleic Acids Res*. 2008;36(Database issue):D480-4.

doi:10.1093/nar/gkm882.
15. Butler JE, Young ND, Lovley DR. Evolution of electron transfer out of the cell: comparative genomics of six Geobacter genomes. *BMC Genomics*. 2010;11(1):40. doi:10.1186/1471-2164-11-40.
16. Logan BE, Call D, Cheng S, et al. Microbial electrolysis cells for high yield hydrogen gas production from organic matter. *Environ Sci Technol*. 2008;42:8630-8640. doi:10.1021/es801553z.
17. Smoot ME, Ono K, Ruscheinski J, Wang P-L, Ideker T. Cytoscape 2.8: new features for data integration and network visualization. *Bioinformatics*. 2011;27(3):431-432. doi:10.1093/bioinformatics/btq675.
18. Nelson KE, Weinstock GM, Highlander SK, et al. A Catalog of Reference Genomes from the Human Microbiome. *Science (80-)*. 2010;328(5981):994-999. doi:10.1126/science.1183605.
19. Borole AP, Lewis AJ. Proton transfer in microbial electrolysis cells. *Sustain Energy Fuels*. 2017;0:1-12. doi:10.1039/C7SE00034K.
20. Hari AR, Katuri KP, Logan BE, Saikaly PE. Set anode potentials affect the electron fluxes and microbial community structure in propionate-fed microbial electrolysis cells. *Sci Rep*. 2016;6:38690. doi:10.1038/srep38690.
21. Sun M, Mu Z-X, Sheng G-P, et al. Hydrogen production from propionate in a biocatalyzed system with in-situ utilization of the electricity generated from a microbial fuel cell. *Int Biodeterior Biodegradation*. 2010;64(5):378-382. doi:10.1016/j.ibiod.2010.04.004.
22. Yin Y, Mao X, Yang J, Chen X, Mao F, Xu Y. dbCAN: a web resource for automated carbohydrate-active enzyme annotation. *Nucleic Acids Res*. 2012;40(W1):W445-W451. doi:10.1093/nar/gks479.
23. Butler JE, Young ND, Lovley DR. Evolution from a respiratory ancestor to fill syntrophic and fermentative niches: comparative fenomics of six Geobacteraceae species. *BMC Genomics*. 2009;10(1):103. doi:10.1186/1471-2164-10-103.
24. Kiely PD, Rader G, Regan JM. Long-term cathode performance and the microbial communities that develop in microbial fuel cells fed different fermentation endproducts. *Bioresour Technol*. 2011;102(1):361-366. doi:10.1016/j.biortech.2010.05.017.
25. Holmes DE, Nevin KP, Lovley DR. Comparison of 16S rRNA, nifD, recA, gyrB, rpoB and fusA genes within the family Geobacteraceae fam. nov. *Int J Syst Evol Microbiol*. 2004;54(5):1591-1599. doi:10.1099/ijs.0.02958-0.
26. Nevin KP, Kim B-C, Glaven RH, et al. Anode biofilm transcriptomics reveals outer surface components essential for high density current production in Geobacter sulfurreducens fuel cells. *PLoS One*. 2009;4(5):e5628. doi:10.1371/journal.pone.0005628.
27. Richter H, Nevin KP, Jia H, Lowy DA, Lovley DR, Tender LM. Cyclic voltammetry of biofilms of wild type and mutant Geobacter sulfurreducens on fuel cell anodes indicates possible roles of OmcB, OmcZ, type IV pili, and protons in extracellular electron transfer. *Energy Environ Sci*. 2009;2(5):506. doi:10.1039/b816647a.
28. Inoue K, Qian X, Morgado L, et al. Purification and characterization of OmcZ, an outer-surface, octaheme c-type cytochrome essential for optimal current production by Geobacter sulfurreducens. *Appl Environ Microbiol*. 2010;76(12):3999-4007. doi:10.1128/AEM.00027-10.

29. Vargas M, Malvankar NS, Tremblay P-L, et al. Aromatic amino acids required for pili conductivity and long-range extracellular electron transport in Geobacter sulfurreducens. *MBio*. 2013;4(2):e00105-13. doi:10.1128/mBio.00105-13.
30. Tan Y, Adhikari RY, Malvankar NS, et al. Expressing the Geobacter metallireducens PilA in Geobacter sulfurreducens Yields Pili with Exceptional Conductivity. *MBio*. 2017;8(1):e02203-16. doi:10.1128/mBio.02203-16.
31. Lemos LN, Pereira R V., Quaggio RB, et al. Genome-Centric Analysis of a Thermophilic and Cellulolytic Bacterial Consortium Derived from Composting. *Front Microbiol*. 2017;8:644. doi:10.3389/fmicb.2017.00644.
32. D'haeseleer P, Gladden JM, Allgaier M, et al. Proteogenomic Analysis of a Thermophilic Bacterial Consortium Adapted to Deconstruct Switchgrass. Xu Y, ed. *PLoS One*. 2013;8(7):e68465. doi:10.1371/journal.pone.0068465.

Appendix

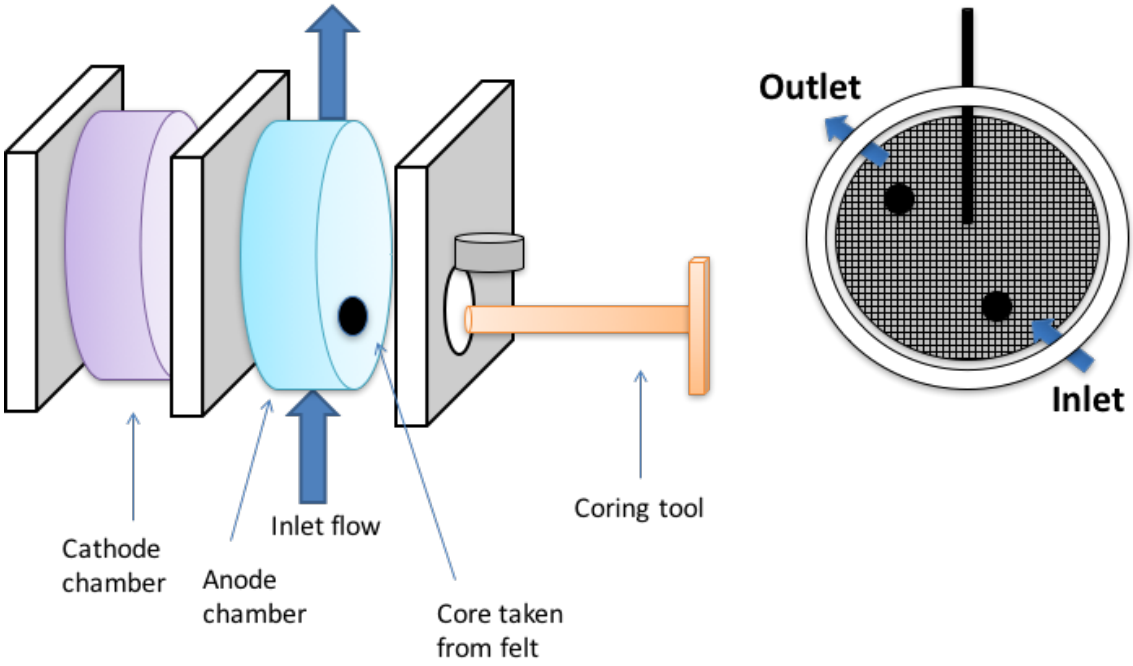

Figure 61: Schematic of MEC reactor design and sampling port.

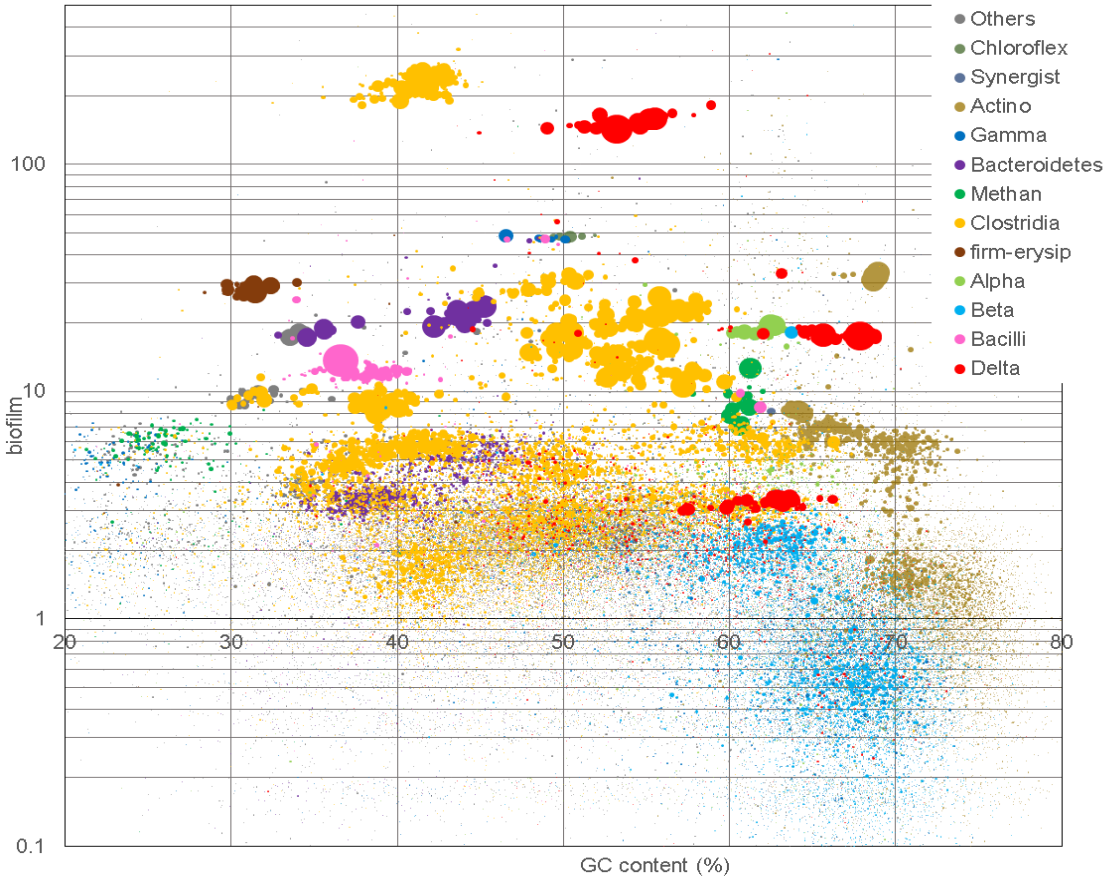

Figure 62: Metagenome contig binning based on average coverage and GC content.

Table 17: Core gene analysis of *Pelobacter Propionicus* using recA, gyrB, rpoB, fusA.

Gene	Taxonomy	%ID	E-value
recA	Pelobacter propionicus DSM 2379, complete genome	98%	0
	Geobacter metallireducens GS-15, complete genome	93%	0
	Geobacter pickeringii strain G13, complete genome	92%	0
	Geobacter anodireducens strain SD-1, complete genome	93%	0
	Geobacter sulfurreducens strain AM-1 genome	87%	0
	Geobacter sulfurreducens PCA, complete genome	87%	0
gyrB	Pelobacter propionicus DSM 2379, complete genome	98%	0
	Geobacter lovleyi SZ, complete genome	98%	0
	Geobacter sp. M18, complete genome	98%	0
	Geobacter pickeringii strain G13, complete genome	84%	0
	Geobacter sulfurreducens strain AM-1 genome	83%	0
	Geobacter sulfurreducens PCA, complete genome	83%	0
rpoB	Pelobacter propionicus DSM 2379, complete genome	99%	0
	Geobacter daltonii FRC-32, complete genome	89%	0
	Geobacter metallireducens GS-15, complete genome	90%	0
	Geobacter lovleyi SZ, complete genome	94%	0
	Geobacter uraniireducens Rf4, complete genome	90%	0
	Geobacter pickeringii strain G13, complete genome	90%	0
	Geobacter anodireducens strain SD-1, complete genome	90%	0
	Geobacter sulfurreducens strain AM-1 genome	90%	0
	Geobacter sulfurreducens PCA, complete genome	90%	0
fusA	Geobacter lovleyi SZ, complete genome	100%	0
	Pelobacter propionicus DSM 2379, complete genome	100%	0
	Geobacter uraniireducens Rf4, complete genome	100%	0
	Geobacter metallireducens GS-15, complete genome	100%	0
	Geobacter daltonii FRC-32, complete genome	100%	0
	Geobacter pickeringii strain G13, complete genome	100%	0
	Geobacter sulfurreducens strain AM-1 genome	99%	0
	Geobacter sulfurreducens PCA, complete genome	99%	0
fusA	Pelobacter propionicus DSM 2379, complete genome	99%	0
	Geobacter lovleyi SZ, complete genome	99%	0
	Geobacter sp. M18, complete genome	99%	0
	Geobacter sp. M21, complete genome	98%	0
	Geobacter bemidjiensis Bem, complete genome	98%	0
	Geobacter sulfurreducens strain AM-1 genome	96%	0
	Geobacter sulfurreducens PCA, complete genome	96%	0
fusA	Pelobacter propionicus DSM 2379, complete genome	98%	0
	Geobacter sulfurreducens strain AM-1 genome	97%	0
	Geobacter sulfurreducens PCA, complete genome	97%	0

FINAL DISCUSSION

Correlating performance to OLR

To better elucidate the association between operational OLR and performance, principle component analysis (PCA) was carried using the data from both replicate reactors at each OLR tested from CHAPTER I (Figure 63). Performance values of CE, HRE, CCE, H_2 productivity (HP), and current density (CD) were included. The 4 conditions were low loading and high flow-rate (L-H), low loading and low flow-rate (L-L), high loading and high flow-rate (H-H), and finally high loading and low flow-rate (H-L). Additionally, each quadrant pair can be analyzed for its shared operational condition, either OLR or flow-rate. The results indicate that for all performance variables, higher flow-rate is associated with better performance, with all arrows directed in the upper two quadrants. Within this quadrant pair for high flow-rate, efficiency values for CE and HRE correlated more with lower OLR while CCE and productivity metrics of HP and CD correlated more strongly with higher loading. Thus, the main correlation is the negative relationship between OLR and CE/HRE, i.e. more electrons are diverted away from sinks outside of current and hydrogen as OLR increases.

The correlation results can be explained and potential pathways for improvement can be identified by linking the parameters to the biochemical aspects of the anode. The low CE and HRE at higher OLR may be limited by the biofilm thickness or microbial density in the anode, leading to diversion of electrons to growth but needs to be investigated further.

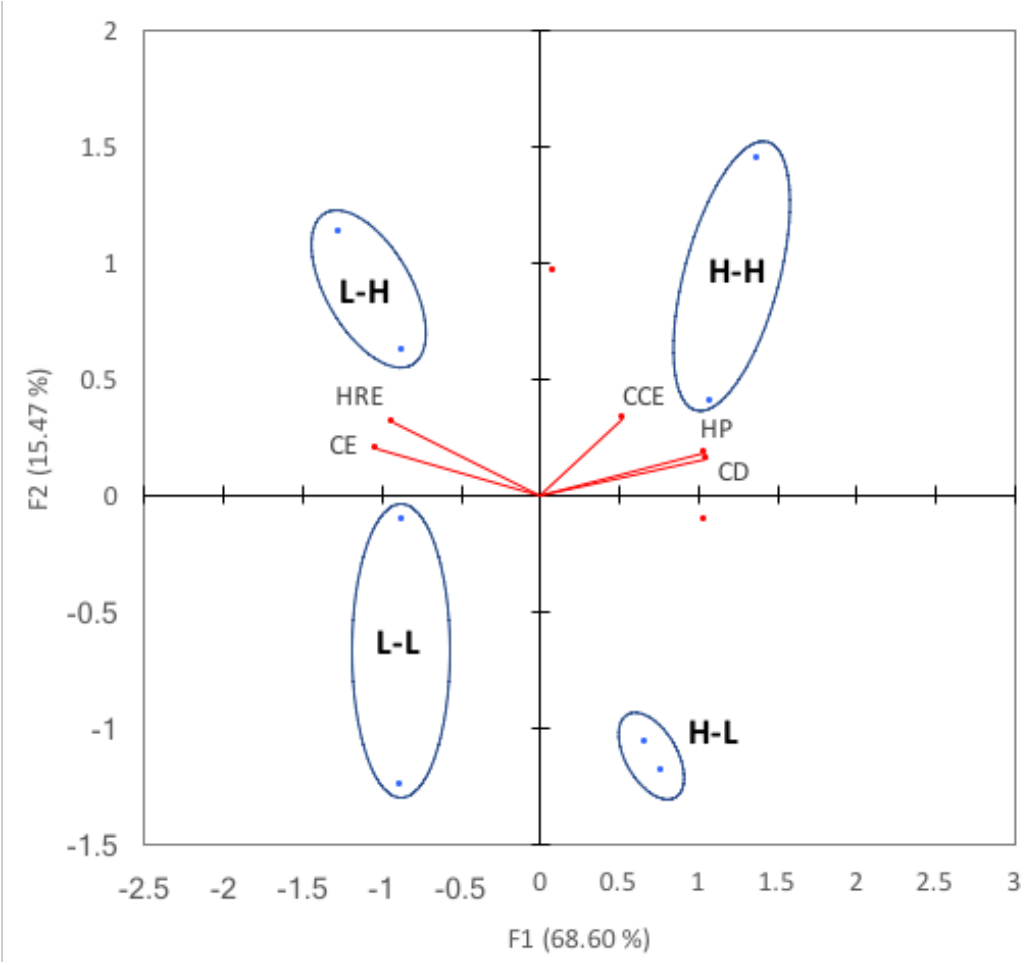

Figure 63: Principal component analysis of operational conditions and performance metrics. (L-H); 2 g/L-d, 4 mL/min. (L-L); 2 g/L-d, 0.4 mL/min. (H-H); 20 g/L-d, 4 mL/min. (H-L); 20 g/L-d, 0.4 mL/min.

Correlating feeding regime to MEC performance

With strong evidence for the impact of substrate on community development, the changes in performance and structure are likely driven by the substrate BOAP, and concentration of its individual components at the levels tested. The conclusions reached for the impact of batch vs continuous addition found a heavy influence from observed changes in individual compound biotransformation as underlying factors impacting current output, COD removal, and CE as function of feeding regime (batch vs continuous) and loading/concentration level (low vs high). Principal component analysis was carried to further elucidate these relationships (Figure 64). The substrate variables are in terms of working concentration rather than percent removal. Thus, higher concentrations of propionic acid, acetate, and catechol are negatively correlated with CE and COD removal which have zero correlation to current density. On the surface, higher acetate and propionic acid concentrations should provide more substrate for exoelectrogens leading to higher current and good CE. However, the positive correlation of higher acetate concentrations with higher concentrations of catechol and higher diversion of electrons to undefined sinks is symptomatic for repressing exoelectrogenesis. These 3 variables are all found correlating to the high batch condition, indicating the high concentration of BOAP related compounds prevents full utilization of acetate and diversion of electrons to growth and other undefined sinks, decreasing anode efficiency while not resulting in any positive correlation for higher current at the high BOAP concentrations. Thus, proper community enrichment in a progressive fashion is needed to develop a denser biocatalyst to handle the more recalcitrant compounds within BOAP, to prevent their accumulation which appears to result in loss in performance.

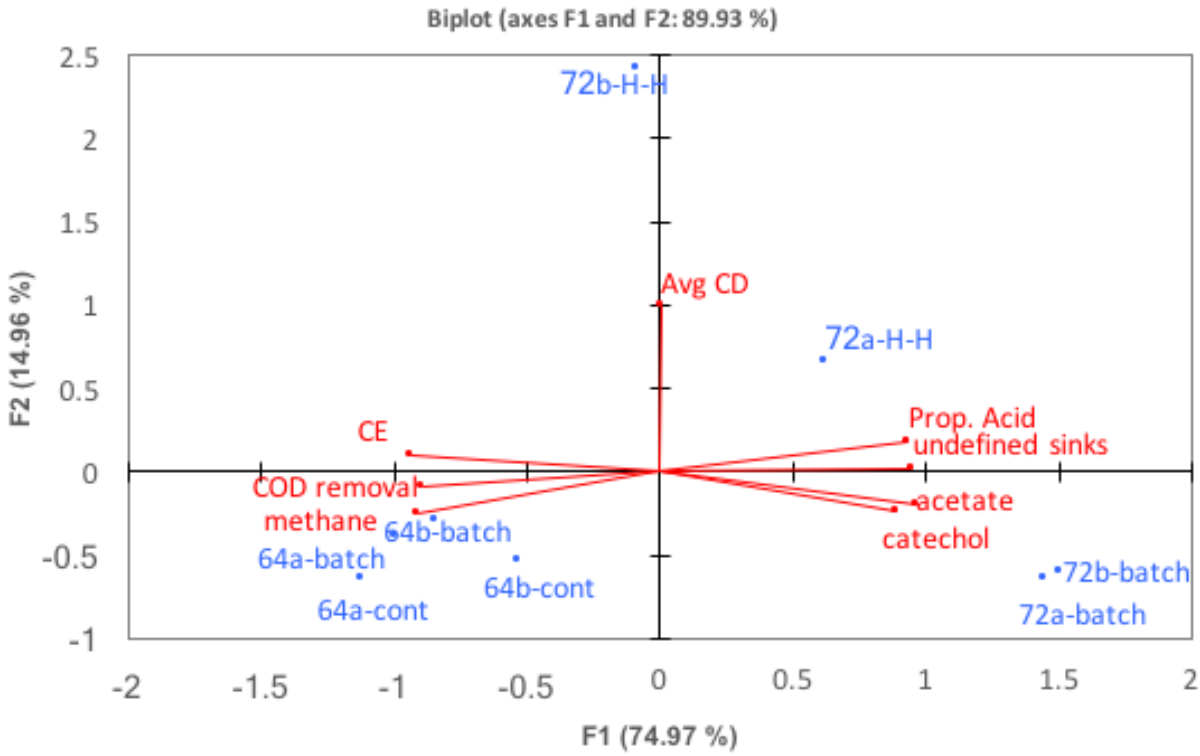

Figure 64: Principal component analysis of feeding regime and substrate concentrations related to performance.

Trends in MEC performance resulting from anode potential shift

Looking deeper into the microbial community response to electrode potential, we can see clearly from Figure 65 that shifting each reactor to the opposite potential level did not result in equivalent short-term responses. The -400 mV reactor was able to maintain and achieve performance after the shift similar to the 0 mV reactor at that level. Thus, conversion of BOAP in current was not inhibited, and both the '-400 mV – end' and '0 mV –pre' were positively correlated with H_2 productivity, and acetate removal rate. However, the 0 mV microbial community did not have the same response, and was unable to mimic the performance of the -400 mV enriched community at that level. This resulted in drop in performance and negative correlation with current density and CE. However, as described in corresponding chapter that

detailed these experiments, proton transport and cathode limitations likely allowed for protons and electrons produced prior to the shift to contribute to H_2 production after the shift, resulting in a positive correlation in CCE and electrical efficiency. The strong correlation between loss in current output and CE provide further evidence that shifting more negative potentials provides stronger selective pressure due to the loss in energy gain available to the microbes, disadvantaging microbes that have been enriched to utilize more positive redox machinery. However, the experiments and long-term studies carried out with -400 mV reactor indicate that if direct enrichment is carried out, the anode community can develop to perform at these more negative anode potentials by utilizing more negative potential terminal cytochromes that can sustain high rates of electron transfer.

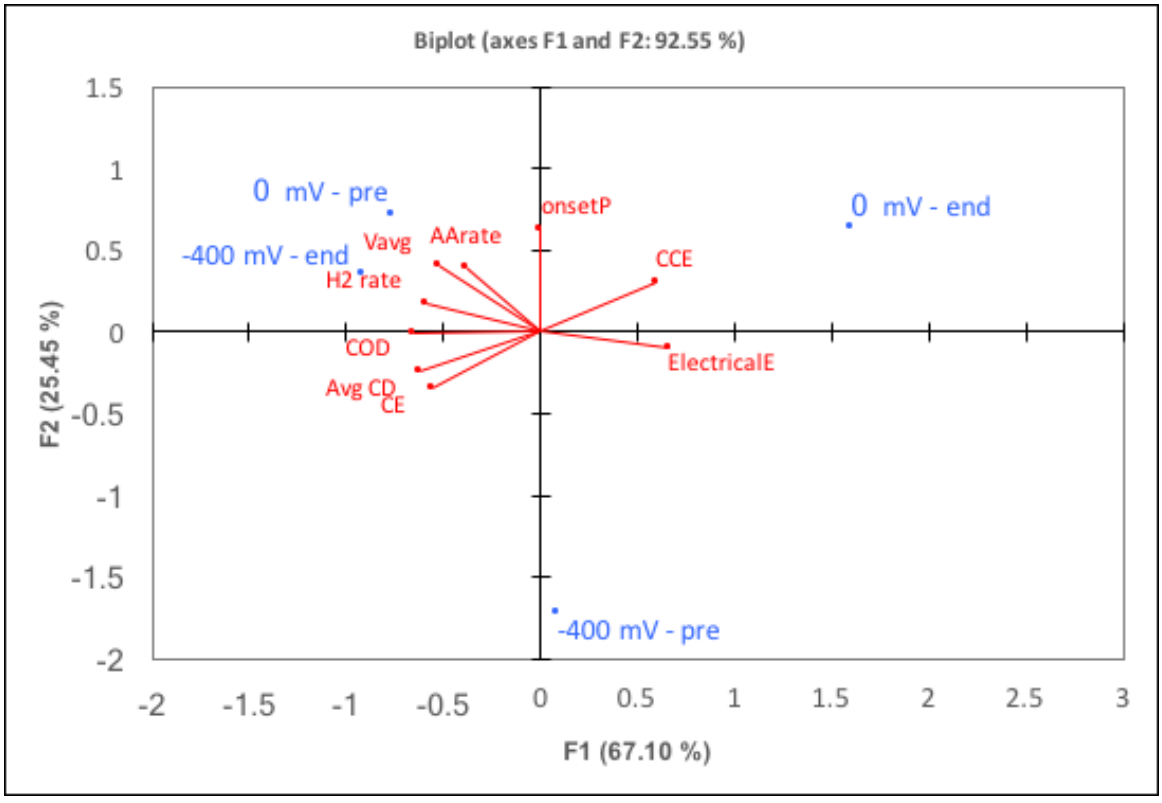

Figure 65: PCA after anode potential shift. (AA); acetic acid, (onsetP); onset potential, (Vavg); average cell voltage.

Correlating operational conditions to performance and microbial community structure

To gain additional insight into the relationship between MEC performance and the operating conditions highlighted in the previous sections, incorporating additional observations in the form of microbial taxa will serve to provide a foundation on which to identify optimal community structures that will result in the best performance for the desired operational condition and output metrics. Combining experimental data from the previous chapters, categorical descriptions were simplified to low, medium, and high loading and batch or continuous addition. Additionally, positive or negative was used to described specific electrode potential conditions (Figure 66). It is clear that high continuous loading rates result in the highest H_2 productivity by allowing high concentrations of substrate to be added without large substrate spikes that can alter metabolism and lead to accumulation of phenolic intermediates and subsequently acetic acid and propionic acid, reducing current as was seen in the fed-batch experiment at 2.5 g/L. To this end, the high batch levels are negatively correlated with COD removal as accumulation of those compounds starts to occur. Meanwhile, COD removal was positively correlated with more positive anode potentials, likely due to the higher energy gain available to the microbes, resulting increased COD removal to growth and other electron sinks. For anode efficiency, we can see that see that CE is most strongly correlated to low continuous organic loadings, that prevent diversion of electrons to undefined sinks, but which also results in low current and H_2 output evidenced by the negative correlation related to those parameters. Now moving to the microbial taxa trends, we can see that *Deltaproteobacteria* are most strongly correlated to H_2 productivity and high continuous loading.

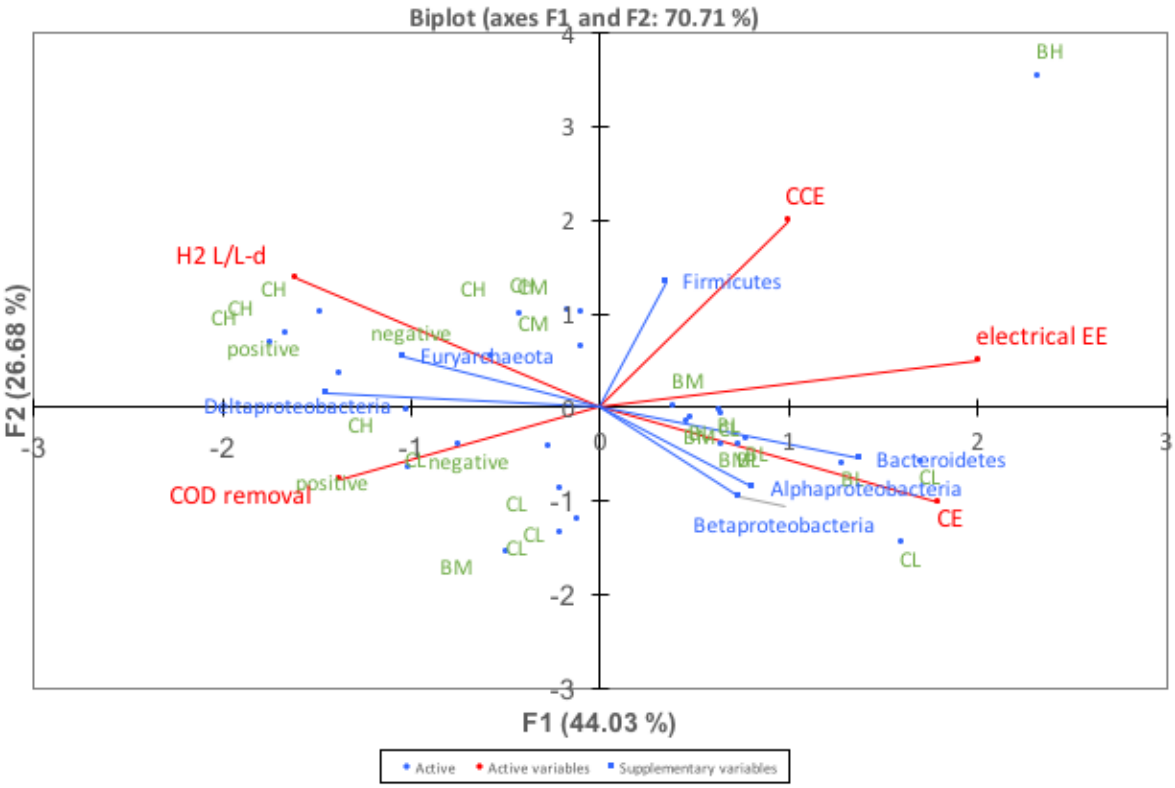

Figure 66: Canonical correspondance analysis (CCA) of all experimental conditions tested and the microbial taxa observed.

Increased hydrogen and current output are observed at the high continuous loading, which is supplied by the growing exoelectrogen population as it feeds on the higher amounts of acetate produced at that level. *Euryaracheota* are also positively correlated with these parameters as more substrate results in more fermentation and more production of intermediates like H_2 and CO_2 for use by methanogens. The *Firmicutes* population is most strongly correlated with CCE and high batch loading. The high batch loading is a strong selective force for growth of this fermenting phylum as saturating amounts of fermentable substrates are added and thus, do not show any correlation to H_2 output and CE. The additional taxonomic groups of *Alphaproteobacteria*, *Betaproteobacteria*, and *Bacteroidetes* show a strong correlation with CE

and low continuous substrate loading. The reasons for this may be two-fold, in that these microbes may be playing a syntrophic and scavenging role that positively contributes to high anode efficiencies. Additionally, these microbes may be more sensitive to recalcitrant compounds and may also be outcompeted by *Firmicutes* resulting in decline in these groups at higher loading, leading to positive correlation with low substrate loadings. The PCA and CCA results demonstrate the intricate relationship among operating parameters, their impact on microbial community structure, and the performance that results from the interaction of the two. The negative correlations between high output and efficiency are driven by impacts on the metabolic pathways of the microbial community, and thus enrichment of key members must take place to prevent cascading impacts that can be detrimental to performance.

FINAL CONCLUSIONS

A comprehensive study of bioelectrochemical conversion of biomass-derived bio-oil aqueous phase (BOAP) to hydrogen using a microbial electrolysis cell (MEC) was undertaken. This included development of an anode community capable of efficient conversion of BOAP and a detailed analysis of the electrochemical, biochemical and genomic aspects of the MEC. The following conclusions were derived from the study.

The research demonstrated that a microbial community capable of efficient conversion of a lignocellulosic-derived stream to electrons and hydrogen can be accomplished via targeted enrichment. An initial hydrogen productivity of 4.3 L/L-day was obtained with an anode coulombic efficiency of 54 ± 6.5%, cathode coulombic efficiency of 94 ± 5.5% and a hydrogen recovery of 50 ± 3.2% at an organic loading rate of 10 g/L-day. The robust microbial community contained a variety of microbial families with population densities ranging from 5-20% based on 16S rRNA analysis. The diversity was likely due to the multiple classes of compounds present in the biomass-derived streams including fatty acids, anhydrosugars, alcohols, aldehydes, ketones, furans and phenolic compounds. Geobacteraceae, the primary known exoelectrogenic family, only made up 7-10% of the population, while other Proteobacteria, Firmicutes, and Bacteroidetes formed the remaining major part of the community.

The MEC process was investigated to understand the impact of process parameters on reactor performance by studying organic loading rate (OLR) and flow rate, while holding concentration constant. Both mass transfer and kinetic limitations were identified to exist in the MEC, depending on the operating conditions. Alleviation of the mass transfer issues was achieved via control of flow rate and OLR. A flow rate of 3.6 mL/min through the MEC anode

was found to minimize mass transfer issues. Substrate limitations were also identified, which were partially alleviated at higher loading rates. Due to the complex nature of the BOAP, a minimum, two-step conversion process was found to be necessary, which included fermentation and exoelectrogenesis. A recycle of the anode stream enabled higher retention time of the substrate in the MEC, minimizing the kinetic limitations at higher flow rates. The benefits of higher flow-rate were masked during one-pass operation due to lower conversion of more complex substrates, resulting in decreased conversion efficiency (ACE), which dropped from 57.9% to 9.9%. Introducing recycle coupled the benefits of faster flow-rate to high conversion rate, resulting in increased COD removal, anode efficiency and current/hydrogen output. A 74.3% COD removal was demonstrated using such an operation, which is remarkable considering the complexity of the biomass-derived substrate.

The impact of process conditions on microbial community was investigated as a follow up to the experiments investigating one-pass vs. recycle operation. This revealed a strong correlation between substrate loading/concentration and the microbial composition. The performance and microbial communities developed during lower loading and flow-rate conditions were reproducible and similar. *Deltaproteobacteria* did increase at the low flow-rate due to higher substrate concentrations of acetate, but did not result in higher performance due to reduced mass transfer at the lower flow rate. At higher substrate loadings, *Deltaproteobacteria* continued to increase but an increase in the population of Firmicutes was also observed. Looking deeper at the changes in *Deltaproteobacteria* , multiple exoelectrogenic strains from the Geobacteraceae family were found to be present under different conditions. The substrate loading affected which *Geobacter* strain/s was dominant in the anode. This implied that a certain trait resulting from the use of higher concentration, such as inhibition tolerance, etc. may be

dictating which microbes can survive in the anode. Furthermore, additional microbes such as *Betaproteobacteria* also changed and were substantially reduced under those conditions. An electron balance showed that more electrons were diverted to undefined sinks at higher loadings, which may have been due to a multi-pronged effect, including a shift in metabolism as evidenced by propionic acid accumulation and a reduction in catechol conversion, as well as increase in population of Firmicutes and *Deltaproteobacteria.* The results provide a basis for optimization of the MEC performance by manipulating the growth or feeding regimes during MEC start-up or initial biofilm development. Alternately, specific exoelectrogenic strains can be isolated, separately grown and introduced to bioaugment the community for achieving higher performance.

To further investigate how the microbial community works to convert BOAP into electrons, a detailed investigation of the reaction products and intermediates and the conversion mechanism was undertaken covering a range of substrate and electrode conditions in batch operation mode. A maximum productivity of 9.35 ± 1.73 L/L-d with BOAP was achieved using the switchgrass-derived BOAP. The productivity was increased 3-fold to 27.6 ± 5.29 L/L-d using pure acetic acid, demonstrating the potential exoelectrogenic capability of the system. The enriched microbial community demonstrated efficient and simultaneous conversion of a wide range of compounds through a synergistic, division of labor strategy and multi-substrate syntrophy. The complex system was investigated via an open-circuit stimulus-response experiment, which demonstrated acetic acid as a primary branching point between fermentation nd exoelectrogenesis. An electron balance showed that the biomass electrons were directed to acetic acid at an efficiency of 68.3% during the open-circuit stimulus provided in the first 4 hours, which increased to ~80% by the end of the run. However, a rate analysis indicated that the rate of

fermentation and conversion of BOAP to produce intermediates which could serve as substrates for exoelectrogenesis limited the system productivity. The experiments provided an understanding of the biocomplexity of bioelectrochemical systems for conversion of biomass-derived streams.

To assess the impact of feeding regime on fermentation limitations and the microbial interactions for BOAP conversion, a direct comparison of the fed-batch and continuous feeding of substrate was conducted at low and high loading conditions. This revealed that the continuous feeding process can solve many problems which limited the performance under fed-batch conditions. The limitations were found to arise from accumulation of phenolic and acidic intermediates. Furthermore, the high concentration observed under fed-batch conditions lead to excessive growth of fermenters with significant loss of electrons to undefined sinks. Inhibition of some exoelectrogens was also observed at high concentration under fed-batch conditions, which did not happen under continuous feeding conditions. Thus, continuous feeding of the substrate is a better option for MEC operation.

To probe deeper into selective pressures on the exoelectrogenic community members, variation in the anode potential was explored, which alters the energy available to the microbes passing electrons to the terminal electrode. A long-term exposure of the anode consortia enriched at -400 mV and 0 mV vs Ag/AgCl resulted in a gradual divergence of the resulting bioanode midpoint potentials by >100 mV over a period of 6 months. Cyclic voltammetry revealed a shift in peak current production to more negative potentials for the reactor poised at -400 mV. Furthermore, chronopotentiometry indicated very different profiles, showing a difference of 500 mV in the potential required to achieve a current of 15 mA (equivalent to 12 A/m^2). The experiments were conducted using the switchgrass-derived BOAP, making this study unique

with potential for biorefinery application for production of hydrogen, fuels or chemicals. Operation at -400 mV resulted in a 1.5-fold higher electrical efficiency reaching 164.9%, while marginally reducing hydrogen recovery by 1.0%. The results provide evidence for adaptation of complex communities to optimize applied potential, while reducing energy input for electrolysis. The community developed here can serve as a model system to understand complex community-function relationships.

To gain a better understanding of all active members of the microbial community, shotgun metagenomics and RNA-seq were carried out during high continuous loading to gain a more in-depth understanding of the structure-function relationship of the community. This was conducted by operating the MEC under continuous feeding at high BOAP loading. An optimized assembly and bin-genome process resulted in the capture of approximately 90% of the sequenced reads into bin-genomes producing, 21 high-quality genomes form the microbial community. The community was found to be dominated by two strains: *Pelobacter propionicus* and *Robinsoniella peoriensis*. The former was demonstrated to possess novel exoelectrogenic behavior for its taxonomy, containing similar numbers of c-type cytochromes with expression of the essential OmcZ, in addition to a pilA sequence which was similar to the ultra-conductive *Geobacter metallireducens* pilA. *Robinsoniella peoriensis* strain contained a substantial number of biomass-degrading genes, with a total of 425 CDS for CAZy related genes. The large amount of Firmicutes in the population totaling 42.5%, and the community as whole containing 2735 CAZy CDs spread across different roles in lignocellulosic degradation highlights selective forces of biomass-derived streams, requiring robust fermenters and cellulolytic microbes to convert the biomass to electrons, which the community demonstrated with high efficiency. The omics analysis thus identified key microbes responsible for the fermentative and exoelectrogenic

function in the community, which can be manipulated to optimize MEC performance.

The resulting data form all operational conditions tested were then analyzed via principle component analysis (PCA) and canonical correspondence analysis (CCA) within and across the operational conditions tested to provide stronger evidence for correlations between operating conditions, performance, and microbial taxa. High OLR and H_2 productivity correlated with *Deltaproteobacteria*, while Firmicutes corresponded strongly to high fed-batch feedings, due to substrate availability for fermentation. Anode CE was strongly correlated to low OLRs, which both correlated with the presence of *Alphaproteobacteria*, *Betaproteobacteria*, and Bacteroidetes. The negative correlations between high output and efficiency are driven by impacts on the metabolic pathways of the microbial community, and thus enrichment of key members must take place to prevent cascading impacts that can be detrimental to performance. Proper enrichment to particular operating conditions is key to this but must be investigated further at the molecular level to prevent the diversion of electrons to undefined sinks at higher loadings while preventing growth and providing conditions that promote community interactions leading to enhanced current output. The collective results advance the understanding of how microbial communities work to degrade biomass-related streams through fermentative, syntrophic, and exoelectrogenic interactions and how control of the operating conditions is essential to manage and enhance reactor and community performance.

RECOMMENDATIONS

While the results from this research considerably advanced the state of the art and knowledge on anode microbial communities in microbial electrolysis cells, further work is necessary to increase and sustain productivities to beyond 20 L/L-day to garner commercial consideration. This research effectively developed a robust microbial community with different interacting groups that efficiently directed different classes of compounds through acetic acid for use by exoelectrogens to produce electrons. However, the evidence shows that at the highest concentration levels tested, this efficient metabolism is impacted, resulting in the accumulation of phenolic and organic acids that likely inhibit the exoelectrogen population and possibly other syntrophic groups coupled to a substantial diversion of electrons to undefined sinks and a decreased performance. While use of 16S rRNA gene analysis can provide limited functional insights into the community, this analysis allowed us to observe shifts in community structure tied to changes in metabolism that indicate functional shifts are occurring at higher concentrations, allowing us to make conclusions about detrimental community shifts and symptoms of bad performance based on these changes and metabolite data that impacts overall community function and reactor performance. The underlying molecular mechanisms driving the observed changes must be better understood so that community structure can be effectively managed at higher loadings to sustain high performance for commercial considerations.

Future work should probe deeper into the sources of electron losses at higher loadings, elucidating the undefined sinks that incorporate growth and additional pathways for electron diversion. Included in this is better determination of the onset of intracellular storage polymers and how these can be abated in addition to how growth can be limited as well as directed toward

needed groups to prevent the negative changes in metabolite profiles observed at higher concentrations. Stable isotope probing could provide powerful means to elucidate the pathways of carbon flow in the system including growth and storage, and how different conditions impact flux of carbon as well as electrons through undesirable as well as desirable pathways. Once better understood, additional environmental controls can be explored to select against these pathways and enhance the driving biochemical force for direction of electrons to current. Likewise, further understanding the biofilms ability and triggers for storing charge extracellularly should be investigated to understand how system limitations may contribute to this and how improvements in reactor design may alleviate it. This will allow establishment of conditions that can enhance fermentation rate and electron flow to acetate without inhibiting exoelectrogenesis. Exploring increased tolerance by exoelectrogens can enhance this as well as enrichment of microbes for detoxification to prevent cascading affects of inhibitory concentrations. Continued efforts in these areas can lead to the development of an optimal microbial community management strategy for developing stable and high performing electroactive biofilms while contributing to overall strategies for engineering microbial communities for additional industrial applications.

VITA

Alex Lewis was born in Auburn, CA to the parents of Greg and Sherry Lewis and has two older brothers, Ryan and Jordan, and one younger sister Kelsey. He attended Del Oro High School in Loomis, CA and later attended the University of California – San Diego where he attained his undergraduate degree in Environmental Systems in 2011. He volunteered as an undergraduate research assistant in the lab of Dr. Stephen Mayfield during this time, and worked as a Laboratory Technician after graduation on the transformation of the chloroplast in marine algal strains for recombinant enzyme production. He then moved on to Synthetic Genomics Inc., where he worked as a Research Associate in Production R&D testing algal strains for biofuel production. Two years later he accepted a fellowship through the Bredesen Center for Interdisciplinary Research and Education at the University of Tennessee in 2013 where he earned his PhD in Energy Science and Engineering. During this time, he worked in the lab of Abhijeet Borole at Oak Ridge National Laboratory studying community dynamics in microbial electrolysis cells for the production of hydrogen from biomass. Alex has a passion of contributing to the development of a renewable energy based economy and plans to pursue starting a company based on technology developed during his dissertation.